2012

Application And Optimization Of Membrane Processes Treating Brackish And Surficial Groundwater For Potable Water Production

Jayapregasham Tharamapalan
University of Central Florida

APPLICATION AND OPTIMIZATION OF MEMBRANE PROCESSES TREATING BRACKISH AND SURFICIAL GROUNDWATER FOR POTABLE WATER PRODUCTION

by

JAYAPREGASHAM THARAMAPALAN
B.Eng (Civil & Structural), Nanyang Technological University, Singapore, 1994
MSc (Environmental), Nanyang Technological University, Singapore, 2003

A dissertation submitted in partial fulfillment of the requirements
for the degree of Doctor of Philosophy
in the Department of Civil, Environmental, and Construction Engineering
in the College of Engineering and Computer Science
at the University of Central Florida
Orlando, Florida

Fall Term
2012

Major Professor: Steven J. Duranceau

ABSTRACT

The research presented in this dissertation provides the results of a comprehensive assessment of the water treatment requirements for the City of Sarasota. The City's drinking water supply originates from two sources: (1) brackish groundwater from the Downtown well field, and (2) Floridan surficial groundwater from the City's Verna well field. At the time the study was initiated, the City treated the brackish water supply using a reverse osmosis process that relied on sulfuric acid for pH adjustment as a pretreatment method. The Verna supply was aerated at the well field before transfer to the City's water treatment facility, either for softening using an ion exchange process, or for final blending before supply.

For the first phase of the study to evaluate whether the City can operate its brackish groundwater RO process without acid pretreatment, a three-step approach was undertaken that involved: (1) pilot testing the plan to reduce the dependence on acid, (2) implementing the plan on the full-scale system with conservative pH increments, and (3) continuous screening for scale formation potential by means of a "canary" monitoring device. Implementation of the study was successful and the annual savings in operating expenditure to the City is projected to be about $120,000.

From the acid elimination study, using the relationship between electrical conductivity in water and total dissolved solids in water samples tested, a dynamic approach to evaluate the performance of the reverse osmosis plant was developed. This trending approach uses the mass transfer coefficient principles of the Homogeneous Solution Diffusion Model. Empirical models

were also developed to predict mass transfer coefficients for solutes in terms of total dissolved solids and sodium.

In the second phase of the study, the use of nanofiltration technology to treat aerated Verna well field water was investigated. The goal was to replace the City's existing ion exchange process for the removal of hardness and total dissolved solids. Different pretreatment options were evaluated for the nanofiltration pilot to remove colloidal sulfur formed during pre-aeration of the groundwater. Sandfilters and ultrafiltration technology were evaluated as pretreatment. The sandfilter was inadequate as a pre-screen to the nanofiltration pilot. The ultrafiltration pilot (with and without a sandfilter as a pre-screen) proved to be an adequate pretreatment to remove particulates and colloids, especially the sulfur colloids in the surficial groundwater source. The nanofiltration pilot, was shown to be an efficient softening process for the Verna well field water, but it was impacted by biofoulants like algae. The algae growth was downstream of the ultrafiltration process, and so chlorination was used in the feed stream of the ultrafiltration process with dechlorination in the nanofiltration feed stream using excess bisulfite to achieve stable operations. Non-phosphonate based scale inhibitors were also used to reduce the availability of nutrients for biofilm growth on the nanofiltration membranes.

The combined ultrafiltration-nanofiltration option for treatment of the highly fouling Verna water samples is feasible with chlorination (to control biofouling) and subsequent dechlorination. Alternatively, the study has shown that the City can also more economically and more reliably use ultrafiltration technology to filter all water from its Verna well field and use its current ion exchange process for removal of excess hardness in the water that it supplies.

Dedicated to my wife Seetha, who has been my inspiration and support and to my boys Sambath and Seshan for making this a fun and enjoyable journey.

ACKNOWLEDGMENTS

This document is the culmination of work that could not have been completed without the support provided by the many individuals involved in this study. Special thanks are given to Dr. Steven J. Duranceau for providing me with the opportunity to be a graduate student, grooming me towards doing research and then serving as my advisor for this dissertation project. His feedback and guidance have been immense and were greatly appreciated during the course of this study. Special thanks are also due to Christopher Boyd for his youthful energy, enthusiasm and research ideas, as we made long trips every week to the field to do our research work. Research work with Christopher Boyd has been one of the main highlights of the work leading to my dissertation.

I would like to thank Dr. C. David Cooper, Dr Andrew A. Randall and Dr Christian A. Clausen for their service as committee members and for offering their time and effort in reviewing this research document. I am also grateful for the time and effort that Laboratory Coordinator Maria Pia Real-Robert has spent towards training and checking to ensure that the quality of laboratory work conducted and reported in this dissertation are of the highest standard. Additional thanks are offered to UCF research students Vito Trupiano, Andrea Cumming, Jennifer Roque, David Yonge, Juan Rueda, Nick Webber, Nancy Holt, Genesis Rios, Yuming Fang, Alyssa Filippi, Paul Biscardi and Marzieh Gasemi who dedicated their efforts to assist with laboratory and field tasks.

I would also like to thank the municipality, companies and individuals who were involved in assisting the UCF research team in this effort. This work would not have been feasible without the City of Sarasota Public Works and Utilities Division (1750-12th Street, Sarasota, FL 34236), particularly Pedro Perez, Katherine Gusie, Javier Vargas, Gerald Boyce and the City's water treatment plant operators. The support offered by Harn R/O Systems, Inc. (310 Center Court, Venice, FL 34285) is also greatly appreciated, notably Julie Nemeth-Harn, Jimmy Harn, Jonathan Harn and Bill Youels.

TABLE OF CONTENTS

LIST OF FIGURES

LIST OF TABLES

LIST OF EQUATIONS

LIST OF ABBREVIATIONS

AOC –Assimilable Organic Carbon

BF – Bag Filters

C_2T – Conductivity to Total Dissolved Solids Ratio

CEB – Chemically Enhanced Backwash

CF – Cartridge Filters

City – City of Sarasota

CIP – Clean-in-Place

$CaCO_3$ – Calcium Carbonate

CO_2 – Carbon Dioxide

DP – Degasified Permeate

EC – Electrical Conductivity

EPS – Extracellular Polymer Substances

Fe – Iron

GPM – Gallons per Minute

gsfd – gal/ft^2.day (gallons per sq. foot-day)

g/min – Grams per Minute

HCl – Hydrochloric Acid

HCO_3^- – Bicarbonate

H_2CO_3 – Carbonic Acid

H_2S – Hydrogen Sulfide

H_2SO_4 – Sulfuric Acid

HS^- – Bisulfite

HSDM – Homogenous Solution Diffusion Model

IC – Ion Chromatograph

ICP – Inductively Coupled Plasma

I-statistic – Industrial Statistic

IX – Ion Exchange

K_{sp} – Solubility Product

K_W – Normalized MTC of Permeate

K_S – Normalized MTC of Solute

LAL – Lower Acceptable Limit

LSI – Langlier Saturation Index

MF – Microfiltration

MG – Million Gallons (equivalent to 3,785m^3)

MGD – Million Gallons per Day

Mo – Molybdenum

MTC – Mass Transfer Coefficient

Na – Sodium

NF – Nanofiltration

NOM – Natural Organic Matter

NTU – Nephelometric Turbidity Unit

OEM – Original Equipment Manufacturer

OSHA – Occupational Safety and Health Administration

PDT – Pressure Decay Test

PES – Polyethersulfone

PLC – Programmable Logic Control

POE – Point-of-Entry

PSI – Pounds per Square Inch

RO – Reverse Osmosis

RSI – Ryznar Stability Index

SF – Sandfilters

S^0 – Sulfur

$S_2O_3^{2-}$ – Thiosulfate

SHMP – Sodium Hexametaphosphate

SMEWW – Standard Methods for the Examination of Water and Wastewater

TDS – Total Dissolved Solids

TEP – Transparent Exopolymer Particulates

TOC – Total Organic Carbon

TP – Total Permeate

UCF – University of Central Florida

UAL – Upper Acceptable Limit

UCL – Upper Control Limit

UWL – Upper Warning Limit

WTF – Water Treatment Facility

WTP – Water Treatment Plant

1. INTRODUCTION

The use of acid and scale inhibitors to control calcium carbonate and sulfate based scale has been around since the 1960s, when commercial water desalination using reverse osmosis (RO) membrane started. Acid addition in the pretreatment process is aimed at suppressing the pH of the feed water to the membrane process, in order to keep the carbonate and bicarbonate in the water in soluble form, so that precipitation of calcium carbonate does not occur in the presence of calcium (Ning & Netwig, 2002). Once concentrated beyond its solubility limit, the calcium carbonate precipitates quickly and so it is the most common scale found in RO systems (Singh, 2006). Sparingly soluble salts in order of formation are $CaCO_3$ > $CaSO_4$ > Silica > $SrCO_3$> $BaSO_4$ > $SrSO_4$> CaF_2 > $CaSiO_4$ > $MgSiO_3$ > $Ca_3(PO_4)_2$> $Fe(OH)_2$ (Cabibbo, Guy, Ammerlaan, Ko, & Singh, 1979). Scale inhibitors are added in pretreatment processes to improve membrane performance by inhibiting the precipitation of sparingly soluble metal salts on the membrane surface (Al-Rammah, 2000).

Scaling potential on the membrane surface at a particular recovery rate is calculated using chemical analysis of the feed water and the solubility of the various salts in the feed water that are likely to precipitate (Al-Shammiri, Salman, Al-Shammari, & Ahmad, 2005). The increasing availability of proprietary scale inhibitors that can achieve scaling control of all salts, and inhibit both alkaline and sulfate based scales has resulted in a re-evaluation of the need to suppress the pH of feed water to RO membranes (Ning & Netwig, 2002) to maintain stable membrane performance. Stable operations in membrane processes are characterized by low increases in

differential pressure which also translates to low decreases in the mass transfer coefficient for water (Bonne, Hofman, & van der Hoek, 2000).

Nanofiltration (NF) technology has increasing application in the water industry for softening purposes (Nanda, Tung, Li, Lin, & Chuang, 2010). The NF technology does not require chemicals for regeneration and minimizes wastes, in comparison to the softening approaches using the ion-exchange (IX) and lime-soda methods of softening. The high pressure membrane systems like the NF and RO systems though they have very high rejection of salts, organic and inorganic micropollutants and pathogens are faced with biofouling which poses a serious problem towards the membrane systems maintaining stable operations. Biofouling is the accumulation of microorganisms on a membrane surface, either by deposition from the feed water or by growth on the surface, or the combination of both deposition and growth, resulting in increases in pressure drop across the membrane system, flux reduction and salt passage increases (Characklis & Marshall, 1990).

Ultrafiltration (UF) process is a low molecular weight cut-off membrane process in comparison to NF and RO processes (Eriksson, Kyburz, & Pergande, 2005). Low molecular cut-off membrane processes like microfiltration (MF) and UF have been proven to be relative good pre-filters in high pressure membrane process like NF to prevent fouling by colloidal and organic fouling (Chellam, Jacangelo, Bonacquisti, & Schauer, 1997).

Project Description

This dissertation is the partial result of a cooperative agreement 16208081 “Reverse Osmosis Process Assessment Study and Verna Nanofiltration Process Evaluation”, between the University of Central Florida (UCF) and City of Sarasota Public Works and Utilities (City). The rising operating costs from the use of sulfuric acid in its reverse osmosis (RO) pretreatment process incentivized the City to explore the possibility of eliminating the use of acid, and reduce the risk associated with its operators having to handle the acid in its water treatment facility (WTF). The City was also ready to explore the possibility of switching to other types of scale inhibitors that would allow its plant to operate without use of acid in pre-treatment of its brackish water source, should the scale inhibitor that it was using prove to be inadequate.

Pilot testing of the acid elimination was carried out in incremental pH steps over 4 months duration. The testing was aimed at evaluating the viability of the City’s RO plant operating with its existing scale inhibitor to prevent the precipitation of sparingly soluble salts, without the complementary use of sulfuric acid to control calcium carbonate scale.

The implementation of the plan to reduce the dependence on acid use in the pretreatment process was then implemented over a 12 months period with five intermediate pH steps from pH 5.8 (i.e. pH of acidified RO feed water before project) to the raw water ambient pH of about 7.1. Another addition to the conservative approach to acid elimination was the installation of a two-membrane element monitoring device (“canary” unit) on the oldest of three RO trains at the plant. The monitoring device was installed at the end of the second stage of the RO train and its feed water

was the concentrate of the second stage, and its feed pressure was the residual concentrate pressure at the end of the second stage. Being installed on the oldest of three trains, with feed water from the concentrate stream of the second stage, meant that any possible scaling in the membrane processes, would be observed on the "canary" unit first.

Monitoring of the "canary" unit during and after the acid elimination, was done in tandem with the monitoring of the whole RO train, to identify trends shifts in the flux of permeate through the membranes in terms of mass transfer coefficient. Feed and differential pressure changes in the first and second stages and the "canary" unit were also concurrently monitored to identify potential signs of scaling/fouling. The standing protocol was to stop the acid elimination if scaling was noted, then the acid use would be partially reduced, and not a complete elimination of use.

The City also treats well water from another well field in Verna using the conventional aeration process for hydrogen sulfide removal, and ion-exchange (IX) technology for hardness removal and blending for stabilization of the soft water from the RO and IX processes. This study was also aimed at evaluating the viability of filtering the aerated water stream from Verna, for additional protection against particle, pathogen and bacterial loadings in the City's water supply. This study included the evaluation of the existing IX process being replaced with a nanofiltration (NF) membrane process.

The Verna well field water has high sulfide content and so it is aerated to remove some of the sulfide in the form of hydrogen sulfide before the water is transferred to a storage tank (10^{th}

Street) closer to the City's water treatment facility (12th Street), which acts as an equalizing tank. From the equalizing tank, water is transferred to the IX process or bypasses the IX process to be used in the final blend. The aerated Verna water has fluctuating turbidity formation potential because of the formation of colloidal sulfur, resulting from the aeration process at Verna. In order to protect the NF membranes from fouling by colloidal sulfur, ultrafiltration (UF) and other pretreatment options are also to be evaluated as part of this study.

Objectives

The purpose of this research is to determine whether a Floridan Water Treatment Facility (WTF) that has been treating brackish groundwater using reverse osmosis (RO) membrane process can be operated without the use of acid in its pretreatment process. The same WTF is also treating a highly fouling surficial groundwater source by aeration for sulfide control and softening the aerated water using ion-exchange technology. The additional objective of this research is to evaluate the alternative treatment technology to treat this highly fouling surficial groundwater source. Specific objectives include:

1. Developing a protocol for the elimination of acid use without compromising the RO membranes. The protocol will encompass:
    a. pilot testing the plan to reduce the dependence on acid;
    b. implementation of the acid elimination plan on the full-scale RO plant in conservative pH increments; and
    c. installation of a "canary" scaling monitoring device to continuously screen for scale formation potential on the RO plant during a staged acid elimination plan.

2. Developing post-treatment options for the RO permeate following the elimination of acid use in the pretreatment process to the RO plant.
3. Developing empirical models for the RO process that uses polyamide membranes to predict the mass transfer of solutes in terms of total dissolved solids and sodium.
4. Developing a tool to allow effective monitoring of performances of RO and NF membrane processes using the Homogeneous Solution Diffusion Model.
5. Pilot testing to evaluate pretreatment options to an NF process to treat a highly fouling groundwater that is aerated for sulfide control. Pretreatment options to nanofiltration process include:
    a. bag filters and cartridge filters on nanofiltration pilot;
    b. sand filtration;
    c. ultrafiltration membrane process in combination with sand filtration;
    d. ultrafiltration membrane process without any additional pre-screening; and
    e. pre-disinfection to control biofouling.

2. REVIEW OF PROJECT SITE

Water Treatment Facility Description

The project site for the research reported in this study is the City of Sarasota Public Works Department's (City) water treatment facility (WTF) located at 1750 – 12th Street, Sarasota, FL 34236. The City's water supply comes from two sources: the Verna well field located 15 miles east of the City and the downtown well field in the northwest area of the City. The Southwest Florida Water Management District regulates the raw water supplies that the City can draw upon.

The City's WTF comprises two major water treatment processes: a reverse osmosis (RO) process; and an ion-exchange (IX) process. The capacity of the WTF is 12 million gallons per day (MGD) from a combination of 4.5 MGD from the RO component of the water treatment facility, 5.2 MGD from the IX component of the WTF and 2.3 MGD of blended bypass water from the Verna well field. Schematic of the water treatment facility is as shown in Figure 2-1.

From the Verna well field about 7.9 MGD of water can be withdrawn based on existing permits to the City. The groundwater is treated using tray aerators atop a structure located at the Verna well field. Chlorine is then added to the aerated groundwater and the water is then stored in a 1 million gallon (MG) ground storage reservoir prior to gravity flow over 22 miles to the 10th Street service reservoir. From the 10th Street service reservoir about 5.6 MGD is withdrawn for treatment at the City's IX process located at the 12th Street WTF, while another 2.3 MGD bypasses the IX process for final blending.

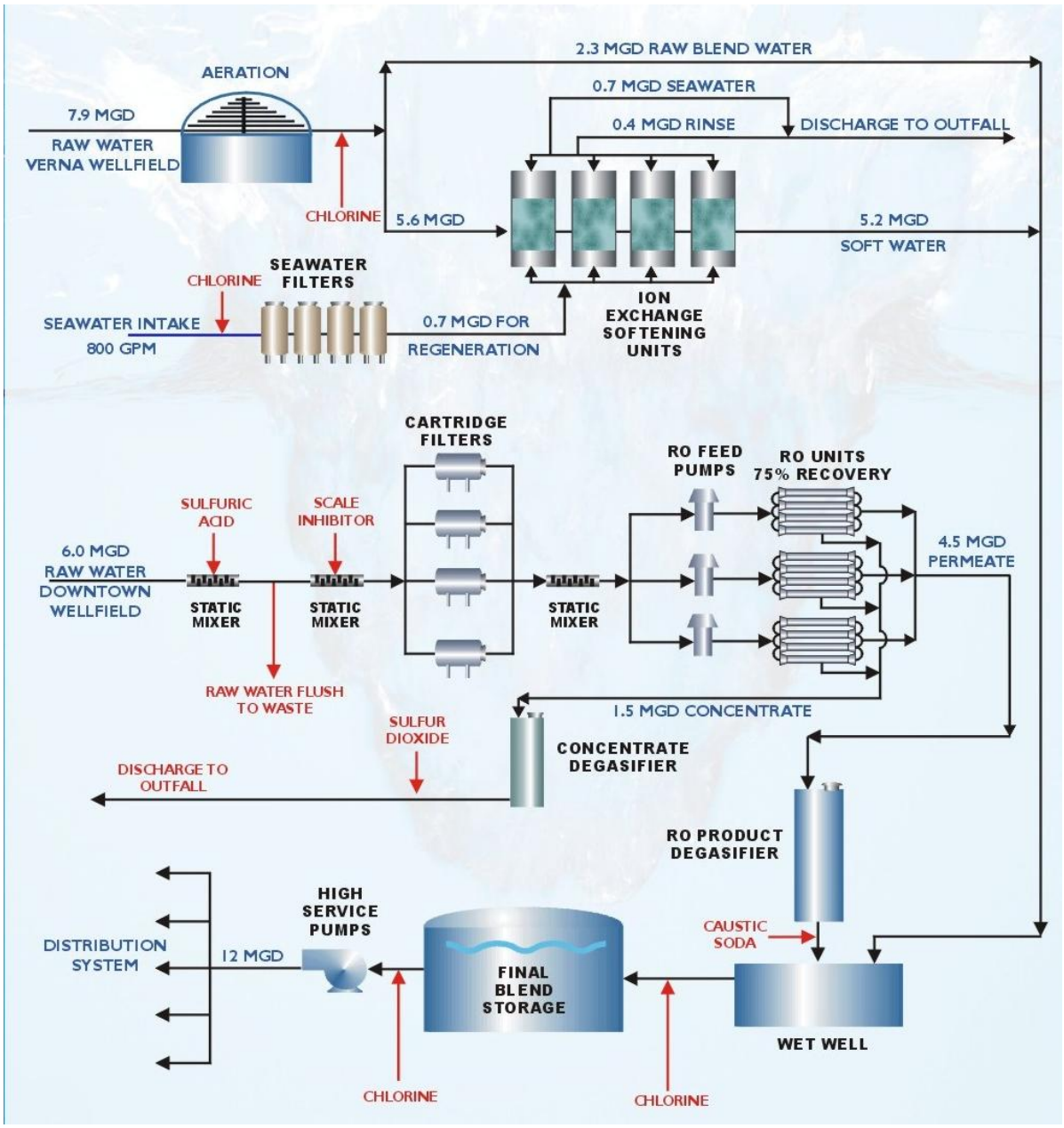

Figure 2-1: Schematic of the City of Sarasota Water Treatment Facility
(Courtesy of City of Sarasota)

For the RO process at the WTF, another 6 MGD of brackish groundwater is withdrawn from a network of 8 deep wells at the downtown well field (Lower Hawthorn Aquifer) in the northwest area of the City of Sarasota. This groundwater is transferred to the RO process and is treated without any physical pretreatment processes.

Despite the fact that the WTF has a capacity of 12 MGD, the overall production at the facility is currently limited to 10.5 MGD in order to be able to comply with secondary drinking water standards (USEPA, 2012). At production levels higher than 10.5 MGD, the WTF's product water to its customers will exceed the secondary maximum contaminant level (MCL) limit of 250mg/L for sulfate. The primary source of sulfate in the City's water supply comes from the Verna well field water that is aerated and processed by IX technology for hardness removal only and the component that is segregated for final blending with the RO permeate and IX soft water.

Ion Exchange Process

Of the 7.9 MGD of Verna well field water, about 5.6 MGD of the water is transferred to the IX process at the WTF, via the 10^{th} Street reservoir. The IX process produces approximately 5.2 MGD of soft water. The remaining 0.4 MGD is used for media rinse. There are four softening units; with three operational at full production, while the fourth is regenerated using chlorinated filtered seawater that is tapped from the nearby Sarasota Bay.

The IX resin is a sodium-based zeolite aimed at removing hardness (mainly calcium and magnesium ions) in the water. Product water from the IX has a hardness of about 8 mg/L, which is a 98% reduction from the feed water hardness of about 500mg/L.

For the regeneration of the media, about 0.7 MGD of seawater is used and this is piped separately to the WTF. The waste stream from the IX process is about 1.1 MGD (0.7 MGD of seawater and 0.4 MGD of media rinse water). As the seawater intake for media regeneration is chlorinated, sulfur dioxide is added to the IX waste stream for the removal of residual chlorine prior to discharge.

Reverse Osmosis Process

The raw brackish water from the Downtown well field that enters the treatment facility is first acidified with sulfuric acid to a pH of about 5.8. The acidification process is aimed at mitigating the formation of calcium carbonate and magnesium hydroxide scale, as well as to suppress organic and biological fouling of the RO membranes((Ghafour, 2003); (Patel & Milligan, 2008)). A scale inhibitor (Aquafeed® 1025) is added as a dispersant, at a dose of 2.0 mg/L as anti-fouling pretreatment to inhibit the formation and growth of sparingly soluble salts, especially strontium sulfate, on the RO membrane as well as to disperse colloids and suspended solids.

The chemically pretreated water is then filtered by 1-micron cartridge filters to remove particles and is pumped into the membrane pressure vessels at pressures of between 150 to 200 pounds per square inch (psi). The RO plant consists of three process trains, each containing 42 pressure vessels configured in a two-stage process. The first stage consists of 28 pressure vessels, while the second stage has 14 pressure vessels. Each pressure vessel holds 6 low pressure, spiral wound RO membrane elements. Operated at 75% recovery, the 3 trains collectively produce 4.5 MGD of RO product water.

Post-Treatment Processes

The RO permeate is first degasified to remove excess hydrogen sulfide and concomitantly carbon dioxide is also stripped in the two RO permeate degasifiers towers in the WTF. Caustic soda is then added for alkalinity recovery in order to stabilize the degasified permeate for corrosion control, prior to blending the water with IX (up to 5.2 MGD) soft water and aerated Verna IX bypass water (up to 2.3 MGD). The blended mix is then disinfected with chlorine before being stored in a ground treated water storage tank, and thereafter sent into the distribution system.

In a two-stage RO process, as in the City's RO plant, the concentrate produced from the first stage becomes the feed water to the second stage. The concentrate water that remains after the second stage flows as wastewater and it is degasified separately from the product water for sulfide control. This RO wastewater stream is combined with the IX waste stream before discharge.

Discharge Permits

The wastewater discharge from the City's WTF consists of the reject water from the RO process and the rinse and regeneration wastewaters from the ion exchange process. The wastewater stream from the WTF is currently permitted to be discharged into the Hog Creek, which is a tributary to Sarasota Bay at a permitted flow of 2.8 MGD (City of Sarasota, 2008). The City is currently exploring a deep well injection system for disposal of its wastewater streams.

3. LITERATURE REVIEW

Overview

In this Chapter, the literature related and relevant to research work carried out in this study is reviewed. The literature review is presented in sections and sub-sections by order of existing and proposed water treatment processes and research work identified as part of this study.

Typical Reverse Osmosis Treatment Processes

One of the primary causes of RO system failure is membrane scaling, which is noted by the increase in differential pressure across the membrane as the accumulation of water-formed or water-borne deposits impede the flow of fluid (Amjad, 1993). Scaling occurs as sparingly soluble salts get concentrated in the reject stream of membrane processes beyond their solubility limit, which is a function of temperature, pressure and pH (Singh, 2006). Three major performance issues are related to scaling membranes: increasing operating pressure (or alternatively a reduced flux at constant pressure), increasing pressure drop across membrane elements, and decreasing salt rejection rates (Kucera, 2010).

The concept of scale inhibition on membranes is “borrowed” from boiler and cooling water technologies, where salt concentration occurs as these processes rely on temperature change to effect evaporation. In membrane processes the same salt concentration occurs without the accompanying temperature change (Darton, 1997). In order to improve RO plant performance, acid and scale inhibitors (also known as antiscalants) are used in pretreatment processes. The

addition of acid and a scale inhibitor to the feed water has been the conventional method of controlling carbonate and sulfate scale formation on membranes respectively. Reducing the process recovery is an option for to control scaling, by ensuring that solubility product is not exceeded, but on an overall basis, it is more economical to use chemicals to condition the feed water thereby maximizing the water production (Nemeth & Seacord, 2000).

Acid pre-treatment of RO feed water reduces the pH to control calcium carbonate scaling by increasing the solubility of calcium carbonate. Hydrochloric [HCl] or sulfuric [H_2SO_4] acids are typically used for acid pre-treatment to reduce the feed water pH to between 5 and 7 pH units (Greenlee, Lawler, Freeman, & Marrot, 2009). Sulfuric acid is sometimes preferred over hydrochloric acid because of the higher membrane rejection of the divalent sulfate ions compared to the monovalent chloride ions (Hydranautics, 2008). A drawback of sulfuric acid addition, however, is that the scaling potential for sulfate-based salts is also increased with increasing sulfate ion concentration.

In order to improve RO plant performance, scale inhibitors are added prior to the feed water entering the RO modules. There are generally three different types of scale inhibitors: sodium hexametaphosphate (SHMP), organophosphonates and polyacrylates (Prihasto, Liu, & Kim, 2009). The scale inhibitor limits precipitation of sparingly soluble salts by increasing the ion concentration threshold required for clustering and by disrupting nuclei ordering and crystal structure. Some scale inhibitors repel other ions in solution by adsorbing onto crystal surfaces or fully chelating with dissolved ions (Greenlee, Lawler, Freeman, & Marrot, 2009). However, scale inhibitors do not completely prevent precipitation, because precipitation will eventually

occur at sufficient salt concentration. On the other hand, the increasing availability of proprietary scale inhibitors that can inhibit both alkaline and sulfate based scales has resulted in a re-evaluation of the need to suppress the pH of feed water to RO membranes (Ning & Netwig, 2002).

When RO feed water is adjusted to approximately pH 6, carbonate species in water is present as either bicarbonate or carbonic acid (i.e. soluble form of carbon dioxide (CO_2)). These species of carbonate do not form scales with calcium. However, the soluble form of CO_2 will freely pass through the membrane into the RO permeate, thereby requiring degassing downstream for corrosion control. If the feed water also contains sulfide (S^{2-}, and HS^-) ions, acidification will generate unionized hydrogen sulfide (H_2S) gas (Gare, 2002). Since H_2S is also a corrosive gas that passes through RO membranes, post-treatment is normally required. Untreated sulfide will be oxidized by chlorine during disinfection resulting in the formation of turbidity and color, which affect the aesthetics of finished water (Lyn & Taylor, 1992).

Permeate from RO facilities have low alkalinity, hardness and pH and require additional treatment to minimize corrosion potential. Post-treatment of permeate at an RO facility typically includes degasification, alkalinity recovery, pH adjustment, corrosion control and disinfection (Duranceau S. J., 2009). In studying alkalinity recovery and corrosion control, Duranceau et al (1999) compared the use of H_2SO_4 and carbonic acid (H_2CO_3) for pH adjustment of water fed to a packed aeration tower. The study showed that pre-treatment with H_2CO_3 did not result in the loss of alkalinity through the packed aeration tower, thereby maintaining the buffering capacity of the product water. However, when sulfuric acid was used, the available bicarbonate (HCO_3^-)

alkalinity was converted to soluble form of CO_2 and was lost during the aeration process. The use of sulfuric acid also resulted in increased sulfate content in the aerated product water.

Membrane Scaling and Control

Traditionally acid and scale inhibitors are used to suppress pH of feed water to RO elements to slow down the scaling of membranes, by ensuring that the solubility product is not exceeded, thereby prolonging the life of the membranes. As water passes through membrane, sparingly soluble salts are concentrated on the feed side, resulting in scaling. Accumulation of salts in the brine is of concern to operators of membrane plants as the sparingly soluble salts will exceed the solubility product (K_{sp}) and precipitate in the concentrate (Kinser, Kopko, Fenske, & Schers, 2007). Solubility product of a solution is dependent on factors such as temperature and ionic strength (AWWA, 1999). The precipitation of salts on the membrane, results in membrane fouling and the membrane productivity declines.

One of the indices used to measure the tendency to form scale is the Langelier Saturation Index (LSI) (Richarson, Blom, & Taylor, 2009). Typically the feed water is pH adjusted so that the LSI remains negative. LSI quantifies the difference between the ambient water pH and the pH at which calcium carbonate ($CaCO_3$) saturation occurs (pH_s) and is dependent upon pH, calcium concentration, alkalinity, temperature and ionic strength as shown in Equations 3-1 and 3-2 (Schock, 1984). A negative LSI indicates that $CaCO_3$ will remain dissolved in solution while a positive LSI indicates that $CaCO_3$ will precipitate.

$$LSI = pH - pHs \tag{3-1}$$

Where: $pHs = (9.30 + A + B) - (C+D)$ (3-2)

A = $\frac{(\log_{10}TDS) - 1}{10}$ where TDS is in mg/L

B = $-13.12 \times \log_{10}(T)+34.55$ where Temperature, T, is in K

C = $\log_{10}[Ca^{2+}]- 0.4$ where $[Ca^{2+}]$ is in mg/L as $CaCO_3$

D = $\log_{10}[Alk]$ where alkalinity, [Alk], is in mg/L as $CaCO_3$

The Langlier Saturation Index calculation for membrane processes is used for instances when total dissolved solids (TDS) concentration of the concentrate stream is less than 10,000 mg/L (ASTM, 2010). When the TDS of the concentrate stream is higher, as in the case of seawater desalination, then the Stiff and David Stability Index is to be used (Stokke J. , Seacord, Maillakakis, & Hawes, 2010).

Another index that is used in many applications, replacing LSI, is the Ryznar Stability Index (RSI). The RSI developed from LSI, uses an empirical database of scale thickness observed to correlate to water chemistry, by relating scale formation to the calcium carbonate saturation state.

$$RSI = 2(pHs) - pH \quad (3\text{-}3)$$

If the RSI value is less than 6.5, the water tends to be scale forming. When the index value is between 6.5 and 7, the water is approximately at saturation equilibrium with calcium carbonate ($CaCO_3$). When the RSI is higher than 8, the water is under saturated and so tends to dissolve any existing solid $CaCO_3$.

Recent developments in proprietary scale inhibitors have suggested that there may not be a need to suppress the pH of feed water to RO membranes (Butt, Rahman, & Baduruthamal, 1995). The concept of acid-free scale control for RO systems involves the application of a scale inhibitor to prevent both alkaline and sulfate based precipitates on the membrane desalting surfaces of the elements or permeators under normal and upset operating conditions (Logan, Nehus, & Smith.A.L., 1985). The availability of scale inhibitors with broad activity spectra would likely present the case for a single scale inhibitor to simultaneously control the carbonate, sulfate and fluoride scales of calcium, sulfate, strontium and barium as well as inorganic foulants resulting from iron, aluminum and reactive silica that may be present in any given water (Ning & Netwig, 2002).

Depending on quality of feed water to membrane plants, different approaches have been adopted in operating membrane plants without acid and/or scale inhibitor pretreatment while still managing membrane fouling potential. A review of some cases in Florida is presented here in the following sub-sections.

City of Cape Coral's North Reverse Osmosis Water Treatment Plant

City of Cape Coral's consultants did a chemical optimization study for the City's new RO plant based on projected water quality of concentrate when the plant was to be operational in 2008 as well as at the end of its 25-year life span in 2033. Three leading scale inhibitor manufacturers were consulted on their proprietary chemicals, and their chemicals tested in pilot scale studies. From these studies projections were made on the dose of their chemicals based on raw feed water

quality to the plant and projected LSI values of the concentrate stream. All projected that the plant can operate without acid, but with only scale inhibitor dose of between 2 - 5 mg/L up to year 2018. Beyond that some level of acid addition may be necessary. Positive LSI values of up to 3 on the brine stream were still acceptable according to the findings of the City's Consultants (Kinser, Kopko, Fenske, & Schers, 2007).

City of Boca Raton's Glade Road Water Treatment Plant

At the City of Boca Raton's 40 MGD Glades Road Water (Nanofiltration) Treatment Plant, the source of fouling on the membranes during pilot testing was adsorption of humic acids onto membrane surfaces, and this fouling was enhanced by the complexing of the humic acid with some of the scale inhibitors and dispersants used. New low fouling membranes were tested and also membranes from multiple suppliers were tested in parallel, without acid and scale inhibitor feed. Stable operations without acid and scale inhibitor pretreatment were noted when using membranes from multiple suppliers, with eventually one membrane being selected for the full-scale plant based on hardness rejection that were within specific ranges as specified by the City (Keifer, Brinson, & Suratt, 2003).

Pilot Testing for United Water Florida's Floridan Aquifer Supply

United Water Florida (UWF) engaged consultants to evaluate membrane options (i.e. either NF/ RO) for its proposed membrane facility treating source water that contains approximately 340 mg/L of sulfate and hydrogen sulfide in excess of 2 mg/L. Pilot testing works showed that it was viable to operate both NF and RO systems without acid pretreatment but with scale inhibitors

only. RO system was eventually selected over NF due to higher rejections and lower capital costs in achieving the same blended water quality. Another consideration was the fact that NF has been noted to remove less assimilable organic carbon that is contributed by the polymeric scale inhibitor that is used and the potential for re-growth in distribution systems. To enhance removal of sulfides, the permeate feed to packed tower was also recommended to be acidified with carbonic acid to a pH of 6. With no acid pretreatment, the concentrate disposal pipelines were expected to have increased scale deposition and this was to be factored into the design of the plant (Seacord, Cushing, White, Grimes, & Dieffenthaller, 2001).

North Lee County RO Water Treatment Plant

North Lee County's RO Water Treatment Plant that became operational in Oct 2006 was faced with numerous challenges in meeting its design production capacity of 6 MGD, including irreversible membrane fouling due to strontium sulfate ($SrSO_4$) scaling. Pilot testing was then commissioned to evaluate the possibility of eliminating sulfuric acid addition to the RO feed. The pilot testing works also included the evaluation of multiple scale inhibitors to minimize membrane fouling. The proprietary scale inhibitors tested proofed viable, though at different dose rates, in minimizing membrane fouling and ensuring stable operations. North Lee County therefore had the option of choosing the most cost effective scale inhibitor to minimize its operations cost. The plant has since been retrofitted to operate without acid addition to RO feed (Stokke J. , Seacord, Maillakakis, & Hawes, 2011).

Existing Pretreatment to Surficial Groundwater from Verna Well field

Biological Sulfur Cycle

Hydrogen sulfide is frequently found in groundwater, and at concentrations of about 1.0 mg/L the odor emitted by hydrogen sulfide in potable water can be considered offensive while as little as 0.05 mg/L of hydrogen sulfide is noticeable (White, 1972). Groundwater obtained from deep wells, where anaerobic conditions prevail, often contain sulfide that is a naturally occurring mineral in some soil and rock (Lovins, Duranceau, King, & Medeiros, 2004). In Florida, many have encountered in shallow irrigation wells the obnoxious odor of hydrogen sulfide gas that is often compared to the 'rotten egg' smell (White, 1999). One reaction pathway in the formation of the 'rotten egg' odor of H_2S is from the anaerobic bacteria action on sulfates (AWWA, 1999). Reduced sulfur compounds are collectively classified as total sulfides, and are most often found in groundwater and at the bottom of water impoundments where anaerobic conditions prevail. If left untreated, the finished water quality is impacted by sulfides, resulting in undesirable taste and odor issues, increased corrosion in the water purveyance system and oxidization to form visible turbidity and color ((Wells, 1954) ,(Lyn & Taylor, 1992)).

Sulfur transformations by microorganisms are complex because of the large number of oxidation states of sulfur and the fact that several transformation of sulfur occurs abiotically. Summary of the oxidation states of key sulfur compounds is given in Table 3-1 (Madigan & Martinko, 2006) below.

Table 3-1: Sulfur Compounds and Oxidation State

Compound	Oxidation state of S atom
Organic S (R-SH)	-2
Sulfide (H_2S)	-2
Elemental sulfur (S^0)	0
Thiosulfate ($S_2O_3^{2-}$)	+2 (average per S)
Sulfur dioxide (SO_2)	+4
Sulfite (SO_3^{2-})	+4
Sulfate (SO_4^{2-})	+6

Oxygen is the terminal electron acceptor, in aerobic systems, and is reduced while organic or inorganic electron donors are being oxidized. In the absence of oxygen, other compounds such as nitrate (NO_3^-), sulfate (SO_4^{2-}) and carbon dioxide (CO_2) may become electron acceptors. The use of sulfate and carbon dioxide requires strictly anaerobic conditions. Sulfate-reducing bacteria use sulfate as electron acceptor, instead of oxygen ((Garcia, Blanco, & Meraz, 2008);(Sungur & Cotuk, 2005)).

In Figure 3-1, the typical reactions for the reduction of sulfide to sulfur, and the oxidation of sulfite to sulfate are shown. The sulfite reduction rate that is mediated by the sulfide reductase is limited by the availability iron (Fe) as cofactor for the enzyme. On the other hand, the sulfite oxidation is mediated by the enzyme sulfite oxidase which requires the cofactors molybdenum (Mo), and Fe (Feng, Tollin, & Enemark, 2007).

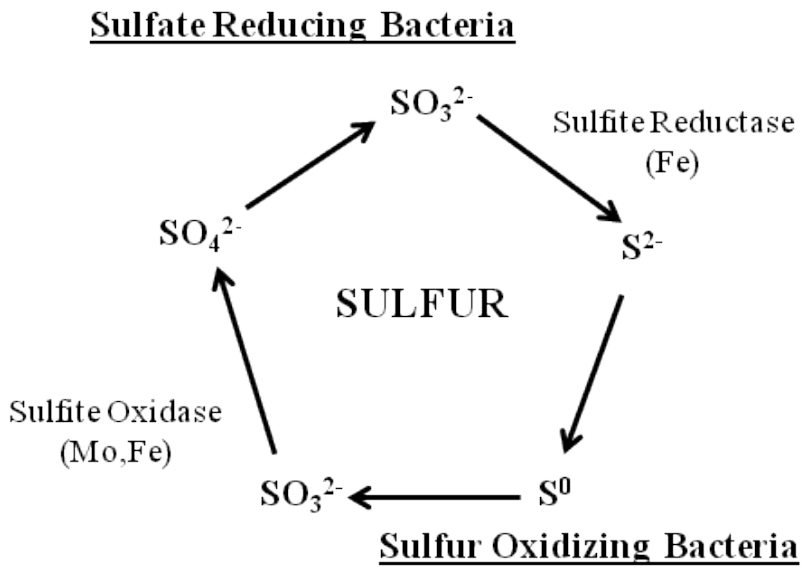

Figure 3-1: Sulfur Oxidation and Sulfate Oxidation

Sulfur Oxidation

In some biological reactions, the sulfur compounds - hydrogen sulfide (H_2S), elemental sulfur (S^0) and thiosulfate ($S_2O_3^{2-}$) - are used as electron donors. The oxidation of sulfur results in the formation of sulfate (SO_4^{2-}), as shown in Equation 3-4.

$$H_2S + 2O_2 \rightarrow SO_4^{2-} + 2H^+ \quad (3\text{-}4)$$

H_2S oxidation occurs in stages, and the first oxidation step yields elemental sulfur, S^0 as shown in Equation 3-5.

$$HS^- + H^+ + \frac{1}{2}O_2 \rightarrow S^0 + H_2O \quad (3\text{-}5)$$

When the supply of H_2S becomes limited, the oxidizing bacteria derive additional energy by oxidation of sulfur to sulfate as shown in Equation 3-6.

$$S^0 + H_2O + \frac{3}{2}O_2 \rightarrow SO_4^{2-} + 2H^+ \quad (3\text{-}6)$$

The sulfur oxidation reactions as depicted in Equations 3-4, 3-5 and 3-6 result in the production of protons (H^+) thereby lowering the pH of the medium.

Another reaction pathway for sulfate (SO_4^{2-}) formation involves the formation of sulfite (SO_3^{2-}) as an intermediate product, from the oxidation of hydrogen sulfide (H_2S), elemental sulfur (S^0) and thiosulfate ($S_2O_3^{2-}$), as shown in Equations 3-7, 3-8 and 3-9. Sulfate is formed when the sulfite is oxidized as depicted in Equation 3-10.

$$H_2S + \frac{3}{2}O_2 \rightarrow SO_3^{2-} + 2H^+ \quad (3\text{-}7)$$

$$S_2O_3^{2-} \rightarrow SO_3^{2-} + S^0 \quad (3\text{-}8)$$

$$S^0 + \frac{3}{2}O_2 + 2e^- \rightarrow SO_3^{2-} \quad (3\text{-}9)$$

$$SO_3^{2-} + \frac{1}{2}O_2 \rightarrow SO_4^{2-} \quad (3\text{-}10)$$

<u>Sulfate and Sulfur Reduction</u>

Sulfate (SO_4^{2-}) is a much less favorable electron acceptor than oxygen (O_2) or nitrate (NO_3^{2-}). The most common electron donors used by sulfate-reducing bacteria are hydrogen, lactate and pyruvate (Cooney, Roschi, Marison, Comminellis, & Stockar, 1996). The reduction of sulfate (SO_4^{2-}) to hydrogen sulfide (H_2S) requires eight electrons, and proceeds through a number of intermediate stages.

In dissimilative sulfate reduction, sulfate (SO_4^{2-}) is reduced biologically under anaerobic conditions to sulfite (SO_3^{2-}), which in turn can combine with hydrogen to form hydrogen sulfide (H_2S). The reactions are detailed in Equations 3-11 and 3-12:

$$SO_4^{2-} + 2H^+ + 2e^- \leftrightarrow SO_3^{2-} + H_2O \quad (3\text{-}11)$$

$$SO_3^{2-} + 8H^+ + 6e^- \leftrightarrow H_2S + 3H_2O \quad (3\text{-}12)$$

Some organisms produce hydrogen sulfide (H_2S) in anaerobic respiration but are unable to reduce sulfate. These organisms are known as elemental sulfur reducers, and these sulfur-reducing bacteria carry out the reaction as shown in Equation 3-13.

$$S^0 + 2H^+ \leftrightarrow H_2S \quad (3\text{-}13)$$

The sulfate and sulfur reductions as depicted by Equations 3-11, 3-12 and 3-13, result in an decrease in pH for the medium.

Aeration

Aeration processes are commonly used for the removal of dissolved gases, such as carbon dioxide (CO_2) and hydrogen sulfide (H_2S) from ground water supplies. CO_2, being a smaller molecule than H_2S, will be released at a faster rate than H_2S (Garrels & Naeser, 1958). In a closed system, CO_2 is a volatile gas that exists in equilibrium with other carbonate species as defined by the following equations and Figure 3-2:

$$CO_{2(gas)} + H_2O \leftrightarrow H_2CO_{3(aq)} \qquad pK_1 = 2.8 \quad (3\text{-}14)$$

$$H_2CO_{3(aq)} \leftrightarrow H^+ + HCO_{3(aq)}^- \qquad pK_2 = 6.33 \quad (3\text{-}15)$$

$$HCO_{3(aq)}^{-} \leftrightarrow H^{+} + CO_{3(aq)}^{2-} \qquad pK_3 = 10.35 \qquad (3\text{-}16)$$

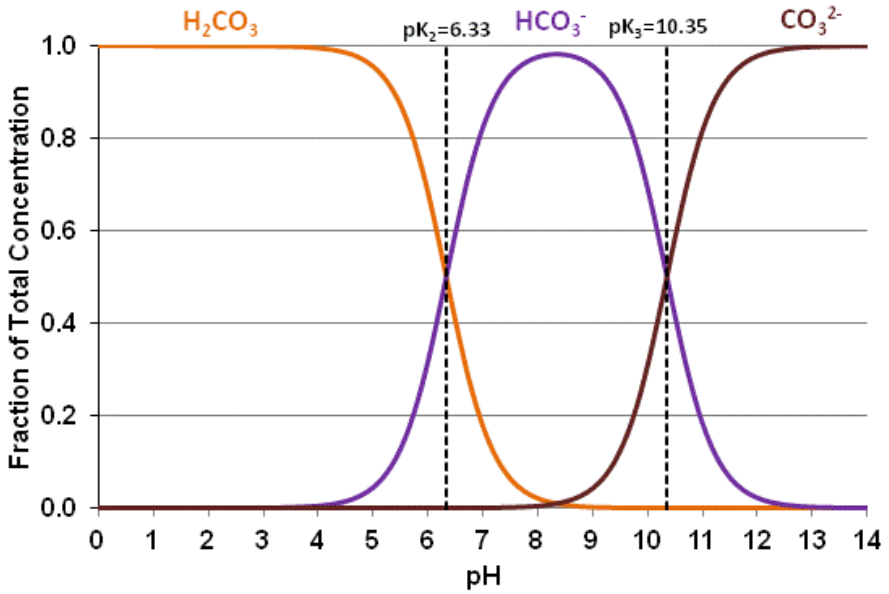

Figure 3-2: Carbonate Species Distribution Diagram

Likewise, H_2S dissociation in aqueous solutions can be described by the following equilibrium equations and Figure 3-3:

$$H_2S_{(gas)} + H_2O \leftrightarrow H_3O^{+} + HS_{(aq)}^{-} \qquad pK_1 = 6.99 \qquad (3\text{-}17)$$

$$HS_{(aq)}^{-} + H_2O \leftrightarrow H_3O^{+} + S_{(aq)}^{2-} \qquad pK_2 = 13.8 \qquad (3\text{-}18)$$

The pK_2 for the dissociation of bisulfide (HS^-) to sulfide (S^{2-}) according to Stumm and Morgan (1996) is 13.8 but other studies have shown that pK_2 is as high as 17.4 (Migdisov, Williams-Jones, Lakshtanov, & Alekhin, 2002), and so the dissociation of HS^- to S^{2-} may not occur in the pH ranges found in nature (Brezonik & Arnold, 2011).

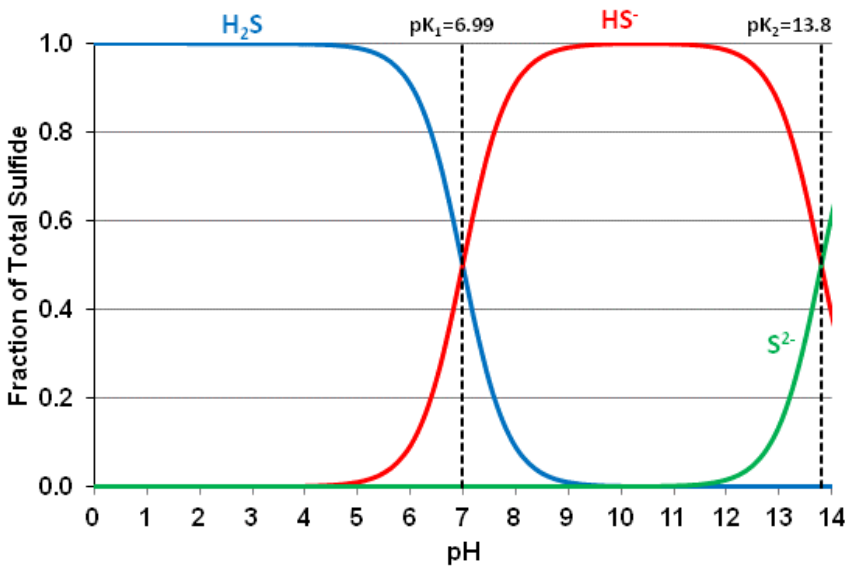

Figure 3-3: Sulfide Species Distribution Diagram

Tray Aerators and Degasifiers

In this research study 2 types of aeration systems are utilized. The first is the tray aeration system used at Verna Well field. The Verna well water is aerated and chlorinated before it is transferred to the City's WTF for either softening treatment by IX process or to bypass the IX treatment and blend with the RO permeate and IX soft water (Tharamapalan, Duranceau, & Perez, 2011). The second aeration system is the RO permeate degasifiers. Both these degasifiers are utilized to strip excess sulfide in the water as part of the City's goal of improving its water quality to customers.

At the Verna well field the aeration system utilized there is a tray aeration system. In this tray aeration system, water that is to be treated flows from entry at the top tray, through a series of perforated trays. The effect of cascading through the perforations in one tier of tray to a lower

tier of trays, allows air-water contact, thereby resulting in mass transfer of dissolved gases from the water to the air (Faborode, 2010).

The RO permeate is degasified using packed tower aeration system, in which the water to be treated is introduced at the top of the degasifier and cascades through packing material in the aerators, countercurrent to the clean air that is introduced from the bottom from the aerator. The water entering the tower is uniformly distributed over the packing material to maximize air-liquid contact (Cooper & Alley, 2012).

The Henry's Law can be used to describe the equilibrium partitioning of a gas between air and water, for the aeration and air stripping applications in water treatment purposes (MWH, 2005). Henry's Law states that at a constant temperature, the amount of a given gas that dissolves in a given type and liquid is directly proportional to the partial pressure of that gas in equilibrium with that liquid (Sawyer, McCarty, & Parkin, 2003). In Equation 3-19 the Henry's law constant relationship for H_2S is illustrated.

$$P_a = HX_a \tag{3-19}$$

Where:

P_a = partial pressure of hydrogen sulfide in the atmosphere

X_a = mole fraction of hydrogen sulfide in the water

H = Henry's law constant for hydrogen sulfide at given temperature

Temperature affects both mass transfer and Henry's constant, and thus affects the removal efficiencies in aeration systems. The solubility of gases in water decreases as temperature

increases (Camp, 1965). From Figure 3-3 at pH of up to 10, total sulfide concentrations in water exists as either H_2S or HS^-. In the study by Yongsiri et al (2004) of sulfide concentrations in this range, as illustrated in Figure 3-4, showed that the proportion of H_2S species in the total sulfide in soluble form is lower at higher temperatures. Therefore the available proportion of total sulfide for stripping in the aeration process is higher at higher temperatures.

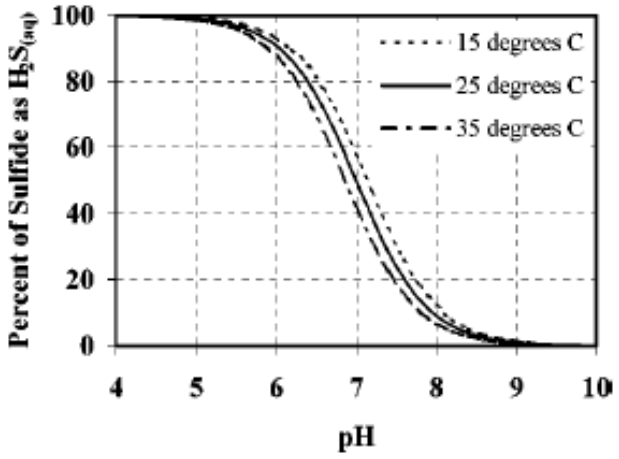

Figure 3-4: Dissociation of Hydrogen Sulfide (H_2S/HS^- equilibrium) at Different pH and Temperatures
(Adapted from Yongsiri et al (2004))

The Henry's Law also shows how far the air-liquid or gas-liquid system is from equilibrium. The rate of removal of H_2S from water in an aeration process is proportional to the difference between the equilibrium concentration in atmosphere as given by Henry's Law at a particular temperature and the actual concentration in water as depicted in Equation 3-20.

$$\frac{dC}{dt} \alpha (C_a - C_s) \tag{3-20}$$

Where:

$\frac{dC}{dt}$ = Rate of stripping of H_2S

C_a = Actual concentration H_2S in water

C_s = Equilibrium concentration of H_2S in atmosphere at particular temperature

In the aeration process, as CO_2 and H_2S are stripped out of water, C_a is greater than C_s, while during the same aeration process C_s is greater than C_a for oxygen gas and oxygen gets transferred into water (Reynolds & Richards, 1995).

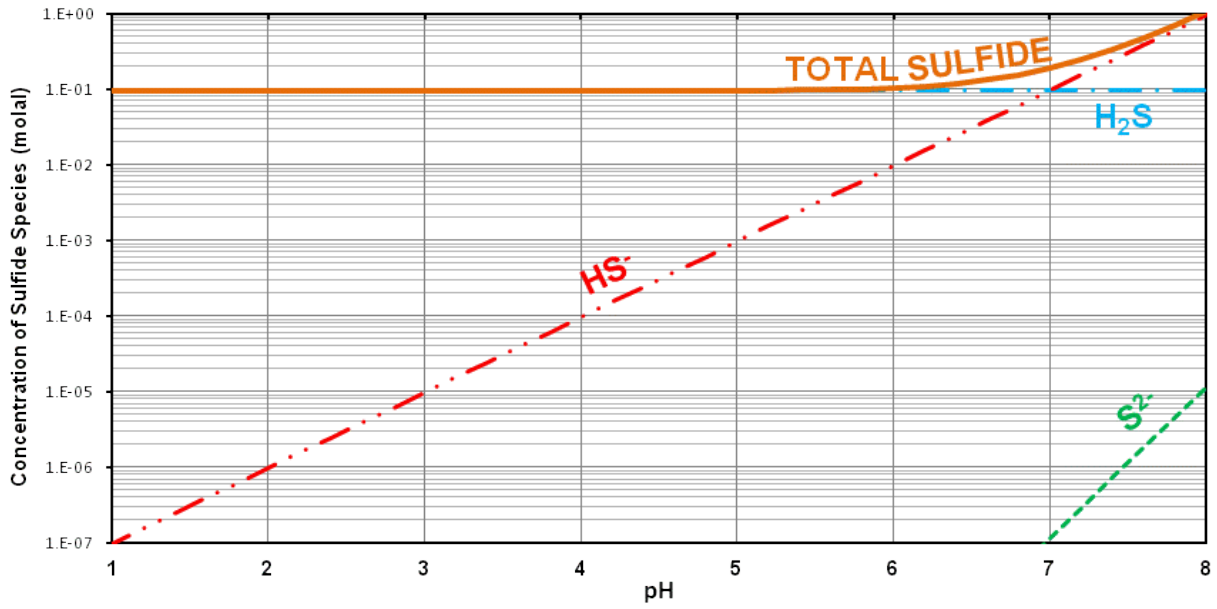

Figure 3-5: Solubility of Hydrogen Sulfide as a Function of the pH at 25°C

In Figure 3-5 the solubility of H_2S as a function of pH in an open system like the aerators, is shown. The concentration of the sulfide (S^{2-}) species is negligible in the pH range as shown in the figure. In addition at higher pHs above 8, the concentration of bisulfate (HS^-) species would become too large and misrepresent the actual solubility levels, if activity coefficients are ignored

(Carroll, 1998). A similar solubility chart for CO_2, in the same pH range, is depicted in Figure 3-6.

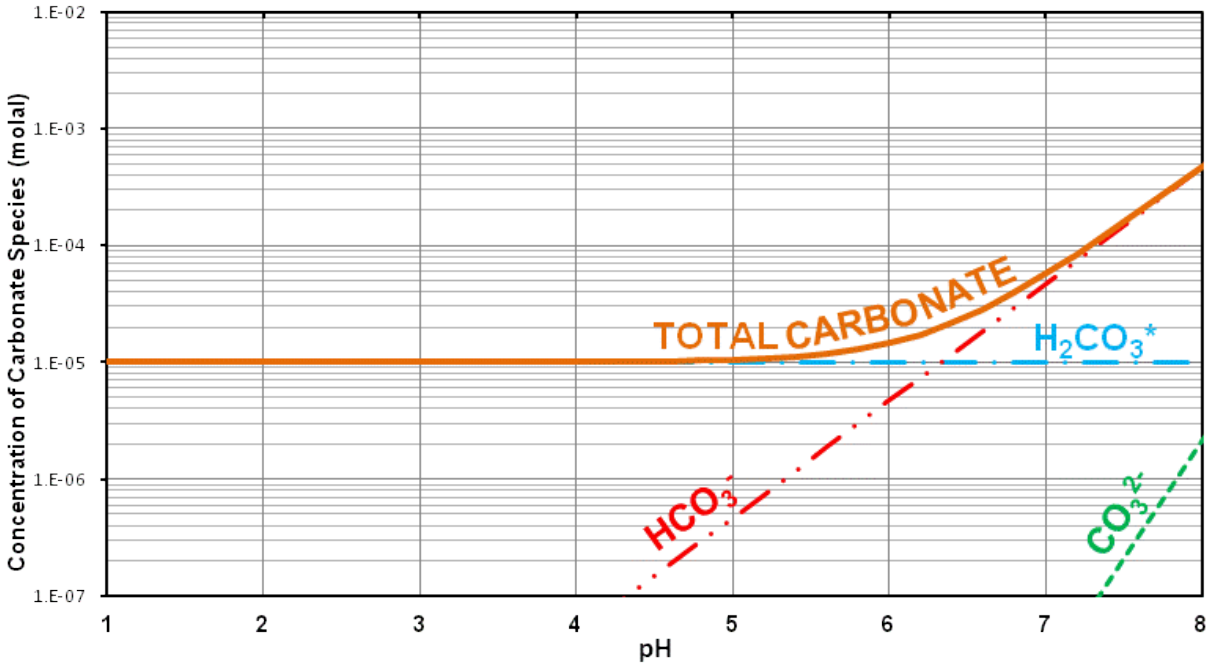

Figure 3-6: Solubility of Carbon Dioxide as a Function of pH at 25°C

As can be seen in Figure 3-5 and Figure 3-6 , H_2S is highly soluble in relation to CO_2 and when aerated the less soluble CO_2 is readily removed (ASCE and AWWA, 1990). In the aeration process, as the CO_2 and H_2S are removed as gases, the pH rises as CO_2 is stripped out more quickly than H_2S as water passes through the tower (Jensen, 2003). At the higher pH, the ionization of H_2S and carbonic acid (H_2CO_3) occurs which decreases the removal efficiency of the aeration process. In order not to concomitantly reduce H_2S stripping, it is common to use acid for pH adjustment prior to packed tower aeration processes. This way of suppressing pH for H_2S

stripping has been demonstrated to be an effective pretreatment method that assists in corrosion control (Powell & von Lossberg, 1948). The pilot-scale study by Duranceau et al (1999) to compare use of sulfuric acid (H_2SO_4) and H_2CO_3 for pH adjustment of water fed to a packed aeration tower, showed that pre-treatment with H_2CO_3 did not result in loss of alkalinity thereby maintaining the buffer capacity through the aeration process. On the other hand, when sulfuric acid was used, the available bicarbonate (HCO_3^-) alkalinity was converted to carbon dioxide (CO_2) and lost during the aeration process. Also the use of H_2SO_4 resulted in increased sulfate content in the aerated product water.

While the aeration processes are aimed at stripping H_2S gases, the process also results in transfer of oxygen from the atmosphere into the water. The oxygen transferred into the water readily oxidizes H_2S to sulfates and elemental sulfur (Mance, O'Donnell, & Harriott, 1988). As groundwater is devoid of oxygen, this presents an opportunity for sulfide that is not stripped by aeration process to be oxidized by the oxygen that is entrapped in the water during the aeration process (Dell'Orco, Chadik, Bitton, & Neumann, 1998). It takes four times the amount of the oxidant oxygen to convert reduced sulfide to sulfate (SO_4^{2-}) as compared to elemental sulfur (S^0) and this is presented in Table 3-2 (Singer & Reckhow, 2011). However, as gas-liquid mass transfer occurs quickly, minimal oxidation of the H_2S actually occurs in aeration (Thompson, Olson, & Wagner, 1993). Formation of colloidal sulfur is therefore favored compared to formation of sulfates.

Table 3-2: Oxidant Requirements for Sulfide Oxidation

Reaction	Oxidant demand, per mg S^{-2}	
$2H_2S+O_2 \rightarrow 2S_{(s)}+2H_2O$	0.5 mg oxygen	(3-21)
$H_2S+2O_2 \rightarrow SO_4^{2-}+2H^+$	2 mg oxygen	(3-22)

Water treatment options are a matter of balancing options. While the suppressing of pH to around 6 enhances H_2S stripping, it also results in stripping of CO_2 that in turn results in lowering of alkalinity in the aerated water. The lowering of alkalinity can potentially contribute to variable pH conditions in the system and lead to corrosion of distribution and metallic plumbing systems. Post-aerated water must therefore be treated for corrosion control and disinfected prior to distribution to customers (Duranceau, Pfeiffer-Wilder, Douglas, Pena-Holt, & Watson.I.C, 2010)

Based on Equation 3-17 and the fact that most groundwaters occur near a neutral pH of 7.0, means that half of the dissolved sulfide species exists as bisulfide [HS^-], while the other half as H_2S. Therefore unless the equilibrium of the system is artificially shifted to cause a change in pH, only a portion of the total sulfide can be removed by aeration (by tray, packed-tower, diffused air, or spray-nozzle methods). The benefits of maximizing H_2S removal by aeration include the elimination of taste and odors; decrease in the corrosive effects of H_2S on metals and concrete in water purveyance and storage systems; and a reduction in chlorine demand in disinfection process (Powell & von Lossberg, 1948).

Chlorination

At the Verna well field, the post-aerated water is chlorinated using, sodium hypochlorite (NaOCl), for disinfection purposes as the water is transported to 10th Street Reservoir before being transferred to the IX plant for softening or bypasses the IX plant for blending purposes. For water sources that do not require extensive treatment, chlorination following aeration, represents a very economical treatment option in comparison to rapid sand filtration or lime-soda softening (Cooper, Dietz, & Reinhart, 2000).

In water, dissolved aqueous chlorine forms hypochlorous acid (HOCl), chloride ions (Cl^-) and protons (H^+) as shown in Equation 3-23 (Downs & Adams, 1973).

$$Cl_{2(aq)} + H_2O \leftrightarrow H^+ + HOCl + Cl^- \quad (3\text{-}23)$$

Hypochlorous acid is a weak acid that dissociates to its conjugate base, hypochlorite ion, at an acid dissociation (pK) constant of 7.6.

$$HOCl \leftrightarrow OCl^- + H^+ \qquad pK=7.6 \quad (3\text{-}24)$$

Therefore in the near neutral pH conditions that exist for water treatment and water supply, both the hypochlorous acid and hypochlorite ion will be present in significant concentration as a fraction of total free chlorine concentration, as depicted in Figure 3-7 (Haas, 2011).

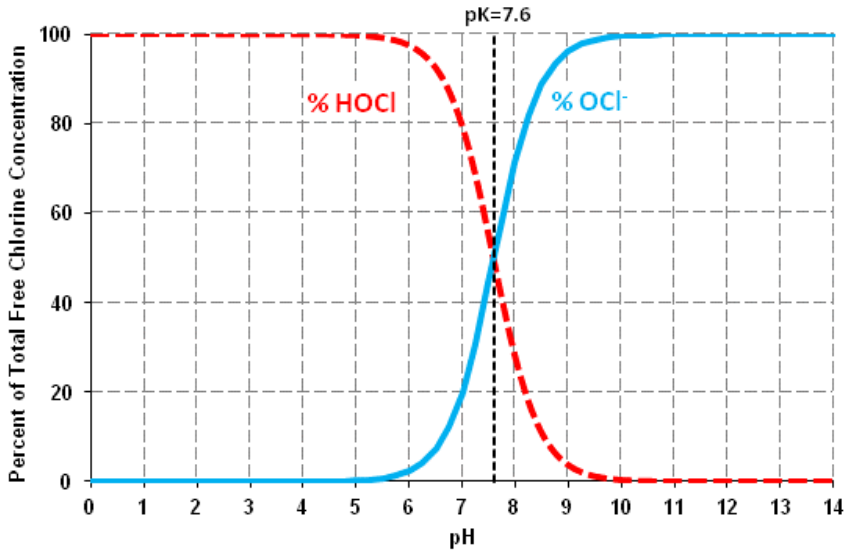

Figure 3-7: Effect of pH on Relative Amount of Hypochlorous Acid and Hypochlorite Ion

Both HOCl and OCl^- contribute to the oxidation of H_2S. The stoichiometric equations relating the oxidation of H_2S and bi-sulfite (HS^-) is shown in Equations 3-25 through 3-32 (Lyn T. , 1991). The equations relating the hypochlorous acid and hypochlorite oxidation of H_2S and HS^- to elemental sulfur (S^0) are shown in Equations 3-25 through 3-28.

$$HOCl + H_2S \rightarrow S^0 + H^+ + Cl^- + H_2O \quad (3\text{-}25)$$

$$HOCl + HS^- \rightarrow S^0 + Cl^- + H_2O \quad (3\text{-}26)$$

$$OCl^- + H_2S \rightarrow S^0 + Cl^- + H_2O \quad (3\text{-}27)$$

$$OCl^- + HS^- \rightarrow S^0 + Cl^- + OH^- \quad (3\text{-}28)$$

Oxidation of H_2S to sulfate is shown stoichiometrically in Equations 3-29 through 3-32.

$$4HOCl + H_2S \rightarrow SO_4^{2-} + 6H^+ + 4Cl^- \quad (3\text{-}29)$$

$$4HOCl + HS^- \rightarrow SO_4^{2-} + 5H^+ + 4Cl^- \quad (3\text{-}30)$$

$$4OCl^- + H_2S \rightarrow SO_4^{2-} + 2H^+ + 4Cl^- \quad (3\text{-}31)$$

$$4OCl^- + HS^- \rightarrow SO_4^{2-} + H^+ + 4Cl^- \quad (3\text{-}32)$$

Sulfate is the most oxidized form of sulfur. Four moles of HOCl (6.17 mg/L) or OCl^- (6.05 mg/L) are required to oxidize 1 mole of H_2S or HS^- to SO_4^{2-}. On the other hand, one mole of HOCl (1.54 mg/L) or OCl^- (1.51 mg/L) is required to convert one mole of a sulfide species (H_2S or HS^-) to elemental sulfur (S^0). Water purveyors would prefer the complete oxidation of sulfide species so that elemental sulfur turbidity is avoided, but in practice however it is not typical to observe complete oxidation (Lyn T. , 1991). The patented process by Kerollis and Mowrey (1993) showed that by suppressing pH of aeration tower feed water to the range of 4.2 to 5.5 and coupled with the addition of a suitable oxidant such as liquid bleach or chlorine gas could result in complete oxidation of sulfide in the feed water. The product of this patented oxidation process is acidic water at a low pH of around 3.5 or below, and before supply to customers must be pH adjusted with a base (Trupiano, 2010).

While chlorine use is beneficial and acts as an oxidant and disinfectant, it also poses a problem to membranes if the oxidant is fed upstream of the membrane process. Chlorine can cause irreversible damage on polyamide RO membranes and the study by Knoell et al. (2005) showed that all polyamide membranes from various manufacturers were susceptible to oxidative degeneration when exposed to both free chlorine and combined chlorine. Therefore when

membrane processes are selected, the compatibility of the specific membrane type must be matched with disinfectants so as to prevent premature membrane degradation (MWH, 2005).

In instances where chorine is used as a disinfectant, strict protocols for dechlorination need to be instituted to protect RO membranes from damage by chlorine oxidation (Sutzkover-Gutman & Hasson, 2010).

Nanofiltration

Applications of nanofiltration (NF) membranes in water treatment have increased significantly especially for water softening (Hajibabania, Verliefde, McDonald, Khan, & LeClech, 2011). The separation characteristics of NF are between the molecule sieving mechanism of ultrafiltration (UF) and the solution diffusion mechanism characteristic of reverse osmosis (RO) (Song, Xu, Xu, Gao, & Gao, 2011). NF is similar to RO and is sometimes called the "loose RO" (Petersen, 1993) or membrane softening (Duranceau, Taylor, & Mulford, 1992). Depending on structure of NF membranes, they have rejection rates in excess of 98% for divalent ions, but low rejection rates for monovalent ions (Wang, Zhang, & Zhao, 2000). NF is used extensively in treating groundwater containing low total dissolved solids (TDS) but with high total hardness, color and organic disinfection-by-product precursors (Hilal, Al-Zhobi, Darwish, Mohammad, & Arabi, 2004). In instances where NF is used to treat surface water, the focus is mainly on organics removal rather than on softening (Van der Bruggen & Vandecasteele, 2003). Fouling of membranes is the major constraint towards the implementation of membranes processes in water treatment. Fouling of membranes is characterized by reduced permeation over time by the

accumulation of materials (adsorption on membrane surface, cake or gel formation and concentration polarization), pore blocking (Meireles, Aimar, & Sanchez, 1991), and adsorption to pore walls (Aimar, Baklouti, & Sanchez, 1986). Adopting suitable pretreatment options can control fouling.

Pre-treatment Options to Nanofiltration

For the efficient operation of NF membranes, high feed water quality is crucial. Without a backwash cycle, presence of any particulate matter, even in low concentrations, can accumulate on membrane surfaces and clog feed channels. Depending on the source water, at a minimum cartridge filtration with 5-µm is employed for pre-filtration (MWH, 2005). Additional options to pretreatment include sand filters, media filters and greensand filters, and the choice is dependent upon the type of contaminant in the feed water.

Other options of pre-filters to NF include the use of membrane processes such microfiltration (MF) or ultrafiltration (UF). The differentiation between MF and UF is the pore size of the membrane. Depending on the source water feeding to the MF/UF membranes, pretreatment may be necessary. Surface water requires more extensive pretreatment as compared to groundwater due to the higher biological and suspended solids content. MF and UF can possibly remove particles and colloids completely and also demonstrate significant advantage in controlling microorganisms and pathogens (Tian, et al., 2010). On the other hand, for the removal of turbidity and natural organic matters, coagulation remains the most common pretreatment process to membrane treatment (Liu, Chen, Yu, Shen, & Gregory, 2011). In surface water

treatment, applying a coagulation process before the membrane filtration helps reduce the organic matter in water, thereby improving the permeate quality (Bergamasco, Konradt-Moraes, Vieira, Fagundes-Klen, & Vieira, 2011). The experience of 2 years of operations of a nanofiltration at the Méry-sur-Oise plant in France showed that with coagulation, flocculation and filtration as pretreatment the overall plant TOC was reduced by a factor of 3 to 5; THMs by a factor of 2, chlorine demand for disinfection by a factor of 3 and viable bacteria population by a factor of 10 (Cyna, Chagneau, Bablon, & Tanghe, 2002).

Colloidal fouling is the most severe of the different types of membrane fouling and membrane systems and operating conditions are very often designed to reduce this risk (Comstock, 1991; Cyna, Chagneau, Bablon, & Tanghe, 2002). One of the options to control colloidal fouling includes pre-filtration (Rajinder, 2006). Where colloids exist in water, as in the case of colloidal sulfur from the aeration process in this study, pre-filtration using UF has surfaced as a common choice as it balances the screening capacity of NF with the flux capacity of MF (Ray & Jain, 2011).

The Silt Density Index (SDI) is used as the measure of fouling potential of feed water (ASTM, 2002). To measure SDI, a sample is filtered at a constant 30 psi (2.07 bars) through a 47 mm diameter 0.45µm membrane filter over a 15-minute period. The SDI is calculated from the time interval to collect first 500mL of permeate and the time interval required to collect another 500mL of permeate after 15 minutes, and is depicted by the following Equation 3-33:

$$SDI_T = \frac{100\left[1-\frac{t_I}{t_F}\right]}{t_T} \tag{3-33}$$

Where:

t_I= time to collect first 500-mL of sample, sec

t_F= time to collect final 500-mL of sample, sec

t_T= test interval between the two test intervals (15 min)

Membrane manufacturers recommend SDI_{15} value of lower than 3 but accept values of 4 (Chua & Malek, 2003) or 5 ((Quevedo, Sanz, Ocen, Lobo, & Tejero, 2011),(Hydranautics, 2008)).

Similar to RO membranes, typical pre-treatment to NF membranes include acid and scale inhibitors. Hydrochloric acid and sulfuric acid are most commonly used to adjust pH. The pH adjustment is to control scaling to some extent by adjusting the feed water pH such that the LSI remains negative. Scale inhibitors are used to control mineral scaling by complexing dissolved calcium (i.e. polyphosphate inhibitors) and/or by limiting crystalline growth rate and altering crystalline structures (i.e. organically based polymeric inhibitors) (Seacord, Cushing, White, Grimes, & Dieffenthaller, 2001). Polyphosphate inhibitors have limited use as it is normally used in combination with an acid to complex calcium and prevent calcium carbonate precipitation. The fact that polyphosphates only help control calcium carbonate scaling and also because some of these types of inhibitors are prone to hydrolysis to orthophosphate, which renders them ineffective, there has been limited use of polyphosphate inhibitors (Snoeyink & Jenkins, 1980). Polymeric inhibitors on the other hand are more stable and are also capable of preventing a scaling of a variety of other salts. Proprietary polymeric scale inhibitors are now available that may control calcium carbonate scaling at LSI value for the concentrate stream as high as 2.5 to 3.0, and this presents an opportunity to eliminate the need for acid in the pretreatment to

membranes to suppress pH of feed water. However when polymeric inhibitors are used in NF processes, it is likely to contribute to assimilable organic carbon (AOC) in permeate water that may contribute to regrowth of bacteria in the distribution system (Escobar & Randall, 1999). At pH of 7.5 the rejection of AOC is greater than 90% whereas when the pH is lowered to around 5.5 the rejection rate is lower at around 75% (Escobar, Hong, & Randall, 2000).

Biofouling

High pressure membrane processes face fouling problems in terms of scaling by inorganic deposits, particulate type fouling caused by colloidal matter and organic fouling and biofouling. Using scale inhibitors and/or acid in pretreatment process, scaling can be controlled. On the other hand particulate fouling can be controlled by pretreatment options such as conventional coagulation and flocculation and UF processes. However, the control of organic and biofouling is more challenging (Vrouwenvelder, 2009).

Organic fouling occurs when the accumulation of natural organic matter (NOM) on membrane surfaces result in decreases in the operating flux of NF or RO systems. The organic matter on the surface of the membrane then propagates biofouling when microorganisms colonize on the layer of organics and multiply by feeding on the nutrients in the feed water, resulting in the formation of a biofilm layer (Villacorte, Kennedy, Amy, & Schippers, 2009).

Bacteria and algae in natural waters and aquatic systems pose biofouling problems firstly by cell growth and multiplication, as well as the production of soluble microbial byproducts. Soluble

microbial products are the organic byproducts of substrate metabolism and biomass decay during the complete mineralization of simple substrates (Park, Kwon, Kim, & Cho, 2005).

The required ratio of nutrient combination for biological growth in terms of carbon, nitrogen, and phosphorus is ~100:20:10. Therefore in comparison, lower amounts of phosphorus are needed for microbial growth (Vrouwenvelder, et al., 2010). Though in natural waters, phosphorus is present in many forms, it is phosphorus that is available in the orthophosphate form that is most readily available for bio-utilization (Maher & Woo, 1998). The study by Vrouwenvendler et al (2010), showed that the use of phosphonate-based scale inhibitors increased the potential for biofouling in the presence of substrate.

Biofilm on membrane surfaces are usually made up of layers of assorted microbial populations, the majority of which are bacteria, held together by a sticky matrix of extracellular polymer substances (EPS) (Berman & Holenberg, Amiad Filtration Systems, 2005). The excessive growth of biofilms in spiral wound NF and RO systems result in increased pressure drop in the feed spacer channel and membrane (Flemming, Schaule, McDonogh, & Ridgway, 1994). The undesirable accumulation of biofilm on a surface is known as biofouling and it degrades equipment and reduces the useful lifetime of equipment (Characklis & Marshall, 1990).

EPS are the protective mass of polysaccharide excreted by bacteria that colonize on membrane surfaces and helps to encapsulate the bacterial cells and entrap nutrients from the feed water for these bacterial cells while impeding the application of biocides that are applied to control the bacterial growth (Kim, Chen, & Yuan, 2006). The buildup of EPS on membrane surfaces result

in a resistance to permeation, thereby increasing the concentration polarization which in turn results in increased osmostic pressure (Chong, Wong, & Fane, 2008; Subramani & Hoek, 2008). Transparent exopolymer particulates (TEP) are similar to EPS and are produced by phytoplankton, bacteriaplankton, microalgae, etc. as a protection of the organism's outer membrane surface (Komlenic, 2010). TEP are microscopic organic particles that range in size from less than 0.4 μm to 100-200 μm and are a source to attract solutes in natural water because of their large and negatively charged surface area (Berman, 2010).

Strategies to control biofouling in membrane processes include biological pre-treatment for nutrient removal (e.g. biofilters); inactivation of bacteria using biocides; membrane surface modification, and chemical cleaning at regular intervals (Mansouri, Harrisson, & Chen, 2010). Even though UF membranes with pore sizes of 0.01 μm can screen off algae, protozoa, bacteria and viruses, it is not uncommon to have biofouling on downstream processes like NF and RO processes. These biogrowth downstream of UF processes do not mean that there is leakage in the UF process due to fiber break, etc. but instead are due to growth of bacteria on surfaces of materials (e.g. filtrate tank) downstream of the UF processes (Vrouwenvelder, 2009).

In the study by Villacorte et al (2009), showed that while UF membranes was the best option in removing particulate TEP of sizes >0.4μm, when compared to microfiltration (MF) processes or conventional treatment processes, the UF process was still not an absolute barrier towards colloidal TEP <0.4μm, that then enters downstream processes. The study by Verdugo (2010), showed that post-filtering through a 0.2 μm membrane filter, the TEP is present in the filtrate as

free polymers and within 5-10 hours of filtration, reassemble into nanogels. It is therefore difficult to remove TEP completely using UF processes.

UF Membranes

Ultrafiltration (UF) membranes, remove virtually all suspended solids from water streams, and also colloidal, microbiological and dissolved organic compounds depending on their molecular mass and on the molecular mass cut-off of the membrane. In well-designed and operated systems, UF membranes can consistently produce filtered water with turbidity values below 0.05 NTU (Duranceau & Taylor, 2011) and can result in SDI<1(Dow Water Solutions, 2010).

The UF system can be operated in either dead-end or cross-flow filtration. In the case of dead-end filtration, water is forced through the filter media which captures and retains particles and the process involves one inlet and outlet stream resulting in 100% of the feed water passing through the UF filter medium without a recycle stream (MWH, 2012). On the other hand in the cross-flow mode of filtration, there are three streams: feed, permeate and concentrate. In this process, the components in the water are separated by a semi-permeable membrane through application of pressure and flow parallel to the membrane surface. With a concentrate stream, the cross-flow mode of filtration has a lower recovery rate compared to dead-end filtration.

There are two different configurations for UF hollow-fiber membranes: flow can be from inside out or outside-in. In the case of the outside-in configuration, there is more flexibility in the amount of feed to flow around the hollow fibers, whereas inside-out configuration has to consider the pressure drop through the inner volume of the hollow fibers. Inside-out

configuration, however, offers much more uniform flow distribution through the lumen of hollow fiber compared to the outside-in configuration (Xu, et al., 2008).

Fouling of UF membranes can be due to operation of membranes beyond a critical flux value (AWWA, 2005); long filtration times that promote compaction that reduce the effectiveness of backwashing (Smith, Vigneswaran, Ngo, Ben-Aim, & Nguyen, 2006); or in selection of the appropriate type of membranes befitting the type of foulant in feed water (e.g. adhesion of high molecular weight NOM fractions to hydrophobic membrane surfaces) (Liu, Caothien, Hayes, & Otoyo, 2001). An UF system can be considered to be fouling if the operating parameters such as feed pressure, temperature and flow rates are held constant but the flux rate or mass transfer coefficient (MTC) rate (i.e. flux rate per unit transmembrane pressure) through the membrane is decreasing (Cheryan, 1998).

Chemical Cleaning of UF Membranes

Chemically enhanced backwash (CEB) involves the routine use of a chemical solution to maintain or restore membrane permeability (Kuzmenko, Arkhangelsky, Belfer, Freger, & Gitis, 2005). The evaluation of the CEB plan to adopt will include determining the appropriate chemicals, concentration of chemicals for CEB and frequency of CEBs. The CEB is performed over and above the regular backwash cycles. During a regular backwash cycle the filtrate water is pumped onto the membranes surfaces at flux rates greater than the forward filtration flux to introduce scouring effect thereby removing matter collected on the fiber surface following a particular forward filtration cycle. On the other hand, a CEB performed at preset intervals

following a predetermined number of forward filtration cycles and is aimed at removing targeted foulants on the fiber surface to restore membrane permeability (Boyd C. C., Duranceau, Harn, & Harn, 2010). A CEB cycle involves injection of the specific chemical onto the fiber surface, soaking of the chemical on the membrane surface for a specified duration, followed by rinsing off of the chemicals before start of another forward filtration cycle.

Chemicals commonly used in CEB cycles include sodium hypochlorite (disinfectant), citric acid (low pH) and caustic (high pH). The type of foulant anticipated on the fibers will determine the type of CEB chemical used. A hypochlorite CEB is preferred when the foulant type is considered to be biological or organic, while a caustic CEB is proposed when there is need for a high pH clean of an organic fouling condition like in the case of algae fouling (Boyd C. C., Duranceau, Harn, & Harn, 2010). In the case of a caustic CEB, it works by breaking the bonds between the membrane surface and foulant (Rajinder, 2006). On the other hand the low pH citric acid CEB is considered when calcium carbonate scaling and iron foulants (Rajinder, 2006) are anticipated. The CEBs are performed individually or in combination depending on whether single or multiple foulants are anticipated on the fiber surfaces. The selection of cleaning chemicals is a trial and error process and the successful cleaning of the foulant off the fiber is dependent on the foulant type, the cleaning chemical used and its concentration, the contact time and flow rates and temperature ((Boyd & Duranceau, 2011); (Rajinder, 2006)).

A clean-in-place (CIP) on the other hand is carried out when there is rapid loss of productivity for the membrane. It involves taking out the membrane system from the operations cycle and may involve using chemicals that are used in the CEB but at higher concentration levels to

remove the foulant. Following each cycle of CIP the transmembrane pressure (TMP) is monitored in order to determine if all or majority of the foulant type is removed. The concentration of each type of CIP chemical and duration of soaking of the chemicals on the fiber surface are all manufacturer specific. The soak time of the cleaning agents can be membrane type, chemical and foulant specific and be as long as 8 hours (Rajinder, 2006).

Blending for Water Supply

The greater salt rejection of RO membranes than NF membranes, results in RO permeate being more corrosive than NF permeate. Either way both these permeates are corrosive and require post-treatment for corrosion control. Corrosion control involves not just protecting the utilities distribution system but also the plumbing system within consumer premises. Depending on the source of the water supply, a portion of the raw water or pretreated membrane feed water can be bypassed around the membrane system to blend with the permeate flow system (Bergman & Elarde, 2005). The study by Taylor et al (2005) on the blending of different source water on distribution water quality, showed that pH, alkalinity, chloride and sulfate composition from different sources in the blend resulted in different levels of corrosion on cast iron, copper and lead pipes that are used in plumbing fittings. Therefore to manage corrosion in distribution and consumer plumbing systems, considerations must be given towards varying the blend ratios of the different source waters.

Normalizing Permeate Flow on RO and NF Membranes

Spiral wound RO membrane systems are designed to operate at a constant flux rate (i.e. producing constant permeate flow). During the life span of the membrane elements, the feed pressure is adjusted to compensate for changes in feed temperature, salinity and permeate flux as fouling and/or compaction of the RO membranes occur (Abdulrazaq, 2011). Equations 3-34 through 3-39 describe the relevant calculations for normalizing the permeate flow.

$$K_W = \frac{J_W}{TCF \times TMP} \tag{3-34}$$

$$J_W = \frac{\left(Q_p \times 1440\ \text{min}/\text{day}\right)}{\text{Area}} \tag{3-35}$$

$$TCF = 1.03^{(T-25)} \quad \text{(MWH, 2012)} \tag{3-36}$$

$$TMP = (\Delta P - \Delta\pi) \tag{3-37}$$

$$\Delta P = \frac{1}{2}(P_f + P_c) + P_p \quad \text{(Bergman R. , 2005)} \tag{3-38}$$

$$\Delta\pi = \frac{1\ \text{psi}}{100\ \text{mg}/\text{L}} \times \left(\frac{1}{2} \times [C_f + C_c] - C_p\right) \quad \text{(Zhao \& Taylor, 2005)} \tag{3-39}$$

where:

K_W = Normalized MTC of water (gal/ft^2.day.psi)

J_W = Flux of water through the membrane (gal/ft^2.day)

Q_p= Permeate flow rate through the membrane stage (gal/min)

Area = Total surface area of membrane elements in each stage (ft^2)

TCF = Temperature Correction Factor

TMP = Transmembrane Pressure

T = Temperature (°C)

P = Pressure (psi)

C = Total Dissolved Solids Concentration (mg/L)

$_{f, c, p}$= feed, concentrate and permeate

Solute Transport in Membrane Processes

Solute transport in RO membranes occurs by diffusion across the membrane or advection/diffusion through a membrane pore (Taylor & Jacobs, 1996). The driving force for solute flux in the diffusion model is by the concentration gradient and is expressed as Equation 3-40 (Ozaki, Sharma, & Saktaywin, 2002).

$$J_S = K_S(\Delta C) \quad (3\text{-}40)$$

Where:

J_S = mass flux of solute (gal/ft^2.day)

K_S = MTC of solute flux (ft^3/ft^2.day or ft/day)

$\Delta C = \frac{C_{Feed}+C_{Conc}}{2} - C_{Permeate}$ (mg/L)

C = Concentration

The flux of solute can also be represented as the flux of water multiplied by the solute concentration in permeate stream, as represented in Equation 3-41.

$$J_S = (C_P)\, J_W \quad (3\text{-}41)$$

Where:

C_P = Concentration of solute in permeate

J_W = Flux of water through the membrane (Equation 3-35)

Equating the Equations 3-40 and 3-41 and rearranging will derive Equation 3-42.

$$Ks = \frac{(C_p)\, Jw}{\Delta C} \tag{3-42}$$

The solute flux in the diffusion model is sometime also rearranged and expressed, in terms of recovery rate, R, as shown in Equation 3-43(Duranceau S. , 1990).

$$C_P = \frac{K_S C_F}{K_W(\Delta P - \Delta\pi)\left(\frac{2-2R}{2-R}\right) + K_S} \tag{3-43}$$

Feed salinity affects the salt passage through a polyamide membrane and is influenced by the feed water composition and the membrane charge and chemistry (Bartels, Franks, Rybar, Schierach, & Wilf, 2005). Polyamide membranes are known to be negatively charged in either a neutral or alkaline solution and positively charged in an acidic solution (Ozaki, Li, & Saktaywin, 2001). Therefore as the pH increases from acidic conditions to near neutral or alkaline solutions the rejection of negatively charged anions like chlorides and sulfates is expected to increase. The shift of ions between the membrane surface and bulk solution is known as the Donnan potential, and this potential determines the degree to which ions diffuse through the membranes (Richarson, Blom, & Taylor, 2009). However increasing the concentration of salts in the bulk solution results in the Donnan potential diminishing and eventually the membrane rejection decreases (Ong, Zhou, Song, & Ng, 2002). The valences of ions influence the Donnan potential and the potential is weakest in solutions with higher concentration of divalent cations, as the

divalent cations at the membrane surface shield the repulsive forces of the membrane's negative charge on the anions (Higa, Tanioka, & Kra, 1998).

Using the hydraulic boundary layer approach, the solute mass transfer coefficient (K_S) can also be expressed by Equation 3-44 ((Hoek, Allred, Knoell, & Jeong, 2008);(Duranceau & Taylor, 1991)). In this approach a boundary layer is assumed to form when the water flows across the solid membrane surface. The friction that results from this flow across the membrane surface is expected to cause the flow near the membrane surface to slow down. Membrane resistance to the flow will not affect the fluid flow at some distance away from the membrane surface. The water boundary layer is defined as the layer that separates the region of lower velocity flow near the membrane surface from the uniform flow seen away from the membrane surface. Concentration polarization occurs when the accumulation of solutes at higher concentration at the membrane surface as water permeates selectively across the membrane, results in a higher concentration of solute at the membrane surface relative to the bulk solution some distance away from the membrane surface (Chong, Wong, & Fane, 2007). The solute diffusion is a much slower process than the crossflow velocity of the water, and so the concentration boundary layer is thinner than the water boundary layer. This in turn means that the transport of solute in the boundary layer occurs by diffusive motion perpendicular to the membrane surface.

$$K_S = Sh\frac{D}{d_H} = 0.065\left(Re^{0.875}\right)\left(Sc^{0.25}\right)\frac{D}{d_H} \quad (3\text{-}44)$$

Where:

Reynolds number, $Re = d_H V \frac{\rho}{\mu}$

Sh = Sherwood number

Schmidt number, $S_C = \frac{\mu.D}{\rho}$

V= Crossflow velocity through spiral wound elements

D = Solute diffusivity

Hydraulic diameter, $d_H = 2\varepsilon_{SP}H$, for a spacer filled thin rectangular channel

ε_{SP} = Effective porosity of the flow channel created by the feed spacer

H = Effective local channel height

μ = Dynamic viscosity of water

ρ = Density of water

Normalizing Filtrate Flow on UF Membranes

UF membrane performance is determined by monitoring trends in MTC and transmembrane pressure (TMP). TMP is calculated as the average of the inlet (P_{IN}) and outlet (P_{OUT}) pressures, minus the permeate pressure (P_P) as shown in Equation 3-47 (Ahmad, Ismail, & Bhatia, 2005). The flux values are normalized and corrected for temperature changes to 20^{O}C using a temperature correction factor. The temperature correction factor is membrane specific, and if it is unavailable a factor of 1.03 is used (MWH, 2005).

$$J_{SP,20} = \frac{J_s}{TMP} \quad (3\text{-}45)$$

$$J_s = J_M(1.03)^{T_S - T_M} \quad (3\text{-}46)$$

$$TMP = \frac{P_{IN} - P_{OUT}}{2} - P_P \quad (3\text{-}47)$$

$$J_M = \frac{Q_F}{Area} \quad (3\text{-}48)$$

Where:

$J_{SP,20}$ = MTC at 20^{O}C (gal/ft^2.day.psi)

J_S = Flux adjusted to 20^{O}C (gal/ft^2.day)

TMP = Transmembrane Pressure (psi)

P_{IN} = Inlet Feed Pressure (psi)

P_{OUT} = Outlet Pressure (psi)

P_P = Atmospheric Permeate Pressure (psi)

J_M = Flux (gal/ft^2.day)

T_S = Standard Temperature (^{O}C)

T_M = Measured Temperature (^{O}C)

Q_F = Filtrate flow rate (gal/day)

Area = Total Fiber Surface Area (ft^2)

Correlating Electrical Conductivity and TDS

The ability of water to conduct an electric current is measured as electrical conductivity (EC). The presence of dissolved ions, in terms of the concentration of ions, temperature and the valence and size, etc. of the ions, affects the EC measurements ((Parameswara & Prasad, 2012),(Eaton, Clesceri, Rice, & Greenberg, 2005)). EC measurements are reported as either microsiemens/cm (μs/cm) or microohms/cm (μmhos/cm).

The Standard Methods for the Examination of Water and Wastewater (SMEWW) provides conductivity factors for ions commonly found in water (e.g. Ca^{2+}, Mg^{2+}, K^{+}, Na^{+}, CO_3^{2-}, HCO_3^{-}, Cl^{-}, SO_4^{2-},and NO_3^{-}). The study by (Parameswara & Prasad, 2012), observed that the actual EC measurements were lower than estimated values from EC factors (i.e. relationship between μs/cm and TDS concentration in mg/L) because the ion-ion and ion-solvent attractions reduced the mobility of the ions and the ion-pairs. Furthermore the complexation of ions also reduced the number of free ions available for the transportation of current, resulting in underestimation of the EC estimates.

Total dissolved solids (TDS) are defined as constituents in water that will pass through a filter with a pore size of 2μm (Berdanier & Ziadat, 2006). TDS is measured by filtering a known volume of sample through a microfilter (typically 0.45μm) and drying the filtrate at 180°C, and the residue is then weighed. TDS is then expressed in terms of the weight of residue to the volume of sample filtered, in units of milligram per litre (mg/L).

The measurement of TDS and EC are two measures for the same parameter (Al Smadi, Al-Zboon, & Al-Azab, 2010). Several studies have been carried out in the past to establish correlation factors between TDS and EC. The study by Day and Nightingale (1984), on groundwater showed a relationship ratio of TDS and EC of 0.527 to 0.597 for waters with an EC of 106-2050 μs/cm. Hem (1985) showed that the conversion factor ranged from 0.54 to 0.96 in most natural water. Whereas the SMEWW (Eaton, Clesceri, Rice, & Greenberg, 2005) gives a correlation between TDS and conductivity of 0.55 to 0.7 with instances of TDS being as high as

0.8 times the EC when poorly dissociated calcium and sulfate ions are present. The SMEWW also states that ratios can be as high as 0.9 for saline or boiler waters.

The study by Walton (1989) highlighted comprehensively the difficulties in correlating EC to TDS. Walton showed that TDS measurement can be impacted by sampling problems and the physical and chemical activities that can happen in the sample bottle between time of collection and the testing. TDS measurements are also dependent in analytical problems, in terms of both the skills of the analysts and also difficulties in analyzing samples with low concentration of solutes like in the case of RO permeates. It was also highlighted that temperature and pH affects EC measurements.

4. EXPERIMENTAL PLAN, MATERIALS AND METHODS

This chapter contains information concerning the experimental plan, methods (pilot testing works, implementation on full-scale plant, etc.), materials and procedures used to conduct the studies involved in this research project. Water quality assessments were done both at the project site and also in University of Central Florida's Environmental Engineering Laboratories. The summary of quality control protocol adopted for this study is also reported in this chapter.

Experimental Plan and Materials

In this study there were 3 phases of experimental plan: the RO pilot study, the acid elimination on the full scale plant and the NF pilot study, which included pretreatment assessments.

Elimination of Acid in Pre-Treatment to Reverse Osmosis Plant

The City and University of Central Florida (UCF) developed a plan to eliminate the use of sulfuric acid as pre-treatment to the City's RO process using a 3-step approach. The 3-Step approach adopted in this study to evaluate and eliminate use of acid in pre-treatment process involved: (1) pilot testing the plan to reduce the dependence on acid, (2) implementing the plan on the full-scale system with conservative pH increments, and (3) continuous screening for scale formation potential by using a "canary" monitoring device.

RO Pilot Study

The RO pilot skid contained two-stages, in a 2-1 array, with 12 elements in the first stage and 6 elements in the second stage. Hydranautics CPA2-4040 and ESPA2-4040 spiral wound polyamide membrane elements were used in the first and second stages, respectively. The pilot unit used the same type of membranes as the RO plant, with the membrane element surface area on the pilot unit being 85 ft^2 each as compared to 400 ft^2 for the membranes on the full-scale plant. The pilot setup mimicked the City's RO water treatment process. The raw feed water to the RO pilot skid was about 21.1 gpm, and at 75% recovery the pilot skid produced 15.8 gpm of water. Process data was automatically recorded on the pilot at ten minute intervals to facilitate data analysis and pilot performance evaluations.

On the RO pilot skid, the sulfuric acid pre-treatment feed reduction and subsequent elimination study was carried out in four phases. Phase 1 involved the operation of the pilot skid at pH 5.8 in order to ripen the new pilot membranes and establish a performance baseline as comparable to the utility's RO full-scale facility. The subsequent three phases represented the stepped reduction in acid feed before the complete elimination of acid in Phase 4. The staged acid pre-treatment feed reduction, the operating feed water pH to the RO skid and the duration of operation during each phase of the study are as summarized in Table 4-1. Aquafeed® 1025, which is the scale inhibitor used in the full-scale plant, was fed to the RO pilot at a dose of 2 mg/L.

Table 4-1: Pilot Scale Evaluation of Post-Acid Elimination Scaling Potential on Membranes

Phase	pH of RO Feed	Runtime (days)	Duration of Operation
1	5.8	0 - 50	25 Mar - 21 May 2010
2	~ 6.3	50 - 87	21 May - 29 June 2010
3	~ 6.6	87 - 94	29 Jun - 6 Jul 2010
4	~ 7.1(i.e. no acid feed)	94 - 124	6 Jul - 6 Aug 2010

Implementation of Acid Elimination in RO Plant

Acid elimination on the 4.5 MGD RO plant, which consists of three 1.5 MGD trains, was carried out in smaller pH increments than the pilot study. The more conservative approach to acid elimination on the full-scale system was selected primarily as a precautionary measure and also because the acid feed injection system could be more easily controlled in the full scale plant. The schedule of the stepped acid elimination for the full-scale system is presented in Table 4-2.

In order to provide a robust monitoring program during the acid elimination phase, a two membrane element pressure vessel, called the “canary” unit, was installed as a third stage on one of the three RO trains. The “canary’ unit was installed at the tail-end of the second stage membrane process and tapped onto two pressure vessels (i.e. a total of 12 membrane elements), out of a total of fourteen pressure vessels in the second stage of Train C. There were no hydraulic limitations as to whether the “canary” vessel could be installed either above or below Train C, and so it was finally decided to install the “canary” vessel below Train C. The fact that there was clearance below Train C for both installation and maintenance work on the “canary” unit, made

it more favorable when compared to the option of working with a "canary" vessel mounted atop Train C.

Table 4-2: Stepped Acid Reduction Sequence for the Full-Scale RO Plant

pH of RO Feed	Runtime (days)	Duration of Operation
5.8	0 - 33	2 Jun – 5 Jul'11
6.05	33 - 60	5 Jul – 1 Aug'11
6.3	60 - 85	1 Aug – 26 Aug'11
6.5	85 - 113	26 Aug – 23 Sep'11
6.7	113 - 245	23 Sep'11 – 3 Feb'12
6.9	245 - 262	3 Feb – 20 Feb'12
7.1	262 - 352	20 Feb – 20 May'12

The "canary" unit was designed as a two membrane element pressure vessel, so that there is sufficient spacing between the feed water and permeate or concentrate sampling and monitoring ports. As the RO membrane process operates at a high system pressure, a two membrane element, "canary" unit would minimize turbulence, allowing the gauges to be more stable.

The "canary" pressure vessel incorporated two Hydranautics ESPA2 spiral wound polyamide membrane elements, which are also used in the second stage of the full-scale RO trains. The "canary" assembly was monitored for pressure and flowrates thrice daily by the City's WTF operators via an instrumentation panel coupled to the "canary". The instrumentation panel for the "canary" unit included feed, permeate and concentrate pressure gauges and permeate and

concentrate flow measurement with rotameters. The recovery rate on the "canary" can be adjusted via adjustments to the feed and concentrate valves.

The configuration of the "canary" unit is shown in Figure 4-1, whereas in Figure 4-2, the as-installed "canary" unit and the instrumentation panel for monitoring the "canary" unit are shown. Upon installation of the "canary" pressure vessel and membranes, the unit was allowed to ripen with the second stage concentrate as feed water for about a month, before the acid elimination plan was instituted in stages.

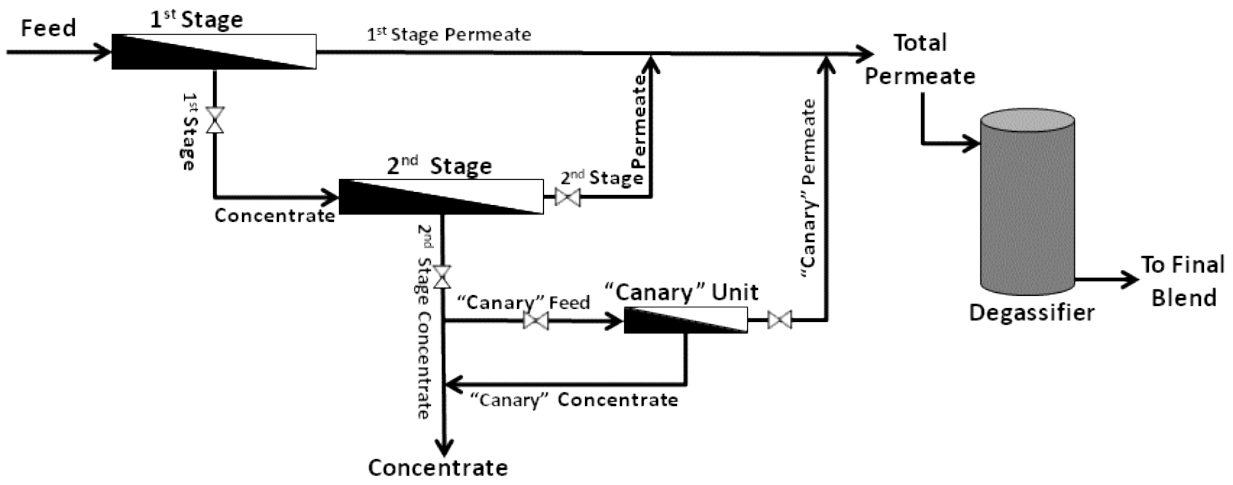

Figure 4-1: Schematic of the "Canary" Unit Setup

Figure 4-2: As Installed “Canary” Unit (left) and Instrumentation Panel (right)

Nanofiltration and Pretreatment Options for a Highly Fouling Surficial Groundwater Source

The study to pilot test membrane softening process using NF membranes, included evaluation of the most economical pretreatment option for the NF process. Pretreatment options evaluated included combinations of bag filters (BF), cartridge filters (CF), mediafilters (MF), sandfilters (SF) and ultrafiltration (UF) membrane. In Table 4-3, the evaluation schedule for pretreatment options to the NF pilot is presented. As each pretreatment option was evaluated, the aim was to operate each filter option as long as possible without causing irreversible fouling on the NF membranes, thereby compromising the NF membrane. The runtime and duration of operation of each pretreatment option as listed in Table 4-3 is the actual duration each pretreatment combination was tested. The runtime presented in Table 4-3, is the runtime on the NF pilot.

The NF pilot skid contained two-stages in a 2-1 array with 12 elements in the first stage and 6 elements in the second stage. Hydranautics ESNA1-LF-4040 spiral wound polyamide NF membrane elements were used in both the first and second stages. On the pilot unit, each of the

pilot membrane elements had a surface area of 85 ft^2. The raw feed water to the RO pilot skid was about 20 gpm, and at 85% recovery the pilot skid produced 17 gpm of water. Process data was automatically recorded on the pilot at ten minute intervals to facilitate data analysis and pilot performance evaluations.

Table 4-3: Evaluation Plan for Pretreatment Options to NF Pilot

Pretreatment Combinations	Scale Inhibitor	Runtime (days)	Duration of Operation
BF + CF	Aquafeed® 1025	0 – 7	Feb 28 – Mar 28'11
MF+ BF + CF	Aquafeed® 1025	7 – 16	May 24 – Jun 2'11
SF+ BF + CF	Aquafeed® 1025	16 – 97	Aug 8 – Dec 3'11
SF+ UF[1] + BF+ CF	Aquafeed® 1025	97 – 119	Feb 1 – Mar 8'12
UF[1] + BF + CF	Aquafeed® 1025	119 – 126	Mar 8 – Mar 29'12
SF + UF[1] + BF + CF	Aquafeed® 1025	126 – 156	Mar 29 – May 5'12
SF + UF[1] + BF + CF	Vitec® 1000	156 – 220	May 15 – Jul 25'12
SF + UF[2]+ BF + CF	Vitec® 1000	220 – 255	Jul 25 – Sep 6'12
UF[2] + BF + CF	Vitec® 1000	255 – 277	Sep 6 – Oct 8'12

Bag filter (BF) was installed as a pre-screen to the cartridge filters on the NF pilot, in the first phase of the study as highlighted in Table 4-3. The BF used in the project was of polypropylene material and has a sieving size of 50μm, which acted a "coarse" screen to the CF used. When the UF pilot testing was commissioned, the BF was retained though it was not necessary, as a precaution against algae and other particulates that may be carried over from the UF filtrate tank to the NF pilot.

[1] UF with no chlorine injection system
[2] UF with chlorine injection system

CF were installed on the NF pilot system as pre-screen to the NF membranes, to prevent any unforeseen suspended particles from coming into direct contact with the NF membranes when feed water is pumped by high pressure feed pumps. Many manufacturers recommend the use of cartridge filters at least 5μm or less (Dow Water Solutions, 2010). In this project as the colloidal sulfur particles are of concern, 1μm cartridge filters made of polypropylene were used. The CFs used were 2.5 inch in diameter and 10 inch long and of the double open end type.

UF Pilot Testing

Pilot testing with UF as pre-screen to NF pilot was started on Feb 1, 2012. The UF pilot incorporated two Toyobo Durasep UPF0860 UF hollow fiber membranes and operated in an inside-outside configuration. Toyobo's UF membrane fibers are composed of hydrophilic polyethersulfone (PES) modified with blended polyvinylpyrrolidone. During the pre-screen phase of the pilot testing, two new modules (each with 430 ft^2 of membrane surface area) but which were not stored in conditions as prescribed by the Toyobo were utilized to test and ascertain possible operating flux rates, identify suitable CEB chemicals and frequency of CEBs. The testing schedule as carried out during the pre-screening phase of the UF pilot testing is in Table 4-4.

Feed water to the UF pilot comes from water being transferred from the Verna well field. The feed water is tapped from the Verna well field line from the location within the WTF, before the water reaches the City's 10^{th} Street reservoir. The 10^{th} Street reservoir tank is to be replaced with a new tank as the existing tank is in a dilapidated state with internal wall corrosion etc. The plan

to bypass the 10th Street reservoir to feed the SF and/or UF and NF pilots, was so that feed water used will be representative in terms of water quality that will feed the future NF plant and its pretreatment facility.

Table 4-4: Schedule for UF Pilot Testing with Pre-Test Module

Flux ($gal/ft^2.day$)	**Forward Filtration Time (min)**	**CEB Type**	**No. of CEBs/day**	**Duration of Operation**
(Operations with SF as pretreatment to UF)				
40	30	NIL	NA	Feb 1 – Feb 9, 2012
60	30	Caustic	1	Feb 9 – Feb 17, 2012
Enhanced CEB with Caustic and Hypochlorite				
45	45	Hypochlorite	2	Feb 17 – Feb 29, 2012
45	45	Hypochlorite	1	Feb 29 – Mar 8, 2012
(SF as pre-treatment to UF bypassed)				
45	30	Hypochlorite	2	Mar 8 – Mar 12, 2012
Enhanced CEB with Caustic and Hypochlorite				
45	45	Hypochlorite	1	Mar 12 – Mar 27, 2012

Pre-screening tests of UF pilot operations were carried out between Feb 1 and Mar 27, 2012. During this pre-screening test, flux rates, forward filtration cycle times and frequency of CEBs were adjusted. UF Pilot operations between Mar 8 and Mar 27, 2012, were without SF as pre-treatment to the UF pilot. Enhanced CEBs were done whenever fouling of the UF membranes was observed, under a specific operating condition, in order to attempt to restore the membranes' productivity. Enhanced CEBs refer to injection of CEB chemicals with longer soak times than normal CEBs, and the chemicals used for these CEBs may also be different to that already being

applied on the membranes during that specific testing period. Identification of fouling on the UF membranes was established by monitoring the increases in transmembrane pressure (TMP) as logged on the UF pilot's programmable logic control (PLC).

Pilot testing with the new Toyobo test modules, were started on Mar 27, 2012 with both UF membrane modules on the UF pilot being replaced. The schedule of pilot testing the new UF membrane modules is in Table 4-5.

Table 4-5 : Schedule for UF Pilot Testing with New Membrane Modules

Flux ($gal/ft^2.day$)	**Forward Filtration Time (min)**	**CEB Type**	**No. of CEBs/day**	**Duration of Operation**
(Operations with SF as pretreatment to UF)				
45	45	Hypochlorite	2	Mar 27 – Apr 17, 2012
45	45	Hypochlorite	1	Apr 17 – Jun 4, 2012
Enhanced CEB with Caustic and Hypochlorite				
45		Hypochlorite	1	Jun 4 – Jun 14, 2012
Enhanced CEB with Caustic and Hypochlorite				
45	45	Hypochlorite	1	Jun 14 – Jun 20, 2012
Enhanced CEB with Citric Acid				
45	45	Hypochlorite	1	Jun 20 – Jun 26, 2012
45	45	Citric + Hypochlorite	1	Jun 26 – Jul 3,2012
45	45	Hypochlorite	1	Jul 3 – Jul 25, 2012
Installation of Hypochlorite Injection to UF Feed Stream				
45	45	NIL	NA	Jul 25 – Aug 10, 2012
Clean-in-Place of UF Module and pilot				
45	45	NIL	NA	10 Jul – Sep 6, 2012
(SF as pre-treatment to UF bypassed)				
45	45	NIL	NA	Sep 6- Oct 8,2012

From the evaluations carried out during the pre-screening phase, a flux rate of 45 gal/ft^2.day, equivalent to filtrate production of approximately 27 gallons per minute (GPM) and a forward filtration time of 45 minutes was adopted. The UF pilot testing was carried out between Mar 27 and Oct 8, 2012.

Several enhanced CEBs were also attempted in this phase of the study, whenever the TMP was noted to be increasing, in order to test whether the fouling condition on the UF membranes can be reversed. Severe algal fouling of the UF pilots was observed during the course of this research study and a chlorine injection system was introduced to the feed stream of the UF pilot on 25 Jul 2012, and thereafter a CIP was carried out on the UF pilot on Aug 10, 2012, to clean up the pilot. The schedule of UF pilot testing with new UF membrane modules is in Table 4-5.

Methods

Membrane Operations Data Analysis

On the NF and RO pilot units, the operations data (i.e. flowrates and pressure readings across process, feed, concentrate and total permeate conductivities, etc.) were logged on the pilot's PLC every 10 minutes. On the UF pilot, the operations data were logged every 2 minutes. The data were analyzed, by taking averages and standard deviations of the data under each testing condition. Data points that were outside ± 3 standard deviations (i.e. 99 percentile) of the average at each operating condition were discarded. The data were then presented in charts, on runtime basis. Runtime demonstrated the overall duration the pilots were operating and did not include any downtime or any data outliers (i.e. outside 99 percentile).

As for the City's RO plant, data were logged and averaged daily. Data stored in the City's database were the daily average of all parameters that were monitored. Therefore no data was discarded from the City's dataset, when analyses were carried out. Only instance when any data was likely to be discarded from the City's dataset, during analysis, was when the RO train was down for CIP.

Water Sampling Plan

Regular sampling for water quality analysis was carried out throughout each of the study phase. For the RO pilot study and acid elimination on the full scale RO plant, regular samplings were done at each pH condition. As the acid elimination plan progressed, over and above the monitoring on the "canary" unit, water sampling analysis was also carried out across the process system at the WTF (i.e. raw water supply, the RO process, the IX process and post-treatment processes). This was aimed at identifying potential impacts to the overall water quality as supplied by the City, as a result of the elimination of acid use in the pretreatment to the RO plant. Full system water quality analyses were carried out during each of the seven pH steps as listed in Table 4-2.

Water Quality Analysis

In Table 4-6 the sample collection and analysis protocol is listed. It also lists the protocol adopted for preservation and storage of samples, if the samples are not analyzed immediately. Turbidity, pH, temperature, conductivity and total sulfide measurements were taken immediately

after sample collection on site. Samples that were stored for analysis later were refrigerated at 4°C.

Table 4-6: Sampling and Handling Requirements

Analyte	**Preservation Technique**	**Holding Time**	
		Recommended	Regulatory*
pH	Analyze Immediately	0.25 hours	0.25 hours
Alkalinity	Refrigerate at 4^oC	24 hours	14 days
Turbidity	Analyze immediately; or store in dark up to 24 hours, refrigerate	24 hours	48 hours
UV Absorbing Organics	Analyze immediately; or refrigerate and add HCl, H_3PO_4 or H_2SO_4 to pH < 2	7 days	28 days
Anions (Cl, SO_4, Br)	Refrigerate at 4^oC	28 days	28 days
Metals	Add HNO_3 to pH < 2	6 months	6 months

**Refer to USEPA. 1992. Rules and Regulations. 40 CFR Parts 100-149* (USEPA, 1992)

The methods and equipment used within the lab and in the field for water quality analysis are presented in Table 4-7. All methods used for the measurement of each constituent were in accordance to the procedures set out in the Standard Methods for the Examination of Water and Wastewater (Eaton, Clesceri, Rice, & Greenberg, 2005).

Alkalinity and total organic carbon (TOC) analysis were carried out within 24 hours of sampling. During the RO pilot testing phase and during testings at pHs 5.8 and 6.05 on the RO plant, the sulfate and chloride were analyzed using the SM:4500 Turbidimetric and Argentometric methods respectively. For all other subsequent testing for sulfate and chloride, the SM:4110B Ion Chromatograph (IC) testing method was adopted. When testing using the IC method, all non-NF/RO permeate samples were filtered using 0.45μm pore membrane before analysis, to prevent any colloidal plugging of the equipment tubings.

Table 4-7: Methods and Equipment for Water Quality Analysis

Analyte	Test Location	Method and/or Equipment Description	Method Detection Level
Barium	Lab	SM: 3120 B. ICP Method/Inductively Coupled Plasma Spectrometer	0.01 mg/L
Calcium	Lab	SM: 3120 B. ICP Method/Inductively Coupled Plasma Spectrometer	0.01 mg/L
Chloride	Lab	SM: 4500 Cl^- B. Argentometric Method	1.0 mg/L
		SM: 4110 B. IC with Chemical Suppression of Eluent Conductivity	0.1 mg/L
Conductivity	Field	HQ40d Portable pH, Conductivity and Temperature Meter	0.01 µS/cm
Magnesium	Lab	SM: 3120 B. ICP Method/Inductively Coupled Plasma Spectrometer	0.03 mg/L
Manganese	Lab	SM: 3120 B. ICP Method/Inductively Coupled Plasma Spectrometer	0.01 mg/L
pH	Field	HQ40d Portable pH, Conductivity and Temperature Meter	0.01 pH Units
Potassium	Lab	SM: 3120 B. ICP Method/Inductively Coupled Plasma Spectrometer	0.1 mg/L
Silica	Lab	SM: 3120 B. ICP Method/Inductively Coupled Plasma Spectrometer	0.02 mg/L
Sodium	Lab	SM: 3120 B. ICP Method/Inductively Coupled Plasma Spectrometer	0.03 mg/L
Strontium	Lab	SM: 3120 B. ICP Method/Inductively Coupled Plasma Spectrometer	0.0005 mg/L
Sulfate	Lab	SM: 4500 SO_4^{2-} E. Turbidimetric Method/HACH Spectrophotometer DR6000	1.0 mg/L
		SM: 4110 B. IC with Chemical Suppression of Eluent Conductivity	0.018 mg/L
Sulfide	Field	SM: 4500-S^{2-} F. Iodometric Method	0.1 mg/L as S
Temperature	Field	HQ40d Portable pH, Conductivity and Temperature Meter	0.01 °C
Total Alkalinity	Lab	SM: 2320 B. Titration Method	5 mg/L as $CaCO_3$
Total Dissolved and Suspended Solids	Lab	SM: 2540 C. Total Dissolved Solids Dried at 180°C, SM: 2540 D. Total Suspended Solids Dried at 103-105°C	2.5 mg/L

Analyte	Test Location	Method and/or Equipment Description	Method Detection Level
Total Organic Carbon	Lab	SM: 5310 C. Persulfate-Ultaviolet Oxidation Method/Tekmarr-Dohrmann Phoenix 8000: The UV- Persulfate TOC Analyzer	0.1 mg/L
Turbidity	Field	Hach 2100q Portable Turbidimeter	0.01 NTU

Laboratory Quality Control

Laboratory quality control measures were instituted for the laboratory testing works and the subsequent analysis of data collected. Samples requiring storage were kept in a cooler at 4°C, and were taken to room temperature before analyses on the samples were carried out for the parameters tested. Preparation for the analysis included thorough cleaning of all glassware used in the data collection with 6N hydrochloric acid (i.e. 1 part HCl and 1 part distilled water) and rinsed with distilled water prior to use. All equipment used like pH meters, weighing scales, electrical conductivity and turbidity meters, spectrophotometers, etc. were calibrated to manufacturer's specifications and all reagents standardized according to procedures set out in the Standard Methods for the Examination of Water and Wastewater (Eaton, Clesceri, Rice, & Greenberg, 2005).

Precision and accuracy of laboratory work were assessed by analysis of duplicate samples and spiked samples. For the work carried out under this research plan, approximately one out of every five samples was collected and analyzed in duplicate to monitor precision via calculation of the industrial (I) statistic.

Equation 4-1 presents the calculation for the I-statistic as described in the Handbook for Quality Control in Water and Wastewater Laboratories (U.S. EPA, 1979). Upper warning limits (UWL) and upper control limits (UCL) were established. The UWL is defined to be the mean I-statistic value for the tested parameter plus two standard deviations from the mean. The UCL is defined to be the mean I-statistic value for the tested parameter plus three standard deviations from the mean. Duplicate samples are said to be in compliance if the I-statistic value did not exceed the UCL or two consecutive I-statistic values for duplicate samples did not exceed the UWL.

$$I = \frac{|A-B|}{[A+B]} \tag{4-1}$$

Where : I = Industrial Statistic; A= Duplicate Value 1; B = Duplicate Value 2

Accuracy was monitored by calculating the percentage recovery (% R) for spiked samples. Equation 4-2 presents the % R calculation for a laboratory-fortified matrix sample. Spiked samples were said to be in compliance if the % R fell within the range of 80 to 120% (Eaton, Clesceri, Rice, & Greenberg, 2005).

$$\%\ R = \frac{\text{Concentration}_{\text{SAMPLE+SPIKE}} - \text{Concentration}_{\text{SPIKE}}}{\text{Concentration}_{\text{SPIKE}}} \text{ X } 100\% \tag{4-2}$$

The precision of laboratory analysis carried out in this study is illustrated using 3 parameters: electrical conductivity, total dissolved solids (TDS) and sodium (Na) measurements. Precision analysis were carried out in the over 6500 water quality parameters tested as part of this research study, but only the three parameters are identified for illustration here, as they form part of the empirical models built as part of this research. The tabulation of the I-statistics for these 3 parameters is presented in Appendix.

For electrical conductivity measurements, a total of 79 duplicate samples were analyzed. Figure 4-3 represents the control chart for precision analysis of EC. The average value of I-statistics for EC is 0.004, indicating a variability of 0.4% between samples. Six sample observations were noted to exceed the UWL of 0.012, however control was re-established on the next duplicate sample which did not exceed the UWL, as seen in Figure 4-3 and Table 0-1 of Appendix. The UCL was not exceeded throughout this set of precision assessment.

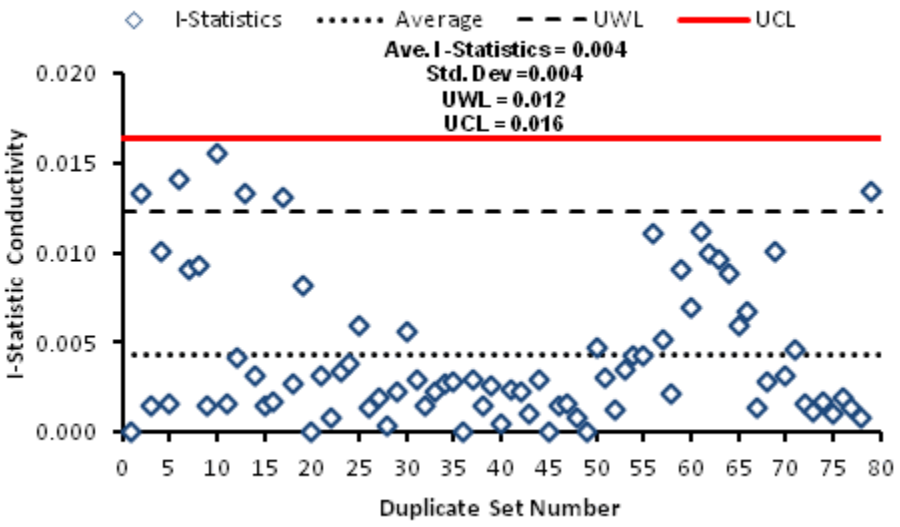

Figure 4-3: Control Chart for Electrical Conductivity Precision Analysis

For total dissolved solids (TDS) analysis, a total of 83 duplicate samples were analyzed. Figure 4-4 represents the control chart for precision analysis of TDS. The average value of I-statistics for conductivity is 0.007, indicating a variability of 0.7% between samples. Six sample observations were noted to exceed the UWL of 0.021, however control was re-established on the

next duplicate sample which did not exceed the UWL, as seen in Figure 4-4 and in Table 0-2 of Appendix. On one duplicate analysis the I-statistic was equal to the UCL but all samples analyzed together with this duplicate sample were accepted, as the both the previous and next duplicate samples in this same analysis did not exceed the UWL and remained within control.

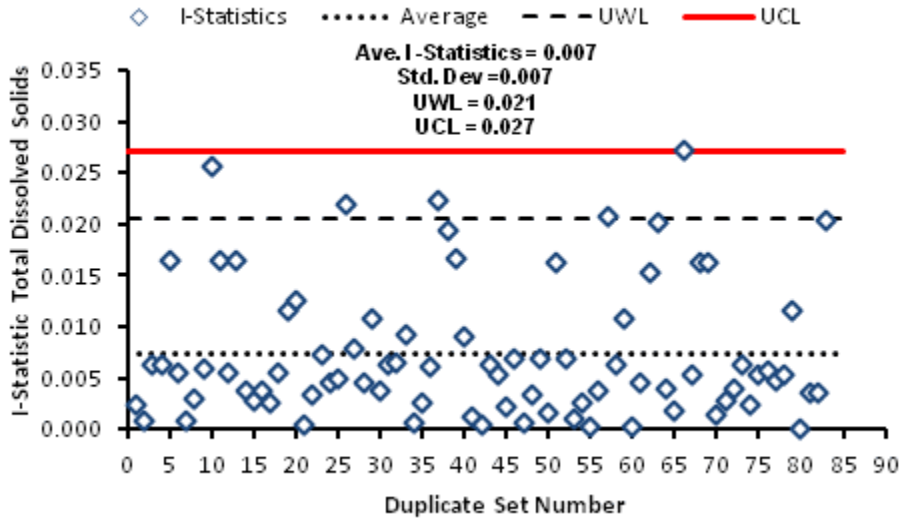

Figure 4-4: Control Chart for Total Dissolved Solids Analysis

For sodium (Na) measurements, a total of 70 duplicate samples were analyzed. Figure 4-5 represents the control chart for precision analysis of Na. The average value of I-statistics for Na is 0.010, indicating a variability of 1.0% between samples. 4 sample observations were noted to exceed the UWL of 0.027, however control was re-established on the next duplicate sample

which did not exceed the UWL, as seen in Figure 4-5 and Table 0-3 of Appendix. The UCL was not exceeded throughout this set of precision assessment.

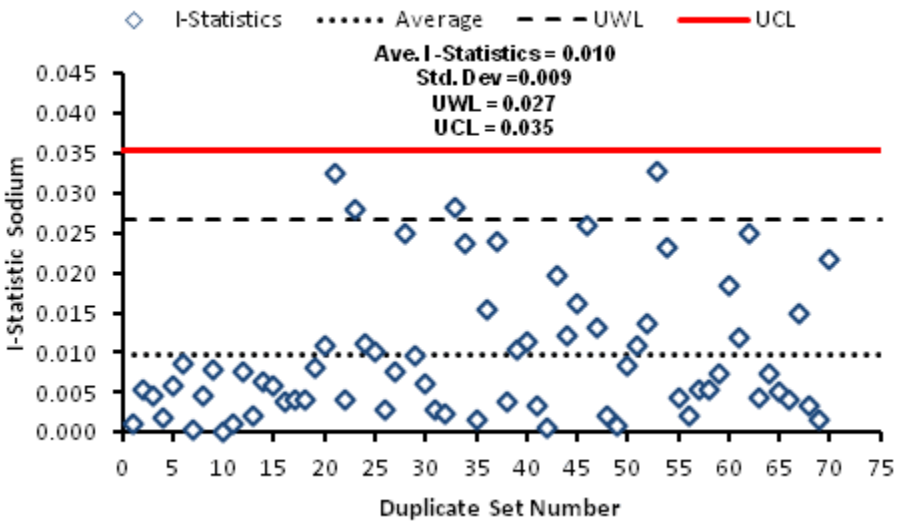

Figure 4-5: Control Chart for Sodium Precision Analysis

The analysis of Na samples is used to illustrate the assessment of accuracy control for laboratory works carried out as part of this research. This is illustrated in Figure 4-6 and also in Table 0-4 of Appendix. A total of 70 samples were spiked for Na analysis and all 70 spiked samples had percentage recovery (% R) of between lower acceptable limit (LAL) of 80% and upper acceptable limit (UAL) of 120%. The average of the recovery rates for Na is 100.4% and the standard deviation of the recovery assessments for Na is 7.5%. Though the average rate of the recovery rate is narrow and close to 100% there is significant variability in the recovery rate.

This can be explained by the fact that Na analysis of the samples in this study was carried out with dilution of samples for analysis on the Inductively Coupled Plasma (ICP) Spectrometer. On the ICP the Na analysis can only be carried out to a concentration range of up to 7.5 mg/L, and hence all samples were diluted in different proportions for measurements, including RO permeate samples which were diluted in ratio of 1:5. In the case of RO concentrate samples the dilution was in the ratio of 1:200. The diluted duplicate samples were then spiked for accuracy control checks and hence the variability in recovery rates.

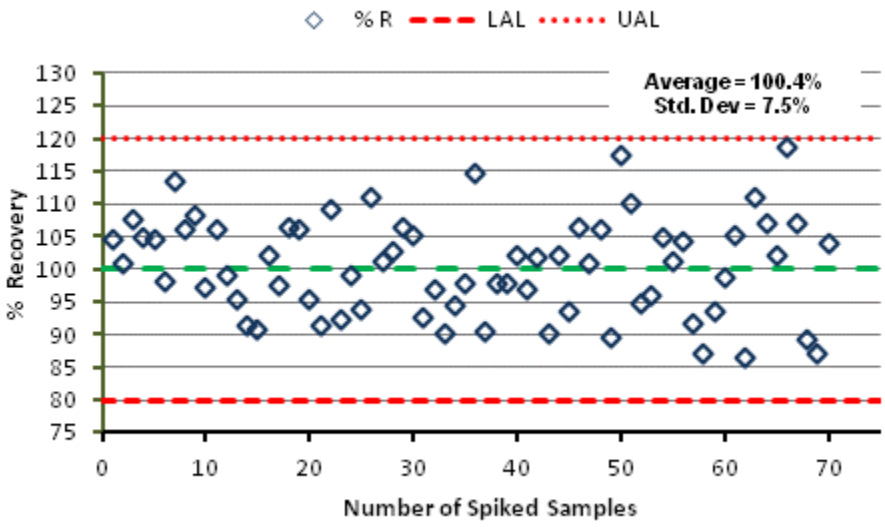

Figure 4-6: Control Chart for Accuracy Sodium Accuracy Analysis

The dilution of samples for analysis is not unique to just the Na analysis. Many parameters that were analyzed had to be diluted for analysis on the ICP, Ion Chromatograph (IC) and even titration analysis. Similar precision and accuracy control checks were carried out for the analysis of these parameters.

Modeling Salt Passage in RO Process

Using the operations and laboratory data collected from this study two empirical models were built to quantify salt passage in terms mass transfer coefficient for solute (K_S). TDS and sodium (Na) were chosen as the two solutes for which the empirical models were built. Both TDS and Na can be measured in the permeate streams in quantifiable quantities using the laboratory equipments and instruments, and so the models were built for these two parameters. The models were built using data from the RO plant, as the process of incremental pH steps allowed for 7 different pH conditions, whereas in the RO pilot there were only 4 pH conditions. The models built using data from the RO plant, were validated using data from the RO pilot.

Chloride, is monovalent like Na, and it also passes into the permeate stream. However, attempts to build models were not possible as two different approaches were adopted for chloride testing in this study. During the RO pilot study and when RO plant were at pHs 5.8 and 6.05, the Argentometric titration method (SM:4500 Cl^-) was used, while the rest of the study on the RO plant at the other 5 pH conditions, the analysis on samples were done using the ion chromatograph (IC) and the dilution range for both these methods were different. When using both these methods, dilution of samples was necessary. For the titration method, using silver nitrate as titrant, dilution of the feed, first and second stage concentrates were necessary, in order to minimize titrant consumption. For the IC method of testing for chloride, the dilution of samples is necessary as part of the manufacturer's requirement on operation of the IC.

The empirical models for K_S were evaluated with the use of the statistical software MINITAB. Solute transfer in the Homogeneous Solution Diffusion Model (HSDM) is based on the relationships presented in Equation 3-34 and Equations 3-40 through 3-42 which are reproduced here.

$$K_W = \frac{J_W}{TCF \times TMP} \tag{3-34}$$

$$J_S = K_S(\Delta C) \tag{3-40}$$

$$J_S = (C_P)\, J_W \tag{3-41}$$

$$Ks = \frac{(C_p)\, Jw}{\Delta C} \tag{3-42}$$

Based on actual measurement of water quality data and RO plant operations data on the dates when the water quality samples were collected, the solute mass transfer co-efficient Ks for TDS and Na were first built for each stage and identified as the actual K_{TDS} and K_{Na} respectively.

A linear regression approach using MINITAB was then taken to identify linear equations that will correlate selected RO plant water quality parameters, used as predictors, to the actual K_{TDS} and K_{Na}, mathematically obtained. The mathematically derived actual K_{TDS} and K_{Na} for each membrane stage, were the known responses as each of the models were built.

Other than the water quality parameters listed in Table 4-7, additional predictors included in the linear regression model evaluations were the ionic strength and viscosity of water. Maung et al (2009) pointed out that removal of salts by RO membranes is not just dependent on factors such as pH, temperature, pressure, feed water quality, etc but also on the ionic strength of the solution. The study by Schäfer et al (2004) showed that ionic strength of solution causes Donnan effect

which affects the transport of ions across membranes. In the study by Mo et al (2008) showed that ionic strength of water affects the zeta potential of RO membranes at different pHs. The ionic strength was calculated using the following Equation 4-3.

$$I = \frac{1}{2}\sum_{i-1}^{n} C_i Z_i^2 \quad (4\text{-}3)$$

Where:

I = Ionic Strength

C_i = molar concentration of ion

Z_i = charge number of ion

Water viscosity is defined as the resistance to flow of the bulk water, and it is temperature dependent (MWH, 2005). As temperature increases the viscosity of water decreases, as intermolecular forces increase. Temperature also influences membrane permeability, osmotic pressure and concentration polarization (Agashichev & Lootah, 2003). Kinematic viscosity inputted as a predictor in the linear regression model building, were interpolated between 3 temperature ranges as shown in Table 4-8.

Table 4-8: Relevant Kinematic Viscosity of Water

Temp(°F)	**Temp (°C)**	**Kinematic Viscosity (ft^2/s)**
70	21.1	1.06×10^{-5}
80	26.7	9.30×10^{-6}
90	32.2	8.26×10^{-6}

The final model selection was to be based on a two-step approach. The first step involves short listing models that give a close fit for predicted values when compared to actual mathematically derived MTC for TDS and Na by the HSDM. The second step involves testing the shortlisted model for predicting the MTC for TDS and Na on the RO pilot. In both steps predicted versus actual charts and statistical "paired t-test" using MINITAB were carried out.

By linear regression on MINITAB, four models were identified as potential empirical good fit of the MTC for TDS for Stage 1 (i.e. K_{TDS1}). The 4 models are represented Models 1 - 4 and Equations 4-4 through 4-7.

Model 1: $$K_{TDS1} = -1.067 \times 10^{-2} + 4.873 \times 10^{3} H^{+} + 6.5 \times 10^{-6} EC \quad (4\text{-}4)$$

Model 2: $$K_{TDS1} = -2.802 \times 10^{-2} + 2.859 \times 10^{3} H^{+} + 7.1 \times 10^{-4} T + 6.14 \times 10^{-6} EC \quad (4\text{-}5)$$

Model 3: $$K_{TDS1} = -2.479 \times 10^{-2} + 2.845 \times 10^{3} H^{+} + 6.1 \times 10^{-6} EC + 3.6 \times 10^{3} \nu \quad (4\text{-}6)$$

Model 4: $$K_{TDS1} = -2.686 \times 10^{-2} + 4.620 \times 10^{3} H^{+} + 7.2 \times 10^{-4} T + 8.05 \times 10^{-6} EC - 0.1284 Ion \quad (4\text{-}7)$$

Where:

K_{TDS1} = MTC for the solute TDS in the 1st Stage (ft/day)

H^{+} = pH expressed in terms of hydronium ion concentration (i.e. 10^{-pH})

EC = Electrical conductivity measurements (μs/cm)

T = Temperature in Celsius

ν = Kinematic viscosity of water (ft^2/sec)

Ion = Ionic strength of feed water

Models 5- 8 represented by Equations 4-8 through 4-11 were developed to fit MTC for TDS for Stage 2 (i.e. K_{TDS2}).

Model 5: $$K_{TDS2} = -1.293 \times 10^{-2} + 4.048 \times 10^{3} H^{+} + 2.91 \times 10^{-6} EC \quad (4\text{-}8)$$

Model 6: $$K_{TDS2} = -1.243 \times 10^{-2} + 4.122 \times 10^{3} H^{+} + 1.96 \times 10^{-5} T + 2.91 \times 10^{-6} EC \quad (4\text{-}9)$$

Model 7: $$K_{TDS2} = -1.372 \times 10^{-2} + 4.109 \times 10^{3} H^{+} + 2.91 \times 10^{-6} EC + 82.1\nu \quad (4\text{-}10)$$

Model 8: $$K_{TDS2} = -1.225 \times 10^{-2} + 4.654 \times 10^{3} H^{+} + 1.8 \times 10^{-5} T + 3.19 \times 10^{-6} EC - 0.016 Ion \quad (4\text{-}11)$$

Where:

K_{TDS2} = MTC for the solute TDS in the 2nd Stage (ft/day)

Similar linear regression was carried out in short listing 2 models to predict MTC for Na in Stage 1. Models 9 and 10 represented by Equations 4-12 and 4-13 were developed to fit MTC for Na for Stage 1 (i.e. K_{Na1}).

Model 9: $$K_{Na1} = 5.115 \times 10^{-2} + 8.68 \times 10^{-6} EC - 1.15 \times 10^{-4} Na \quad (4\text{-}12)$$

Model 10: $$K_{Na1} = 2.018 \times 10^{-1} + 2.41 \times 10^{-5} EC - 2.41 \times 10^{-4} Na - 19311\nu \quad (4\text{-}13)$$

Where:

K_{Na1} = MTC for the solute Na in the 1st Stage (ft/day)

Na = Sodium concentration (mg/L)

Models 11 and 12 represented by Equations 4-14 and 4-15 were developed to fit MTC for Na for Stage 2 (i.e. K_{Na2}).

Model 11: $$K_{Na2} = 4.159 \times 10^{-2} + 4.92 \times 10^{-6}\,EC - 4.82 \times 10^{-5} Na \quad (4\text{-}14)$$

Model 12: $$K_{Na2} = 1.372 \times 10^{-1} + 5.43 \times 10^{-6} EC - 6.27 \times 10^{-5} Na - 9965\nu \quad (4\text{-}15)$$

Where:

K_{Na2} = MTC for the solute Na in the 2nd Stage (ft/day)

The evaluation and determination of the final representative empirical models to predict the MTC for TDS and Na are discussed in the next chapter.

5. RESULTS AND DISCUSSIONS

Overview

This research study covers two major assessments: elimination of acid in the pre-treatment to RO plant and the evaluation of NF for the treatment of an aerated surficial groundwater that is highly fouling. In this chapter, the assessments of the findings in these two major studies are presented. From the monitoring of water quality during the stepped pH adjustments, as use of acid in the pre-treatment process to the RO plant was eliminated, four empirical models were developed as tools to ascertain salt passage, in terms of TDS and Na, in an RO plant using polyamide membranes.

Elimination of Acid in Pre-Treatment to Reverse Osmosis Plant

The elimination of the use of sulfuric acid as pre-treatment to the City's RO plant was carried out in a 3-step approach. The 3-Step approach involved: (1) pilot testing the plan to reduce the dependence on acid, (2) implementing the plan on the full-scale system with conservative pH increments, and (3) continuous screening for scale formation potential, using a "canary" monitoring device.

Raw Water Quality

The pilot study for acid elimination was carried out between Mar 25 and Aug 6, 2010 while the actual elimination on the 4.5 MGD RO plant was carried out in steps between Jun 2, 2011 and May 20, 2012. As the window of pilot study and the implementation and completion of the acid

elimination on the full scale RO plant spanned over 2 years, an assessment of the variability of the raw water feeding the RO pilot and the RO plant was critical in order to have a better appreciation of the findings of this study. Furthermore the City adopts different well rotations in its operation to feed water to its RO plant and also refurbished and added new wells into its circuit.

The comparison of the raw water quality between the RO pilot study and that during the implementation acid elimination on the RO plant is presented in Table 5-1. The City's 4.5 MGD RO plant is made up of three 1.5 MGD trains named Trains A, B and C. The acid elimination on the RO plant was monitored and studied on Train C, as part of this research study.

From the raw water quality tabulation it was noted that the raw water as received at the RO plant during the acid elimination phase in 2011 and 2012 was of better quality (i.e. lower concentration on analytes) than that noted in 2010 during the pilot study. The main reason for this was the City's refurbishment of its Well No.4 in early 2011 that has improved the overall feed water quality to the RO plant.

Table 5-1: Raw Brackish Water Quality Comparison

Parameter		**Units**	**RO Pilot**[1]	**Train C**[2]
pH	Max:		7.31	7.26
	Min:		6.95	6.87
Temp	Max:	°C	30.6	29.9
	Min:	°C	23.1	25.0
Turbidity		NTU	0.12 ± 0.07	0.13 ± 0.04
Conductivity		µs/cm	3330 ± 120	3430 ± 200
TOC		mg/L	1.37 ± 0.11	1.21 ± 0.37
SO_4^{2-}		mg/L	857.8 ± 25.0	803.1 ± 58.6
Cl^-		mg/L	587.8 ± 52.3	521.1 ± 43.3
Total Alkalinity		mg/L as $CaCO_3$	136.2 ± 5.3	138.5 ± 4.2
Ca		mg/L	278.7 ± 16.4	229.2 ± 11.6
Mg		mg/L	134.8 ± 5.6	116.3 ± 5.1
Sr		mg/L	26.5 ± 1.0	24.2 ± 1.5
Ca Hardness		mg/L as $CaCO_3$	695.3 ± 40.8	571.8 ± 29.0
Total Hardness		mg/L as $CaCO_3$	1279.0 ± 62.6	1077.9 ± 49.5
Si		mg/L	21.9 ± 1.1	21.0 ± 1.3
K		mg/L	6.6 ± 0.9	7.7 ± 0.6
Na		mg/L	293.7 ± 24.3	256.7 ± 20.4
Ba		µg/L	16.2 ± 0.9	13.0 ± 1.9
Mn		µg/L	<10	< 10
Fe		µg/L	<10	< 10
TDS		mg/L	2398.8 ± 46.6	2225.4 ± 76.4
TSS		mg/L	3.5 ± 1.4	2.7 ± 1.2
Sulfide		mg/L as S^{2-}	Not Tested	2.68 ± 0.18

[1] RO Pilot Testing Period Mar 25 – Aug 6, 2010
[2] RO Plant Train C Testing Period Jun 2, 2011 – May 20, 2012

RO Pilot Assessment

The pilot scale acid elimination evaluation was carried out in 4 phases as mentioned in Table 4-1. Three aspects of the performance of the pilot were monitored. First was the comparison of the performance of the membranes as acid was eliminated, to ascertain any membrane productivity deterioration. The other two performance monitoring was carried out to ascertain the changes in total permeate water quality and also the concentrate water quality as acid elimination progressed.

The assessment membrane performance, was carried out by normalizing permeate flow using Equation 3-34 and is presented graphically in Figure 5-1. In tandem with monitoring the normalized MTC, the feed pressure and differential pressure across the pilot was also monitored as presented in Figure 5-2.

The RO pilot membranes were ripened and monitored at pH 5.8 during Phase 1 for 50 days with sulfuric acid and scale inhibitor feed before the first stepped acid feed reduction was carried out. Phase 2 operations occurred at a pH of 6.3 (i.e. acidity constant pK_1 of carbonic acid) for approximately 37 days. The next two stepped acid reduction phases increased the pH to 6.6 and then 7.1 when the acid feed was completely eliminated after 94 days of runtime.

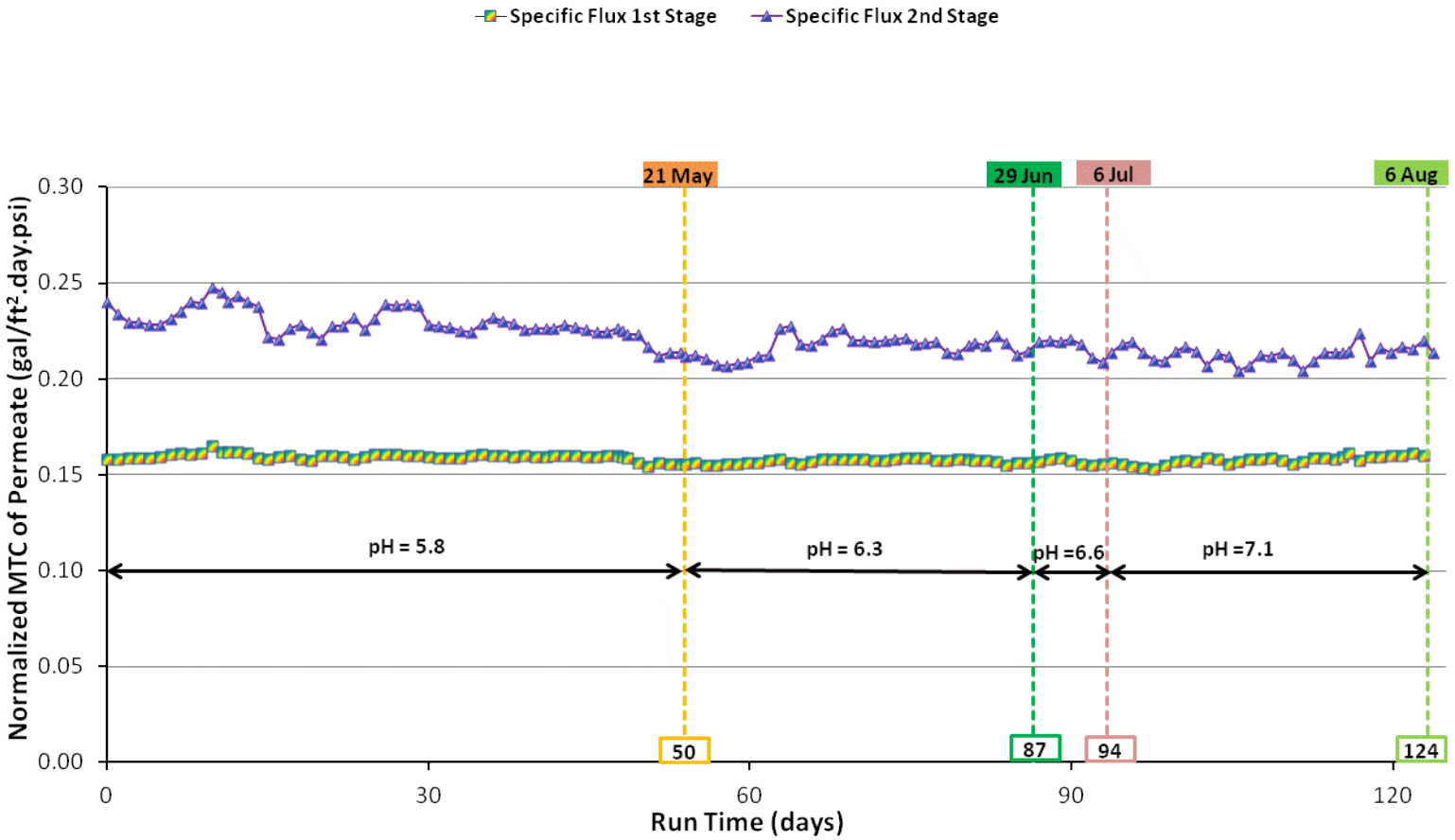

Figure 5-1: Average Daily Normalized Mass Transfer Coefficient of RO Pilot Operations

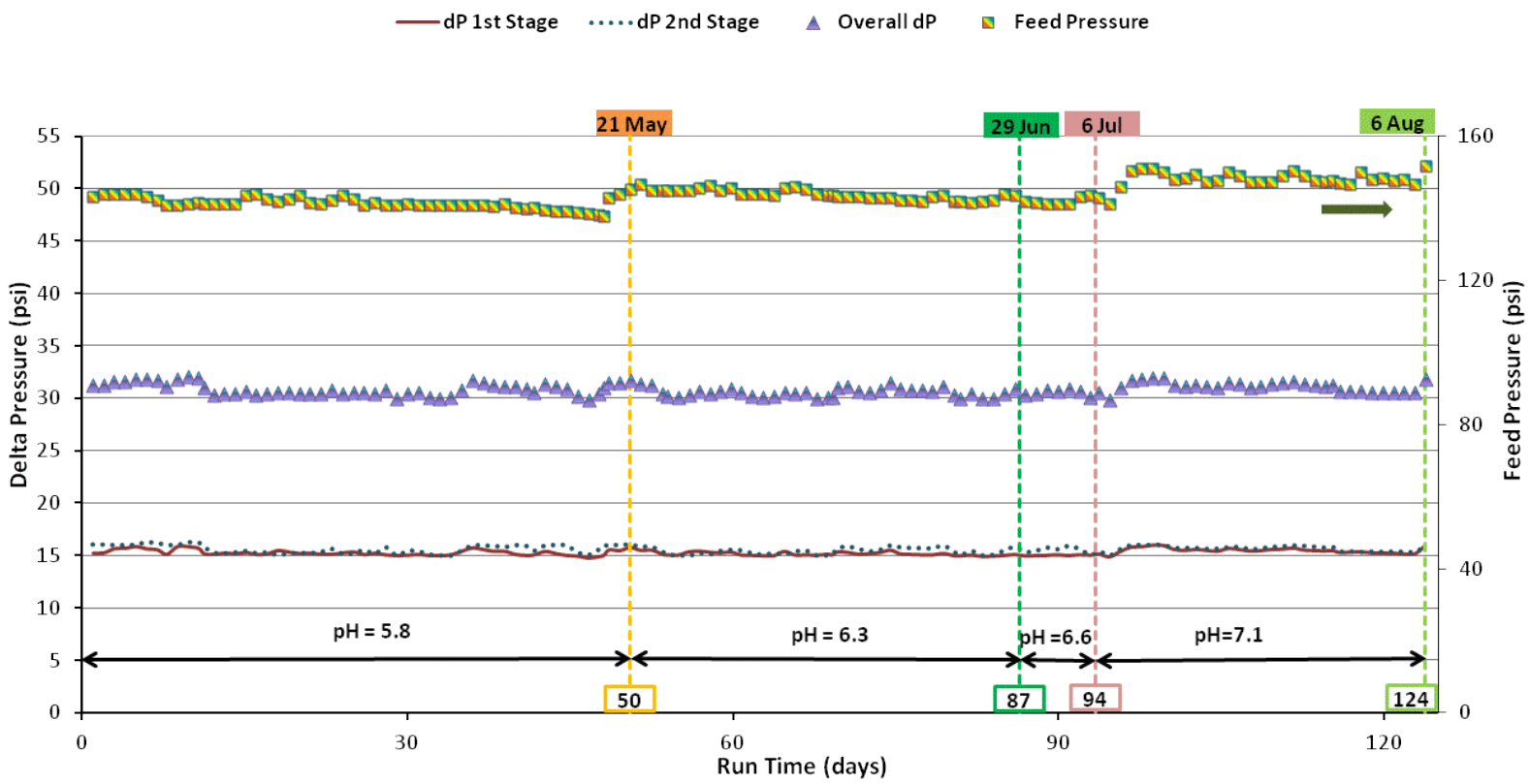

Figure 5-2 : Average Daily Feed Pressure and Differential Pressure on RO Pilot

As observed in Figure 5-1, during the first 94 days of the study, the normalized MTC of the first Stage remained relatively stable. Fluctuations in the MTC rates were observed during pilot testing, especially on the second stage. Maintaining the proper pH set-points at the low pilot flow and sulfuric acid feed rates presented an operational challenge. Phase 3 of pilot operations was concluded after one week of runtime as a result of issues faced with calibration of the acid feed system. Hence, after a week of relatively stable operation at pH 6.6, acid feed as pre-treatment to the RO pilot skid was discontinued.

The normalized second stage MTC during Phase 1 was 0.23 gal/ft^2-day-psi. Following acid elimination after 94 days of runtime, the normalized second stage MTC was marginally lower at 0.21 gal/ft^2-day-psi. The lower MTC was expected as acid elimination is expected to result in calcium carbonate ($CaCO_3$) scaling (Bonne, Hofman, & van der Hoek, 2000). Monitoring the feed pressures showed that the feed pressure to the pilot increased from about 142 psi to 150 psi as the acid elimination progressed. When the permeate production is held constant, and fouling/scaling propagates, the feed pumps are expected to ramp up to maintain the pre-determined permeate production. The increase in feed pressure is another indication that as acid elimination progressed, some level of scaling has occurred, and this is supported by the observed lower normalized MTC of permeate production.

As acid elimination progressed, the total permeate and concentrate water qualities were also monitored. The comparisons of the total permeate quality at pH 5.8 and at pH 7.1 when the use of acid in pre-treatment to the RO pilot was discontinued is shown in Table 5-2. Similar

comparison of the concentrate water quality is presented in Table 5-3. In comparing the total permeate quality between the operations in Phases 1 and 4, it can be noted that the pH of the permeate has increased by 0.7 pH units on average to 6.2 pH units. Chloride and Na concentration and also TDS in the total permeate increased as the RO feed pH was increased upwards to ambient pH of 7.1. The concentrate pH increased by over 1 pH unit to 7.4 on average, while the total alkalinity, and Na and chloride concentrations also increased. Acid addition suppresses pH and converts available carbonate and bicarbonate species to carbonic acid, and hence the increase in total alkalinity can be attributed directly to the removal of acid use in the pretreatment (Duranceau, Anderson, & Teegarden, 1999). Likewise sulfate concentration reduced as acid use was tapered down and this is again because of reduced sulfate in RO feed water as sulfuric acid was eliminated.

As the City was rotating its wells to the RO plant, the feed to the RO pilot was also changing and this variability will also translate to variable permeate and concentrate water quality. Therefore the permeate and concentrate water qualities were not used as primary factors in deciding whether to proceed with the acid elimination on the RO plant.

The autopsy of the last membrane element on the second stage (performed by Avista Technologies) showed that "the active membrane surface was free of any visual foulant material". This and the fact that relatively stable operations as seen by the normalized MTC for permeate in Figure 5-1, were the key factors in the City deciding to discontinue the use of sulfuric acid feed as pre-treatment to its brackish water RO plant at 75% recovery.

Table 5-2: Comparison of Total Permeate Water Qualities at pHs of 5.8 and 7.1

Parameter	Units	Total Permeate	
		pH = 5.8	**pH=7.1**
pH		5.49 ± 0.11	6.2 ± 0.08
Temp	°C	27.2 ± 2.1	28.9 ± 0.3
Turbidity	NTU	0.07 ± 0.02	0.08 ± 0.02
Conductivity	µS/cm	81.4 ± 3.0	140.9 ± 5.2
TOC	mg/L	< 0.1	< 0.1
SO_4^{2-}	mg/L	2.5 ± 0.5	2.4 ± 0.9
Cl^-	mg/L	13.2 ± 3.7	19.9 ± 1.3
Total Alkalinity	mg/L as $CaCO_3$	12.7 ± 0.80	9.8 ± 1.2
Ca	mg/L	< 1.0	< 1.0
Mg	mg/L	< 1.0	< 1.0
Si	mg/L	0.33 ± 0.01	0.40 ± 0.07
K	mg/L	0.26 ± 0.02	0.24 ± 0.02
Na	mg/L	13.6 ± 0.2	15.2 ± 5.8
Ba	µg/L	< 10	< 10
Mn	µg/L	< 10	< 10
Fe	µg/L	< 10	< 10
Sr	mg/L	< 0.2	< 0.2
Ca Hardness	mg/L as $CaCO_3$	< 2.5	< 2.5
Total Hardness	mg/L as $CaCO_3$	< 6.8	< 6.8
TDS	mg/L	40.1 ± 7.9	78.3 ± 2.9
TSS	mg/L	0.1 ± 0.2	0.2 ± 0.3

Table 5-3: Comparison of Concentrate Water Quality at pHs of 5.8 and 7.1

Parameter	Units	Concentrate	
		pH = 5.8	**pH=7.1**
pH		6.23 ± 0.06	7.39 ± 0.05
Temp	°C	27.4 ± 2.0	29.2 ± 0.2
Turbidity	NTU	0.15 ± 0.09	0.14 ± 0.01
Conductivity	µS/cm	9963 ± 160	9315 ± 173
TOC	mg/L	4.2 ± 1.4	5.5 ± 0.2
SO_4^{2-}	mg/L	3400 ± 236	3202 ± 123
Cl^-	mg/L	1970 ± 83	2095 ± 58
Total Alkalinity	mg/L as $CaCO_3$	146 ± 21	485 ± 17
Ca	mg/L	1005 ± 37	955 ± 25
Mg	mg/L	491 ± 11	480 ± 11
Si	mg/L	70 ± 2	68 ± 3
K	mg/L	25 ± 1	23 ± 3
Na	mg/L	1000 ± 41	1112 ± 30
Ba	µg/L	48 ± 9	46 ± 1
Mn	µg/L	<10	<10
Fe	µg/L	<10	<10
Sr	mg/L	98 ± 3	98 ± 22
Ca Hardness	mg/L as $CaCO_3$	2506 ± 93	2382 ± 63
Total Hardness	mg/L as $CaCO_3$	4601 ± 129	4467 ± 105
TDS	mg/L	8589 ± 151	8801 ± 152
TSS	mg/L	17 ± 3	13 ± 3

Acid Elimination RO Plant

The acid elimination on the 4.5 MGD RO plant was staged in 6 pH increases from pH 5.8: pHs 6.05, 6.3, 6.5, 6.7, 6.9, 7.1, spanning close to 12 months as highlighted in Table 4-2. Additional control over potential scaling of the membranes in the RO plant was done by installation of a "canary" monitoring device on Train C (one of the three RO trains in the plant).

Monitoring Results

The normalized MTC for the Stages 1 and 2 of Train C, throughout the time-frame of the study is shown in Figure 5-3. Acid elimination study and evaluation on the full-scale system began following the installation and commissioning of the "canary" monitoring device on Jun 2, 2011. In order to benchmark the productivity of the full-scale RO membranes during acid elimination, process data was collected for 4 months (120 days) prior to the commissioning of the "canary" pressure vessel (runtime 0 days), which was following the last chemical clean-in-place of the full-scale RO Train C. Unfortunately, the City had problems with the instrumentation on all three of its RO trains for approximately 30 days prior to the start of the acid elimination study resulting in erratic data values. However, this problem was fixed in time for the start of the study. Therefore, about 4 months of pre-acid elimination data was utilized for comparison with data collected during the 6 acid elimination steps listed in Table 4-2. The "Canary" unit was operational for approximately 33 days before the first stepped acid reduction to increase the feed water pH to 6.05 was instituted, allowing time for the ripening of the two membrane elements in the "canary" unit.

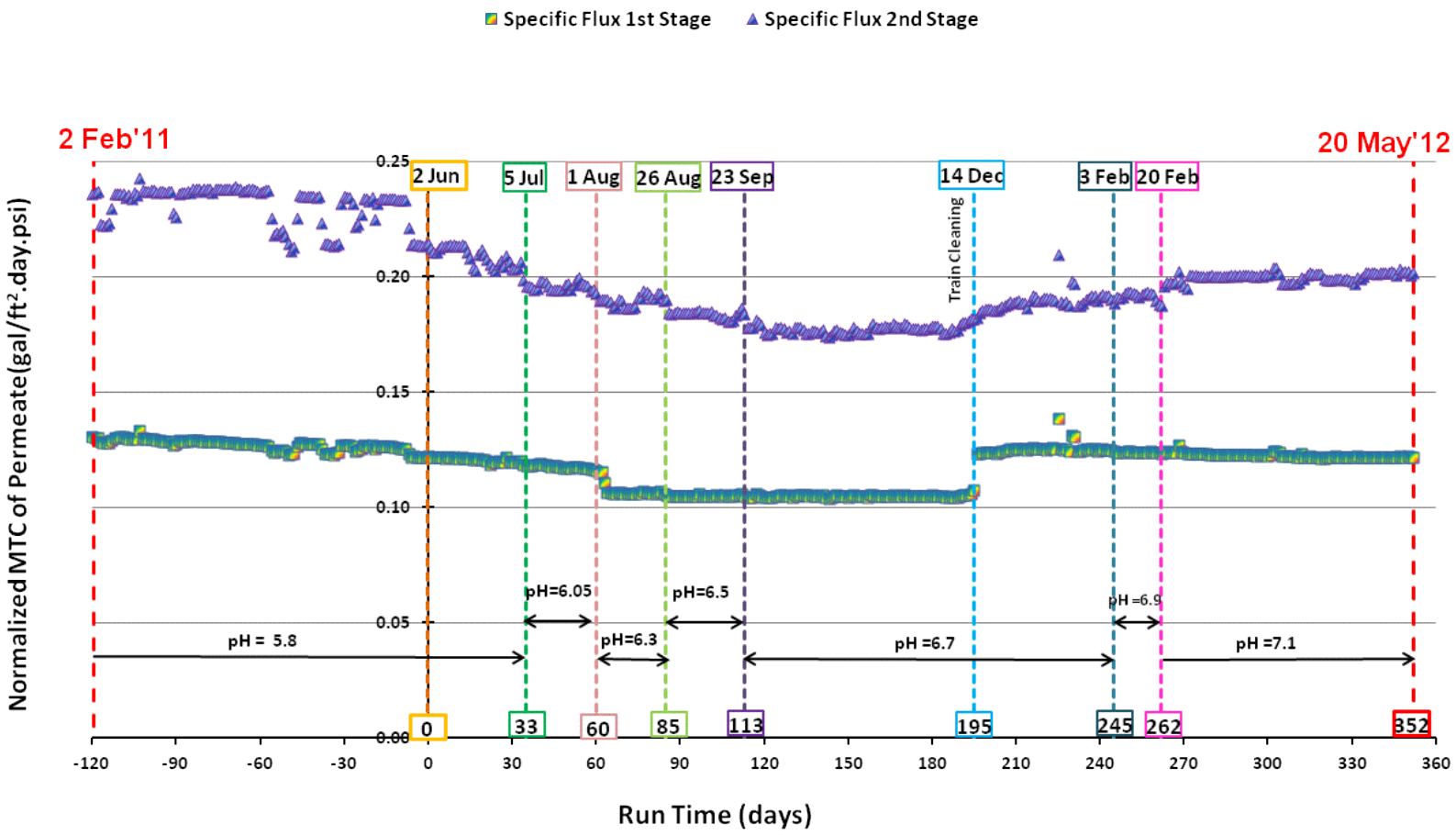

Figure 5-3: Normalized MTC of Permeate for Stages 1 and 2 of Train C

As the acid elimination progressed, the permeate flow rate and concentrate flow rates were logged by the operators thrice a day, and from this the recovery rates on the "canary" unit were computed. In Table 5-4 is the tabulation of the average observed permeate flow, concentrate flow and from this the corresponding recovery rate.

Table 5-4: "Canary" Unit Recovery Rate

pH	Permeate Flow (gpm)	Concentrate Flow (gpm)	Total Flow (gpm)	Recovery (%)
5.8	5.5	34.5	40.0	13.8
6.05	5.5	35.0	40.5	13.6
6.3	5.5	35.0	40.5	13.6
6.5	5.5	35.0	40.5	13.6
6.7	4.0	34.8	38.8	10.3
6.9	2.5	30.0	32.5	7.7
7.1	4.5	34.5	39.0	11.5

The MTC before acid elimination on the RO train at pH 5.8 was comparable to that seen on the RO pilot (see Figure 5-1), at approximately 0.22 gal/ft^2-day-psi. As the acid elimination program progressed, the MTC on the second stage membranes was observed to decline before stabilizing at pH 6.5 and remained stable during the early stages of pH 6.7. With regards to the first stage membranes, the MTC decline was not attributable to the acid elimination program but more probably to plugging problems related to the City's brackish water wells.

In Figure 5-4, the feed pressure to the first and second stages of the RO train, as well as the "canary" unit, are shown along with the differential pressure across each stage. By approximately pH 6.3, the feed pumps to the RO train had already reached their maximum operating capacity of 200 psi, and with no intermediate boosting to the second stage, the MTC stabilized until runtime day 195 (i.e. Dec 14, 2011) when the City cleaned its full-scale RO train.

Following the cleaning of the RO train and "canary" unit, the feed pressure dropped to 180 psi. As the acid elimination study progressed to completion 90 days after the acid elimination, the feed pressure to the first stage only increased to 185 psi.

At pH 6.7 the recovery rate across the "canary" unit was noted to be dropping, as seen in Table 5-4. This coincided with the period during which the feed pump to the Train C had reached its maximum feed pressure of 200 psi. As the acid elimination progressed since Jun 2, 2011 (i.e. runtime 0 day), the differential pressure across the second stage was increasing. The total permeate production by Train C remained relatively constant at around 1040 gpm, and so the increase in feed pressure could correspond to either scaling/fouling of the membranes as the acid elimination progressed.

While the feed pumps reached their maximum operating pressure of 200 psi, the differential pressures across the first and second stages were also increasing, due to membrane plugging and scaling/fouling problems. Overall this translated to the second stage concentrate pressure dropping, thereby meaning that the available feed pressure to the "canary" was also dropping. As the feed pressure to the "canary" dropped, correspondingly the permeate production on the "canary also dropped. On Oct 11 (i.e. runtime 131 days), Oct 13 (i.e. runtime 133 days) and Nov 1 (i.e. runtime 152 days), high and low pH cleaners were used to clean the "canary" unit in isolation of Train C to recover the lost productivity. These cleanings did not help to improve the permeate production by the "canary" unit and strengthened the position that the feed pressure to the "canary" unit being the primary cause of low permeate production and not any significant fouling on the membranes in "canary" unit.

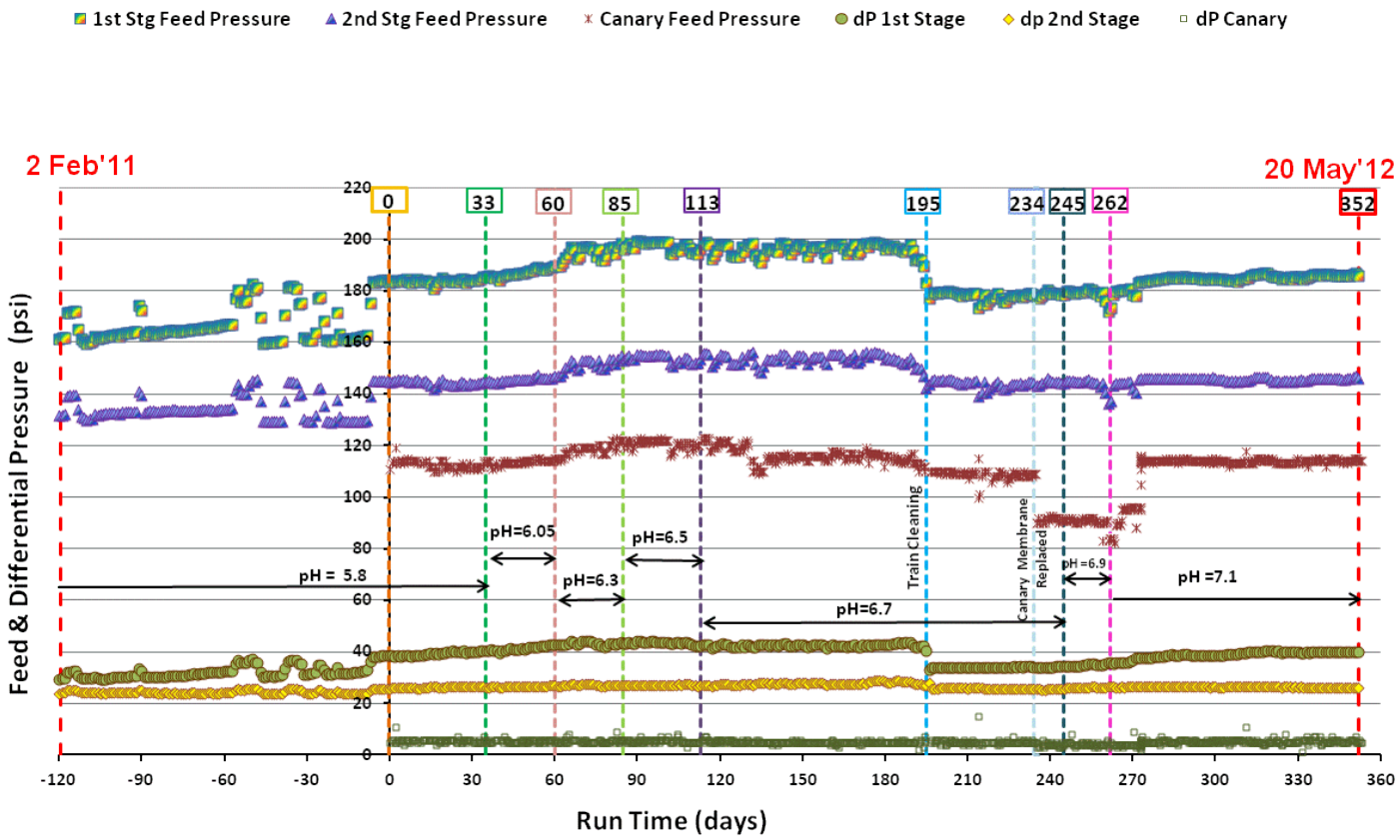

Figure 5-4: Comparison of Feed and Differential Pressure across Train C and Canary Unit

In Figure 5-5, the MTC of the second stage is compared to that of the "canary" unit. Initially, the "canary" unit was operated at a recovery rate of about 13.8%, which resulted in a MTC rate of about 1.0 gal/ft^2-day-psi. In comparison, the 84 element second stage of the RO plant Train C was operating at a recovery rate of 54% with a MTC of approximately 0.23 gal/ft^2-day-psi. The MTC value for the "canary" was 4 to 5 times the MTC of the second stage. By runtime day 33 (i.e. Jul 5, 2011), the MTC rate of the "canary" narrowed to approximately 0.5 gal/ft^2-day-psi or about 2.5 times that of the second stage, as the "canary" membranes ripened.

During the time period between runtime day 33 (i.e. Jul 5, 2011) and 195 (i.e. Dec 14, 2011), a downtrend in the MTC was noted. This reduction in flux rate was the consequence of the removal of acid pre-treatment, which resulted in the increased potential for calcium carbonate scaling. Following the low pH cleaning of the RO train on runtime day 195 (i.e. Dec 14, 2011), the MTC of the "canary" rebounded to 0.65 gal/ft^2-day-psi and remained stable until runtime day 234 (i.e. Jan 23, 2012) when one of the "canary" membrane elements was taken out for autopsy and both the "canary" membrane elements were replaced. The rebound in the MTC at runtime day 195 was also a clear indicator that the productivity of the RO membranes was recoverable following a cleaning for calcium carbonate scale using low pH cleaners. The autopsy report for the "canary" element was similar to the autopsy for the pilot unit with no discernible foulant material identified on the membrane surface. The most likely cause of the autopsy report returning with no foulant material on the membrane surface, could be because the RO train C and "canary" unit were all cleaned with low pH cleaners at runtime day 195, before the "canary" element was taken out for autopsy.

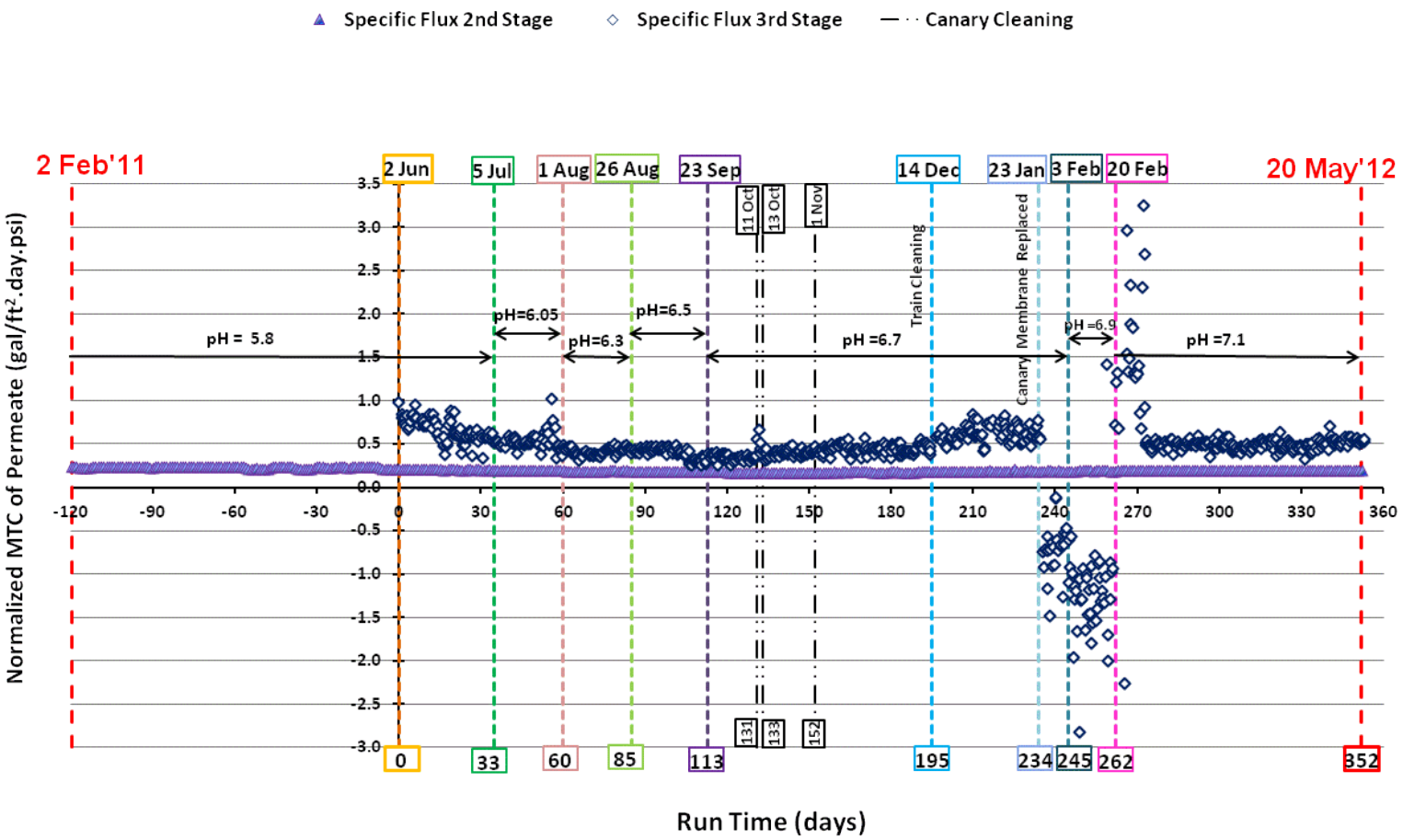

Figure 5-5: Comparison of Normalized MTC of Permeate between "Canary" Unit and 2nd Stage of Train C

Negative Osmotic Pressure

Following the replacement of the two "canary" elements at runtime day 234 (i.e. Jan 23, 2012), attempts were made to operate the "canary" unit at a lower MTC rate comparable to the second stage. The attempts to lower the MTC were aimed at having comparable MTCs between the second stage and "canary" unit, since the "canary" is being utilized as a monitoring device and having comparable MTCs will probably enhance the position of the "canary" vessel as a monitoring device. However, the efforts to regulate the "canary" feed valve resulted in feed pressures lower than the osmotic pressure. As a consequence, the MTC computations yielded negative values indicating that the "canary" unit was not operating as a RO process when the recovery rate was reduced. The negative MTC during the window (i.e. between runtime days 234 and 270) when the osmotic pressure was higher than the feed pressure to the "canary" is as depicted in Figure 5-6. Hydraulic limitations are the most likely cause of the insufficient third stage feed pressure, as only 2-second stage pressure vessels were tapped to feed the "canary" unit. The incorporation of additional second stage pressure vessels and concentrate flows would be required to allow the feed pressure to be throttled so that the "canary" can be operated at lower recoveries. Other systems that incorporated intermediate boosting to the second stage may have allowed more flexibility towards adjusting feed flow, while maintaining adequate feed pressure to a "canary" unit, to overcome the osmotic pressure at the lower recovery rates.

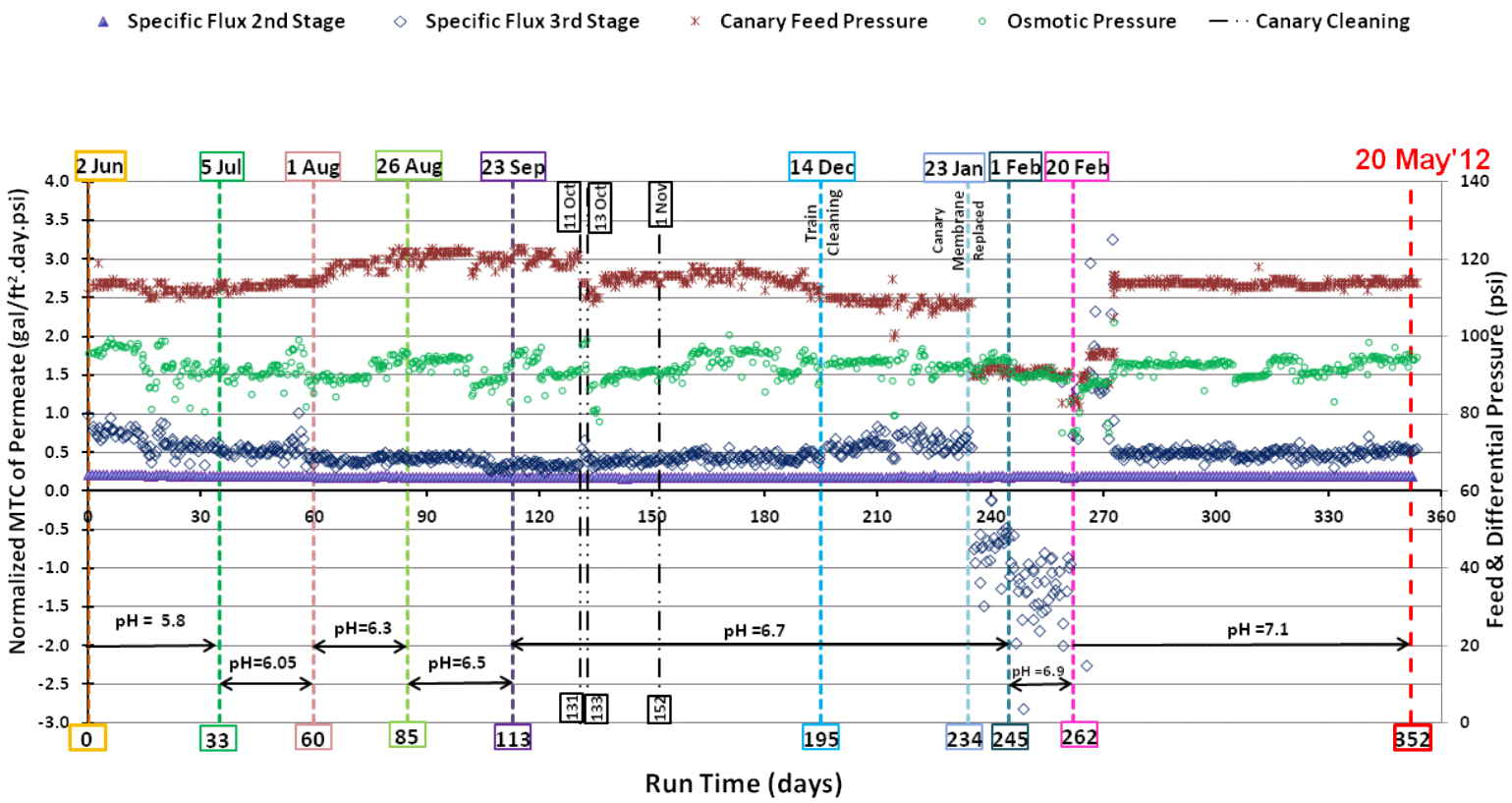

Figure 5-6: Normalized MTC of Permeate Comparison with Feed and Osmotic Pressure

Acid pre-treatment was completely removed from the full-scale system on runtime day 262. Following a reset of the "canary" unit to its original operating condition on runtime day 270, both the "canary" unit and RO train demonstrated stable performance during 90 days of post-acid elimination monitoring till the end of this study on May 20, 2012.

Solute Flux Monitoring

During the acid elimination, solute flux in terms of total dissolved solids (TDS) concentration were monitored using Equation 3-42 and is plotted in Figure 5-7. At the pH of 5.8 before acid elimination started, the solute flux on the first stage in terms of TDS was 0.022 ft/day and as the acid elimination progressed to pH 6.7 the salt passage increased to about 0.024 ft/day. When the Train C was cleaned with low pH cleaners at runtime day 195 (i.e. Dec 14, 2011), the solute flux increased to 0.027 ft/day. Increased solute flux is anticipated when membranes are cleaned and between runtimes days 195 and 262, as the pH increased from 6.7 to 6.9 the solute flux was slowly declining as the membranes "tightened". Following the elimination of acid in pretreatment at runtime day 262 and till the end of this study some 90 days after, the solute flux on the first stage stabilized at about 0.025 ft/day. Overall the solute flux in terms of TDS on the first stage increased by about 0.003 ft/day between pHs 5.8 and 7.1.

On the second stage the solute flux in terms of TDS was at 0.013 ft/day at pH 5.8 and it stabilized at about 0.015 ft/day post-acid elimination. Overall the solute flux on the second stage increased by about 0.002 ft/day between pHs 5.8 and 7.1.

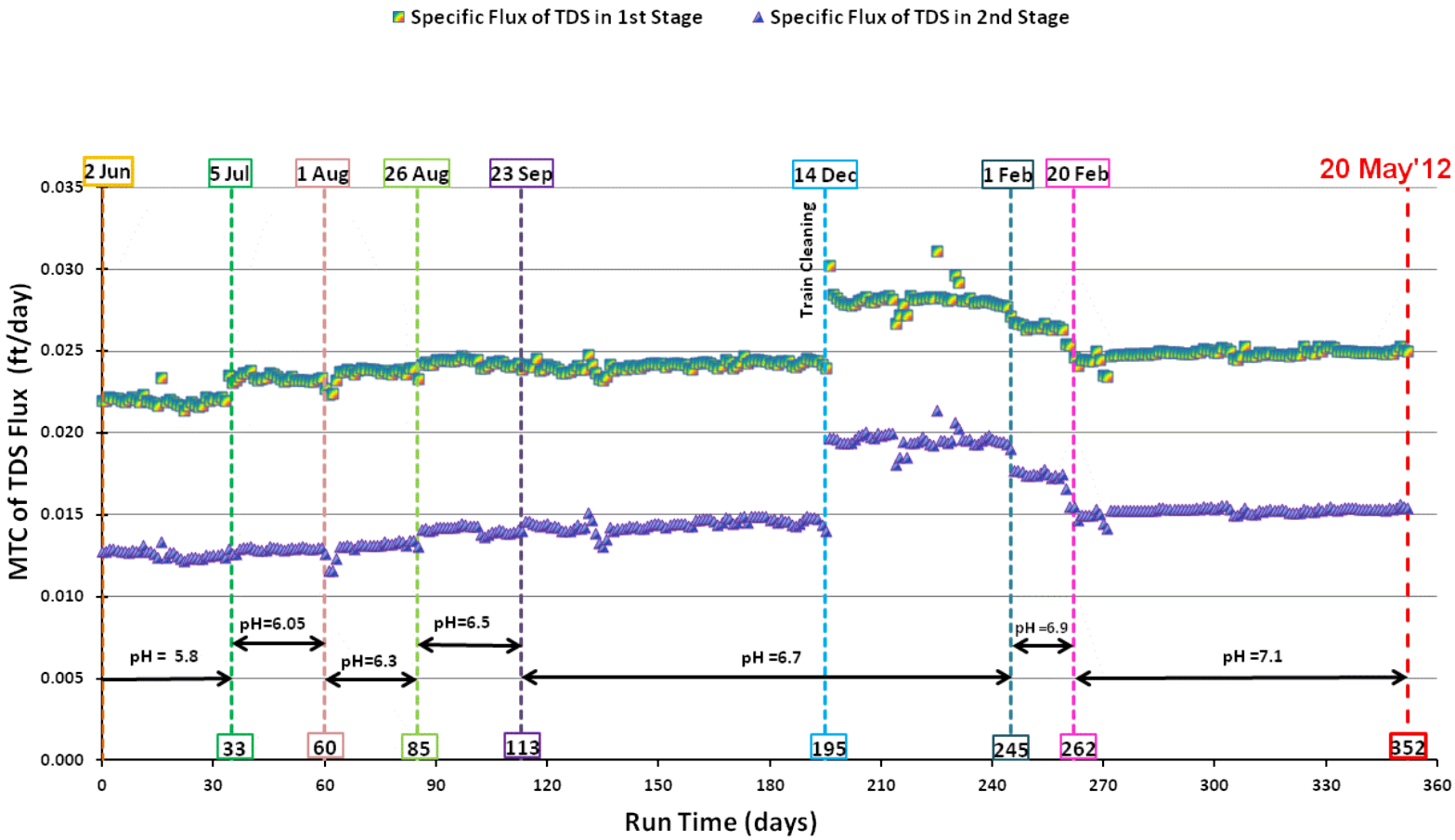

Figure 5-7: MTC of TDS Flux on RO Plant

Water Quality Comparison

As the acid elimination plan progressed, water samples were collected across the RO process, as well as the different source waters that make up the final blend of water that the City supplies to its customers. The final blend consists of the degasified RO permeate, IX soft water and Verna raw water that bypasses the IX. The Verna raw water that bypasses the IX and the feed water to the IX all come via the City's 10^{th} Street Reservoir, which the City is moving towards replacing.

In Table 5-5 the total permeate water quality at pH 5.80 (i.e. before the acid elimination) and at pH 7.10 (i.e. after completely elimination of acid in pretreatment) are tabulated for comparison. The total permeate pH has increased from 5.47 $\pm$ 0.04 at pH 5.80, to 6.46 $\pm$ 0.13 at pH 7.10. At the higher pH of the total permeate the total sulfide content at 3.43 $\pm$ 0.27 mg/L as S^{2-} is higher than the total sulfide content at pH 5.80 of 2.61 $\pm$ 1.05mg/L as S^{2-}. The higher sulfide content means that H_2S stripping efficiency on the degasifier will be lower for the same air-water ratios. And this is noted in the higher turbidity values of the degasified permeate water at pH 7.10 compared to at pH 5.80, as shown in Table 5-6. The degasified permeate turbidity at pH 7.10 is 0.38 $\pm$ 0.05 NTU while the turbidity at pH 5.80 was lower at 0.08 $\pm$ 0.02. Going through the degasifier the pH of the product water is higher than the total permeate, while the alkalinity has dropped. The higher pH is the result of the degassing of the dissolved carbon dioxide as the water goes through the degasifier and this is further substantiated by the lower alkalinity in the degasified permeate water as compared to the alkalinity of the total permeate from the RO plant (Kinser, Kopko, Fenske, & Schers, 2008).

In Table 5-7 is the comparison of the concentrate water quality pre and post-acid elimination. The wastewater discharge from the City's WTF consisting of the reject water from the RO process and the rinse and regeneration wastewaters from the IX process, is currently permitted to be discharged to the Hog Creek, which is a tributary to Sarasota Bay at a permitted flow of 2.8 MGD. There is little impact to the City's discharge permit following the acid elimination plan for the RO plant. Post acid elimination the concentrate pH, total alkalinity and sodium and chloride concentrations are higher while the total sulfide content is lower. The lower total sulfide content post acid elimination of 0.93 $\pm$ 0.11 mg/L as S^{2-}, is about half before acid elimination at 1.86 $\pm$ 0.21 mg/L as S^{2-}, and so reduces the impact on sulfide stripping in the concentrate degasifiers at the higher concentrate pH. The fact that acid is eliminated means that the available bicarbonate alkali is not being converted to soluble form of carbon dioxide and so it would not have diffused through the RO membrane to the permeate stream. Therefore the majority of the available bicarbonate is rejected by the membrane process resulting in the higher total alkalinity of the total concentrate as noted in Table 5-7. This information on the concentrate quality post acid elimination as highlighted will be useful for the City in planning for its new deep well injection system for its wastewater discharge.

Table 5-5: Comparison of Total Permeate Quality at pHs 5.8 and 7.1

Parameter	Units	Total Permeate	
		pH = 5.8	**pH=7.1**
pH		5.47 ± 0.04	6.46 ± 0.13
Temp	°C	29.3 ± 0.6	27.7 ± 0.2
Turbidity	NTU	0.08 ± 0.00	0.08 ± 0.02
Conductivity	µS/cm	77.4 ± 0.5	95.0 ± 5.1
TOC	mg/L	< 0.1	< 0.1
SO_4^{2-}	mg/L	2.8 ± 0.2	4.6 ± 0.2
Cl^-	mg/L	13.5 ± 0.8	18.0 ± 0.7
Alkalinity	mg/L as $CaCO_3$	13.0 ± 0.7	16.6 ± 5.8
Ca	mg/L	< 1.0	< 1.0
Mg	mg/L	< 1.0	< 1.0
Si	mg/L	0.46 ± 0.01	0.52 ± 0.03
K	mg/L	0.34 ± 0.02	0.39 ± 0.02
Na	mg/L	12.9 ± 1.8	15.4 ± 0.8
Ba	µg/L	< 10	< 10
Mn	µg/L	< 10	< 10
Fe	µg/L	< 10	< 10
Sr	mg/L	< 0.2	< 0.2
Ca Hardness	mg/L as $CaCO_3$	< 2.5	< 2.5
Total Hardness	mg/L as $CaCO_3$	< 6.8	< 6.8
TDS	mg/L	44.3 ± 2.5	56.8 ± 3.6
TSS	mg/L	0	0
Total Sulfide	mg/L as S^{2-}	2.61 ± 1.05	3.43 ± 0.27

Table 5-6 : Comparison of Degasified Permeate Water Quality at pHs 5.8 and 7.1

Parameter	Units	Degasified Permeate	
		pH = 5.8	**pH=7.1**
pH		7.33 ± 0.27	7.79 ± 0.01
Temp	°C	29.6 ± 0.6	27.8 ± 0.3
Turbidity	NTU	0.15 ± 0.03	0.37 ± 0.07
Conductivity	µS/cm	75.0 ± 0.7	103.2 ± 0.3
TOC	mg/L	< 0.1	< 0.1
SO_4^{2-}	mg/L	2.31 ± 0.37	5.0 ± 0.5
Cl^-	mg/L	14.3 ± 2.0	20.9 ± 0.3
Alkalinity	mg/L as $CaCO_3$	12.6 ± 0.7	10.1 ± 0.1
Ca	mg/L	< 1.0	< 1.0
Mg	mg/L	< 1.0	< 1.0
Si	mg/L	0.53 ± 0.08	0.65 ± 0.01
K	mg/L	0.34 ± 0.02	0.44 ± 0.01
Na	mg/L	13.1 ± 1.0	16.8 ± 0.2
Ba	µg/L	< 10	< 10
Mn	µg/L	< 10	< 10
Fe	µg/L	< 10	< 10
Sr	mg/L	< 0.2	< 0.2
Ca Hardness	mg/L as $CaCO_3$	< 2.5	< 2.5
Total Hardness	mg/L as $CaCO_3$	< 6.8	< 6.8
TDS	mg/L	38.5 ± 16.9	31.0 ± 2.8
TSS	mg/L	0	0
Total Sulfide	mg/L as S^{2-}	0.64 ± 0.15	0.41 ± 0.01

Table 5-7: Comparison of Total Concentrate Quality at pHs 5.8 and 7.1

Parameter	Units	Total Concentrate	
		pH = 5.8	**pH=7.1**
pH		6.33 ± 0.03	7.55 ± 0.12
Temp	°C	29.5 ± 0.3	27.7 ± 0.5
Turbidity	NTU	0.14 ± 0.02	0.18 ± 0.05
Conductivity	µS/cm	10435 ± 31	12222 ± 292
TOC	mg/L	4.20 ± 0.22	5.30 ± 0.05
SO_4^{2-}	mg/L	3580 ± 133	3525 ± 119
Cl^-	mg/L	1891 ± 179	2400 ± 65
Alkalinity	mg/L as $CaCO_3$	148 ± 2	531 ± 9
Ca	mg/L	944 ± 7	994 ± 56
Mg	mg/L	485 ± 3	502 ± 26
Si	mg/L	84.4 ± 0.2	81.3 ± 1.2
K	mg/L	19.0 ± 2.6	34.2 ± 1.5
Na	mg/L	967 ± 13	1121 ± 93
Ba	µg/L	42.1 ± 0.9	48.7 ± 0.7
Mn	µg/L	< 10	< 10
Fe	µg/L	< 10	< 10
Sr	mg/L	97.6 ± 1.8	105.9 ± 4.3
Ca Hardness	mg/L as $CaCO_3$	2354 ± 17	2480 ± 140
Total Hardness	mg/L as $CaCO_3$	4462 ± 27	4665 ± 252
TDS	mg/L	8642 ± 50	9438 ± 237
TSS	mg/L	8.6 ± 1.2	15.2 ± 8.4
Total Sulfide	mg/L as S^{2-}	1.86 ± 0.21	0.93 ± 0.11

Canary Feed Water Quality

The two membrane element "canary" unit received its feed water from two second stage pressure vessels in Train C, each with six membrane elements. There are a total of fourteen second stage pressure vessels in each Train and out of this only the two lower vessels in Train C were tapped to feed the "canary" unit. The "canary" unit was to monitor fouling potential on the second stage and so comparisons were made to the average concentrate quality of the second stage and compare it to the quality of feed water to the "canary", in order to see if the feed to the "canary" is representative of the second stage. The tabulation of water quality for the second stage concentrate and the feed water to the "canary" unit at startup of this study at pH 5.80, is presented in Table 5-8. In all aspects the "canary" unit feed water was of higher concentration than the second stage concentrate except in the case of total sulfide content, where at the higher pH of the "canary" feed water, the total sulfide content is lower.

In Figure 5-8, the concentrate stream in Train C is depicted schematically. As shown in this figure the "canary" unit feed comes from 2 membrane pressure vessels in the second stage. Tracing the hydraulics of the feed to the "canary" shows that the head loss across the first and second stages and then the "canary" in this part of Train C, is higher than the rest of Train C, where the head loss is only across the first and second stages. The higher "canary" feed concentration can be explained by the fact that the feed stream that enters the membrane element becomes progressively more concentrated as the permeate passes through the membrane surface. Therefore the feed stream becomes more concentrated for successively elements. In this case of Train C, the segment of feed stream to the "canary" unit is longer in terms of both piping and

appurtenances as well as total membrane elements. At the same feed pressure, because of head losses, the feed stream to the “canary” becomes the path of highest resistance to permeate flow and so becomes more concentrated.

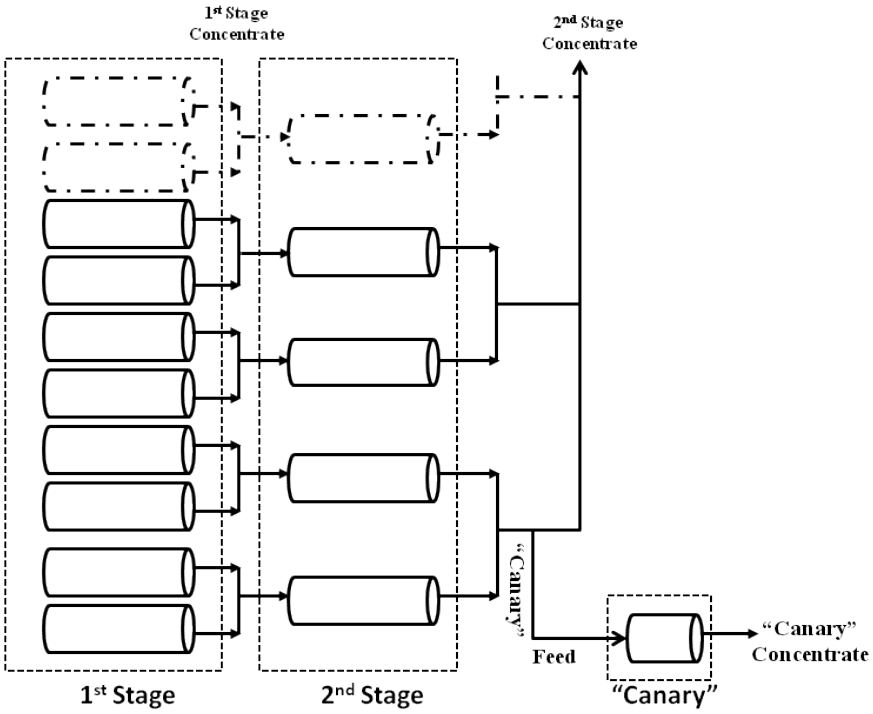

Figure 5-8: Schematic of Concentrate Stream in part of Train C

At the end of the acid elimination, at pH 7.10, the feed stream to the “canary” continued to be more concentrated than the second stage concentrate (i.e. total concentrate of membrane process). Overall this goes to show that using a “canary” unit as a monitoring device to track potential scaling in the second stage is very conservative, as the “canary” feed is more concentrated than the second stage concentrate and so the scaling potential on “canary” membrane elements is higher than the second stage elements.

Table 5-8: Comparison of 2nd Stage Concentrate and "Canary" Feed Water Quality at pH 5.80

Parameter	Units	pH=5.80	
		2nd Stage Conc.	**"Canary" Feed**
pH		6.33 ± 0.03	6.44 ± 0.09
Temp	°C	29.5 ± 0.3	29.3 ± 0.7
Turbidity	NTU	0.14 ± 0.02	0.15 ± 0.07
Conductivity	µS/cm	10435 ± 31	11076 ± 407
TOC	mg/L	4.20 ± 0.22	4.53 ± 0.44
SO_4^{2-}	mg/L	3580 ± 133	3926 ± 148
Cl^-	mg/L	1891 ± 179	1994 ± 55
Alkalinity	mg/L as $CaCO_3$	148 ± 2	149 ± 5
Ca	mg/L	944 ± 7	977 ± 30
Mg	mg/L	485 ± 3	499 ± 13
Si	mg/L	84.4 ± 0.2	87.2 ± 1.0
K	mg/L	19.0 ± 2.6	19.5 ± 2.3
Na	mg/L	967 ± 13	980 ± 18
Ba	µg/L	42.1 ± 0.9	43.2 ± 0.3
Mn	µg/L	< 10	< 10
Fe	µg/L	< 10	< 10
Sr	mg/L	97.6 ± 1.8	101 ± 1
Ca Hardness	mg/L as $CaCO_3$	2354 ± 17	2439 ± 74
Total Hardness	mg/L as $CaCO_3$	4462 ± 27	4576 ± 168
TDS	mg/L	8642 ± 50	9072 ± 323
TSS	mg/L	8.6 ± 1.2	11.5 ± 3.4
Total Sulfide	mg/L as S^{2-}	1.86 ± 0.21	1.60 ± 0.22

Table 5-9: Comparison of 2nd Stage Concentrate and "Canary" Feed Water Quality at pH 7.10

Parameter	Units	pH=7.10	
		2nd Stage Conc.	**"Canary" Feed**
pH		7.55 ± 0.12	7.61 ± 0.10
Temp	°C	27.7 ± 0.5	27.6 ± 0.4
Turbidity	NTU	0.18 ± 0.05	0.12 ± 0.03
Conductivity	µS/cm	12222 ± 292	12211 ± 361
TOC	mg/L	5.30 ± 0.05	5.18 ± 0.36
SO_4^{2-}	mg/L	3525 ± 119	3699 ± 164
Cl^-	mg/L	2400 ± 65	2504 ± 126
Alkalinity	mg/L as $CaCO_3$	531 ± 9	549 ± 6.3
Ca	mg/L	994 ± 56	983 ± 50
Mg	mg/L	502 ± 26	502 ± 27
Si	mg/L	81.3 ± 1.2	88.1 ± 14.4
K	mg/L	34.2 ± 1.5	34.6 ± 1.5
Na	mg/L	1121 ± 93	1169 ± 110
Ba	µg/L	48.7 ± 0.7	48.4 ± 2.7
Mn	µg/L	< 10	< 10
Fe	µg/L	< 10	< 10
Sr	mg/L	105.9 ± 4.3	109.5 ± 3.8
Ca Hardness	mg/L as $CaCO_3$	2480 ± 140	2452 ± 124
Total Hardness	mg/L as $CaCO_3$	4665 ± 252	4640 ± 233
TDS	mg/L	9438 ± 237	9355 ± 358
TSS	mg/L	15.2 ± 8.4	24.1 ± 8.3
Sulfide	mg/L as S^{2-}	0.93 ± 0.11	0.83 ± 0.14

Checking Scaling Potential

In Table 5-10 the "Canary" unit's LSI and RSI values were compared to that of Train C. These trends were monitored throughout the acid elimination process. The LSI values for Train C were also compared to earlier observed indices from the RO pilot study for the acid elimination. As the autopsy studies on the second stage membrane from the RO pilot showed no discernible fouling, comparing the evaluation using the two indices between the RO pilot and Train C would allay any concerns of fouling on the second stage of the RO plant. In the case of the LSI index, a more positive value indicates increasing scaling potential, while in the RSI index, as values get significantly below 6, the scaling tendency increases.

The LSI values for the concentrate on the RO pilot were higher at all pHs except marginally at ambient pH of 7.1 when compared to Train C. At the same time the RSI values for the RO pilot were consistently lower than that for Train C, except again marginally at pH 7.1.

In comparing the 'Canary" unit to Train C, similar trends were observed for both the LSI and RSI on the concentrates. The LSI index for both demonstrated a positive, increasing trend, indicating a shift from mild corrosion potential to moderate scale formation. The RSI calculations demonstrated a decreasing trend, which indicated a possible increase in scale tendency as the value decreased below 6.

Table 5-10: Comparison of RSI and LSI Values

Canary Pressure Vessel														
pH	**5.8**		**6.05**		**6.3**		**6.5**		**6.7**		**6.9**		**7.1**	
	Feed	Conc.	Feed	Conc.	Feed	Conc.	Feed	Conc.	Feed	Conc.	Feed	Conc.	Feed	Conc.
LSI	0.32	0.3	0.54	0.77	0.98	1.11	1.03	1.2	1.37	1.5	1.19	1.25	1.46	1.55
RSI	6.0	5.9	5.6	5.2	5.0	4.8	4.9	4.6	4.5	4.3	4.4	4.3	4.1	3.8
Train C - RO Plant														
pH	**5.8**		**6.05**		**6.3**		**6.5**		**6.7**		**6.9**		**7.1**	
	Feed	Conc.	Feed	Conc.	Feed	Conc.	Feed	Conc.	Feed	Conc.	Feed	Conc.	Feed	Conc.
LSI	-1.35	0.03	-1.08	0.52	-0.61	0.91	-0.5	0.99	-0.2	1.23	-0.77	0.81	0.12	1.7
RSI	8.7	6.3	8.3	5.6	7.7	5.1	7.6	5	7.2	4.7	8.0	5.7	6.8	4.1
RO Pilot														
pH	**5.8**				**6.3**			**6.6**					**7.1**	
	Feed	Conc.			Feed	Conc.		Feed	Conc.				Feed	Conc.
LSI	-1.37	0.06			-0.57	1.00		-0.13	1.25				0.38	1.61
RSI	8.6	6.2			7.6	5.0		7.1	4.7				6.4	4.2

Overall the use of LSI and RSI indices showed that calcium carbonate fouling potential on the Train C is probable but it will be at a rate lower or comparable to that noted in the RO pilot and it can be cleaned using low pH cleaners, as noted in Figure 5-3 and Figure 5-5 when the "canary" unit and Train C were cleaned.

Post-Treatment Options for RO Permeate

As the use of the acid in the pretreatment process was reduced, RO feed pH increased from pH 5.8 to the ambient raw feed water pH of about 7.1. This in turn resulted in the increase of the permeate pH. In Table 5-11, is the tabulation of the feed pH condition at the RO plant, and the resulting permeate pH and corresponding total sulfide concentration during the sampling period of the acid elimination study between June 2011 and May 2012. This same information is presented in Figure 5-9. On average basis the total sulfide content in the total permeate increased about 10 percentage from 3.2 mg/L as S^{2-} at the RO feed pH of 5.8 to reach about 3.5 mg/L as S^{2-} at RO feed pH of 7.1.

When factoring in the flow rate of each stream, the same total sulfide content in each stream is represented as mass flow rate in Figure 5-10.

Table 5-11: Comparison of Target Feed pH to Total Sulfide Concentration and Permeate pH

Target RO Feed pH	1st Stage Permeate		2nd Stage Permeate		Total Permeate	
	pH	S^{2-} (mg/L)	pH	S^{2-} (mg/L)	pH	S^{2-} (mg/L)
5.8	5.50 ± 0.03	3.18 ± 0.15	5.49 ± 0.02	2.67 ± 0.45	5.47 ± 0.04	3.21 ± 0.14
6.05	5.61 ± 0.05	3.12 ± 0.14	5.59 ± 0.03	2.77 ± 0.21	5.68 ± 0.03	3.07 ± 0.07
6.3	5.82 ± 0.04	3.89 ± 0.11	5.90 ± 0.03	2.55 ± 0.15	5.83 ± 0.06	3.26 ± 0.0
6.5	5.76 ± 0.01	4.50 ± 0.29	5.72 ± 0.01	2.15 ± 0.0	5.77 ± 0.01	3.38 ± 0.14
6.7	5.99 ± 0.01	4.36 ± 0.28	5.83 ± 0.11	2.18 ± 0.0	5.81 ± 0.04	3.51 ± 0.07
6.9	5.94 ± 0.07	4.37 ± 0.36	5.97 ± 0.0	1.75 ± 0.15	5.98 ± 0.06	3.45 ± 0.07
7.1	6.41 ± 0.12	4.45 ± 0.27	6.35 ± 0.19	1.75 ± 0.14	6.46 ± 0.13	3.43 ± 0.27

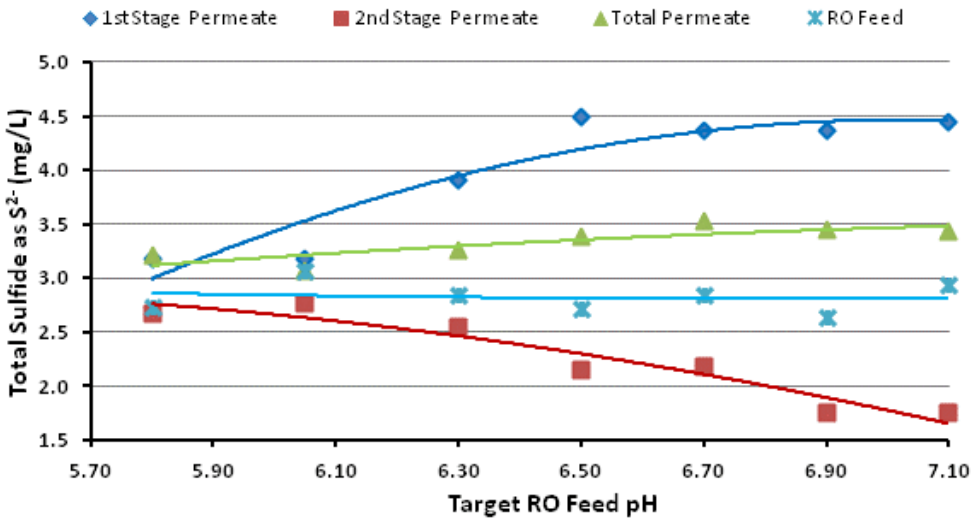

Figure 5-9: Total Sulfide Concentration as RO Feed pH is Increased.

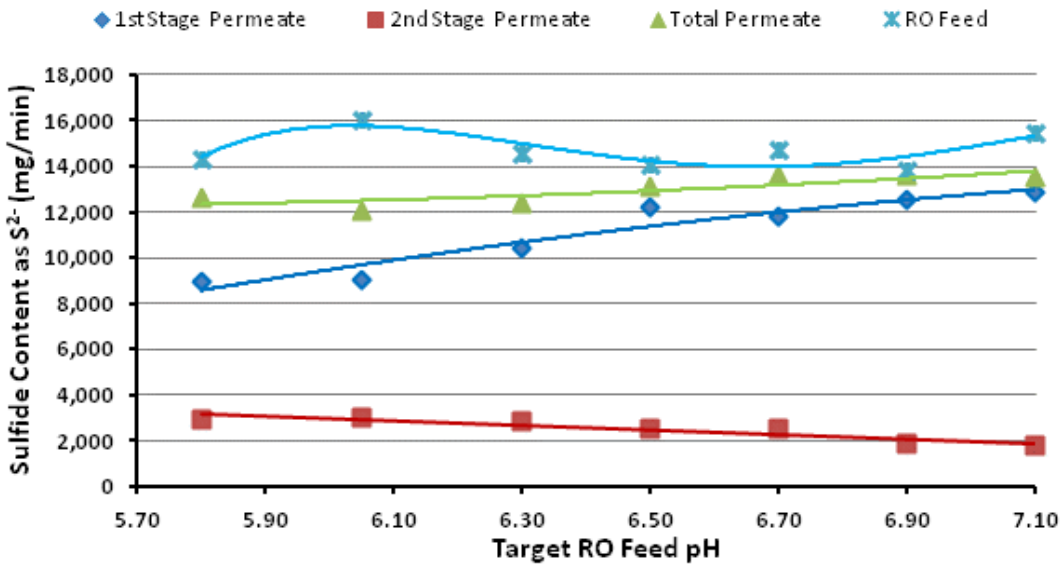

Figure 5-10: Mass Flow Rate of Total Sulfide as RO Feed pH is Increased

The molecular structure of water (H_2O) is similar to H_2S as shown in Figure 5-11. The bond angle in water is 104.5° while that of H_2S is 92.5°, and the O—H bond is stronger in comparison to the compared to the S—H bond. This overall makes H_2S more reactive than water (Tro, 2008).

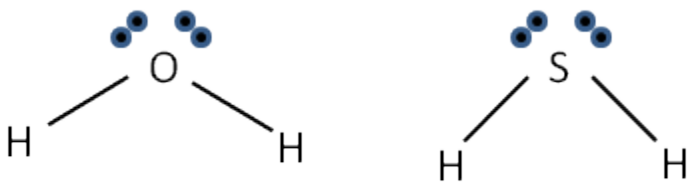

Figure 5-11: Molecular Structures of Water and Hydrogen Sulfide

The first stage of the RO plant uses the Hydranautics CPA2-4040 membranes which are hydrophilic (i.e. “water loving”) membranes. The Hydranutics ESPA2-4040 membranes are used in the second stage of the RO plant and the canary unit, and are known to be more hydrophobic. At the lower RO feed pH and 1st Stage permeate pH, more of the total sulfide in the form of H_2S, is being carried into the permeate stream, via the more hydrophilic membrane.

The difference in the total sulfide content between the RO feed and the total permeate streams as shown in Figure 5-10, is the amount of total sulfide that is passed into the concentrate stream. As the acid elimination progressed, lesser amounts of total sulfide is passed into the concentrate stream of the RO process. The well combinations have been variable during the period of the study, and the highest RO feed total sulfide loading was about 16 grams per min (g/min) as noted on Train C of the RO plant. At pH 7.1, the total sulfide loading in the total permeate stream was about 14 g/min.

The total permeate pH increased by about 1 pH unit to 6.5, by the time the acid use in the pretreatment was completely discontinued. The total sulfide concentration in the total permeate at pH 7.1 is about 3.5 mg/L as S^{2-} , and at an average total permeate pH of 6.5, close to pK_1 of 6.99 (see Figure 3-3), about 75% of the total sulfide exists as H_2S and the remaining as HS^-. The fraction of total sulfide, in the form of H_2S and HS^- in the total permeate stream, as the RO feed pH is adjusted upwards is shown in Figure 5-12.

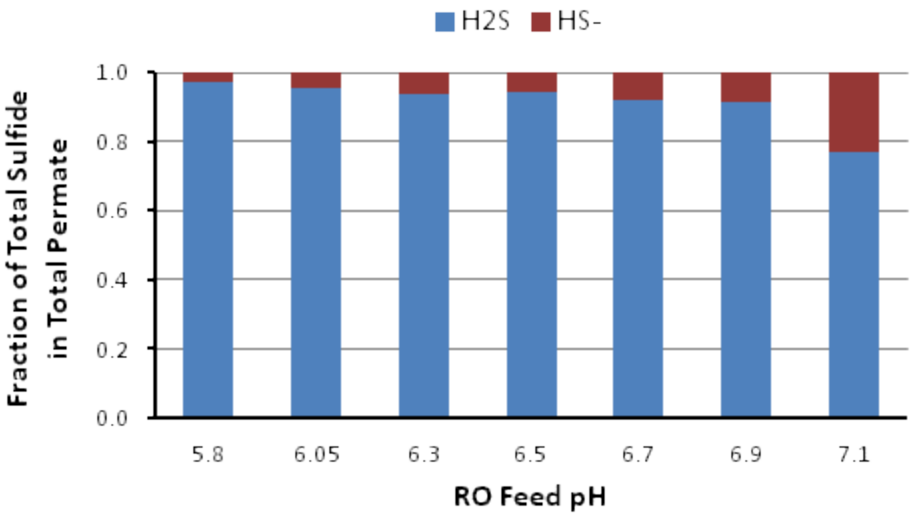

Figure 5-12: Fraction of Total Sulfide as H_2S and HS^- in Total Permeate as pH Varied

The fraction of HS^- increased from about 3% at pH 5.8 to about 23% at the RO feed pH of 7.1. This observation is comparable to the estimated HS^- content as per the sulfide speciation chart in Figure 3-3, at about 25%. The total permeate from the RO plant is then channeled through the degasifiers, and H_2S is vented out of the permeate into the air stream, the proportion of H_2S and HS^-, in the degasified permeate stream changes significantly and is as shown in Figure 5-13.

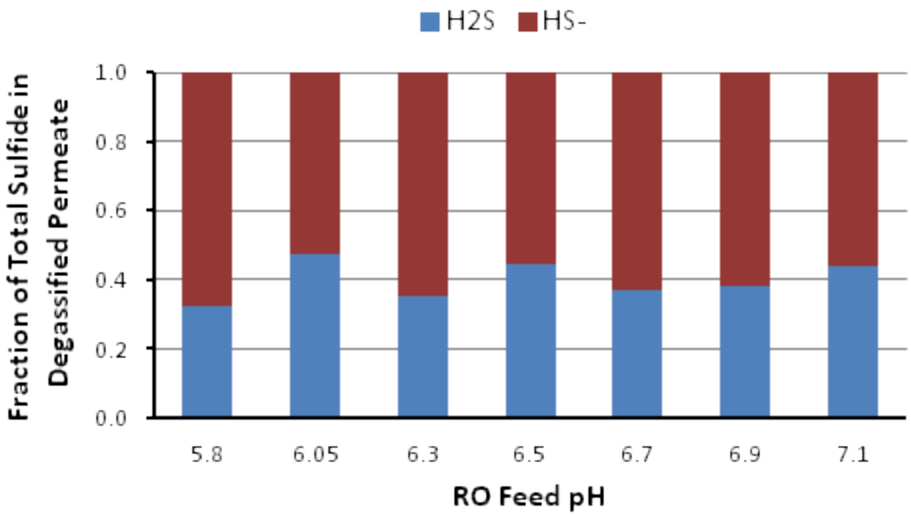

Figure 5-13: Fraction of Total Sulfide as H_2S and HS^- in Degasified Permeate Water Stream as pH Varied

At pH 5.8, the fraction of HS^- in the degasified permeate is about 68% of the total sulfide, and at pH 7.1 the fraction of HS^- is about 55%. One of the reasons for the higher fraction of HS^- at pH 5.8, is the lower permeate pH, allowing more of the H_2S to be vented out of water leaving the proportion of HS^- to be higher in the degasified permeate stream. The mass loading of sulfide content in the degasified permeate is as shown in Figure 5-14. Another reason for the higher fraction of HS^- , is that as more of the dissolved CO_2 in lost from the water to the atmosphere in the aeration process, it will result in higher pH of the permeate as it goes through the degasifier, thereby converting some fraction of the H_2S species to HS^- species.

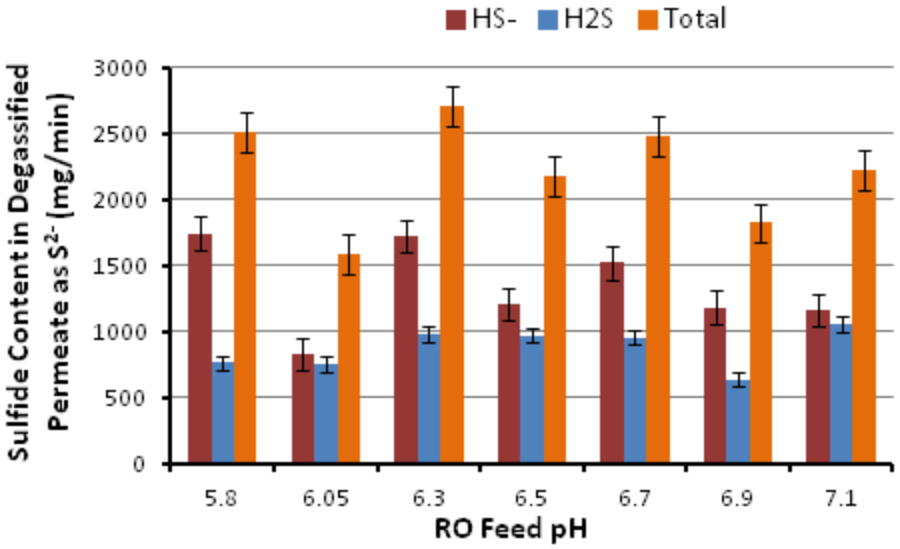

Figure 5-14: Mass Fraction by Sulfide Species in Degasified Permeate Stream as pH Varied

At RO feed pH 7.1 about 2.2 g/min of total sulfide is present in the degasified permeate, of which about 1.2 g/min (about 55 %) is in the form of HS^- . The mass loadings of total sulfide content in the total permeate and degasified permeate streams are as shown in Figure 5-15. The degasifiers were maintaining very high removal efficiencies for total sulfide. The data as observed in this study shows that at pH 7.1 the removal efficiency of total sulfide in the degasifiers is about 85%, which is slightly higher than the 80% at pH 5.8. However the proportion of H_2S and HS^- in the total permeate (TP) and degasified permeate (DP) streams vary significantly as noted in Figure 5-12 and Figure 5-13, and the mass loading comparison is as shown in Figure 5-16.

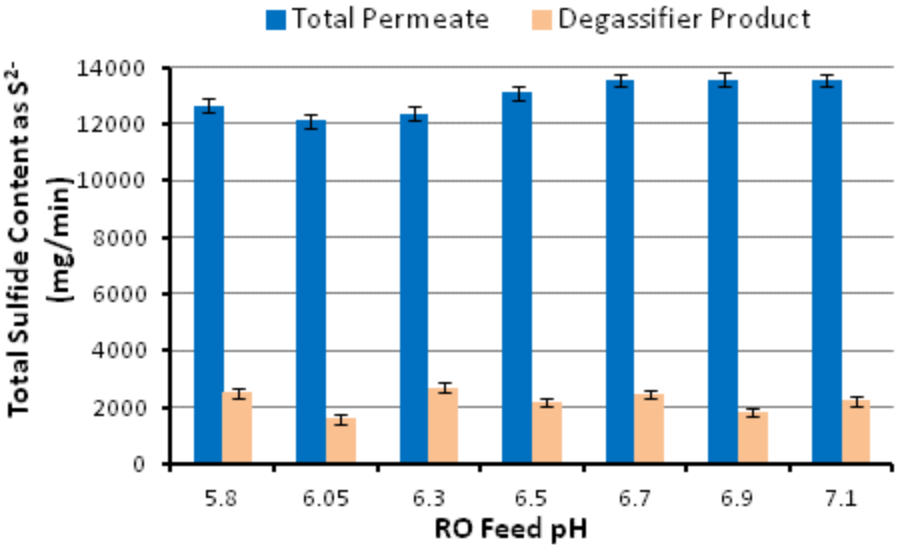

Figure 5-15: Mass Loading in terms of Total Sulfide in the Total Permeate and Degasified Permeate Streams.

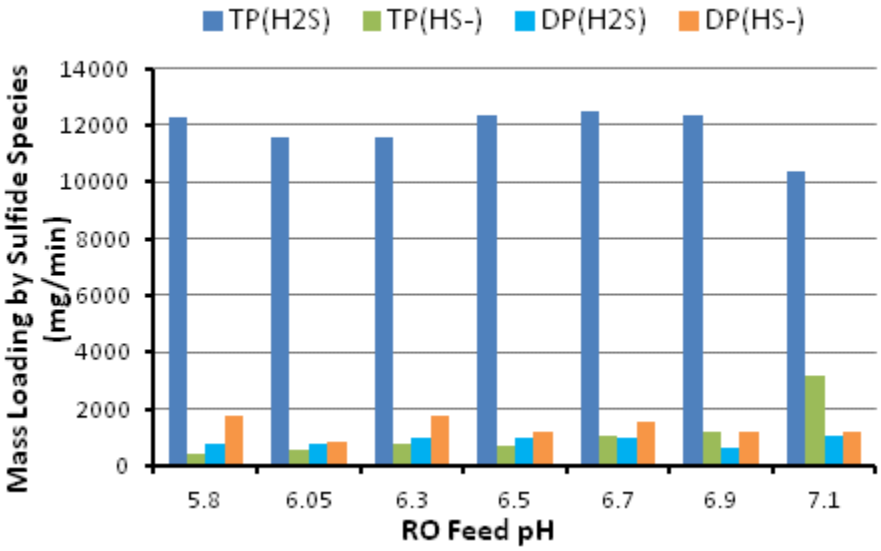

Figure 5-16: Mass Loading in terms of H_2S and HS^- in the Total Permeate and Degasified Permeate Streams

The efficiency of the degasifier depends on the air-water ratio. Though the City normally operates both its RO permeate degasifiers, the City's RO plant is not operating at its capacity of 4.5 MGD. In year 2010 and 2011 the City's RO plant produced on average 3.8 MGD and 3.6 MGD of RO permeate respectively. The variability of the permeate production will mean that at times the air-water ratio in the degasifier may be higher resulting in more stripping of H_2S, while at other times the H_2S stripping efficiency may be lower. In this study the variability of RO permeate production was not monitored but the H_2S removal efficiency in the degasifier is noted be very high, as seen in Figure 5-16 and Table 5-12.

Table 5-12 : Change in H_2S and HS^- Loading Post-Degasifier at pHs 5.8 and 7.1

pH	**Average H_2S Loading (g/min)**			**Average HS^- Loading (g/min)**		
	TP	**DP**	**Change (%)**	**TP**	**DP**	**Change (%)**
5.8	12.3	0.8	- 94	0.4	1.7	+325
7.1	10.4	1.1	- 90	3.2	1.2	-63

Another factor in the removal of total sulfide in the degasifier, is the presence of aerobic bacteria like *Beggiatoa* and *Thiothrix* that oxidize reduced sulfide (i.e. both H_2S and HS^-) to elemental sulfur and subsequently to sulfate (Gottschalk, 1986). *Beggiatoa* and *Thiothrix* derive energy from the oxidation of reduced sulfide, but require organic carbon for growth (Atlas, 1984). Though RO processes remove very high fractions of organic carbon in water, traces of organic carbon can still be noted in RO permeates (Kegel, Rietman, & Verliefde, 2010), and be food source to the aerobic bacteria. As seen in Table 5-12, the average HS^- loading at pH 7.1 post degasifier has decreased by almost 63%, even though, the degasifiers are targeted at primarily

stripping H_2S. This would mean that the aerobic bacteria are removing a combination of H_2S and HS^- and multiplying in the degasifiers on the surface of the packing materials. The resulting problem of the increased aerobic bacteria activity is the sloughing off of these organisms from the surfaces of the packing materials, that would cause increased turbidity downstream (Duranceau, Trupiano, Lowenstine, Whidden, & Hopp, 2010b). The average loading in terms of HS^- , reduced post-degasifiers as the RO feed pH increased from 5.8 to 7.1, but the average H_2S loading increased post-degasifier, at the same time. The turbidity post-degasifier increased significantly at pHs 6.9 and 7.1, compared to the lower feed pH conditions, as shown in Figure 5-17.

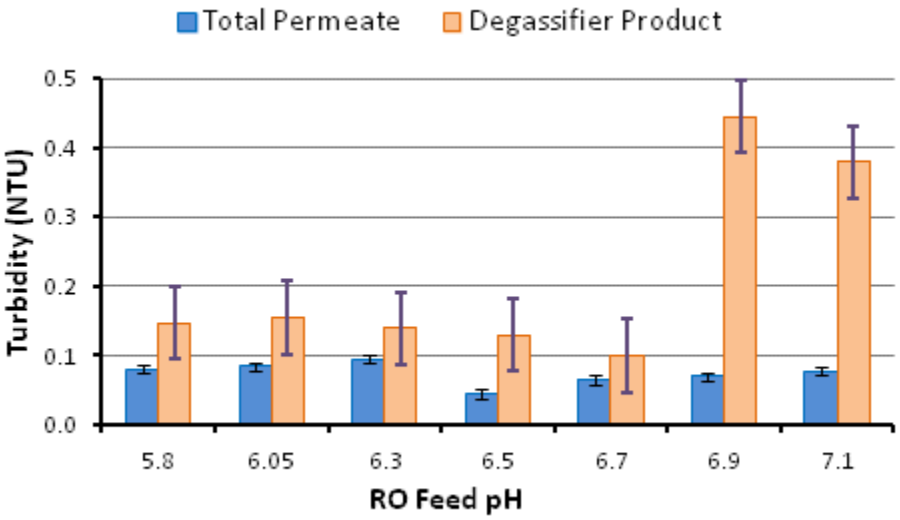

Figure 5-17: Comparison of Permeate Turbidity Pre and Post Degasifier

The post-degasifier turbidity is high probably due to the sloughing off of aerobic bacteria from the packing material as more of the reduced sulfide is converted to sulfate. The excess sulfide in the form of H_2S (1.1 g/min per operational RO train of 1.5MGD) and HS^- out the degasifier (1.2 g/min per operational RO train of 1.5MGD) will react with the hypochlorite used in the disinfection process and potentially form about 2.2 g/min (per operational RO train of 1.5MGD) of sulfur turbidity in the form of colloidal sulfur (S^0), as shown in Equation 3-25 and 3-26. Based on data collected in this study, at pH 5.8 assuming that all the H_2S and HS^- are converted to S^0, instead of to sulfate, the colloidal sulfur formation rate would be higher at 2.3g/min (per operational RO train of 1.5MGD). However, the additional sloughing off of biological mass would add to the increased turbidity overall following the elimination of acid in the pretreatment to the RO feed, and this could explain the higher turbidity post-acid elimination at pHs 6.9 and 7.1.

One of the options to control turbidity for the City will be to increase its frequency of cleaning its degasifiers, to control the sloughing off of biological material. Another option would be to suppress the feed pH of the total permeate to the degasifiers, to increase the proportion of H_2S in the feed stream to the degasifier, thereby enhancing the removal of more of the total sulfide in the form of H_2S. Acidifying the total permeate to the degasifier, will reduce the proportion of HS^-, thereby possibly helping to reduce the multiplication of aerobic bacteria on the packing material in the degasifiers.

If the City is considering the option of lowering the RO permeate feed pH to the degasifier, the use of carbonic acid is recommended as it would not suppress the alkalinity in the water but in

fact add to the buffering capacity of the water, thereby reducing the need for post-degasifier addition of caustic to increase pH before supply (Duranceau S. J., 2009). The City has been using about 83mg/L of sulfuric acid on average to suppress its feed water pH to the RO plant. In the case of the City, instead of dosing sulfuric acid to 6 MGD of feed water, it will only need to acidify the 4.5 MGD of RO permeate. Furthermore, the amount of acid required to depress the permeate pH to the baseline pH of 5.5 (permeate pH pre-acid elimination) from about pH 6.5 , will only be a fraction of the amount of acid required on the RO feed, as the RO permeate has a lower buffering capacity. The lower buffering capacity in the RO permeate is because the bicarbonate and carbonate species that contribute to alkalinity are rejected during the RO treatment. It is estimated that a carbonic acid dose of about 12 $\pm$ 3 mg/L will be required to suppress the permeate pH before the degasifier to pH 5.5.

Economic Analysis of Acid Elimination

The primary driver is the City exploring the viability of operating its RO plant without use of acid in the pretreatment process, was the fluctuating bid prices that the City received from its supplier since 2007. In Table 5-13, is the unit bid price of sulfuric acid to the City between Sep 1007 and Dec 2012.

The RO plant has a capacity of 4.5 MGD, but between 2009 and 2012 the City's RO plant has not been producing at its full capacity as seen in Table 5-14. During this period the highest average daily production was 3.8 MGD in 2010.

Table 5-13: Unit Price of Sulfuric Acid to City

Acid Bid Period		Price/Ton ($)
Sep-1997	Sep-2007	60.00[1]
Oct-2007	Jun 2008	78.80
Jul-2008	Dec-2008	138.00
Jan-2009	Mar-2010	343.91
Apr-2010	Mar-2011	139.50
Apr-2011	Oct-2011	134.50
Nov-2011	Dec-2012	159.50

Table 5-14: RO Permeate Production

RO Permeate Sum/MONTH (MG)				
	2009	**2010**	**2011**	**2012**
Jan	116.7	127.3	106.4	110.4
Feb	103.2	96.9	100.0	116.6
Mar	128.9	105.4	119.0	137.9
Apr	105.5	110.6	118.6	131.5
May	99.1	126.6	117.3	136.3
Jun	92.3	122.2	116.0	119.1
Jul	96.0	118.1	110.3	
Aug	98.8	117.7	110.3	
Sep	97.9	116.5	101.4	
Oct	109.7	125.0	109.0	
Nov	189.3	115.6	99.8	
Dec	104.3	114.1	100.9	
Year Total (MG)	1341.6	1395.8	1308.9	751.9
Daily Ave. (MGD)	3.7	3.8	3.6	4.1

The information of permeate production was used to co-relate the corresponding use of sulfuric acid in the pretreatment to the RO plant. The daily sulfuric acid use between 2009 and the end of acid use in pretreatment to RO plant on Feb 20, 2012, is tabulated in Table 5-15 .

[1] Based on previous 10-year average of acid bid prices to City

Table 5-15: Tabulation of Acid Use and Expenditure on Acid Since Year 2009

Period	Acid Use (Gal)	Acid Use (lbs)	Acid Use (Tons)	Price/Ton	Cost	Year Total Cost	Daily Ave. Cost
Jan - Dec 2009	81378	1249152	624.6	343.91	$214,798	$214,798	$588.49
Jan - Mar 2010	19994	306908	153.5	343.91	$52,774	$122,467	$335.53
Apr - Dec 2010	65093	999178	499.6	139.50	$69,693		
Jan - Mar 2011	20399	313125	156.6	139.50	$21,840	$47,105	$253.25
Apr - 5 Jul 2011	24474	375676	187.8	134.50	$25,264		
6 Jul - Oct 2011	13211	202789	101.4	134.50	$13,638	$17,110	$95.59
Nov - 31 Dec 2011	2837	43548	21.8	159.50	$3,473		
1 Jan – 20 Feb 2012	2364	36287	18.1	159.50	$2,894	$2,894	$56.74

In 2009, when the supplier's price of acid to the City was a high $343.91/ton, the total expenditure on sulfuric acid during the year was about $215,000. In 2010, the expenditure was about $122,000 and in 2011 before the acid elimination in stages started on Jul 5, 2011, the total expenditure was about $47,000. Between Jul 6, 2011 and Feb 20, 2012, when the acid used was being tapered down the total expenditure on acid was about $20,000. Savings were already being realized by the City while the acid elimination progressed over 12 months. The computation of the average acid consumption between 2009 and Jun 2012 is shown in Table 5-16. The average use of sulfuric acid in the RO plant is about 0.46 ton per million gallon (MG) of permeate produced.

Table 5-16: Computation of Average Acid Use per MG of Permeate Production

Timeframe	**Acid Use (Tons)**	**Permeate Production (MG)**	**Average Acid Use (tons/MG)**
Year 2009	625	1342	0.466
Year 2010	653	1396	0.468
Year 2011 (1 Jan -30 Jun)	285	677	0.421
Average per day	1.77	3.88	0.460

The tabulation of cost savings as the acid elimination progressed is tabulated in Table 5-17 . The projected expenditure on acid reflects the expenditure that would have been incurred at the prevailing acid bid price, if the acid use was not progressive discontinued. The actual expenditure on acid use is extracted from Table 5-15. If the average permeate production at the RO plant is about 3.5 MGD for the period Jul – Dec 2012, the projected savings realized from the acid elimination project by end Yr 2012, will be about $123,000 at prevailing acid bid prices.

Table 5-17: Projected Savings from Acid Elimination Project

Timeframe	Permeate Production (MG)	Projected Acid use @ 0.46tons/MG	Projected Expenditure on Acid ($)	Actual Expenditure on Acid Use ($)	Estimated Savings ($)
6 Jul – Oct'11	415	191	25,700	13,600	12,100
Nov'11-Jun'12	952.5	438	69,900	6,400	63,500
Jul- Dec'12[1]	644	296	47,300	-	47,300
				Total Savings	122,900

If the City chooses to suppress the RO permeate pH to the degasifier to about pH 5.5 (i.e. the pre-acid elimination permeate pH), it is anticipated that at prevailing carbonic acid supply price of $160/ton, the City will have an annual operating expenditure of about $13,000 at full production of 4.5 MGD. Off-setting this expenditure from the $120,000 annual savings from eliminating sulfuric acid use in the pretreatment for the same 4.5 MGD of full capacity production, would result in net savings of about $107,000 annually.

Over and above the direct savings from the non-use of acid, other additional savings come from the reduced maintenance and replacement costs on the storage system, piping, fittings, pumps, appurtenances and instruments on the sulfuric acid injection system. The savings in manpower time and cost in complying with Occupational Safety and Health Administration (OSHA) requirements in dealing with the supply and handling of sulfuric acid is another additional benefit to the City.

[1] Projected savings from non-use of sulfuric acid in pretreatment based on 3.5 MGD permeate production.

RO Performance Monitoring using Electrical Conductivity and Total Dissolved Solids Relationship

In developing one proprietary software to trend and monitor RO membrane processes, Saad (2004), highlighted the problems faced by operators in monitoring membrane system performance and detecting membrane scaling and/or fouling. Trending and monitoring in accordance to the standard method ASTM D-4516, was pointed out to be difficult as it involved collection of large amounts of data. The ASTM method of performance monitoring was developed by DuPont and is considered to be more representative of DuPont's membranes. This method requires a large amount of data to arrive at log mean average concentrations to input into equations provided and does not consider factors that affect mass transfer like fluxes, recoveries, foulants and temperature (Zhao & Taylor, 2005b). The proprietary system (Fouling Monitor™) by Saad, uses a database of historical data from many major membrane plants, to trend alongside the ASTM D-4516 method of trending to warn/advice operators of potential fouling. This proprietary system therefore requires the inputs of specific data as well the cumbersome amount of data that the ASTM D-4516 method requires.

The trending and monitoring of the RO pilot and full scale RO plant's Train C in this study were done using the Homogeneous Solution Diffusion Model (HSDM) with Equations 3-34 through 3-39. Combining Equations 3-34 through Equation 3-37, the normalized MTC for permeate (K_W) can be re-written as Equation 5-1.

$$K_W = \frac{Q_P}{\text{Area} \times 1.03^{(T-25)} \times \left\{\left[\frac{1}{2}(P_f+P_c)+P_p\right] - 0.01 \times \left[\frac{1}{2}(C_f+C_c)-C_p\right]\right\}} \quad (5\text{-}1)$$

From Equation 5-1, it can be noted that the continuous trending to monitor the permeate flux is dependent on continuous monitoring of the feed, concentrate and permeate TDS concentrations. Therefore the variation in TDS is the critical parameter of importance, in being able to trend the MTC. As TDS concentration increases, it will mean that the osmotic pressure component of the TMP also increases, resulting in the RO process needing to overcome this osmotic pressure, by increasing the driving pressure, to provide an acceptable flux through the membrane (Fuqua, Bowen, & Creighton, 1991). It is common practice to use TDS measurements, in the monitoring of the K_W on a membrane plant, as it is representative of the anions and cations in water. While permeate flowrate, temperature and pressure measurements can be logged continuously and accurately using some of the very advanced equipments and instruments, the direct measurement of TDS is still not feasible. The common practice is to use relationship between electrical conductivity (EC), more commonly known as conductivity, and TDS. EC is related to TDS by a constant, which is shown as the C_2T ratio (i.e. EC to TDS ratio) in Equation 5-2.

$$\mathrm{TDS} = (C_2T) * \mathrm{EC} \tag{5-2}$$

In order to be able to monitor the K_W by each stage, using the EC readings and relating it to TDS, EC measurements are necessary on the RO plant at 5 locations: feed, 1st Stage Permeate, 1st Stage Concentrate, 2nd Stage Permeate and 2nd Stage Concentrate (or also known as Total Concentrate). However, on the RO plant, online EC measurements were only available on 4 locations but not for the 2nd Stage Concentrate. For the "canary" unit, thrice daily EC measurements were done by plant operators. The schematic showing the EC monitoring locations is as shown in Figure 5-18.

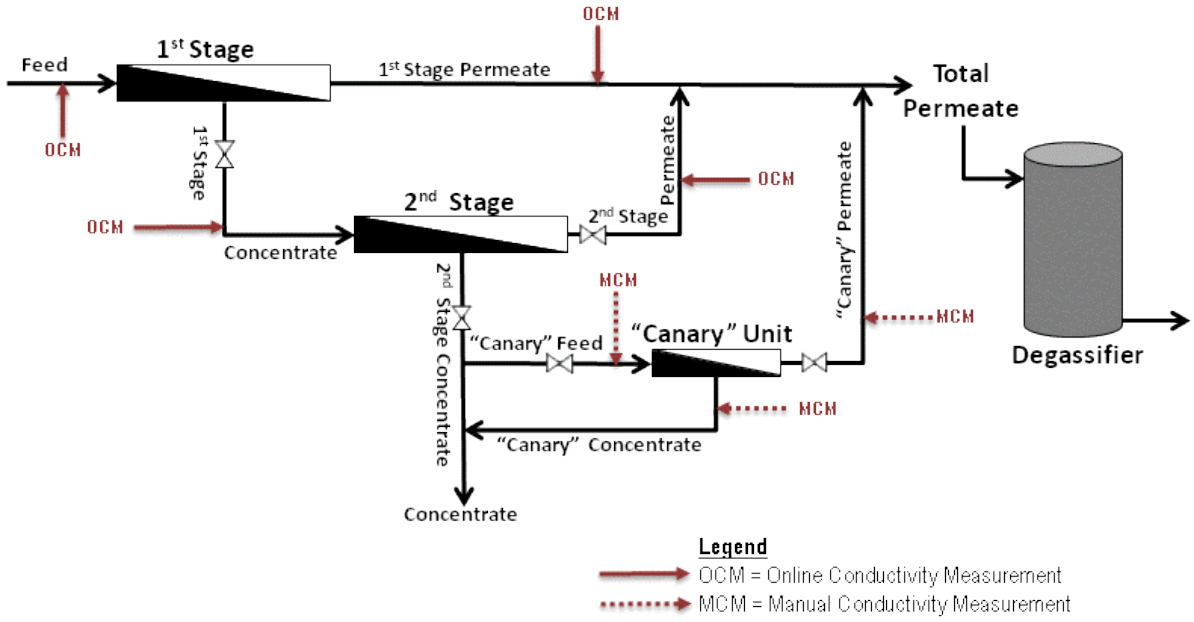

Figure 5-18: Conductivity Monitoring on RO Plant and "Canary' Unit

As samples were collected at the plant for TDS enumeration in UCF laboratories, field measurements of EC for the same water streams were carried out. The EC measurements and TDS results were co-related for each pH condition and the C_2T ratios is tabulated in Table 5-18 for the RO plant and Table 5-19 for the "canary" unit. As the RO plant and "Canary" were cleaned on Dec 14, 2011 at pH 6.7, the C_2T ratios pre and post-cleaning are tabulated separately in the tables.

Table 5-18: EC to TDS Ratio for RO Plant

Target Feed pH	RO Feed	1st Stage Permeate	1st Stage Concentrate	2nd Stage Permeate	Total Concentrate
5.80	0.68	0.72	0.75	0.45	0.83
6.05	0.67	0.75	0.73	0.46	0.80
6.30	0.65	0.73	0.70	0.42	0.78
6.50	0.66	0.75	0.69	0.44	0.76
6.70[1]	0.63	0.75	0.67	0.44	0.74
6.70[2]	0.67	0.70	0.75	0.52	0.76
6.90	0.63	0.69	0.68	0.49	0.76
7.10	0.65	0.69	0.70	0.44	0.77
Ave.	**0.65**	**0.72**	**0.71**	**0.46**	**0.77**

Table 5-19: EC to TDS Ratio for "Canary" Unit

Target Feed pH	Canary Feed	Canary Permeate	Canary Concentrate
5.80	0.82	0.55	0.83
6.05	0.80	0.36	0.81
6.30	0.78	0.43	0.79
6.50	0.77	0.40	0.78
6.70[1]	0.78	0.37	0.79
6.70[2]	0.80	0.54	0.80
6.90	0.77	0.41	0.79
7.10	0.77	0.47	0.78
Ave.	**0.78**	**0.44**	**0.79**

[1] Samples tested before Train C cleaning on Dec 14, 2011 at pH 6.70
[2] Samples tested after Train C cleaning on Dec 14, 2011 at pH 6.70

The C_2T obtained from field measurements are used to convert the online EC measurements recorded on the RO plant, to TDS values which are then inputted into Equation (5-1, to obtain the K_W values, which is then graphed and trended. As the total concentrate (or second stage concentrate) conductivity measurements were not logged, a conductivity balance approach was used to derive the conductivity values as shown in Equation 5-3.

$$EC_{C2} = \frac{(EC_{C1} \times FLOW_{C1}) - (EC_{P2} \times FLOW_{P2})}{FLOW_{C2}} \quad (5\text{-}3)$$

Where:

EC_{C2} – 2nd stage concentrate conductivity (µs/cm)
EC_{C1} – 1st stage concentrate conductivity (µs/cm)
EC_{P2} – 2nd stage permeate conductivity (µs/cm)
$FLOW_{P2}$ – 2nd stage permeate flow (gal/min)
$FLOW_{C1}$ – 1st stage concentrate flow (gal/min)
$FLOW_{C2}$ – 2nd stage concentrate flow (gal/min)

The EC values obtained by for the total concentrate stream using Equation (5-3, was compared with actual field measurements taken during this research study and were found to be between -5 and +4 % accuracy.

Similar C_2T tabulation was done for the field conductivity and laboratory measurement of TDS during the RO pilot study phase to eliminate acid use in pretreatment. The tabulation is presented in Table 5-20.

Table 5-20: EC to TDS Ratio for RO Pilot

Target Feed pH	RO Feed	1st Stage Permeate	1st Stage Concentrate	2nd Stage Permeate	Total Concentrate
5.80	0.72	0.71	0.80	0.40	0.89
6.30	0.73	0.76	0.83	0.35	0.89
6.60	0.70	0.71	0.81	0.37	0.87
7.10	0.74	0.81	0.84	0.36	0.94
Ave.	**0.72**	**0.75**	**0.82**	**0.37**	**0.90**

On the RO pilot, online conductivity measurements were only available for the feed and total permeate streams. Hence weekly or fortnightly TDS sampling was used as basis to obtain the K_W and the TDS value was assumed to be representative of the pilot's operations during the window between sampling.

When comparing the trend of the C_2T ratio tabulated, it can be seen that one single ratio is not practical for the computation and trending of the normalized MTC for all the streams. It can be observed that as the water stream gets concentrated, the C_2T ratio increases. On the other hand, the C_2T ratio for the second stage permeate is lower than in the case of the first stage permeate. Furthermore, the average C_2T ratio was higher and different in all cases on the RO pilot as compared to the RO plant, except for the second stage permeate where it was lower.

In this study, as pH of feed water was a variable, the K_W was monitored and trended for the RO plant and "canary" unit using the average C_2T ratio under each pH condition and is presented in Figure 5-3 and Figure 5-5 respectively. Both these figures were updated, for the project duration and the K_W compared to that using the single averaged C_2T ratio for each stream over the whole project duration. The comparison of the K_W on the RO plant using the moving average and single averaged C_2T ratio are shown in Figure 5-19 and Figure 5-20 respectively.

Though the trend of the K_W is somewhat similar when using both methods, it is noted that when using the single average C_2T ratio, the K_W is lower at pH 5.8 as compared to pH 7.1. Intuitively looking at the overall trend after the whole acid elimination plan is complete, it can be understood that this was not possible, as the elimination of acid in the pretreatment was expected to reduce the permeate flux rate as scaling potential on the membrane increased.

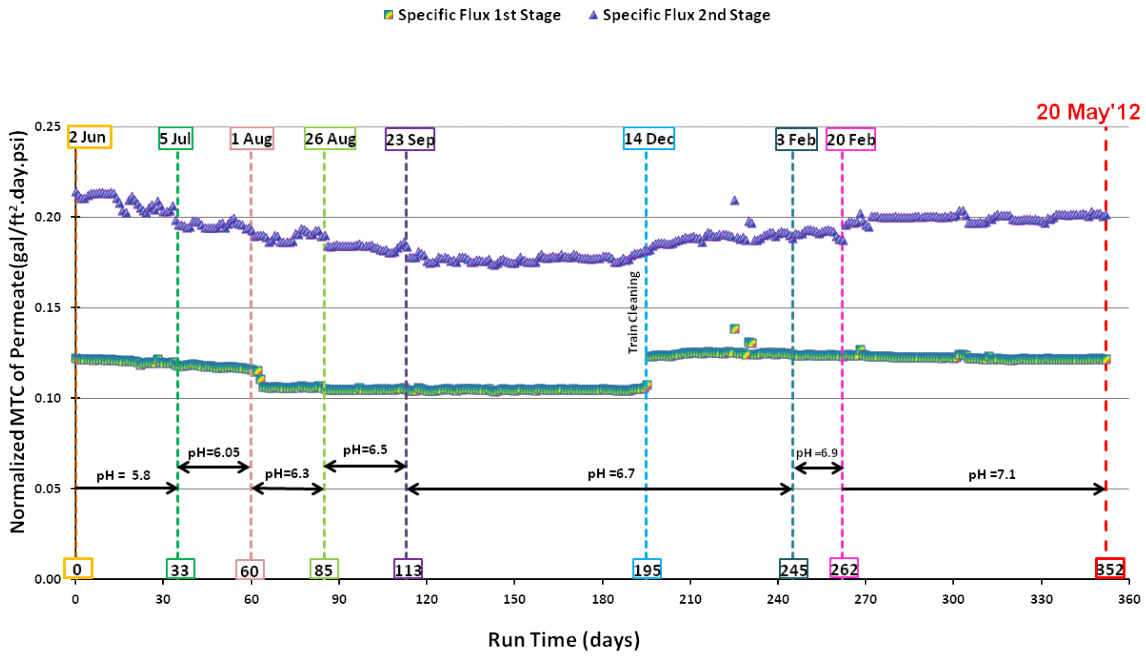

Figure 5-19: Normalized K_W of RO Plant Using Moving Average of C_2T Ratio as pH Varied

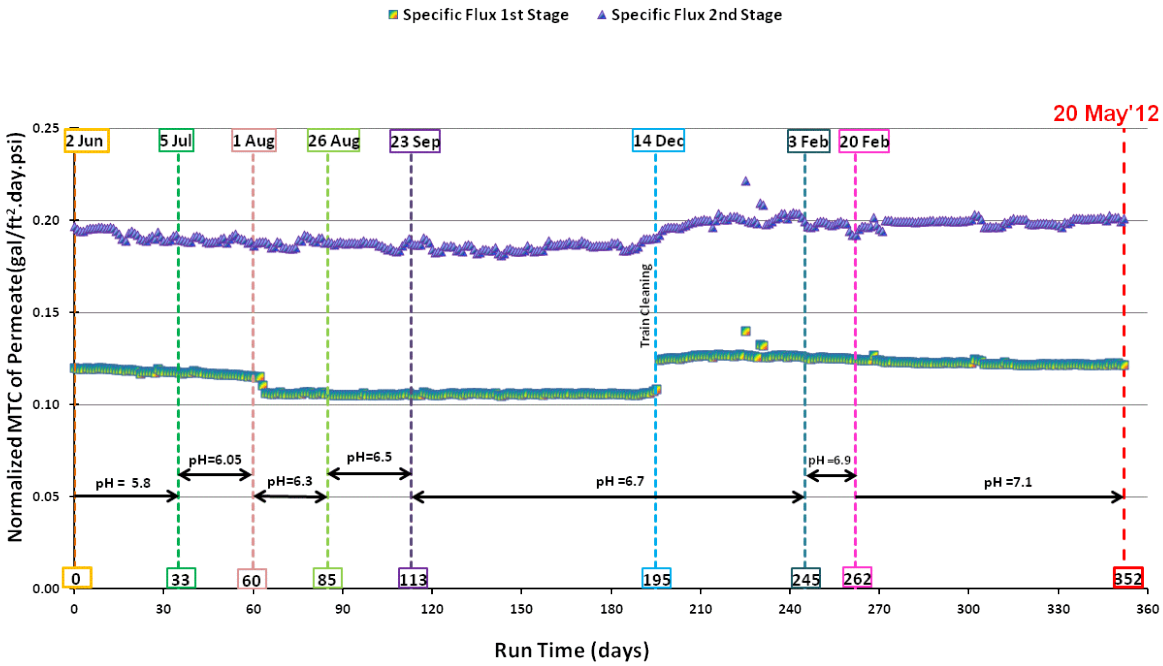

Figure 5-20: Normalized K_W of RO Plant Using Average of C_2T ratio

The comparison of the K_W on the "canary" unit using the moving average and single averaged C_2T ratio are shown in Figure 5-21 and Figure 5-22 respectively. In this case when using the single averaged C_2T ratio, the trend of the K_W is 50 per cent lower at startup of the "canary", and is similar across all pH conditions, which again is not representative of the conditions on the canary unit's membranes as acid is eliminated.

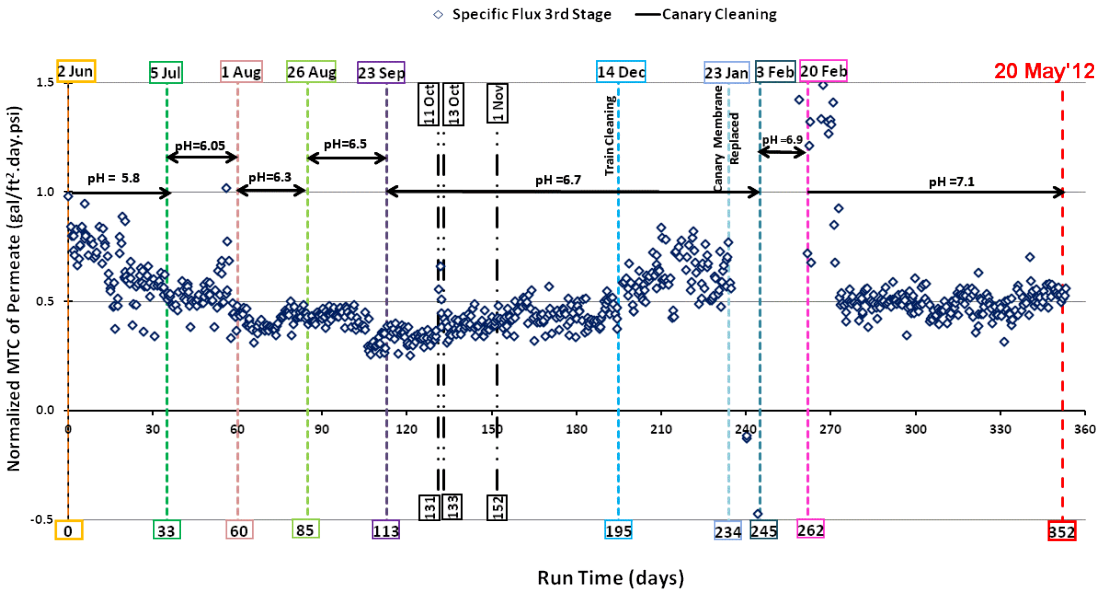

Figure 5-21: Normalized K_W of "Canary" Unit Using Moving Average of C_2T Ratio as pH Varied

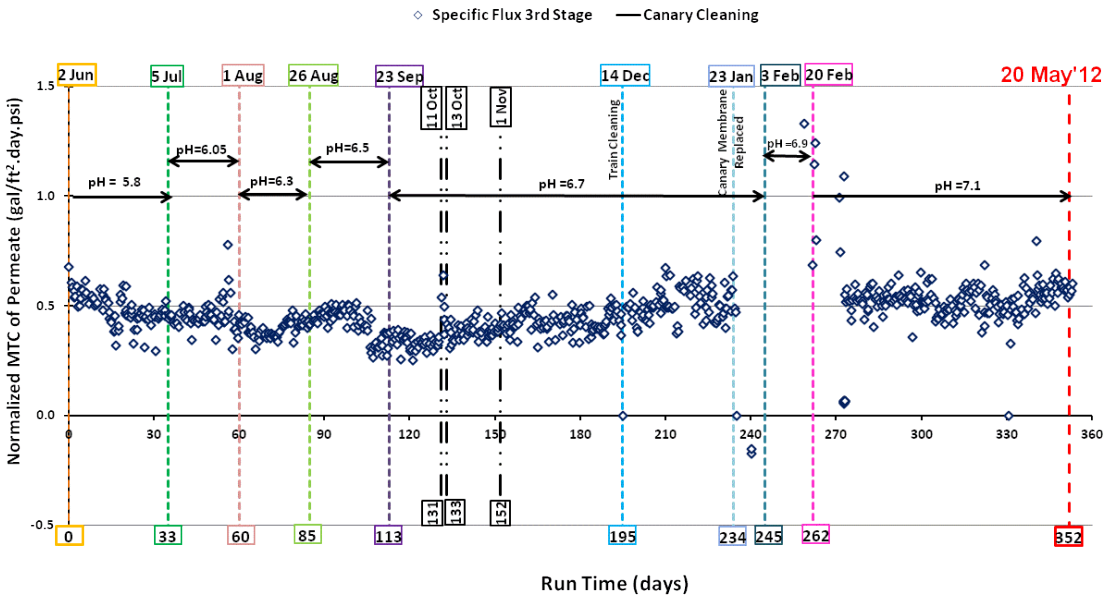

Figure 5-22: Normalized K_W of "Canary" Unit Using Average of C_2T ratio

The overall assessment is that using the moving ratio of C_2T ratio for each individual stream in a RO plant, as conditions vary, will be more realistic and representative, even though the C_2T ratio may seem similar.

Modeling Salt Passage in RO Process

A total of 4 models using parameters that allow close prediction of the MTC for TDS (K_{TDS}) were shortlisted for evaluation. The selection of models is based on same set of parameters being able to closely represent the K_{TDS} on both stages of the RO plant. Likewise 2 models were shortlisted to represent the MTC for Na (K_{Na}). The equations representing the models shortlisted for the K_{TDS} are Equations 4-4 through 4-11, while the equations representing the models shortlisted for the K_{Na} are Equations 4-12 through 4-15.

Selection of MTC Model for TDS

The evaluation and short listing of models were done using the t-statistics test. The t-statistic is used to compare the actual versus the predicted by each of the 4 models for K_{TDS1} and the next 4 models for K_{TDS2}. The t-statistics (commonly known as t-test) uses the approach of checking the difference between the averages of 2 different sets of data. The test of actual K_{TDS1} being compared against each individual set of predicted K_{TDS1} is known as the paired t-test. In the paired t-tests the t-distribution is a distribution of the differences between actual and predicted values (Knoke, Bohrnstedt, & Mee, 2002).

In the t-test, one of the key outputs is the P-value. The P-value in the paired t-test is defined as the chance or probability of obtaining a value for the difference in the distribution of the actual versus predicted that is more extreme than what is actually observed (Johnson, 2005). The P-value is interpreted in relation to the hypothesis testing. Using the example of one of the paired t-test analysis carried out in this study, the null hypothesis is that the mean of the actual K_{TDS1} is equal to the mean of the predicted K_{TDS1}. The alternative hypothesis is that the actual K_{TDS1} is not equal to predicted K_{TDS1}, and so the tests were all two-tailed t-tests.

In this study a 90% confidence interval was adopted for a two tailed t-test. Hence the acceptable P-value is larger than or equal to 0.05. A P-value smaller than 0.05 would therefore signify that the alternative hypothesis is valid, and that the mean of the actual is different from the predicted. The 90% confidence interval also means the differences in mean between the actual and predicted are valid 90% of the time.

Using the paired t-test and the 90% confidence interval, the P-values obtained by analysis on MINITAB for the determination of MTC for TDS (K_{TDS}) on the RO Plant, are shown in Table 5-21.

Table 5-21: Comparison of P-Values by Stages and Model on the RO Plant for TDS

Model Number	P-Value K_{TDS1}	P-Value K_{TDS2}	Model Number
Model 1	0.926	0.347	**Model 5**
Model 2	0.676	0.350	**Model 6**
Model 3	0.685	0.349	**Model 7**
Model 4	0.944	0.390	**Model 8**

Models 1 and 5, are a function of hydronium ion concentration (H^+) and electrical conductivity (EC) on the 1st Stage and 2nd Stage of the RO plant respectively. While Model 4 and Model 8 are a function of H^+, temperature (T), EC and ionic strength (Ion) for the 1st and 2nd Stage of the RO plant respectively. As both sets of parameters show high P-values, the combination of models 1 and 5 and models 4 and 8, were then used for a second T-test on the RO pilot at the same 90% confidence interval. The P-values obtained by analysis on MINITAB, for the determination of MTC for TDS (K_{TDS}) on the RO pilot, is as shown in Table 5-22.

Table 5-22: Comparison of P-Values by Stages and Model on the RO Pilot for TDS

Model Number	P-Value K_{TDS1}	P-Value K_{TDS2}	Model Number
Model 1	0.806	0.940	**Model 5**
Model 4	0.007	0.311	**Model 8**

Models 1 and 5 were therefore selected as the best fit empirical models to predict MTC TDS in the 1st Stage and 2nd Stage respectively, as a result of the consistently high P-values.

Model 1: $$K_{TDS1} = -1.067 \times 10^{-2} + 4.873 \times 10^{3} H^{+} + 6.5 \times 10^{-6} EC \quad (4\text{-}4)$$

Model 5: $$K_{TDS2} = -1.293 \times 10^{-2} + 4.048 \times 10^{3} H^{+} + 2.91 \times 10^{-6} EC \quad (4\text{-}8)$$

The actual versus predicted for K_{TDS1} on the RO plant is presented in Figure 5-23. The chart on the left shows the overall clustering of the actual versus predicted values around the 45 degrees equal line. The chart on the right gives a close up view of the actual versus predicted values, in order to be able to compare better, how the actual versus predicted values vary as the pH varied.

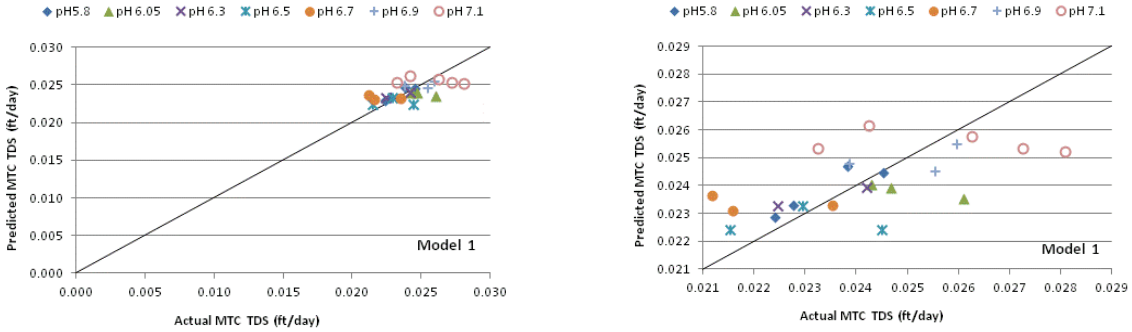

Figure 5-23: Actual versus Predicted of K_{TDS1} for 1st Stage of RO Plant

A detailed review of the prediction of the models was also carried out, in terms of the deviation of the predicted value from the actual value. The comparison of the actual against the predicted values for K_{TDS1} on the RO plant is presented in Table 5-23. In the table, the comparison is done by each pH level, as well as on an overall basis.

Table 5-23: Comparison of Actual versus Predicted Values of K_{TDS1} on the RO Plant

pH	Mean of Actual K_{TDS1} (ft/day)	Mean Difference of Predicted K_{TDS1} from Actual @ 90% Confidence Interval (ft/day)	Deviation of Prediction from Actual (%)	
			Low	High
5.8	0.02339	-0.00092 ; 0.00002	- 0.1	+ 3.9
6.05	0.02503	-0.00083 ; 0.00324	- 13.0	+ 3.3
6.3	0.02334	-0.00369 ; 0.00319	- 13.7	+ 15.2
6.5	0.02300	-0.00234 ; 0.00300	- 13.0	+ 10.2
6.7	0.02210	-0.00358 ; 0.00107	- 4.9	+ 16.2
6.9	0.02513	-0.00148 ; 0.00191	- 7.6	+ 5.9
7.1	0.02584	-0.00184 ; 0.00242	- 9.4	+ 7.1
Overall	0.02414	-0.00049 ; 0.00054	- 2.3	+ 2.0

The mean of actual K_{TDS1}, represents the average of the calculated values of K_{TDS1}. In comparing the various models on a t-test, the actual values were used as the base. Hence the mean difference of predicted K_{TDS1} from actual at 90% confidence interval in the table represents the range of mean difference of the predicted from actual K_{TDS1}. That is to say, at pH 5.8, with 90% confidence, the predicted K_{TDS1} will be between 0.00092 ft/day more than actual K_{TDS1} of 0.02339 ft/day and 0.00002 ft/day lower than the same actual K_{TDS1}. This same difference by confidence interval is presented in percentage terms as low and high. For the same pH 5.8, the predicted value is between 0.1% below and 3.9% above the actual K_{TDS1}, at a 90% confidence level.

The overall predicted K_{TDS1} on the RO plant is between -2.3 and +2.0% of the actual K_{TDS1} during the whole acid elimination phase. The percentage difference at the various pH conditions, with negative and positive values indicates that there is a spread of the difference between the actual and predicted.

The actual versus predicted for K_{TDS2} on the RO plant is presented in Figure 5-24.

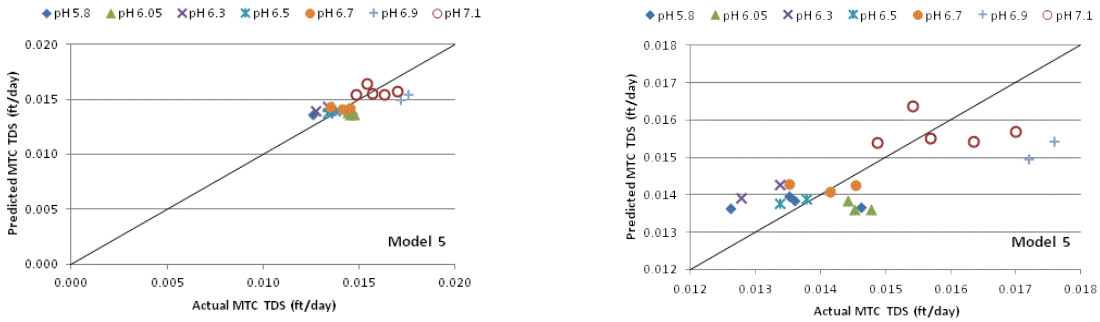

Figure 5-24: Actual versus Predicted of K_{TDS2} for 2nd Stage of RO Plant

The overall predicted K_{TDS2} on the RO plant is between -4.0 and +1.1% of the actual K_{TDS2} during the whole acid elimination phase, as seen in Table 5-24. However, at pH condition 6.05 and 6.9, the actual K_{TDS2} value is consistently higher than the predicted K_{TDS2} value. The Model 5 is under predicting at pH 6.05 by up to about 10% and at pH 6.9 by up to 15%. On the other hand, at pH 6.3, the model is over predicting by between 2 and 13%. This is also noted in Figure 5-24.

Table 5-24: Comparison of Actual versus Predicted Values of K_{TDS2} on the RO Plant

pH	Mean of Actual K_{TDS2} (ft/day)	Mean Difference of Predicted K_{TDS2} from Actual @ 90% Confidence Interval (ft/day)	Deviation of Prediction from Actual (%)	
			Low	High
5.8	0.01359	-0.00118 ; 0.00078	- 5.7	+ 8.7
6.05	0.01457	0.00040 ; 0.00137	- 9.4	- 2.8
6.3	0.01309	-0.00175 ; -0.00025	+ 1.9	+ 13.4
6.5	0.01358	-0.00121 ; 0.00075	- 5.6	+ 8.9
6.7	0.01407	-0.00109 ; 0.00080	- 5.7	+ 7.7
6.9	0.01740	0.00200 ; 0.00247	- 14.7	- 11.5
7.1	0.01587	-0.00070 ; 0.00111	- 7.0	+ 4.4
Overall	0.01465	-0.00017 ; 0.00059	- 4.0	+ 1.1

The comparison of the predicted versus actual K_{TDS1} on the RO pilot is as shown in Figure 5-25 and as tabulated in Table 5-25.

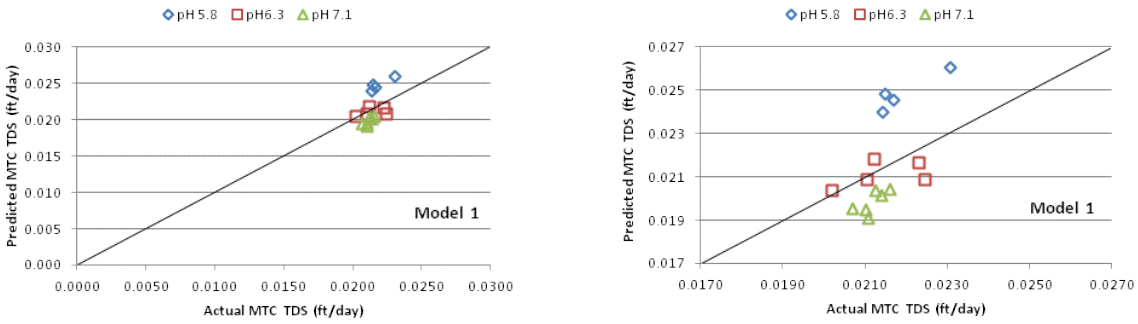

Figure 5-25: Actual versus Predicted of K_{TDS1} for 1st Stage of RO Pilot

Table 5-25: Comparison of Actual versus Predicted Values of K_{TDS1} on the RO Pilot

pH	Mean of Actual K_{TDS1} (ft/day)	Mean Difference of Predicted K_{TDS1} from Actual @ 90% Confidence Interval (ft/day)	Deviation of Prediction from Actual (%)	
			Low	High
5.8	0.02192	-0.00329 ; -0.00255	+ 11.6	+ 15.0
6.3	0.02145	-0.00045 ; 0.00115	- 5.4	+ 2.1
7.1	0.02118	0.00104 ; 0.00166	- 5.0	- 7.9
Overall	0.02147	-0.00097 ; 0.00073	- 3.4	+ 4.5

On the RO pilot, the overall predicted K_{TDS1} using Model 1 1ies between -3.4 and +4.5% of the actual K_{TDS1}. However at pH 5.8, the Model 1 is over predicting 90% of the time by as much as 15%, and at pH 7.1, the Model 1 is under predicting by between 5 and 8 %.

The comparison of the predicted versus actual K_{TDS2} on the RO pilot is as shown in Figure 5-26 and as tabulated in Table 5-26.

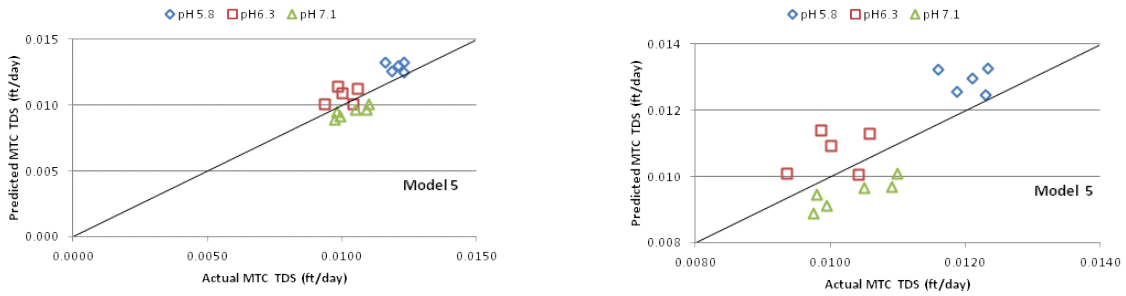

Figure 5-26: Actual versus Predicted of K_{TDS2} for 2nd Stage of RO Pilot

Table 5-26 : Comparison of Actual versus Predicted Values of K_{TDS2} on the RO Pilot

pH	Mean of Actual K_{TDS2} (ft/day)	Mean Difference of Predicted K_{TDS2} from Actual @ 90% Confidence Interval (ft/day)	Deviation of Prediction from Actual (%)	
			Low	High
5.8	0.01229	-0.00104 ; -0.00016	+ 1.3	+ 8.4
6.3	0.00997	-0.00151 ; -0.00001	+ 0.5	+ 15.1
7.1	0.01058	0.00084 ; 0.00135	- 1.3	- 8.0
Overall	0.01092	-0.00047 ; 0.00043	- 3.9	+ 4.3

On the RO pilot, the overall predicted K_{TDS2} by Model 5 is between -3.9 and +4.3% of the actual K_{TDS2}. However at pH 5.8 and pH 6.3, the Model 5 is over predicting 90% of the time by as much as 8% and 15% respectively, and at pH 7.1, the Model 5 is under predicting by between 1 and 8%.

Selection of MTC Model for Sodium

Similar approach as taken to identify the empirical model to determine the MTC for TDS (K_{TDS}), was taken to determine the model which would determine the MTC for Na (K_{Na}). Using the paired t-test and the 90% confidence interval, the P-values obtained by analysis on MINITAB for the determination of K_{Na} on the RO Plant, is as shown in Table 5-27.

Table 5-27: Comparison of P-Values by Stages and Model on the RO Plant for Na

Model Number	P-Value K_{Na1}	P-Value K_{Na2}	Model Number
Model 9	0.821	1.000	**Model 11**
Model 10	0.238	0.049	**Model 12**

Models 9 and 11 were therefore selected as the best fit empirical models to predict MTC Na in the 1st Stage and 2nd Stage respectively.

Model 9: $$K_{Na1} = 5.115\times 10^{-2} + 8.68\times 10^{-6}\ EC - 1.15 \times 10^{-4} Na \quad (4\text{-}12)$$

Model 11: $$K_{Na2} = 4.159\times 10^{-2} + 4.92\times 10^{-6}\ EC - 4.82 \times 10^{-5} Na \quad (4\text{-}13)$$

Models 9 and 11, show that the MTC for Na (K_{Na}) decreases as the Na ion concentration increases. Higa et al (1998), showed that when the concentration of divalent cations is high in solutions, the Donnan potential is weakened as the divalent cations at the membrane surface shield the membrane's negative charges. In this study the concentrate streams of the first stage of the RO plant had calcium and magnesium concentrations of about 500mg/L and 260 mg/L respectively. The second stage had calcium and magnesium concentrations of about 970mg/L and 490 mg/L respectively. The high concentrations of divalent ions in the concentrate streams are therefore the more likely the cause of the decrease in MTC for Na.

The study by Bartels et al (2005), showed that at mid range TDS values of between 1000mg/L and 3000mg/L is when Donnan potential is greatest. When the TDS values get higher than 3000mg/L the Donnan potential is weakened, and leads to increased salt passage. In this study

the average feed brine channel concentration in the first stage was 3600mg/L and 7000mg/L in the second stage. Therefore higher concentration of ions measured in terms of TDS and the fact that there are high concentrations of divalent cations, would better explain the less negative predictor coefficient for Na for the second stage (Equation 4-13) as compared to that in the first stage (Equation 4-12).

The actual versus predicted for K_{Na1} on the RO plant using Model 9 is presented in Figure 5-27 and Table 5-28.

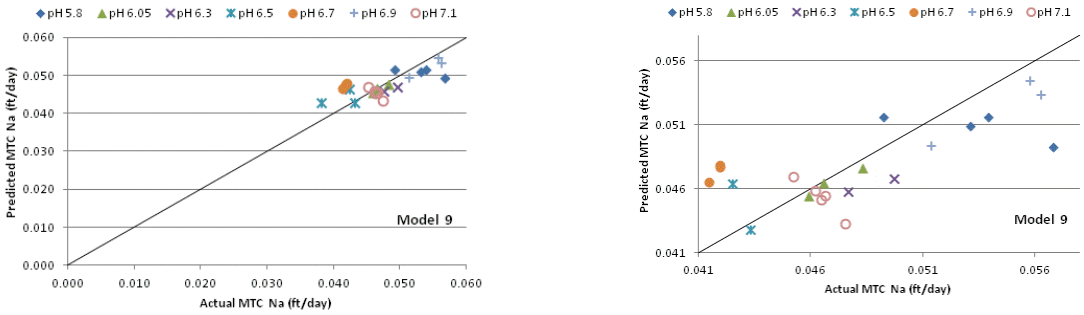

Figure 5-27: Actual versus Predicted of K_{Na1} for 1st Stage of RO Plant

On the RO plant, the overall predicted K_{Na1} using Model 9 1ies between -2.9 and +2.2% of the actual K_{Na1}. However at pH 6.8, the Model 9 is over predicting 90% of the time by as much as 15%.

Table 5-28: Comparison of Actual versus Predicted Values of K_{Na1} on the RO Plant

pH	Mean of Actual K_{Na1} (ft/day)	Mean Difference of Predicted K_{Na1} from Actual @ 90% Confidence Interval (ft/day)	Deviation of Prediction from Actual (%)	
			Low	High
5.8	0.05329	-0.00231 ; 0.00723	- 13.6	+ 4.3
6.05	0.04695	-0.00008 ; 0.00097	- 2.1	+ 0.2
6.3	0.04872	-0.00098 ; 0.00591	- 12.1	+ 2.0
6.5	0.04139	-0.00724 ; 0.00205	- 5.0	+ 17.5
6.7	0.04180	-0.00632 ; -0.00482	+ 11.5	+ 15.1
6.9	0.05450	0.00073 ;0.00355	- 6.5	- 1.3
7.1	0.04646	-0.00092 ;0.00320	- 6.9	+ 2.0
Overall	0.04769	-0.00106 ; 0.00138	- 2.9	+ 2.2

The actual versus predicted for K_{Na2} using Model 11, on the RO plant is presented in Figure 5-28 and Table 5-29.

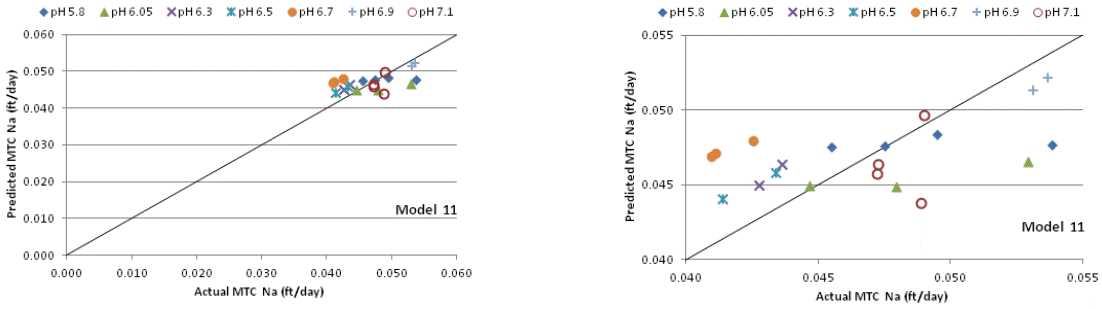

Figure 5-28: Actual versus Predicted of K_{Na2} for 2nd Stage of RO Plant

On the RO plant, the overall predicted K_{Na2} using Model 11 1ies between -2.9 and +2.9% of the actual K_{Na1}. However at pHs 6.3, 6.5 and 6.7 the Model 11 is over predicting 90% of the time by

as much as 9%, 6% and 15% respectively. At pH 6.9 the Model 11 is under predicting by about 5%.

Table 5-29: Comparison of Actual versus Predicted Values of K_{Na2} on the RO Plant

pH	Mean of Actual K_{Na2} (ft/day)	Mean Difference of Predicted K_{Na2} from Actual @ 90% Confidence Interval (ft/day)	Deviation of Prediction from Actual (%)	
			Low	High
5.8	0.04908	-0.00280 ; 0.00542	- 11.0	+ 5.7
6.05	0.04852	-0.00255 ; 0.00869	- 18.0	+ 5.3
6.3	0.043212	-0.00405 ; -0.00078	+ 1.8	+ 9.4
6.5	0.04566	-0.00252 ; -0.00061	+ 1.3	+ 5.5
6.7	0.041532	-0.00638 ; -0.00520	+ 12.5	+ 15.4
6.9	0.053425	0.00068 ; 0.00273	- 1.3	- 5.1
7.1	0.048166	-0.00017 ; 0.00392	- 8.1	+ 0.4
Overall	0.046922	-0.00136 ; 0.00136	- 2.9	+ 2.9

The comparison of the predicted versus actual K_{Na1} on the RO pilot is as shown in Figure 5-29 and as tabulated in Table 5-30.

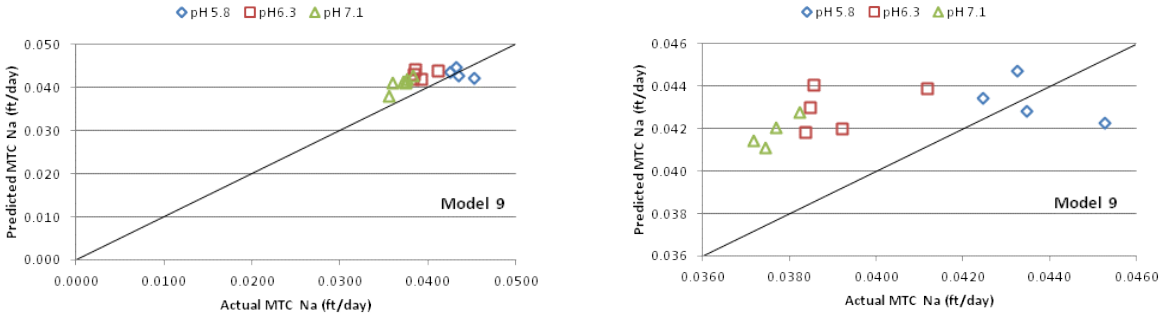

Figure 5-29: Actual versus Predicted of K_{Na1} for 1st Stage of RO Pilot

Table 5-30 : Comparison of Actual versus Predicted Values of K_{Na1} on the RO Pilot

pH	Mean of Actual K_{Na1} (ft/day)	Mean Difference of Predicted K_{Na1} from Actual @ 90% Confidence Interval (ft/day)	Deviation of Prediction from Actual (%)	
			Low	High
5.8	0.04362	-0.00206 ; 0.00268	- 6.1	+ 4.8
6.3	0.03917	-0.00491 ; -0.00264	+ 6.7	+ 12.5
7.1	0.03703	-0.00479 ; -0.00323	+ 8.7	+13
Overall	0.03950	-0.00383 ; -0.00173	+ 4.4	+9.7

On the RO pilot, the overall predicted K_{Na1} using Model 9 is consistently over predicting by about 10%. At pHs 6.3 and 7.1 the Model 11 is over predicting 90% of the time by as much as 13% on both cases. At pH 5.8 on the RO pilot, at 90% confidence, the predicted K_{Na1} is between -6% and +5% of the actual calculated K_{Na1}.

The comparison of the predicted versus actual K_{Na2} on the RO pilot is as shown in Figure 5-30 and is as tabulated in Table 5-31.

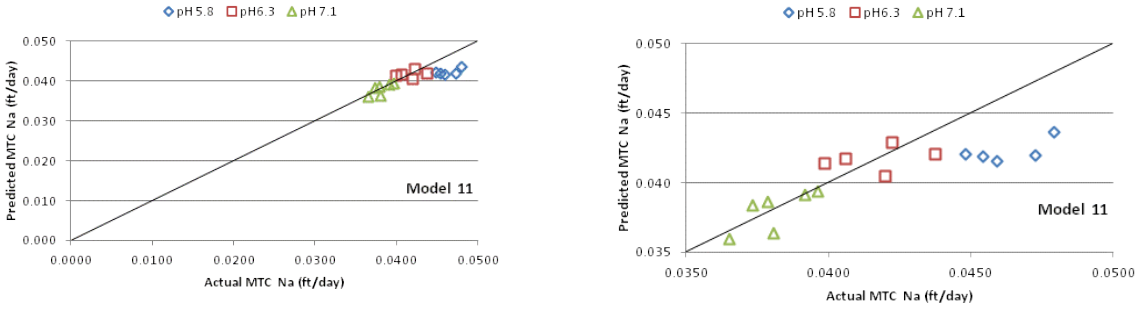

Figure 5-30: Actual versus Predicted of K_{Na2} for 2nd Stage of RO Pilot

Table 5-31: Comparison of Actual versus Predicted Values of K_{Na2} on the RO Pilot

pH	Mean of Actual K_{Na2} (ft/day)	Mean Difference of Predicted K_{Na2} from Actual @ 90% Confidence Interval (ft/day)	Deviation of Prediction from Actual (%)	
			Low	High
5.8	0.04627	0.00315 ; 0.00493	- 6.8	- 10.7
6.3	0.04170	-0.00146 ; 0.00144	- 3.4	+ 3.5
7.1	0.03810	-0.00067 ; 0.00092	- 2.4	+ 1.8
Overall	0.04178	0.00035 ; 0.00227	- 5.4	+ 0.8

On the RO pilot, the overall predicted K_{Na2} at 90% confidence interval is between -5.4% and +0.8% of the actual K_{Na2} using Model 11. At pH 5.8, Model 11 is under predicting 90% of the time by as much as 11%.

Nanofiltration and Pretreatment Options for a Highly Fouling Surficial Groundwater Source

The nanofiltration (NF) pilot study is driven with the objective of possibly substituting the City's IX process, for softening of water from the Verna well field. NF is a proven technology that is able to remove microorganisms, turbidity and hardness, as well as a small fraction of dissolved salts (Hilal, Al-Zhobi, Darwish, Mohammad, & Arabi, 2004). NF membranes are operated at higher flux than RO membranes, as it has lower rejection of monovalent and certain fractions of divalent ions. In this study the NF pilot was operated at a recovery rate of about 85 per cent. Though the primary aim of the study was to evaluate the UF technology as a pretreatment to the NF process to control fouling on the NF membranes, early evaluations included the use of just bag filters (BF) and cartridge filters (CF), before media filters (MF) and sand filters (SF) were used. The monitoring the NF membrane process involved the similar approach adopted for the

RO pilot and RO plant, using Equations 3-34 through 3-39 and trending the MTC for permeate (K_W) using weekly or biweekly sampling and analysis of TDS from the NF feed, NF 1st and 2nd Stage Permeates and the 1st and 2nd Stage Concentrate streams.

Upgrading of Tray Aeration System at Verna Well Field

As part of the City's strategy to improve the overall water quality of its water supply, the City embarked on a project to improve the aeration system at the Verna well field. The original deep tray aeration system with four tiers of trays, was found to be inefficient in stripping the sulfides in water, as the distribution of water over the trays was not uniform and all the tray area was not being utilized to maximize aeration. The retrofitting works to improve aeration at Verna started in 2011 and the replacement works were completed in Jul, 2012. The improved tray aeration system has a piping system to spread the well water over all the surface area on the top tray and the system had five tiers of tray. The old and new tray aerators at the Verna well field are as shown in

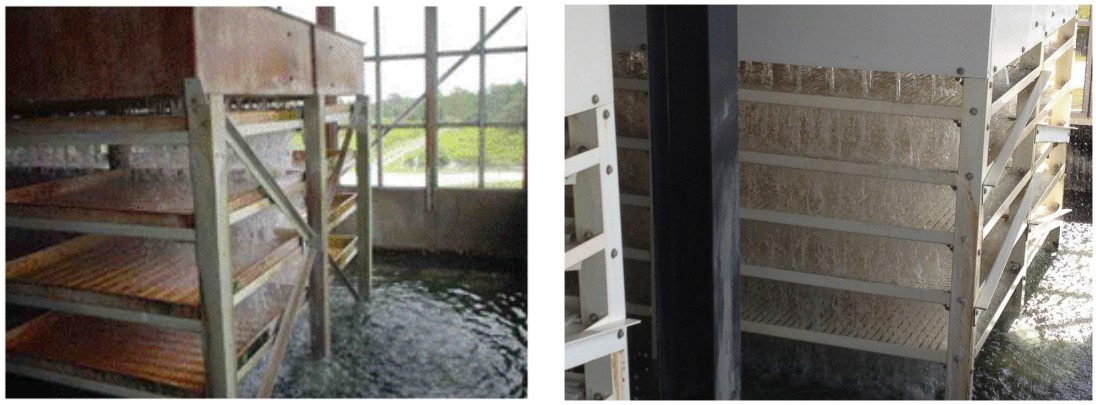

Figure 5-31: Old Tray Aeration System (left) and New Tray Aeration System (Right) at Verna

Sulfide testing was carried out before (Jun, 2010) and after (Aug, 2012) the retrofitting works to the tray aeration system at Verna and the results are summarized in Table 5-32.

Table 5-32: Efficiencies of Tray Aerators at Verna Well Field

Sample Type	**Old Tray Aerators**		**New Tray Aerators**	
	S^{2-} (mg/L)	**Turbidity (NTU)**	**S^{2-} (mg/L)**	**Turbidity (NTU)**
Raw Verna	5.8	0.3	2.6	0.23
Degasified Verna	3.0	0.9	0.9	2.0
Efficiency	- 48%	+ 200%	- 65%	+ 770%

The sulfide removal efficiency in the tray aerators at Verna has increased to about 65% from 48% previously. The turbidity formed as the sulfides are oxidized has also increased to close to 770% as compared to about 200% increase previously. The higher sulfide content of the raw Verna water in Jun 2010 compared to Aug 2012, is due to well rotations and the City could not bring the same sets of wells online in Aug 2012 for direct comparison with the earlier analysis.

The higher turbidities formed are expected to settle in the ground storage tank at Verna or at the 10^{th} Street Reservoir, near the City WTF. For the nanofiltration and its pretreatment study, as the feed to the pilots bypass the 10^{th} Street Reservoir, some of the turbidity directly impacted the pretreatment processes.

Evaluation of Bag Filters, Cartridge Filters, Media and Sand Filters as Pretreatment

The schematic layout of the process units when the bag filters, cartridge filters and media and sand filters were evaluated as pretreatment to the NF process is as shown in Figure 5-32. The trend of the K_W during the period from startup on Feb 28, 2011 till Jun 2, 2011 is shown in Figure 5-33. The operations with just BF and CF (1μm nominal) lasted only about 2 days, as the performance on the NF dropped steeply and sharp increases in feed pressure were noted. The post cartridge filter Silt Density Index (SDI) on the feed water to the NF was as high as 4.5 to 5, indicating that the NF fouling rates were potentially high.

After a shutdown (Mar 2 till Mar 23) of about 3 weeks, the 1μm nominal CF were then replaced with 1μm absolute CF on 23 Mar 2011, but the SDI values of the NF feed water remained high at about 4.5. During this same window of operating with the NF pilot with 1μm absolute CF, an attempt was made to bypass the aeration at Verna well field, to test the possibility of operating the NF pilot with feed water that bypasses the aeration at Verna. However, the City had to resume aeration at the Verna Well field, as the water quality at the Point-of-Entry (POE) at the WTF was deteriorating with high turbidity of between 1.32 and 1.56 NTU, and a yellow tinge was noted in water supplied. With the 1μm (absolute) CF the SDI as measured at the NF Pilot skid was only marginally lower at 3.7 but higher than the targeted SDI value of less than 3 for feed to NF membranes. The NF pilot operations were then stopped again on Mar 28, 2011.

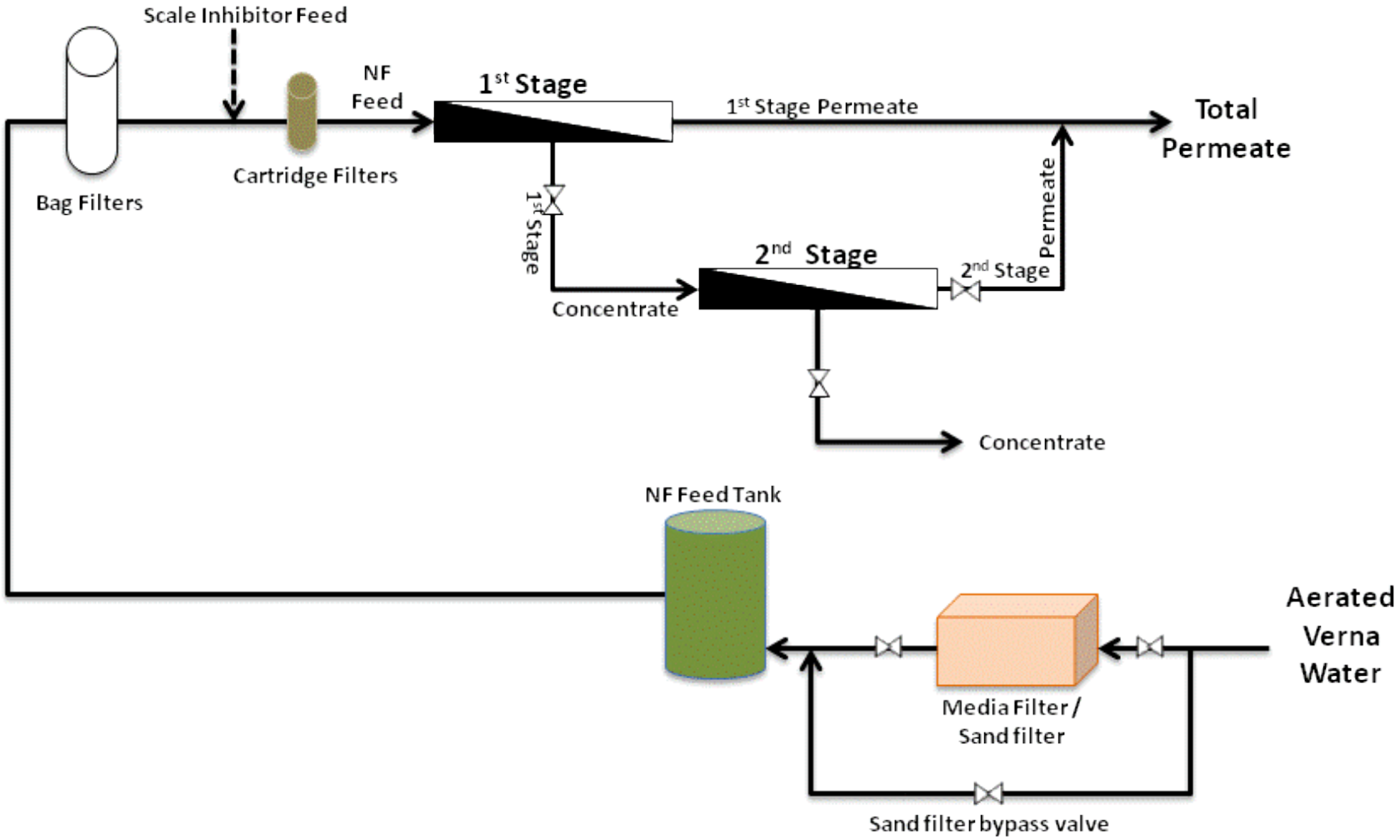

Figure 5-32: Schematic Layout of Pre-Treatment Systems to NF Pilot

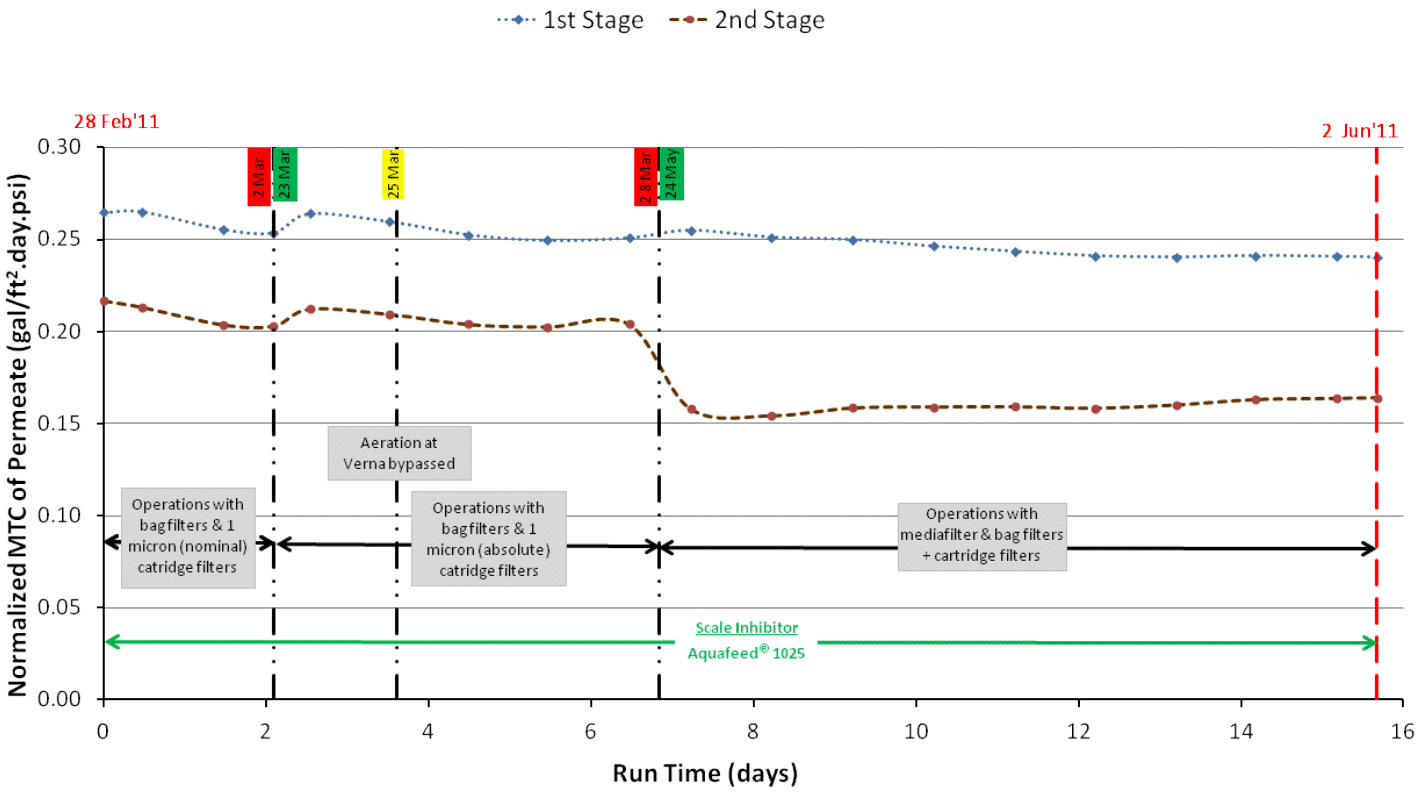

Figure 5-33: Normalized MTC of Permeate for Stages 1 and 2 of NF Pilot (Feb 28 – Jun 2, 2011)

Figure 5-34: Cartridge Filter Taken out of NF Pilot (left), New Cartridge Filter (middle) and Cartridge Filter after Exposure to Atmosphere (right)

An analysis was done of the CF taken out of the NF pilot following the shutdown that occurred as a result of the short duration of stopping aeration at Verna Well field.

In Figure 5-34, is the black colored CF taken out of the NF pilot. Two days after the black CF was exposed to atmosphere, (i.e. when it was taken out of the NF), it was analyzed to identify the possible constituents that fouled the fibers. By the time of the analysis, the black colored appearance of the CF completely disappeared and the fibers appeared orange-brown.

Analysis of the fibers of the CF showed that the TOC content ranged between 54 and 65 mg/L when the regular TOC of the NF feed water only ranged between 1.7 and 1.85 mg/L. Also the iron (Fe) content was high at between 29 and 56 mg/L, when the feed water Fe content was less than 0.010 mg/L. The high turbidity and sudden deterioration of the water quality from Verna

well field is therefore explained by the loss of aeration, as dissolved oxygen level in the Verna water dropped from about 8.3 mg/L to about 1.3 mg/L. This resulted in the "kill" of the aerobic biogrowth and slime layers in the pipeline transferring water from Verna to 10th Street Reservoir that then caused the high turbidity and increased organics level.

It was then decided that the evaluation of the NF will continue with aerated water (for H_2S removal) from Verna, as there was only one pipeline to transfer the Verna water to the City's WTF, via the 10th Street Reservoir. With only one 22 mile long pipeline transferring water from Verna to the WTF, and the City concurrently operating its IX and IX bypass to meet supply to customers; it was not feasible to test the non-aerated Verna water at the WTF location.

On May 24, 2011, a media filtration bed (anthracite and sand filter bed) was setup as pretreatment to the NF pilot. The anthracite had effective size range of 0.7 – 1.7 mm, while the sand had effective size of 0.3 – 0.7mm. The operations only lasted about a week till Jun 2, 2011, as the media filtration unit developed a leak that would not allow backwash cycles. With the old media filtration unit the SDI values for feed water to the NF was still high at around 3.5, and the though the K_W on the 2nd Stage improved, the 1st Stage K_W was dropping, showing that fouling by "plugging" mechanism was happening on the 1st stage membranes, as seen in Figure 5-35.

The NF pilot study that stopped on Jun 2, 2011 was resumed on Aug 8, 2011 with sandfilters (SF) using commercially available pool sand of diameter 0.45–0.55mm, which gives a screening range of particles in the range 20-100 μm as pretreatment to the NF. The operations with SF as pre-filter to the NF (with BF and CF still on the pilot) continued till Dec 3, 2011, as shown in

Figure 5-35. The SF bed was operated with backwashes being carried out by monitoring the head loss across the SF. The SDI values were also monitored at the CF location on the NF pilot throughout the evaluation of SF as pre-filter to the NF. The SDI values varied, and was about 2 when the media was new or just after a backwash, increasing to as high as 4 just before a backwash cycle. The frequency of the backwash was determined at about 6 - 8 days.

The comparison of the raw Verna water (that bypasses 10^{th} Street Reservoir) and the filtrate of the SF are as shown in Table 5-33. The turbidity of the filtrate from the SF is about 0.15 NTU and it only seems to screen some of the turbidity or particulate material in the raw Verna water.

As the K_W of both the 1^{st} and 2^{nd} stages on the NF was dropping during the period of evaluation between Aug 8 and Dec 3, 2011, the evaluation of SF as pre-filter as to the study was concluded on Dec 3, 2011. The NF pilot membrane were cleaned with high pH cleaners and stored in sodium bisulfite solution till the start of UF pilot study as pre-filter to the NF pilot in Feb, 2012.

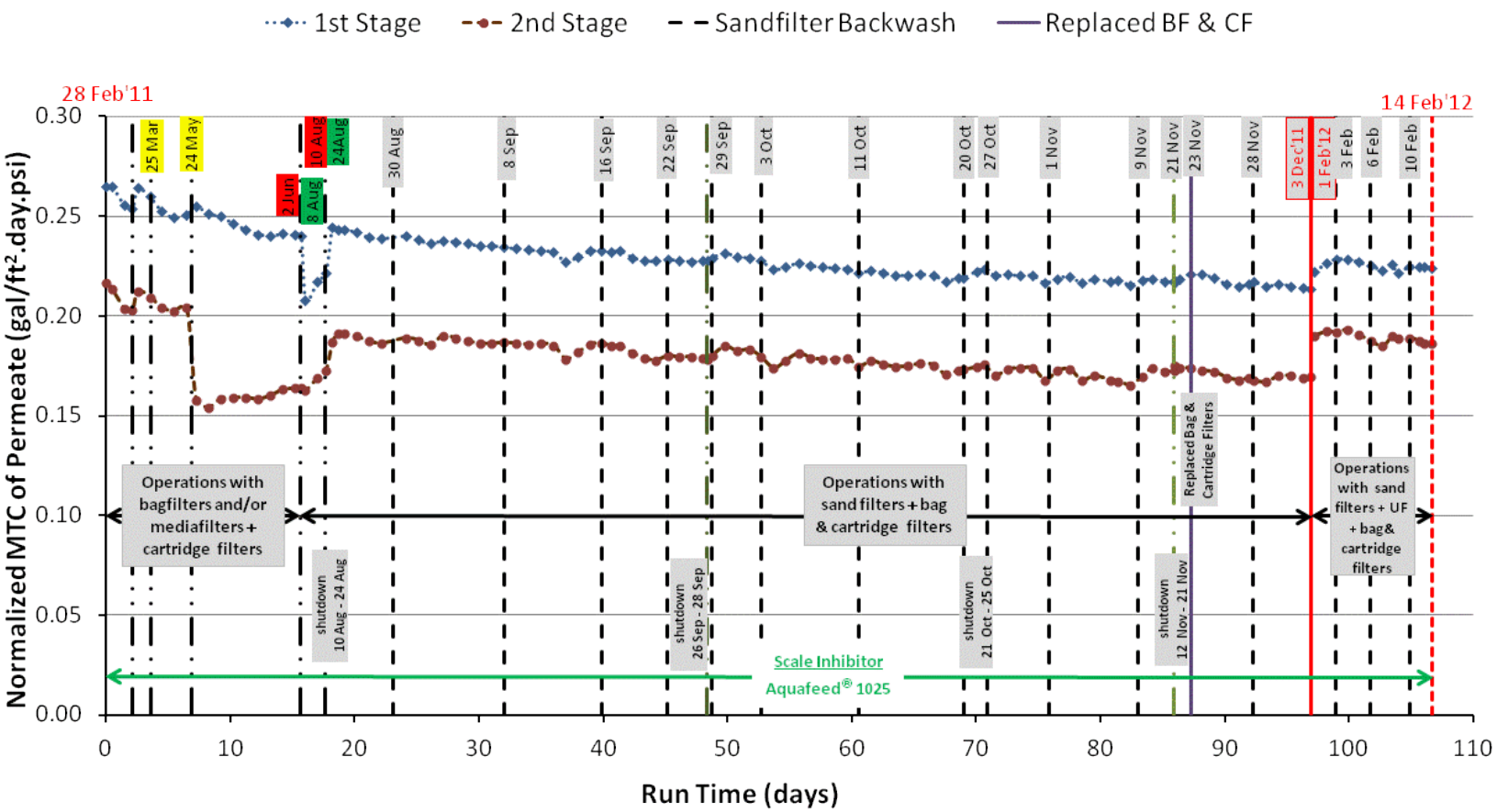

Figure 5-35: Normalized MTC of Permeate for Stages 1 and 2 of NF Pilot (Feb 28, 2011 – Feb 14, 2012)

Table 5-33: Comparison of Raw Verna Water and Sand Filtrate Water Quality

Parameter	**Units**	**Raw Verna**	**Post SF**
Turbidity	NTU	0.20 ± 0.05	0.15 ± 0.02
Conductivity	µS/cm	1015 ± 33	991 ± 16
TOC	mg/L	2.0 ± 0.4	1.7 ± 0.1
SO_4^{2-}	mg/L	344 ± 47	348 ± 6
Cl^-	mg/L	26.0 ± 6.2	17.6 ± 1.1
Total Alkalinity	mg/L as $CaCO_3$	166 ± 6	157 ± 5
Ca	mg/L	97.2 ± 7.0	94.9 ± 0.4
Mg	mg/L	49.9 ± 3.5	49.1 ± 0.3
Si	mg/L	26 ± 1.4	26 ± 0.1
Ba	µg/L	30.4 ± 2.8	29.2 ± 0.2
Sr	mg/L	20.6 ± 1.0	21.8 ± 0.3
Ca Hardness	mg/L as $CaCO_3$	243 ± 18	237 ± 1
Total Hardness	mg/L as $CaCO_3$	471 ± 32	464 ± 2
TDS	mg/L	730 ± 33	731 ± 25
TSS	mg/L	1.0 ± 0.8	0.8 ± 0.3

Evaluation of Ultrafiltration as Pretreatment

The evaluation of ultrafiltration (UF) as pretreatment to NF started on Feb 1, 2012. At this point the UF pilot operations started with the SF as a pre-screen to the UF process. Also UF testing started with the use of two UF membrane modules from TOYOBO that were new but not stored in the conditions as prescribed by the manufacturer. This phase of evaluation using the UF filters was called the pretest phase and during this phase a quick evaluation was made in identifying the appropriate flux rates to operate the UF membranes, the types of chemically-enhanced-backwashes (CEBs) that would be appropriate for the type of fouling and the frequency of such CEB. The operations of the UF and the NF were then both monitored. The schematic layout of the UF and NF pilots and sand filter as pre-treatment is as shown in Figure 5-36.

Following the cleaning and storage of the NF membranes, when the SF-UF-NF combination started on Feb 1, 2012, an increase of about 0.02 gal/ft2.day.psi was noted on both the 1st and 2nd stages of the NF pilot, as seen in Figure 5-35. These K_Ws for each stage then became the reference to the evaluation of the NF process.

The operations of the UF pilot with the 2 pretest UF membrane modules is as shown in Figure 5-37. Between the periods of Feb 1 to Feb 9, while the CEB injection system on the UF pilot was still being programmed and assembled, the UF pilot was operating with no CEBs. During this window the pilot was producing about 24 gpm of UF filtrate and with the total fiber surface area of 860 ft^2, this was equivalent to about 40 gal/ft^2.day (gsfd). During this window the MTC on the UF pilot stabilized to about 18 gal/ft^2.day.psi.

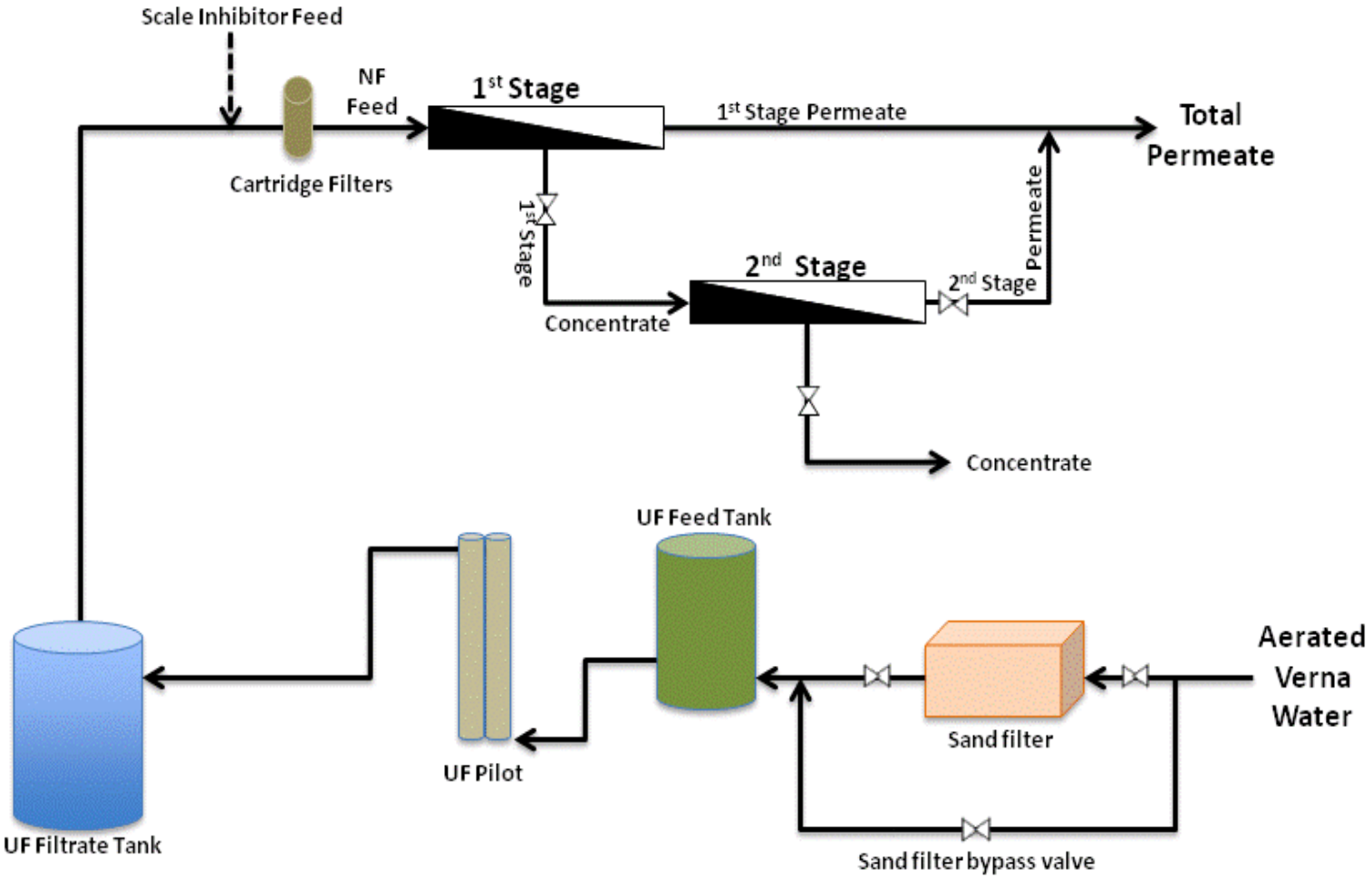

Figure 5-36: Schematic Layout of UF and NF Pilots with Sand Filter Pre-Treatment System

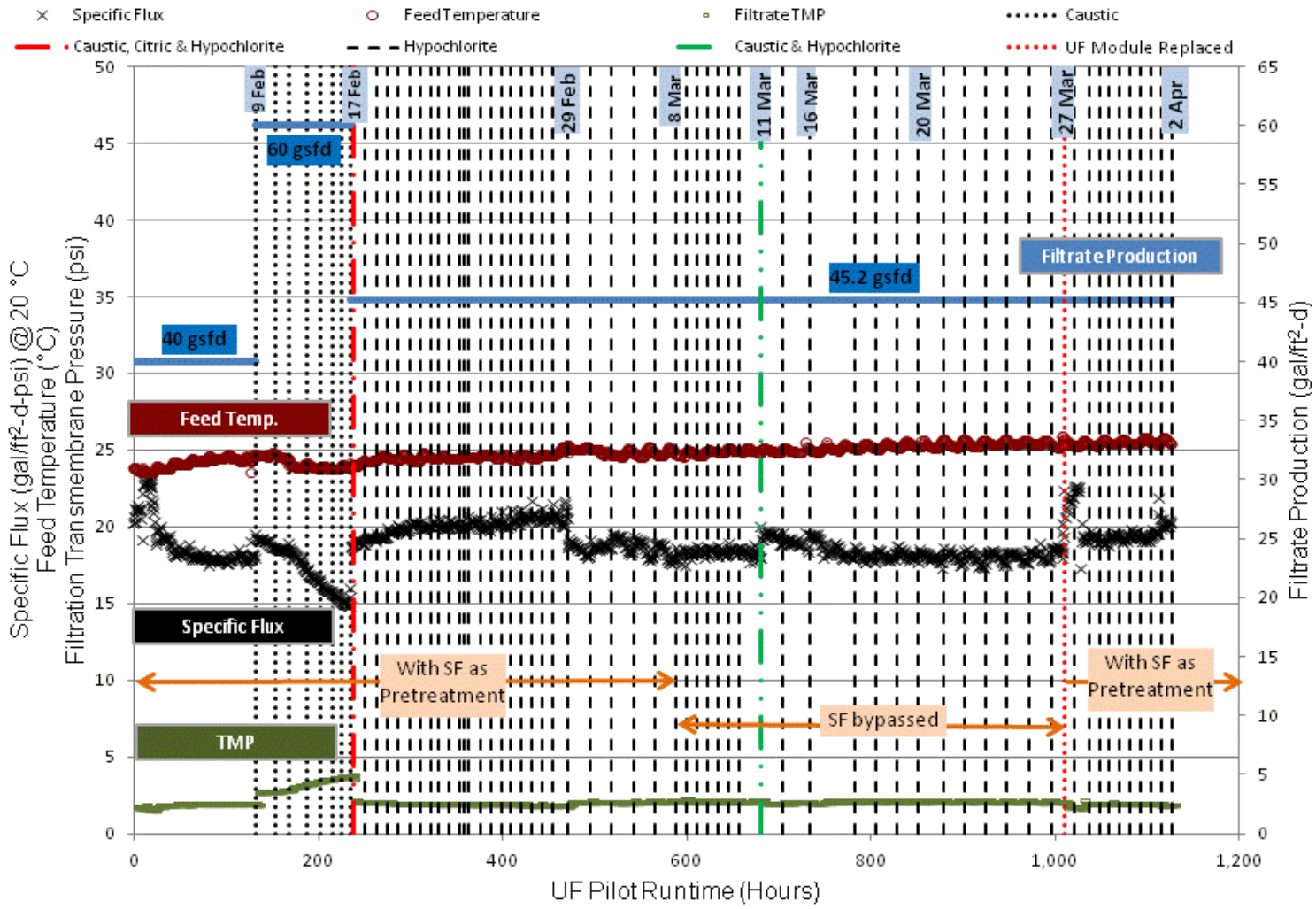

Figure 5-37: UF Pilot Operations with Pretest Modules (Feb 1 – Apr 2, 2012)

When the CEB system was ready, the UF pilot was pushed to the manufacturer's limit on the filtrate production of 35.8 gpm (equivalent to 60 gsfd). Between the period Feb 9 -17, the UF pilot was operated with once per day caustic CEB. The high pH caustic CEB was chosen as caustic is known to break the bonds between the membrane surface and foulant material (Rajinder, 2006).

At the very high flux rate, the transmembrane pressure (TMP) (i.e. average pressure between feed and outlet of membrane modules) of the membrane system was noted to be increasing steeply and the specific flux of the UF process was also noted to be dropping. The specific flux and TMP conditions were not improving with the daily caustic CEBs.

On Feb 17, 2012 a cycle of CEBs were performed to restore the performance of the UF membrane modules. Caustic CEB with an extended soak time of 20 minutes was first attempted. The regular daily CEBs were with 8 minutes of soak time. When this did not improve the TMP, an extended soak duration of 20 minutes with citric at a concentration of about 10,000mg/L (1 % concentration) was attempted. Citric acid CEBs are performed to target and remove calcium carbonate scaling. The citric acid also had very little impact in improving the TMP on the membrane modules. Finally a hypochlorite CEB was performed with a chlorine strength soaking on the fibers of about 1600 mg/L. The hypochlorite CEB restored about 1 psi on the TMP and so the pilot operations were started up again, with twice daily hypochlorite CEBs with chlorine strength of about 150 mg/L soaking on the fiber during the CEB. The UF pilot was also readjusted to produce about 27 gpm (45.2 gsfd) on the forward filtration cycle. Between Feb 17

and Feb 29, the specific flux on the UF pilot improved to about 20 gal/ft^2.day.psi. Hypochlorite CEBs are normally performed to control biological fouling, and the need to use hypochlorite CEB to restore performance were the first indications that the UF and NF processes will potentially be impacted by biofouling.

Between Feb 29, and Mar 8 the UF pilot was operated with once a day hypochlorite CEB and there was an immediate impact, as compared to the twice daily CEBs, as the MTC dropped to 18 gal/ft^2.day.psi, but remained stable.

On Mar 8, the SFs were bypassed and the UF pilot (with the test UF modules) was filtering the raw Verna water directly. The UF pilot was then operated till Mar 29, with no SF to pre-screen the Verna water. Between Mar 8 and 12 the frequency of the hypochlorite CEB was twice per day with 30 minutes forward filtration cycle, which was then increased to once per day on Mar 12 with 45 minutes forward filtration cycle. On Mar 12, a caustic CEB was carried out as a test to check if it could help improve the membrane's performance. The improvement following the CEB was only momentary and the UF pilot returned to its stable operating point at about 18 gal/ft^2.day.psi. On Mar 27, the pre-test modules were replaced with the new membrane modules from TOYOBO, and the UF operations started again with SF as pre-screen to the UF pilot. It was also decided that all evaluation of the UF operations, will be at an operating flux of 45.2 gsfd (i.e. 27 gpm)

While the UF evaluation was being carried out using the pre-test UF modules, the NF pilot was concurrently being monitored. In Figure 5-38, is the evaluation of the NF performance during the

same window as the UF pretest modules were being tested. The NF pilot performance was relatively stable up to Feb 29, when the CEB frequency with hypochlorite was decreased to once per day. From Feb 29, onwards the NF performance on the 1st Stage seemed to be declining and this decline was more evident since the SF as pre-screen to the UF pilot was removed on Mar 8, 2012, as noted in Figure 5-39.

On Mar 18, the NF pilot was shutdown as the differential pressure (i.e. pressure difference between feed and outlet) of the 1st Stage increased steeply by about 7 psi. The UF pilot continued operating but the NF pilot was shutdown between Mar 18 and 29, till the NF membranes were cleaned with proprietary high pH cleaners from Avista Technologies. The cleaning with the high pH cleaners restored the 1st Stage membrane's performance (see Figure 5-38) and it was as comparable to the NF pilot study startup conditions (see Figure 5-33).

The SF-UF-NF operations resumed on Mar 29, with the UF pilot operating with new UF modules. The operations of the UF pilot since Mar 29 till Oct 8 is shown in Figure 5-40, Figure 5-41, and Figure 5-42. The UF operations were with SF as pre-screen up till Sep 6. Throughout the duration of the testing of the UF membranes to treat raw Verna, with and without SF as pre-screen the flux rate was maintained at 45.2 gsfd (27 gpm) with 45 minutes forward filtration cycle. The principal CEB chemical was also hypochlorite as biofouling was identified as the key foulant that needs to be managed, for the Verna water, together with the original target foulant of colloidal sulfur that arise from the aeration of groundwater at the Verna well field.

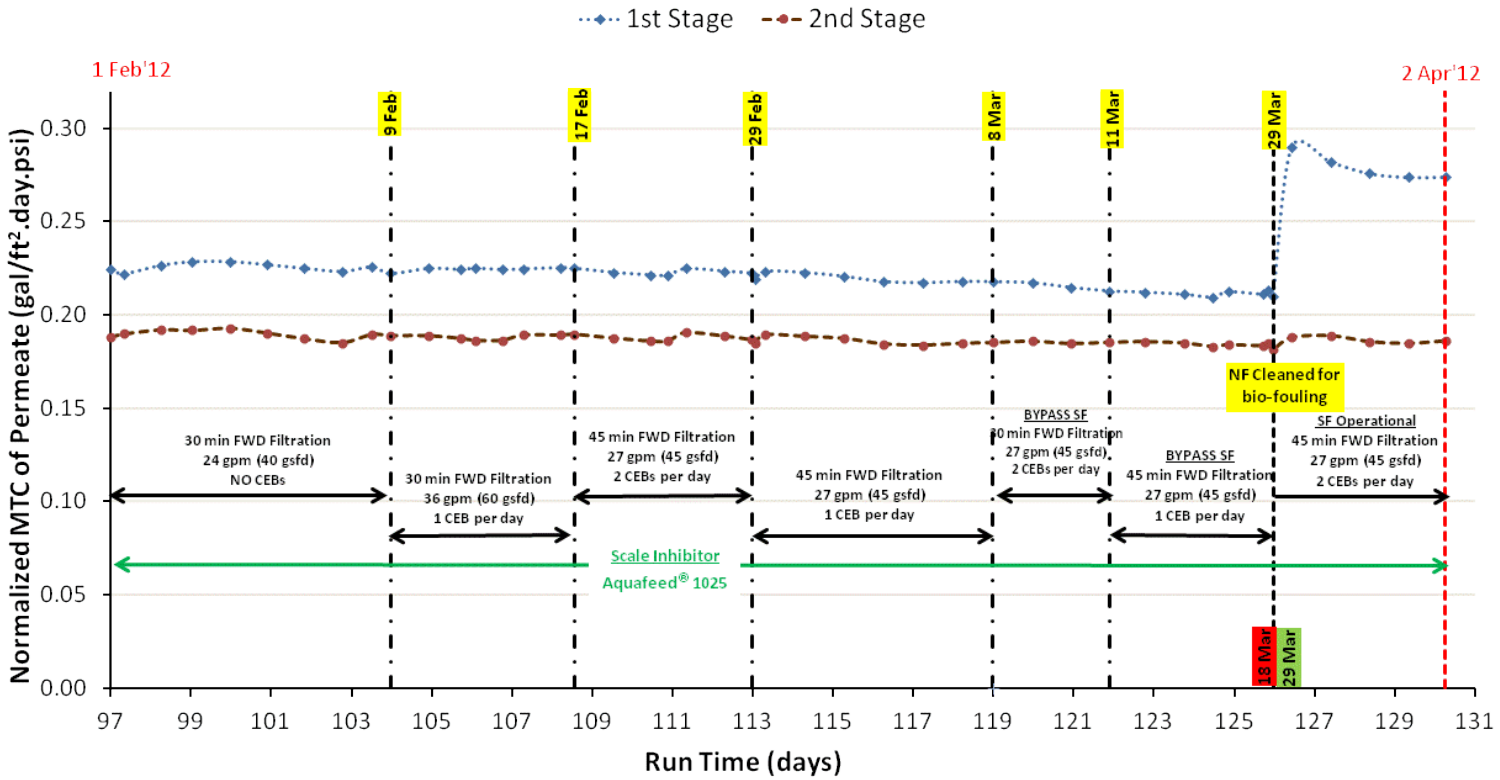

Figure 5-38: Normalized MTC of Permeate for Stages 1 and 2 of NF Pilot (Feb 1 – Apr 2, 2012)

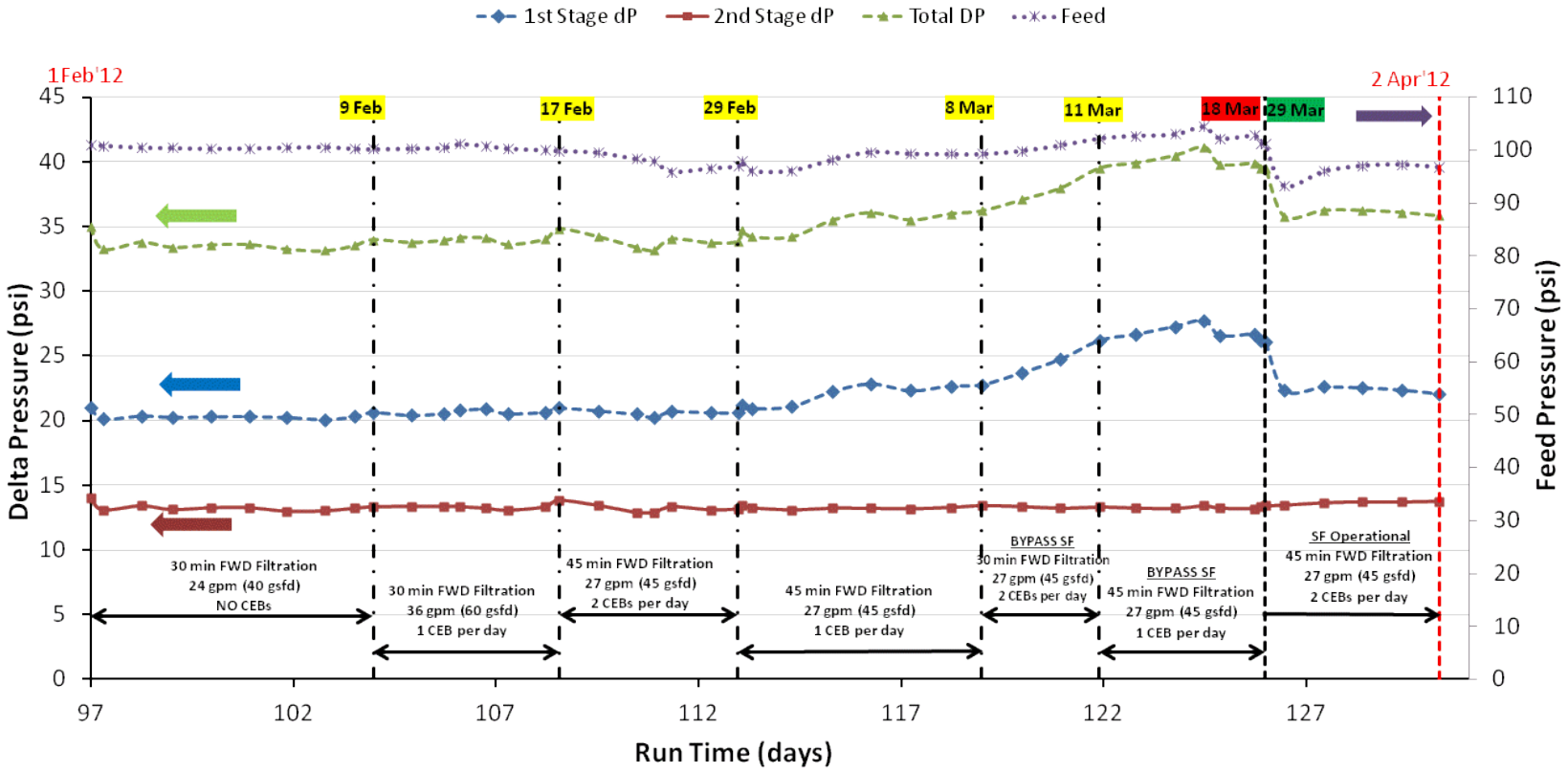

Figure 5-39: Feed and Differential Pressure Condition by Stages on NF Pilot (Feb 1 – Apr 2, 2012)

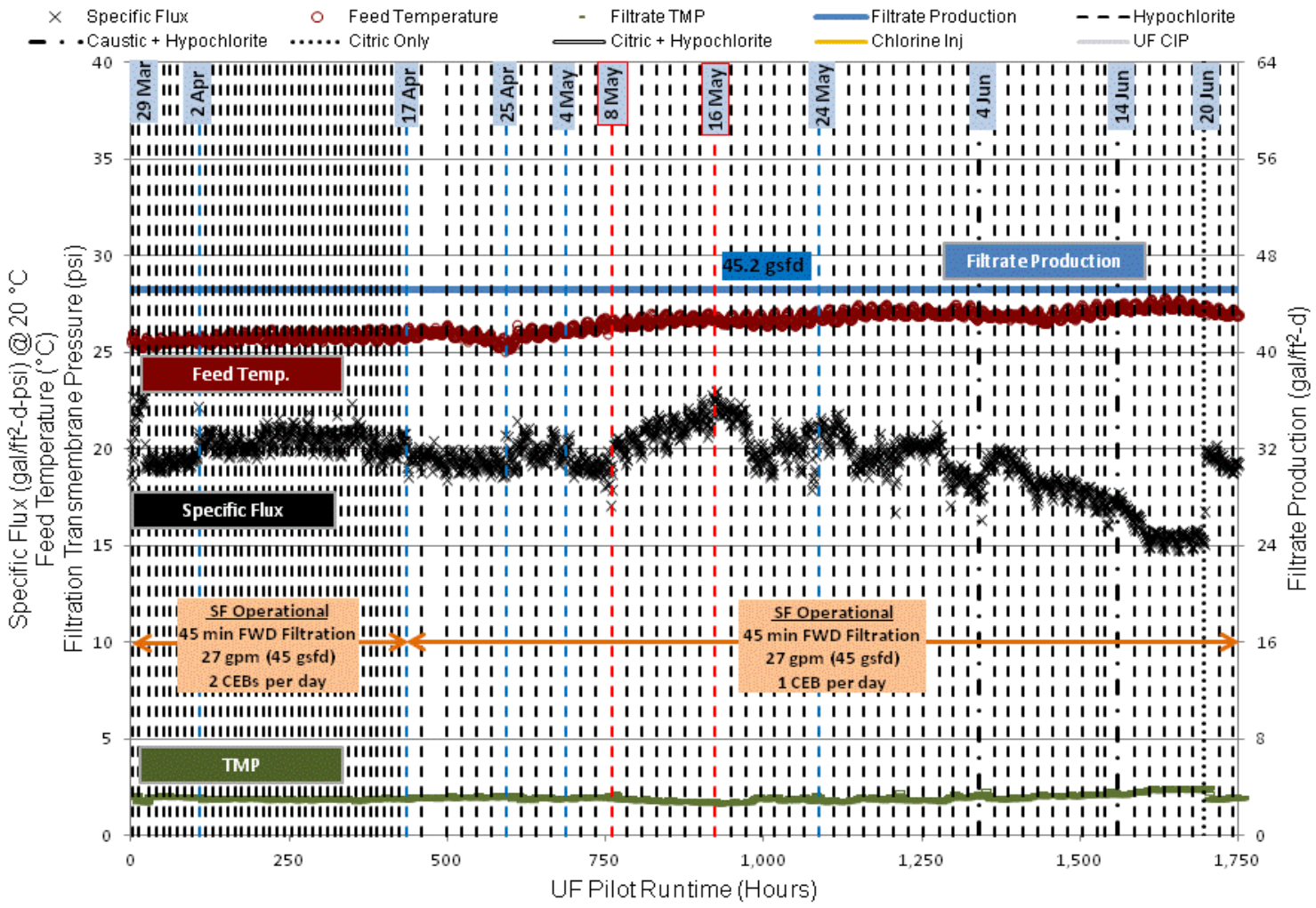

Figure 5-40: UF Pilot Operations (Mar 29 – Jun 22, 2012)

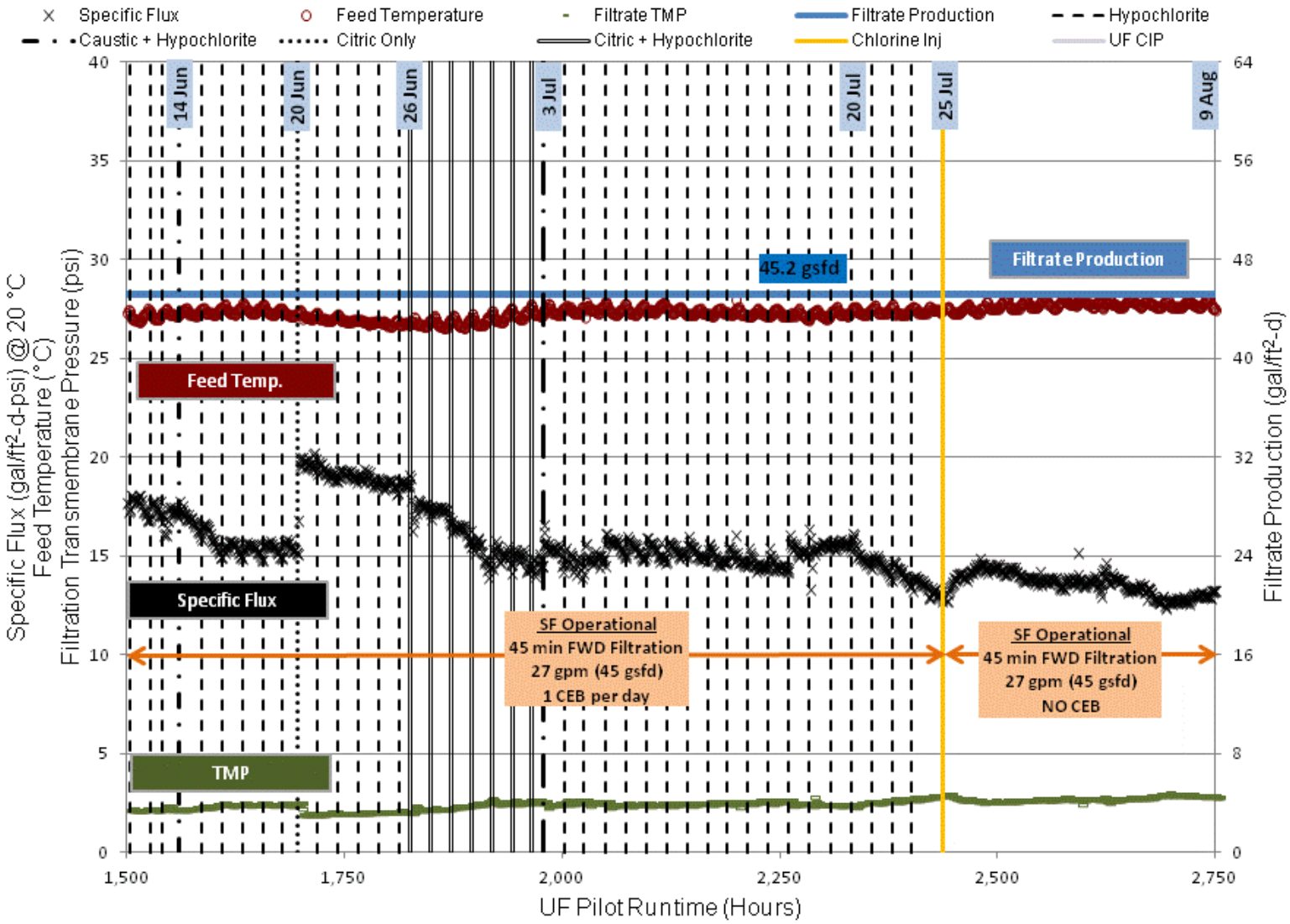

Figure 5-41: UF Pilot Operations (Jun 11 – Aug 9, 2012)

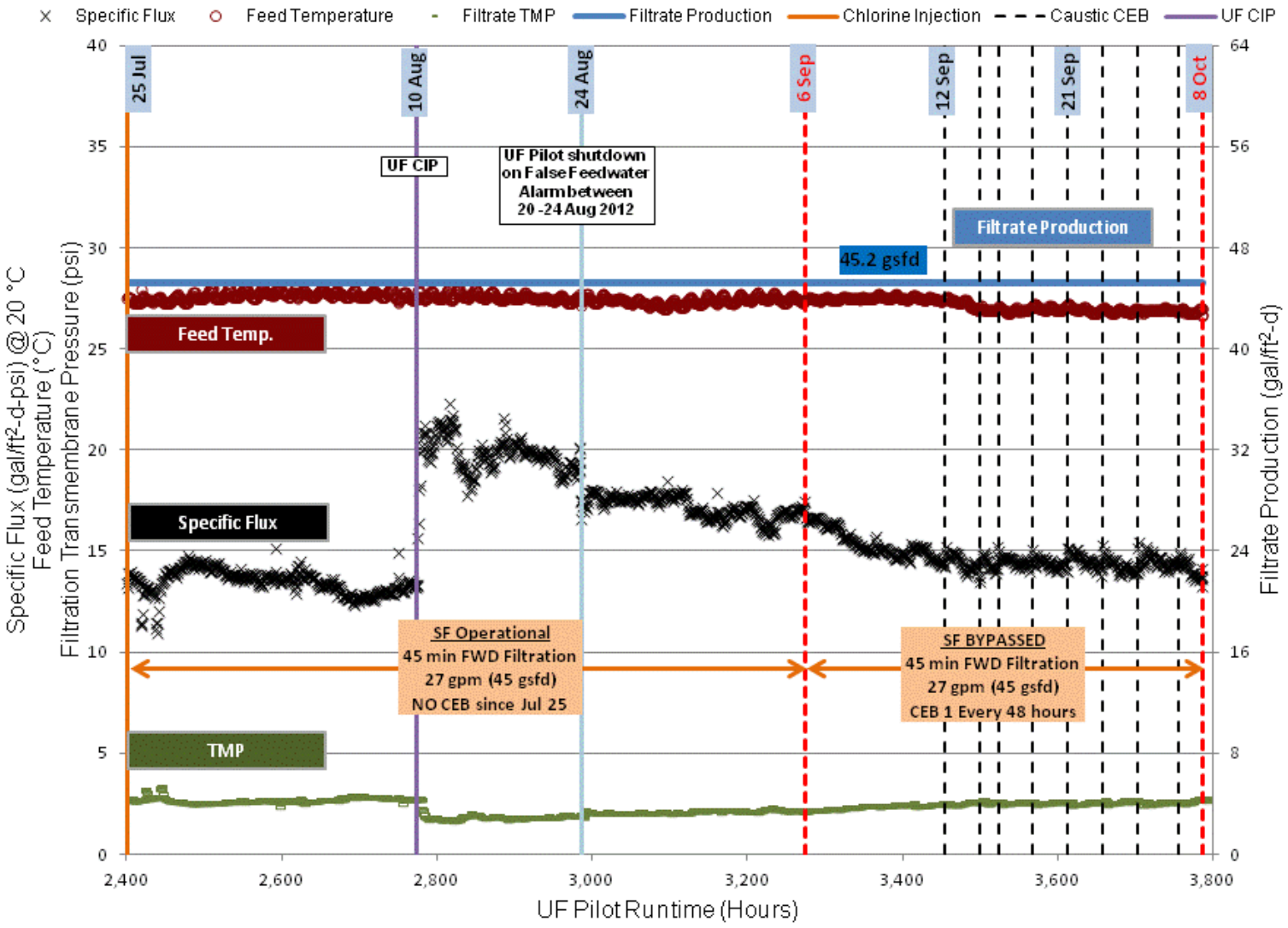

Figure 5-42: UF Pilot Operations (Jul 25 – Oct 8, 2012)

During the period between Mar 29 and Apr 17, the CEB frequency with hypochlorite was twice per day and the MTC was stable at about 20 gal/ft^2.day.psi. Since Apr 17, the CEB frequency with hypochlorite was decreased to once per day till Jul 25. The UF pilot was shutdown on alarm, during the period Apr 25 – 30, as the compressor on the UF pilot failed. The compressor was replaced on Apr 30.

Stable UF operations were observed following the change to once per day hypochlorite CEB up till May 8. Between May 8 and May 16, the MTC was noted to be increasing steeply. Pressure decay tests (PDT) to check if there was fiber breaks causing the MTC to increase, showed that the UF membrane modules were not holding pressure. Additional tests on the pilot eventually showed that one of the check valves on the pilot was loose. The check valve was fixed and the subsequent PDT tests on the feed and filtrate side at 16 psi and 18 psi respectively showed only a pressure loss of 0.01 psi/min and 0.02 psi/min respectively. The PDT is used to test the integrity of membrane unit, based on the principle of measuring pressure drop on the feed and/or filtrate side of the membranes after the membranes have been drained and then pressurized (Zondervan, Zwijnenburg, & Roffel, 2007). The PDT test is membrane manufacturer specific, as the pressure must be below the bubble point pressure of the membrane, which is the pressure required to overcome capillary forces that hold water in membrane pores (USEPA, 2005).

While the filtrate production was consistent at 45.2 gsfd, the TMP was observed to be increasing steadily. On Jun 4, and Jun 14, combination of caustic and hypochlorite CEB were tried as one-off CEBs to see if membrane performance can be improved. Though on Jun 4 there was some

performance improvement of about 3 gal/ft^2.day.psi, this was quickly lost, and a similar caustic and hypochlorite CEB on Jun 14, did not give result in any improvement to the UF performance.

Citric acid CEB done on Jun 20 and the combination of citric and hypochlorite done between Jun 26 and Jun 30, and the caustic-hypochlorite CEB, did not improve the MTC of the UF membrane which stabilized at about 15 gal/ft^2.day.psi.

Between Jul 20 and Jul 25 the daily hypochlorite CEB was noted to be insufficient, and the MTC was noted to be dropping. The performance drop was most likely caused by the algae from the UF filtrate tank. By Jun 14, it was noted that the UF filtrate tank, which serves as the storage tank of feed water to the NF pilot, was acting as a source for algae growth. This algae growth was initially thought to be only affecting the NF pilot (BF and CF) and NF membranes. In Figure 5-43, is the picture taken of the inside of the filtrate tank. The greenish stain is the algae, while the brown stains are the stains that appear when the hypochlorite is used to control algae.

Figure 5-43: Greenish Algae in UF Filtrate Tank

The algae problem was not only noted in the UF filtrate tank. The problem existed in the UF feed tank which stores the feed water to the UF. The source water in the UF feed tank comes from either the SF filtrate or the raw Verna water, if the SF is bypassed. The UF feed tank was regularly cleaned with hypochlorite and flushed, to remove algae. The problem of the algae in the UF filtrate tank only started during the hotter summer months, and the cleaning of this filtrate tank is normally done by the UF pilot vendor, as the use of any hypochlorite that is used in cleaning the UF filtrate tank, must not carry over to the NF pilot. Hypochlorite is an oxidant and even in small quantities, it can damage the polyamide NF membranes.

The algae in the UF filtrate tank though was initially affecting the NF pilot, eventually it started impacting the UF pilot, by way of the rinse cycle following a CEB cycle. The UF pilot was set as once a day hypochlorite CEB to control biofouling problems. However after an 8 minutes soak time on a hypochlorite CEB, the UF filtrate (with algae) is used as rinse water at 3 times the regular forward filtration cycle (i.e. at 81 gpm) for a 2 minutes rinse. This rinse cycle therefore resulted in a very high loading of algae on the outside surface of the hollow UF fibers. By Jul 20, the regular daily hypochlorite CEB was insufficient to take off the algae foulant loaded on the UF fiber before start of the 45 minutes forward filtration cycle, and hence the UF pilot's MTC was decreasing steeply.

On Jul 25, a chlorine injection system was installed on the feed stream to the UF pilot. The target concentration of chlorine in the feed water was about 1.7 mg/L and this resulted in residual chlorine in the UF filtrate tank of about 0.25 ± 0.2 mg/L. Following the installation of the chlorine injection system in the feed stream, the UF pilot was operated in the same conditions as

previously except with no CEBs. Between Jul 25, and Sep 6, when the SF was eventually bypassed, the UF pilot was operated without any CEB. On Aug 10, a clean-in-place (CIP) was performed on the UF pilot, in order to clean the fibers off any biofoulant that was still on the fibers surfaces, especially on the outside surface (see Figure 5-42). The CIP resulted in an increase in the MTC as expected and with no CEB, but with regular backwashes with UF filtrate after every 45 minutes of forward filtration cycle, the pilot continued to produce filtrate at 45.2 gsfd.

On Sep 6, the SF was bypassed and the UF pilot was then directly filtering raw Verna water. The TMP was noted to be increasing while the MTC was dropping, and so on Sep 12 a once in two days caustic CEB cycle was instituted, and by Oct 8, it was noted that the MTC was stable at around 14 gal/ft^2.day.psi.

The UF filtrate water quality was compared to the water quality of the raw Verna water as shown in Table 5-34. The water quality was relative similar, but the UF was noted to consistently screen turbidity causing particulates in the water, with a filtrate turbidity of about 0.08 NTU. The SDI from the UF filtrate as measured at the CF location on the NF pilot was between 2.1 to 2.6, outside of the window of the biofouling problem. During the biofouling problem the SDI as measured at the CF was as high as 3.8.

The UF pretreatment of Verna water has shown, that if it is managed well, for both biofouling and fluctuating turbidity due to formation of colloidal sulfur, can be a more efficient process, when compared to SF.

Table 5-34 : Comparison of Raw Verna Water, Sand Filtrate and UF Filtrate Water Quality

Parameter	Units	Raw Verna	Post SF	UF Filtrate
Turbidity	NTU	0.20 ± 0.05	0.15 ± 0.02	0.08 ± 0.02
Conductivity	µS/cm	1015 ± 33	991 ± 16	1022 ± 35
TOC	mg/L	2.0 ± 0.4	1.7 ± 0.1	2.1 ± 0.4
SO_4^{2-}	mg/L	344 ± 47	348 ± 6	348 ± 67
Cl^-	mg/L	26.0 ± 6.2	17.6 ± 1.1	26.9 ± 4.2
Total Alkalinity	mg/L as $CaCO_3$	166 ± 6	157 ± 5	167 ± 5
Ca	mg/L	97.2 ± 7.0	94.9 ± 0.4	95.1 ± 8.5
Mg	mg/L	49.9 ± 3.5	49.1 ± 0.3	49.1 ± 3.7
Si	mg/L	26 ± 1.4	26 ± 0.1	26 ± 1.2
Ba	µg/L	30.4 ± 2.8	29.2 ± 0.2	30.7 ± 3.3
Sr	mg/L	20.6 ± 1.0	21.8 ± 0.3	20.2 ± 0.8
Ca Hardness	mg/L as $CaCO_3$	243 ± 18	237 ± 1	237 ± 21
Total Hardness	mg/L as $CaCO_3$	471 ± 32	464 ± 2	462 ± 36
TDS	mg/L	730 ± 33	731 ± 25	727 ± 31
TSS	mg/L	1.0 ± 0.8	0.8 ± 0.3	1.4 ± 1.0

Nanofiltration in Conjunction with Ultrafiltration Pretreatment

The new UF modules were installed and operational by Mar 27, and at the same time the NF pilot was also cleaned for biofouling on Mar 29 (see Figure 5-38). Between Mar 29 and Apr 17, the UF pilot was operational with twice a day CEB (see Figure 5-40) and then between Apr 17 and Apr 25, the UF was operating at once a day CEB. During this window the MTC for the 1st

Stage on the NF pilot was dropping, though the 2nd Stage performance remained relatively stable (see Figure 5-44). There was clear indication of biofouling on the NF pilot and after the NF pilot was shut between Apr 25 and Apr 30 for the compressor on the UF pilot to be replaced, the biofouling problem was more obvious and the NF pilot was eventually shutdown on May 5, as the differential pressure drop across the membranes on the 1st Stage increased steeply as seen in Figure 5-45.

The NF pilot operations were started on May 15, with a non-phosphonate based scale inhibitor Vitec® 1000 (Vitec). The study by Vrouwenvendler et al (2010), showed that the use of phosphonate based scale inhibitors increased the potential for biofouling in the presence of substrate. The previous scale inhibitor Aquafeed® 1025 that is also used in the City's RO process is a phosphate based synthetic scale inhibitor. On the NF pilot the dose of Aquafeed® 1025, was about 5 mg/L, while the Vitec scale inhibitor has slightly higher density and at the same feed rate, it was equivalent to a dose of about 5.1 mg/L. The high scale inhibitor dose was the consequence of testing the NF pilot operations without any acid pretreatment to control calcium carbonate scaling.

Even with the non-phosphonate based scale inhibitor the biological fouling problem persisted and the MTC on the first stage was dropping, and the CF on the NF pilot had to be replaced on Jun 5 and Jun 21. The differential pressure across the 2nd stage remained relatively stable as seen in Figure 5-45. Even though the NF feed tank (also the UF filtrate tank) was cleaned for algae growth, the problem was exacerbated by the hot summer months, which resulted in the algae

problem persisting. It was then decided to pre-chlorinate the feed to the UF pilot to control the biofouling problems caused by algae.

The chlorination system on the UF pilot at a dose of about 1.7 mg/L resulted in residual chlorine levels in the UF filtrate tank of about 0.25 ± 0.2. mg/L. As the polyamide NF membranes had zero tolerance for free chlorine, a bisulfate injection system was installed ahead of the NF feed, ahead of the membranes in the NF pilot as shown in Figure 5-46.

The bisulfite feed concentration on the NF pilot was targeted at, at least three times the residual chlorine level and the dose rate was about 2 mg/L. The excess bisulfite was to minimize the possibility of any free chlorine coming into contact with the polyamide membranes. A new ORP (oxidation-reduction potential) electrode probe was installed downstream of the CF. The excess bisulfite suppressed the feed water ORP, and so when the predetermined ORP set point was exceeded due to presence of oxidants like chlorine, the NF pilot's high pressure feed pumps would be shut down automatically with an alarm.

Upon installation of the chlorine injection system on the UF pilot on Jul 25, the MTC on the 1st Stage increased by more than 0.04 gal/ft^2.day.psi, and upon cleaning of the NF membranes on Jul 31, the MTC on the 1st Stage increased to the same levels as the new NF membranes (See Figure 5-33 and Figure 5-38).

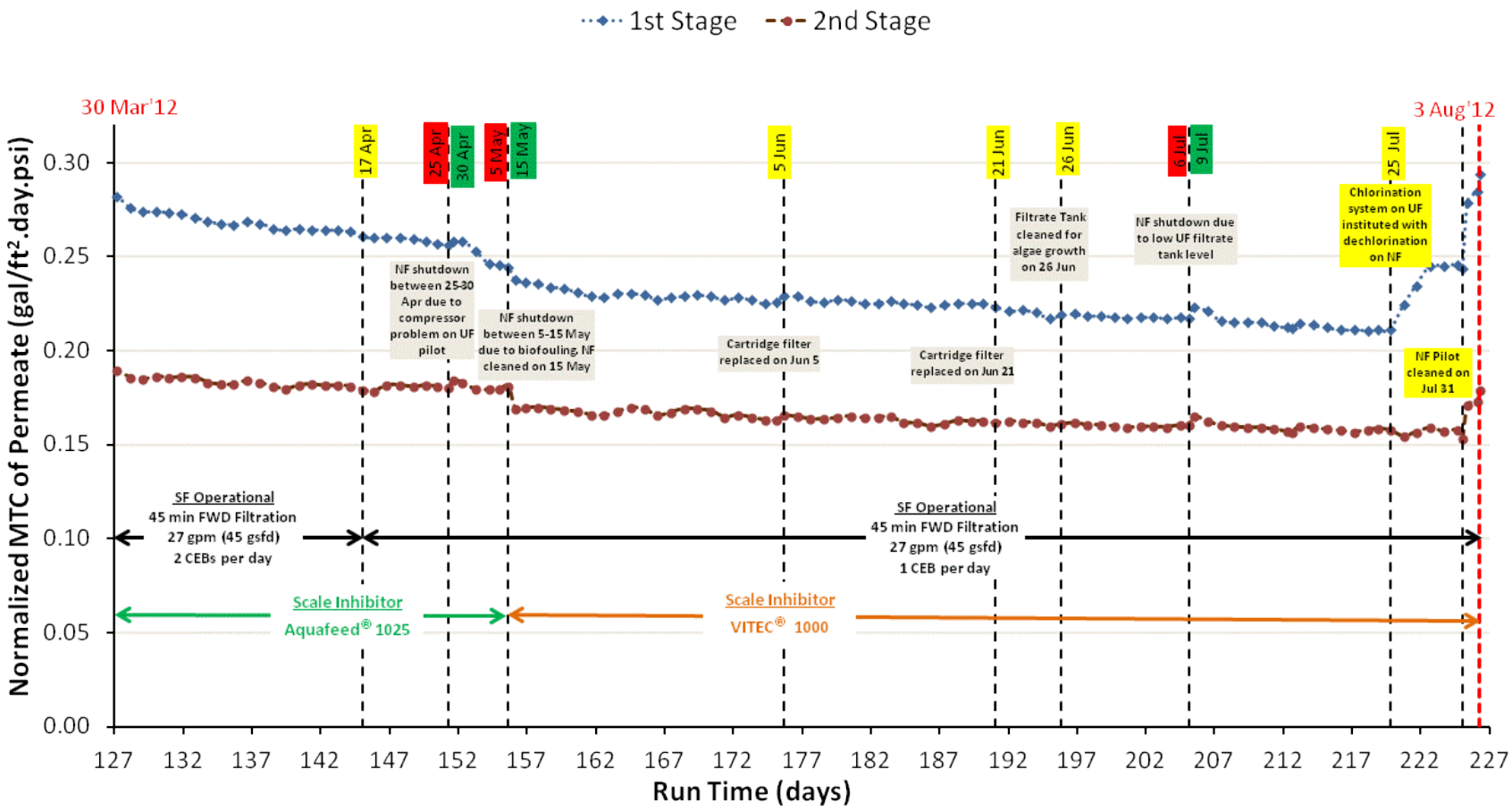

Figure 5-44: Normalized MTC of Permeate for Stages 1 and 2 of NF Pilot (Mar 30 – Aug 3, 2012)

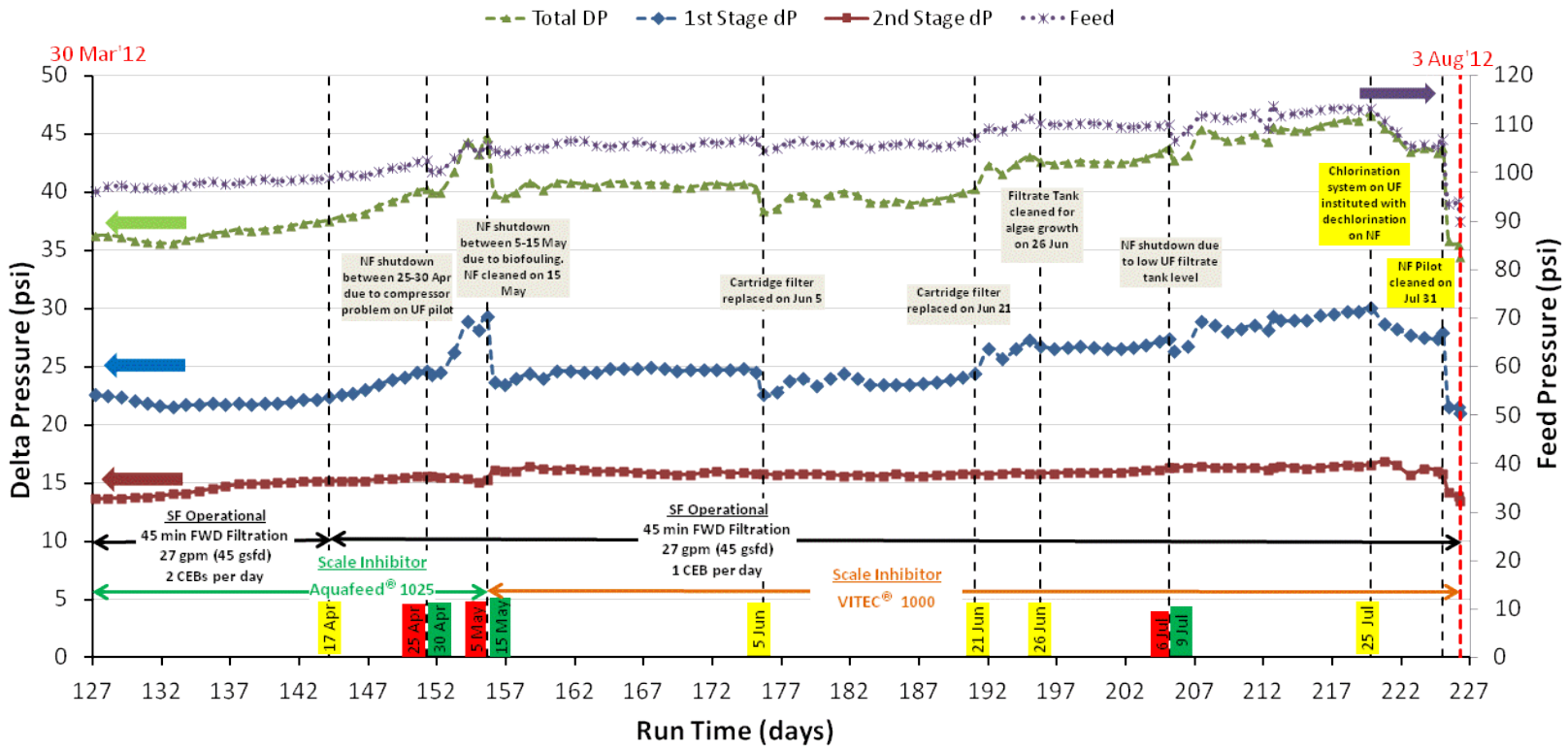

Figure 5-45: Feed and Differential Pressure Condition by Stages on NF Pilot (Mar 30 – Aug 3, 2012)

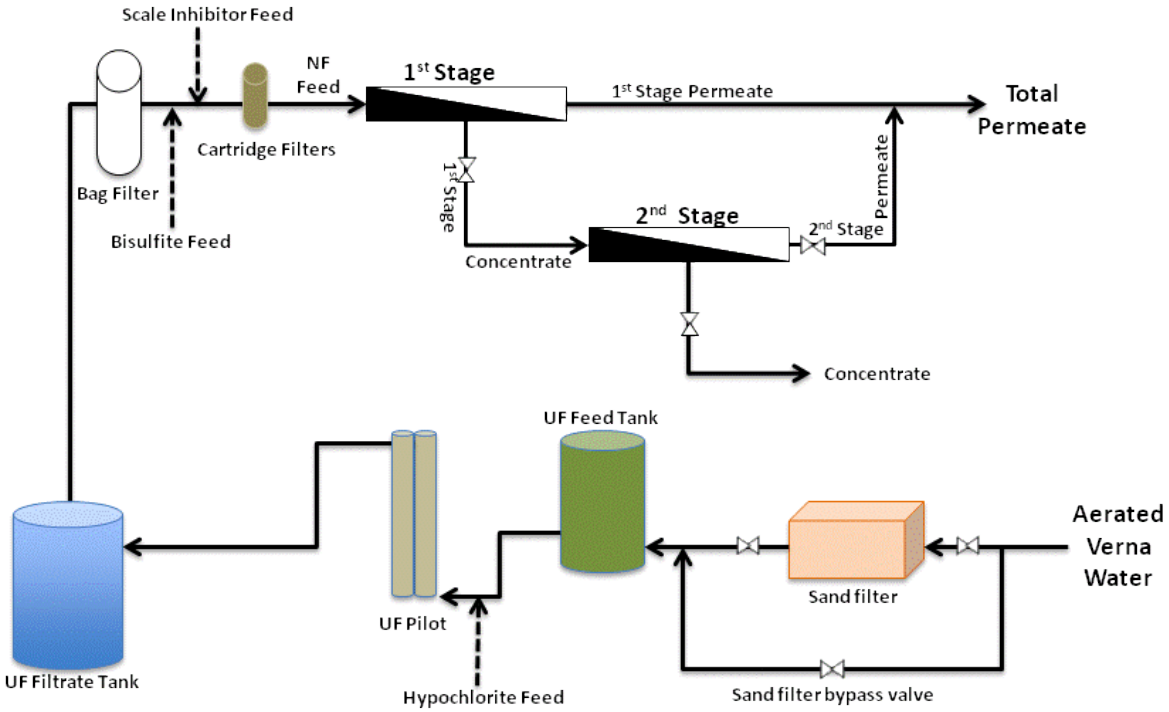

Figure 5-46: Schematic Layout of UF and NF Pilot and Chemical Injections

The NF performance since the installation of the chlorine injection system to the UF feed and dechlorination with bisulfite on the NF feed is as shown in Figure 5-47. The NF performance has been stable with the chlorine injection system in place for close to 22 days before the SF as pre-screen to the UF pilot was bypassed on Sep 6. Extended monitoring of the NF pilot is needed to see if the particulate plugging on the 1st Stage membranes is going to stabilize without the SF as pre-screen to the UF pilot.

The comparison of water quality between the permeate of the NF process and the IX product water from the City's existing IX process is as shown in Table 5-35.

Table 5-35: Comparison of NF Permeate and IX Product Water Quality

Parameter	**Units**	**NF Permeate**	**IX Product**
pH		7.32 ± 0.28	7.81 ± 0.18
Turbidity	NTU	0.06 ± 0.01	0.18 ± 0.06
Conductivity	µS/cm	181 ± 30	1298 ± 91
TOC	mg/L	0.12 ± 0.23	1.8 ± 0.5
SO_4^{2-}	mg/L	4.0 ± 0.7	429 ± 68
Cl^-	mg/L	9.2 ± 2.6	26.4 ± 6.9
Alkalinity	mg/L as $CaCO_3$	63 ± 14	162 ± 9
Ca	mg/L	11.2 ± 1.9	< 1.0
Mg	mg/L	6.3 ± 1.2	< 1.0
Na	mg/L	7.6 ± 3.4	271 ± 24
Ca Hardness	mg/L as $CaCO_3$	28 ± 5	< 2.5
Total Hardness	mg/L as $CaCO_3$	60 ± 15	< 6.7
TDS	mg/L	72 ± 25	783 ± 70

The IX process adopted by the City's is aimed at removing hardness in the water but as sodium zeolite resins are used, the IX product has a higher sodium content when compared to the NF permeate. Though the concentration of sodium in the IX permeate (and also the IX bypass) are higher than the Florida Department of Environmental Protection's drinking water standard of

160mg/L (FDEP, 2011), the actual concentrations at the POE is only about 71 ± 13mg/L as a result of blending with the RO permeate.

From Table 5-35, it can be seen that the NF process does not achieve as high removal efficiency for total hardness in the water, mainly in the form of calcium, magnesium and strontium, when acting as a membrane softening process when compared to the UF process. The raw Verna water has a total hardness concentration of about 500mg/L, and the NF process achieves about 88% removal efficiency while the IX process achieves almost 99% removal efficiency. On the other hand the NF process removes almost 90% of the TDS from the Verna water (between 730 -850 mg/L), while the IX process hardly removes any.

The comparison of the average NF permeate water quality during this study to the UF filtrate water quality, is as shown in Table 5-36. It can therefore be concluded that stable operations can be achieved on the NF pilot treating the highly fouling Verna water with SF and UF as pretreatment to control colloidal plugging problems on the 1st stage and a chlorine injection with a bisulfite injection to quench the excess chlorine, will likely be needed to control biofouling especially from algae. Extended testing will be needed to determine if the operations with UF-NF, without SF, will be stable.

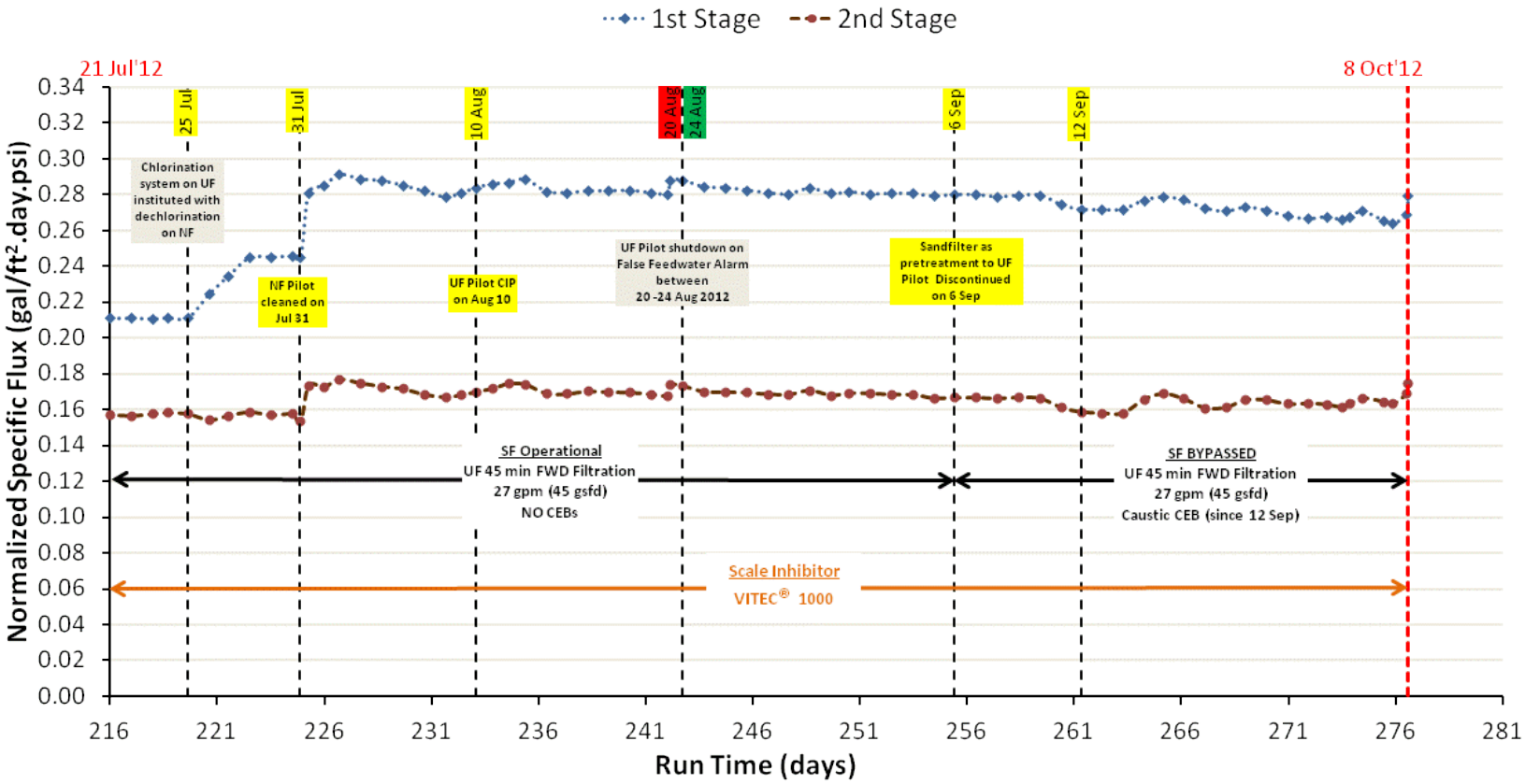

Figure 5-47: Normalized MTC of Permeate for Stages 1 and 2 of NF Pilot (Jul 21 – Oct 8, 2012)

Table 5-36: Comparison of NF Permeate and UF Filtrate Water Quality

Parameter	Units	NF Permeate.	UF Filtrate
pH		7.32 ± 0.28	7.38 ± 0.14
Temp	°C	25.7 ± 1.0	25.7 ± 0.9
Turbidity	NTU	0.06 ± 0.01	0.08 ± 0.02
Conductivity	µS/cm	181 ± 30	1022 ± 35
TOC	mg/L	0.12 ± 0.23	2.1 ± 0.4
SO_4^{2-}	mg/L	4.0 ± 0.7	339 ± 67
Cl^-	mg/L	9.2 ± 2.6	26.9 ± 4.2
Alkalinity	mg/L as $CaCO_3$	63 ± 14	167 ± 5
Ca	mg/L	11.2 ± 1.9	95.1 ± 8.5
Mg	mg/L	6.3 ± 1.2	49.1 ± 3.7
Si	mg/L	17 ± 2.2	26 ± 1.2
K	mg/L	3.8 ± 2.1	2.1 ± 0.2
Na	mg/L	7.6 ± 3.4	20.2 ± 3.2
Ba	µg/L	< 10	30.7 ± 3.3
Mn	µg/L	< 10	< 10
Fe	µg/L	< 10	< 10
Sr	mg/L	2.4 ± 0.5	20.2 ± 0.8
Ca Hardness	mg/L as $CaCO_3$	28 ± 5	237 ± 21
Total Hardness	mg/L as $CaCO_3$	60 ± 15	462 ± 36
TDS	mg/L	72 ± 25	727 ± 31
TSS	mg/L	0.9 ± 1.5	1.4 ± 1.0

6. CONCLUSIONS

UCF and the City successful implemented a 3-Step approach towards acid elimination on the RO plant. The pilot testing of the whole process was the first step, and that was carried out over 4 months at 2 intermediate pHs (i.e. pHs 6.3 and 6.6) between pH 5.8 and ambient pH of 7.1. The second of the 3-step approach was the full-scale implementation of the acid elimination over 5 intermediate pHs between pH 5.8 and pH 7.1 on the RO plant. And the final step was the use of a 2-membrane element "canary" monitoring device, as the 3rd Stage of the membrane process, to act as an early warning device if any unforeseen fouling/scaling occurred as acid was progressively eliminated on the RO plant. During each of the step increments of pH, the LSI and RSI indices were used as tracking tools for comparison of the scaling potential of the 2nd Stage of the RO plant, in comparison to the "canary" unit and the observed trends during the RO pilot study. The acid elimination on the City's RO plant using the 3–step approach was successfully completed over 12-months duration.

The productivity of the second stage of full-scale RO membranes post-acid elimination was lowered by about 0.03 gal/ft^2-day-psi to 0.20 gal/ft^2-day-psi as the result of an increase in the calcium carbonate scaling potential. However, chemical cleaning with low pH cleaners can remove the calcium carbonate scale as seen with the cleanings conducted during the project. The elimination of sulfuric acid pre-treatment is estimated to save the City over $120,000 annually at full capacity production of 4.5 MGD, based on Year 2012 bid prices for sulfuric acid. The total permeate pH following the acid elimination, has risen by about 1 pH unit, and as a result the H_2S removal efficiency in the permeate degasifiers was noted to be marginally lower at 90%. If the

City desires to install a carbonic acid injection system for the permeate before the degasifiers, to improve the H_2S removal efficiency to levels before the acid elimination of about 95%, the additional annual chemical costs is expected to be about $13,000 based on Year 2012 bid prices for carbonic acid. However, it was identified that more frequent maintenance cleaning of the degasifier and its packing material would be a more economical option, as the overall bisulfite removal efficiency on the degasifier seemed to have increased since the elimination of acid use in pre-treatment, resulting in biogrowth of aerobic bacteria like Beggiatoa and Thiothrix. The increased biogrowth could potentially be the main cause of increased turbidity post-degasifier since the acid elimination was completed.

The monitoring and trending of the RO plant performance during the acid elimination was done using the Homogeneous Solution Diffusion Model (HSDM). One of the key weaknesses of trending with HSDM, in the need to input concentrations of the various feed, permeate and concentrate streams on each of the two stages of the RO plant. However there were instruments measuring electrical conductivity (EC) on all points of the RO process except the total concentrate. Using the EC measurements and TDS measurements on samples collected, the correlation factor C_2T was created for each stream on the RO plant. These C_2T factors varied as pH was changed on the RO plant, and were used as inputs in trending the mass transfer coefficient (MTC) for permeate (K_W) for the RO plant and "canary" unit. This same high level of trending to track potential fouling, was not possible on the pilot scale study of the acid elimination, as the online EC measurements were only available on the RO feed and total permeate streams.

Four empirical models were built to predict MTC for solute in terms of TDS and sodium (Na) with data collected in the acid elimination study on the RO plant. The models were validated with data on the RO pilot, as the data collected also reflect similar trends in pH changes and both the pilot and plant used the same types of spiral wound polyamide membranes.

As the MTC is different on each stage of the RO process, two MTC models were built to predict the MTC for TDS and Na on each stage. For the models for the 1st Stage, representing the MTC for TDS (K_{TDS1}) and MTC for Na (K_{Na1}) are as follows:

$$K_{TDS1} = -1.067 \times 10^{-2} + 4.873 \times 10^{3} H^{+} + 6.5 \times 10^{-6} EC$$

$$K_{Na1} = 5.115 \times 10^{-2} + 8.68 \times 10^{-6}\ EC - 1.15 \times 10^{-4} Na$$

The MTC for TDS (K_{TDS2}) and MTC for Na (K_{Na2}) on the 2nd Stage are as follows:

$$K_{TDS2} = -1.293 \times 10^{-2} + 4.048 \times 10^{3} H^{+} + 2.91 \times 10^{-6} EC$$

$$K_{Na2} = 4.159 \times 10^{-2} + 4.92 \times 10^{-6}\ EC - 4.82 \times 10^{-5} Na$$

The models for the MTC of TDS (K_{TDS}) were a function of EC and pH (in terms of hydronium ions), whereas the models for the MTC for Na (K_{Na}) were in terms of EC and concentration of sodium (Na) ions. The models were validated with low deviation from the actual calculated MTC values on an overall basis, though variations were noted at each individual pH condition.

A nanofiltration (NF) pilot was evaluated as an alternative to the City's current operations of treating aerated surficial groundwater from Verna well field using IX process. The principle

problem identified in being able to treat Verna water using NF technology was the colloidal sulfur in the water that comes about as a consequence of oxidation of sulfide in the water during the aeration process. The use of ultrafiltration (UF) filters as pre-screen to the colloidal sulfur, before the water softened using the NF process, was also evaluated. Earlier studies of using different combinations of bag filters, cartridge filters, multi media filters and sand filters did not result in stable operations on the NF pilot. The NF operations without acid use in the pretreatment process were stable with just the use of scale inhibitors, as noted by the MTC for the 2nd Stage. However the MTC for NF permeate on the 1st Stage was noted to drop as a result of fouling by either biofoulants or plugging problems by colloids in the NF feed water, when bag filters, cartridge filters and sand filters were used.

The testing to use UF as a pre-filter to the NF pilot, involved testing the UF operations with and without the use of sand filters as a process ahead of the UF. With sand filters and UF as pretreatment the 1st Stage MTC did not stabilize and the UF was cleaned for biofouling issues. In order to starve off biological growth on the NF membranes, a polyacrylic acid based scale inhibitor Vitec®1000 was used instead of the phosphonate based Aquafeed®1025. As stable operations were not maintained on the NF pilot and the UF filtrate tank was breeding algae, it was decided to chlorinate the UF feed water to control the biofouling and then to dechlorinated the NF feed water with sodium bisulfite ahead of the membranes. Bisulfite feed was pegged at about 4 times the DBP residual chlorine levels, and stable operations were noted on the UF and NF. Stable operations were noted on the NF, with and without the sand filters as pretreatment to the UF pilot.

Both the UF pilot and NF pilots have been shown to withstand high and low pH cleans to restore membrane productivity. Pressure decay tests on the UF fibers have also shown that after more than 3600 runtime hours (equivalent to 150 days), there has been no fiber breaks.

The UF pilot has proven to be an adequate pre-filter of colloids in the Verna water, especially for colloidal sulfur, to the NF pilot. In order to control biofouling on the NF membranes, chlorination or treatment with other biocides is necessary for the Verna water. This approach will also need to be coupled with a non-phosphonate based scale inhibitor, so that the operations of the NF can be stable.

However, it is not a sustainable and cost effective approach to dechlorinate the UF filtrate ahead of the polyamide NF membranes, as any failure to completely dechlorinate the filtrate water will damage the NF membranes. If the City is still keen on adopting the NF membrane technology to improve the quality of its water supply, it will need to investigate controlling the nutrients in the water to control biofouling and/or use of alternative biocides like chloramines. The composite polyamide membranes by Hydranautics (2008) have estimated chloramine tolerance of between 50,000 to 200,000 hours, at the manufacturer's recommended chloramines level of 1.9 mg/L in the feed stream. This chloramines tolerance translates to operating periods of between 3 and 12 years before salt passage increases and membranes need to be replaced. However, as chloramines are formed by mixing chlorine and ammonia, strict controls must be in place to prevent free chlorine from existing by adding excess ammonia.

An alternative solution for the City is to filter all of the Verna water using UF technology and then using part of the filtered water as bypass water for blending while the other fraction of the UF filtrate is softened using the City's existing IX process. The UF pilot studies have shown that it is possible to effectively screen Verna water samples for sulfur and other colloids and particulate matter. Furthermore the membranes have been shown to withstand cleaning with both low and high pH cleaners to restore its performance. Based on this study, biannual clean-in-place of the UF membranes will probably be necessary to maintain sustainable and economical long term operations.

7. RECOMMENDATIONS

The lessons learned from the successful implementation of the 3-step approach towards acid elimination can serve as a guide to other utilities when evaluating and implementing a similar acid elimination plan on their RO/NF processes. Some or all of these lessons can improve the overall process of eliminating use of acid in the pretreatment processes:

1. The instrumentation on pilots and full scale plants should include online EC measurements for the feed, permeate and concentrate of each stage of the membrane process. This would allow better correlation of EC to TDS to arrive at representative correlation factors for C_2T ratios for each part of the membrane process.
2. Sufficient numbers of TDS sampling on all water samples on the process must be done, so that there is sufficient representation of the feed water should well rotations be exercised. Similar TDS analysis should also be done when there are changes to operating conditions, like changes to feed pH and/or scale inhibitor use, etc..
3. No one EC-to-TDS (C_2T) ratio can be representative of all the sample streams on the RO process. The 1st Stage permeate of the RO process has been shown to have a higher C_2T ratio when compared to the 2nd stage permeate.
4. If a "canary" monitoring unit is installed, the feed stream to this 3rd stage unit should come from multiple 2nd stage pressure vessels. Tapping the feed from multiple 2nd stage pressure vessels will allow the feed pressure to the "canary" unit to be sufficiently high so that there is no false alarm towards fouling by monitoring the "canary" unit. Tapping

from multiple 2nd stage pressure vessels, will also allow for throttling of feed flow with little reduction in feed pressure.

5. Trending and monitoring of membrane processes, on full scale RO plant can use the HSDM. The original equipment manufacturer (OEM) shall provide monitoring software that will allow operators to input the varying TDS and EC measurements for the various streams, into the membrane monitoring programs. Using a simple HSDM model, with the flexibility of inputting EC and TDS measurements, the trending of membrane processes by monitoring the MTC in terms of permeate or salt like TDS, as the membrane ages, or conditions in the feed are changed, or when the pretreatment chemicals are varied, will become easier and more representative.

6. Before the acid elimination is implemented on a full scale plant, it is important to check on the plants operating conditions, like for example the available spare capacity on the high pressure feed pumps to ascertain that it is not maxed out. During acid elimination it is anticipated that some level of scaling may happen, and if the spare head on the pumps are inadequate then the overall permeate production of the plant will drop. If necessary it may be best to carry out a membrane cleaning cycle before the acid elimination process is started. That will allow the pumps to be operating at lower head, at the start of the acid elimination exercise. If the membrane is already cleaned, at the start of the acid elimination exercise, then any loss of MTC can be directly attributed to the reduction in acid feed, and it can be easily quantified.

The pilot testing for UF and NF has highlighted the concerns of biofouling on the membrane surfaces. With adequate screening of sunlight by use of black tanks for feed and filtrate tanks, there may not severe biofouling problems with algae, as was seen in this project.

Extended evaluation of the use of chlorine in the feed stream to the UF membranes and dechlorination with sodium bisulfite before the polyamide membranes will be necessary, in order to determine if it will be economical to use this approach towards treating the highly fouling Verna water using NF technology. Other options could include assessment of the use of sodium bisulfite in the feed stream to the UF process. Studies have shown that with exposure time of 30 minutes and at sodium bisulfite concentrations of about 500 ppm, 99% kill rates can be achieved for sea water microorganisms while in other instances only 75% kill is achieved after 4 hours of contact time at same 500 ppm bisulfite concentration (Baker & Dudley, 1998). If bisulfite can be injected into the UF feed stream, and the residual levels can be maintained in the UF filtrate stream to control biofouling, the excess bisulfite can be removed in the NF process (Singh, 2006).

If disinfection using chlorine or monochloramine is considered as pretreatment to the UF process to control biofouling, then additional studies will be required to evaluate the formation potential for disinfection byproducts in the Verna water. NF permeate will be blended with the RO water and Verna bypass water that is filtered or unfiltered by UF an UF process, and chlorinated once again for disinfection purposes before supply. Comparisons of DBP formation of this approach to treatment, to the DBP formation as a result of treatment of Verna water using UF technology

and then chlorinating of the final blended for disinfection for supply, ought to be part of the overall assessment of the treatment technology that the City will adopt for its Verna water.

APPENDIX:
WATER QUALITY AND MODEL BUILDING DATA

The Appendix contains the water quality data used for the precision analysis of conductivity, total dissolved solids and sodium and the accuracy analysis data for sodium. Precision analysis is done on samples collected, with duplicates taken on every 5 samples taken. Accuracy analysis is carried out by spiking samples with known concentration of the parameter (i.e. in this case Sodium) being analyzed.

Also included in this Appendix is the water quality tabulations that were used in the derivation of the EC to TDS (C_2T) ratios and the empirical models built to predict the mass transfer coefficient for TDS and sodium.

Table 0-1: Laboratory Precision Analysis of Electrical Conductivity

Set Number	Conductivity (µs/cm)		
	Dupe A	Dupe B	I
1	3320	3320	0.000
2	84.1	81.9	0.013
3	3270	3280	0.002
4	54.9	53.8	0.010
5	6210	6190	0.002
6	80.3	82.6	0.014
7	142.9	145.5	0.009
8	3190	3250	0.009
9	3390	3380	0.001
10	3180	3280	0.015
11	6210	6190	0.002
12	6020	5970	0.004
13	84.1	81.9	0.013
14	3210	3230	0.003
15	3340	3330	0.001
16	5800	5820	0.002
17	92.6	90.2	0.013
18	9350	9400	0.003
19	9060	9210	0.008
20	3170	3170	0.000
21	3130	3150	0.003
22	6240	6250	0.001
23	10390	10460	0.003
24	11740	11650	0.004
25	10920	11050	0.006
26	10800	10770	0.001
27	12720	12670	0.002
28	11940	11930	0.000
29	1307	1313	0.002
30	1062	1074	0.006
31	519	516	0.003
32	3280	3270	0.002
33	6530	6500	0.002
34	10900	10840	0.003
35	12490	12560	0.003
36	12340	12340	0.000
37	519	516	0.003
38	3490	3480	0.001
39	11500	11440	0.003
40	11660	11650	0.000
41	12470	12530	0.002
42	12900	12960	0.002
43	1463	1466	0.001
44	1184	1177	0.003
45	649	649	0.000
46	3240	3250	0.002
47	3230	3240	0.002
48	6560	6570	0.001
49	12420	12420	0.000
50	11670	11560	0.005
51	13010	12930	0.003
52	1224	1227	0.001
53	1003	996	0.004
54	3560	3530	0.004
55	3490	3460	0.004
56	6840	6690	0.011
57	11720	11600	0.005
58	11610	11660	0.002
59	13280	13040	0.009
60	506	499	0.007
61	3600	3520	0.011
62	3560	3490	0.010
63	7360	7220	0.010
64	11970	11760	0.009
65	1174	1160	0.006
66	976	963	0.007
67	3640	3630	0.001
68	3610	3590	0.003
69	7370	7520	0.010
70	12630	12550	0.003
71	12120	12010	0.005
72	12160	12200	0.002
73	12480	12510	0.001
74	14520	14470	0.002
75	13720	13690	0.001
76	1289	1284	0.002
77	1068	1065	0.001
78	590	589	0.001
79	529	515	0.013

Average I-Statistic =	**0.004**
Standard Deviation =	**0.004**
Upper Warning Limit (UWL) =	**0.012**
Upper Control Limit (UCL) =	**0.016**

Table 0-2: Laboratory Precision Analysis of Total Dissolved Solids

Set Number	TDS (mg/L)		
	Dupe A	Dupe B	I
1	2321	2332	0.002
2	2330	2334	0.001
3	2394	2424	0.006
4	39	39.5	0.006
5	62	60	0.016
6	8495	8589	0.006
7	2363	2367	0.001
8	2410	2396	0.003
9	42.5	42	0.006
10	40	38	0.026
11	62	60	0.016
12	8495	8589	0.006
13	42.1	43.5	0.016
14	5021	5059	0.004
15	2367	2380	0.003
16	4973	4936	0.004
17	5069	5043	0.003
18	8496	8589	0.005
19	43.6	42.6	0.012
20	8709	8493	0.013
21	2463	2461	0.000
22	2429	2413	0.003
23	2442	2478	0.007
24	2425	2403	0.005
25	4966	5015	0.005
26	5132	4912	0.022
27	8690	8555	0.008
28	8866	8946	0.004
29	2192.5	2145.5	0.011
30	2182	2165.5	0.004
31	4712	4772	0.006
32	8681	8570	0.006
33	9538	9364	0.009
34	8847	8859	0.001
35	9958	9905	0.003
36	849	859.5	0.006
37	856	818.5	0.022
38	288.5	277.5	0.019
39	2146.5	2219.5	0.017
40	2160	2121	0.009
41	4734	4721.5	0.001
42	8699	8689.5	0.001
43	10073	9946	0.006
44	374	378	0.005
45	2287	2277	0.002
46	8897	9021	0.007
47	9106	9095	0.001
48	10235	10303	0.003
49	901.5	889	0.007
50	889.5	892.5	0.002
51	362	374	0.016
52	2131.5	2161	0.007
53	2151.5	2147	0.001
54	4549.5	4572.5	0.003
55	9416.5	9412.5	0.000
56	8991	8922	0.004
57	9664	10074	0.021
58	699.5	708.5	0.006
59	684	699	0.011
60	2248	2249.5	0.000
61	2204.5	2225	0.005
62	4638	4498.5	0.015
63	1074.1	1031.6	0.020
64	8789	8720	0.004
65	9707	9671	0.002
66	340.5	322.5	0.027
67	2246.5	2271	0.005
68	2204	2276.5	0.016
69	500.34	516.8	0.016
70	9284	9312	0.002
71	697	693	0.003
72	675.5	681	0.004
73	278.89	282.5	0.006
74	2353.5	2342	0.002
75	5243.5	5299.5	0.005
76	9675.5	9786.5	0.006
77	9383	9296	0.005
78	9354	9453	0.005
79	11152	11412	0.012
80	10850	10848	0.000
81	767	761.5	0.004
82	749	754.5	0.004
83	78.22	75.09	0.020

Average I-Statistic =	**0.007**
Standard Deviation =	**0.007**
Upper Warning Limit (UWL) =	**0.021**
Upper Control Limit (UCL) =	**0.027**

Table 0-3: Laboratory Precision Analysis of Sodium

Set Number	Na (mg/L)		
	Dupe A	Dupe B	I
1	289.3	289.9	0.001
2	289.8	286.6	0.005
3	8.6	8.6	0.005
4	8.2	8.2	0.002
5	288.7	292.1	0.006
6	575.6	565.9	0.009
7	22.9	22.9	0.000
8	12.1	12.2	0.005
9	1040.8	1024.5	0.008
10	298.1	298.2	0.000
11	288.0	287.4	0.001
12	284.1	288.4	0.008
13	276.5	275.3	0.002
14	576.0	583.3	0.006
15	632.7	625.2	0.006
16	1072.8	1081.0	0.004
17	1132.6	1141.7	0.004
18	225.0	226.8	0.004
19	225.1	228.8	0.008
20	476.3	486.9	0.011
21	14.3	15.3	0.032
22	1096.9	1105.7	0.004
23	542.4	573.5	0.028
24	278.6	272.4	0.011
25	959.5	979.3	0.010
26	62.4	62.8	0.003
27	1111.3	1094.2	0.008
28	258.9	246.3	0.025
29	975.7	957.2	0.010
30	1062.7	1050.0	0.006
31	62.4	62.8	0.003
32	260.7	262.0	0.002
33	250.4	236.7	0.028
34	1061.2	1112.5	0.024
35	1271.2	1267.4	0.002
36	308.3	317.9	0.015
37	17.9	18.8	0.024
38	93.1	92.4	0.004
39	264.4	269.9	0.010
40	275.0	281.3	0.011
41	611.2	607.1	0.003
42	1137.3	1138.9	0.001
43	1329.1	1277.8	0.020
44	264.6	258.3	0.012
45	15.5	16.0	0.016
46	263.8	250.5	0.026
47	257.6	264.4	0.013
48	581.4	583.9	0.002
49	8535.5	8520.0	0.001
50	1110.3	1091.9	0.008
51	1261.6	1289.6	0.011
52	53.0	54.4	0.014
53	270.2	253.0	0.033
54	268.4	256.2	0.023
55	4958.5	5002.5	0.004
56	44.6	44.8	0.002
57	237.6	235.1	0.005
58	1.9	1.9	0.005
59	2315.0	2349.0	0.007
60	282.2	272.0	0.018
61	647.0	662.7	0.012
62	1040.8	990.4	0.025
63	49.5	49.1	0.004
64	45.4	46.0	0.007
65	58.2	57.6	0.005
66	55.0	54.6	0.004
67	268.3	276.3	0.015
68	18.3	18.2	0.003
69	307.0	308.0	0.002
70	284.0	272.0	0.022

Average I-Statistic =	**0.010**
Standard Deviation =	**0.009**
Upper Warning Limit (UWL) =	**0.027**
Upper Control Limit (UCL) =	**0.035**

Table 0-4: Laboratory Accuracy Analysis of Sodium

Sample (mg/L)	Spike (mg/L)	Determined Value (mg/L)	% Recovery
2.89	5.5	8.64	104.5
2.95	5.5	8.49	100.7
2.80	5.5	8.72	107.6
2.87	5.5	8.63	104.7
2.90	5.5	8.65	104.5
1.71	5.5	7.1	98.0
4.58	5.5	10.82	113.5
2.83	5.5	8.66	106.0
5.20	5.5	11.15	108.2
1.64	5.5	6.99	97.3
4.46	5.5	10.29	106.0
2.42	5.5	7.86	98.9
2.98	2.3	5.17	95.2
2.84	2.3	4.94	91.3
2.88	2.3	4.97	90.9
5.36	2.3	7.71	102.2
2.88	2.3	5.12	97.4
3.16	2.3	5.61	106.5
5.66	2.3	8.1	106.1
3.47	2.3	5.66	95.2
3.56	2.3	5.66	91.3
3.72	2.3	6.23	109.1
2.25	2.3	4.37	92.2
2.25	2.3	4.53	99.1
2.38	2.3	4.54	93.9
4.8	2.3	7.35	110.9
4.39	2.3	6.72	101.3
3.79	2.3	6.15	102.6
4.88	2.3	7.33	106.5
5.57	2.3	7.99	105.2
0.71	2.3	2.84	92.6
2.37	2.3	4.6	97.0
2.59	2.3	4.66	90.0
2.70	2.3	4.87	94.3
5.31	2.3	7.56	97.8
6.79	2.3	9.43	114.8
3.12	2.3	5.2	90.4
5.56	2.3	7.81	97.8
6.36	2.3	8.61	97.8
4.66	2.3	7.01	102.2
5.31	2.3	7.54	97.0
6.36	2.3	8.7	101.7
0.94	2.3	3.01	90.0
2.64	2.3	4.99	102.2
2.75	2.3	4.9	93.5
6.11	2.3	8.56	106.5
5.79	2.3	8.11	100.9
5.10	2.3	7.54	106.1
0.77	2.3	2.83	89.6
4.34	2.3	7.04	117.4
4.28	2.3	6.81	110.0
2.64	2.3	4.82	94.8
2.58	2.3	4.79	96.1
5.81	2.3	8.22	104.8
5.37	2.3	7.7	101.3
6.31	2.3	8.71	104.3
2.65	2.3	4.76	91.7
2.70	2.3	4.7	87.0
2.68	2.3	4.83	93.5
5.00	2.3	7.27	98.7
5.51	2.3	7.93	105.2
0.80	2.3	2.79	86.5
3.75	2.3	6.3	110.9
3.34	2.3	5.8	107.0
3.55	2.3	5.9	102.2
6.67	2.3	9.4	118.7
6.26	2.3	8.72	107.0
3.75	2.3	5.8	89.1
5.75	2.3	7.75	87.0
5.53	2.3	7.92	103.9

Average	**=**	**100.4 %**
Standard Deviation	**=**	**7.5 %**

Table 0-5: TDS to Electrical Conductivity Relationship for RO Pilot's Feed

Date	Target Feed pH	pH RO Feed	TDS (mg/L)		Conductivity [EC] (µs/cm)		TDS/EC Ratio	
			RO Feed	Ave RO Feed	RO Feed	Ave RO Feed	RO Feed	Ave RO Feed
4/2/10	5.80	5.94	2330	2361	3320	3281	0.70	0.72
4/2/10		5.94	2334		3320		0.70	
4/9/10		6.23	2365		3310		0.71	
4/16/10		6.00	2324		3280		0.71	
4/23/10		5.89	2332		3160		0.74	
4/30/10		5.90	2383		3200		0.74	
5/14/10		5.97	2394		3330		0.72	
5/14/10		5.97	2424					
5/21/10		5.85	2367		3330		0.71	
5/25/10	6.30	6.42	2406	2393	3230	3266	0.74	0.73
6/1/10		6.51	2367		3300		0.72	
6/1/10		6.51	2380					
6/8/10		6.44	2422		3310		0.73	
6/15/10		6.51	2414		3340		0.72	
6/22/10		6.53	2407		3160		0.76	
6/22/10		6.57			3280			
6/29/10		6.61	2356		3240		0.73	
7/6/10	6.60	6.81	2407	2407	3450	3450	0.70	0.70
7/13/10	7.10	7.13	2442	2419	3210	3280	0.76	0.74
7/13/10		7.20	2478		3230		0.77	
7/20/10		7.02	2381		3320		0.72	
7/28/10		7.11	2425		3340		0.73	
7/28/10		7.15	2403		3330		0.72	
8/6/10		7.13	2384		3250		0.73	

Table 0-6: TDS to Electrical Conductivity Relationship for RO Pilot's 1st Stage Permeate

Date	Target Feed pH	pH 1st Stg Permeate	TDS (mg/L)		Conductivity [EC] (µs/cm)		TDS/EC Ratio	
			1st Stage Permeate	Ave 1st Stg Permeate	RO Feed	Ave 1st Stg Permeate	1st Stage Permeate	Ave 1st Stg Permeate
4/2/10	5.80	5.34	46.0	40.8	55.2	57.3	0.83	0.71
4/9/10		5.58	43.0		58.8		0.73	
4/16/10		5.37	41.0		53.6		0.76	
4/23/10		5.57	40.0		56.0		0.71	
4/30/10		5.36	40.0		55.8		0.72	
4/30/10		5.36	35.0					
5/14/10		5.54	44.0		63.4		0.69	
5/21/10		5.65	39.0		58.3		0.67	
5/21/10		5.65	39.5					
5/25/10	6.30	5.81	40.0	40.6	56.9	53.6	0.70	0.76
6/1/10		5.81	42.0		51.7		0.81	
6/8/10		5.78	42.5		49.9		0.85	
6/8/10		5.80	42.0					
6/15/10		5.80	40.5		54.9		0.74	
6/15/10		5.80			50.7			
6/22/10		5.72	40.0		50.8		0.79	
6/29/10		5.86	40.0		64.0		0.63	
6/29/10		5.77	38.0		50.1		0.76	
7/6/10	6.60	6.18	37.0	37.0	51.8	51.8	0.71	0.71
7/13/10	7.10	6.35	40.0	39.9	52.3	49.4	0.76	0.81
7/20/10		6.36	40.0		47.6		0.84	
7/28/10		6.21	40.5		47.6		0.85	
8/6/10		6.35	39.0		50.2		0.78	

Table 0-7: TDS to Electrical Conductivity Relationship for RO Pilot's 1st Stage Concentrate

Date	Target Feed pH	pH 1st Stg Conc	TDS (mg/L)		Conductivity [EC] (µs/cm)		TDS/EC Ratio	
			1st Stage Conc.	Ave 1st Stg Conc.	1st Stage Conc.	Ave 1st Stg Conc.	1st Stage Conc.	Ave 1st Stg Conc.
4/2/10	5.80	6.08	4895	4918	6150	6110	0.80	0.80
4/9/10		6.14	4986		6070		0.82	
4/16/10		6.15	4919		6100		0.81	
4/23/10		5.99	5014		6020		0.83	
4/30/10		6.00	4846		5930		0.82	
5/14/10		6.05	4828		6230		0.77	
5/21/10		5.98	4938		6270		0.79	
5/25/10	6.30	6.52	4973	5034	5950	6055	0.84	0.83
5/25/10		6.52	4936					
6/1/10		6.55	5059		5950		0.85	
6/8/10		6.51	5143		6120		0.84	
6/15/10		6.55	5069		6200		0.82	
6/15/10		6.59	5043					
6/22/10		6.71	5056		6140		0.82	
6/29/10		6.68	4991		5970		0.84	
7/6/10	6.60	6.83	5021	5040	6210	6200	0.81	0.81
7/6/10		7.01	5059		6190		0.82	
7/13/10	7.10	7.26	5014	5020	5970	5950	0.84	0.84
7/20/10		7.10	4966		6020		0.82	
7/20/10		7.21	5015		5970		0.84	
7/28/10		7.28	4972		6120		0.81	
8/6/10		7.23	5132		5800		0.88	
8/6/10		7.26	4912		5820		0.84	

Table 0-8: TDS to Electrical Conductivity Relationship for RO Pilot's 2nd Stage Permeate

Date	Target Feed pH	pH 2nd Stg Permeate	TDS (mg/L)		Conductivity [EC] (µs/cm)		TDS/EC Ratio	
			2nd Stage Permeate	Ave. 2nd Stage Permeate	2nd Stage Permeate	Ave. 2nd Stage Permeate	2nd Stage Permeate	Ave. 2nd Stage Permeate
4/2/10	5.80	5.42	65.0	58.0	138.7	144.7	0.47	0.40
4/9/10		5.60	62.0		150.7		0.41	
4/16/10		5.45	59.0		148.1		0.40	
4/23/10		5.50	56.0		144.3		0.39	
4/30/10		5.54	54.0		135.4		0.40	
5/14/10		5.59	53.0		148.7		0.36	
5/21/10		5.52	55.0		147.0		0.37	
5/21/10		5.52	60.0					
5/25/10	6.30	5.73	49.0	48.4	139.5	139.8	0.35	0.35
6/1/10		5.73	48.0		137.3		0.35	
6/8/10		5.69	47.4		137.8		0.34	
6/15/10		5.73	46.0		142.9		0.32	
6/15/10		5.73			145.5			
6/22/10		5.94	52.0		141.1		0.37	
6/29/10		5.73	46.5		136.0		0.34	
6/29/10		5.75	50.0		138.2		0.36	
7/6/10	6.00	5.80	53.0	53.0	144.5	144.5	0.37	0.37
7/13/10	7.10	6.19	45.0	47.0	129.5	128.9	0.35	0.36
7/20/10		5.96	49.0		130.1		0.38	
7/28/10		6.14	50.0		130.6		0.38	
8/6/10		6.05	44.0		125.3		0.35	

Table 0-9: TDS to Electrical Conductivity Relationship for RO Pilot's 2nd Stage Concentrate

Date	Target Feed pH	pH 2nd Stg Conc.	TDS (mg/L)		Conductivity [EC] (µs/cm)		TDS/EC Ratio	
			2nd Stage Conc.	Ave. 2nd Stage Conc.	2nd Stage Conc.	Ave. 2nd Stage Conc.	2nd Stage Conc.	Ave. 2nd Stage Conc.
4/2/10	5.8	6.23	8630	8589	9880	9663	0.87	0.89
4/9/10		6.32	8852		9750		0.91	
4/16/10		6.28	8495		9640		0.88	
4/16/10		6.28	8589					
4/23/10		6.22	8740		9720		0.90	
4/30/10		6.12	8400		9420		0.89	
5/14/10		6.21	8445		9490		0.89	
5/21/10		6.26	8565		9740		0.88	
5/25/10	6.3	6.74	8377	8560	9940	9617	0.84	0.89
6/1/10		6.77	8238		9230		0.89	
6/8/10		6.78	8879		9620		0.92	
6/15/10		6.79	8615		9820		0.88	
6/22/10		6.84	8493		9670		0.88	
6/29/10		7.01	8760		9420		0.93	
7/6/10	6.6	7.10	8637	8594	9820	9841	0.88	0.87
7/6/10		7.20	8551		9862		0.87	
7/13/10	7.1	7.49	8932	8801	9300	9315	0.96	0.94
7/20/10		7.35	8690		9350		0.93	
7/20/10		7.36	8555		9400		0.91	
7/28/10		7.37	8819		9570		0.92	
8/6/10		7.39	8866		9060		0.98	
8/6/10		7.40	8946		9210		0.97	

Table 0-10: TDS to Electrical Conductivity Relationship for RO Plant's Feed

Date	Target Feed pH	pH RO Feed	TDS (mg/L)		Conductivity [EC] (µs/cm)		TDS/EC Ratio	
			RO Feed	Ave RO Feed	RO Feed	Ave RO Feed	RO Feed	Ave RO Feed
6/17/11	5.80	6.04	2182	2144	3130	3133	0.70	0.68
6/17/11		6.02	2162		3150		0.69	
6/17/11		5.96	2100		3130		0.67	
6/17/11		5.91	2134		3120		0.68	
7/14/11	6.05	6.15	2160	2162	3250	3250	0.66	0.67
7/14/11		6.09	2121		3260		0.65	
7/14/11		6.20	2204		3240		0.68	
8/16/11	6.30	6.44	2287	2282	3490	3485	0.66	0.65
8/16/11		6.49	2277		3480		0.65	
9/16/11	6.50	6.51	2152	2173	3230	3293	0.67	0.66
9/16/11		6.56	2147		3240		0.66	
9/16/11		6.53	2221		3410		0.65	
10/21/11	6.70	6.74	2205	2196	3490	3483	0.63	0.63
10/21/11		6.71	2225		3460		0.64	
10/21/11		6.76	2160		3500		0.62	
1/17/12	6.70	NM[1]	2167	2271	3316	3413	0.65	0.67
1/28/12		NM	2376		3510		0.68	
2/9/12	6.90	6.78	2204	2218	3560	3507	0.62	0.63
2/9/12		6.80	2276		3490		0.65	
2/9/12		6.82	2172		3470		0.63	
3/1/12	7.10	7.17	2428	2363	3860	3652	0.63	0.65
3/1/12		7.10	2312		3580		0.65	
5/8/12		7.18	2342		3610		0.65	
5/8/12		7.19	2354		3590		0.66	
5/8/12		7.35	2381		3620		0.66	

[1] NM – Not measured

Table 0-11: TDS to Electrical Conductivity Relationship for RO Plant's 1st Stage Permeate

Date	Target Feed pH	pH 1st stg Permeate	TDS (mg/L)		Conductivity [EC] (µs/cm)		TDS/EC Ratio	
			1st Stage Permeate	Ave.1st Stage Permeate	1st Stage Permeate	Ave.1st Stage Permeate	1st Stage Permeate	Ave.1st Stage Permeate
6/17/11	5.80	5.48	39.0	40.3	57.1	56.4	0.68	0.72
6/17/11		5.53	40.0		55.8		0.72	
6/17/11		5.49	42.0		56.3		0.75	
7/14/11	6.05	5.64	41.0	42.0	56.8	55.8	0.72	0.75
7/14/11		5.57	43.0		54.7		0.79	
8/16/11	6.30	5.79	46.0	44.0	59.4	60.2	0.77	0.73
8/16/11		5.84	42.0		60.9		0.69	
9/16/11	6.50	5.77	38.0	40.5	52.6	54.0	0.72	0.75
9/16/11		5.75	43.0		55.3		0.78	
10/21/11	6.70	5.99	38.0	41.0	55.2	54.8	0.69	0.75
10/21/11		5.98	44.0		54.4		0.81	
1/17/12	6.70	NM[1]	48.0	46.0	63.5	65.6	0.76	0.70
1/28/12		NM	44.0		67.6		0.65	
2/9/12	6.90	5.89	46.0	44.5	65.3	64.5	0.70	0.69
2/9/12		5.99	43.0		63.7		0.68	
3/1/12	7.10	6.33	47.0	48.5	69.0	70.5	0.68	0.69
3/1/12		6.28	44.0		64.2		0.69	
5/8/12		6.51	50.0		83.4		0.60	
5/8/12		6.50	53.0		65.2		0.81	

[1] NM – Not measured

Table 0-12: TDS to Electrical Conductivity Relationship for RO Plant's 1st Stage Concentrate

Date	Target Feed pH	pH 1st Stg Conc	TDS (mg/L)		Conductivity [EC] (µs/cm)		TDS/EC Ratio	
			1st Stage Conc.	Ave. 1st Stage Conc.	1st Stage Conc.	Ave. 1st Stage Conc.	1st Stage Conc.	Ave. 1st Stage Conc.
6/17/11	5.80	6.46	4712	4702	6240	6258	0.76	0.75
6/17/11		6.35	4772		6250		0.76	
6/17/11		6.11	4660		6270		0.74	
6/17/11		6.12	4663		6270		0.74	
7/14/11	6.05	6.36	4734	4745	6530	6507	0.72	0.73
7/14/11		6.40	4722		6500		0.73	
7/14/11		6.38	4778		6490		0.74	
8/16/11	6.30	6.85	4711	4700	6570	6675	0.72	0.70
8/16/11		6.76	4689		6780		0.69	
9/16/11	6.50	6.71	4550	4533	6560	6610	0.69	0.69
9/16/11		6.70	4573		6570		0.70	
9/16/11		6.88	4478		6700		0.67	
10/21/11	6.70	6.94	4638	4554	6840	6750	0.68	0.67
10/21/11		6.91	4499		6690		0.67	
10/21/11		6.91	4525		6720		0.67	
1/17/12	6.70	NM[1]	4784	5023	6513	6724	0.73	0.75
1/28/12		NM	5261		6934		0.76	
2/9/12	6.90	7.02	4958	4935	7360	7247	0.67	0.68
2/9/12		7.03	5003		7220		0.69	
2/9/12		7.01	4843		7160		0.68	
3/1/12	7.10	7.27	5349	5270	7870	7508	0.68	0.70
3/1/12		7.30	5254		7390		0.71	
5/8/12		7.54	5300		7520		0.70	
5/8/12		7.61	5244		7370		0.71	
5/8/12		7.45	5207		7390		0.70	

[1] NM – Not measured

Table 0-13: TDS to Electrical Conductivity Relationship for RO Plant's 2nd Stage Permeate

Date	Target Feed pH	pH 2nd Stg Permeate	TDS (mg/L)		Conductivity [EC] (µs/cm)		TDS/EC Ratio	
			2nd Stage Permeate	Ave. 2nd Stage Permeate	2nd Stage Permeate	Ave. 2nd Stage Permeate	2nd Stage Permeate	Ave. 2nd Stage Permeate
6/17/11	5.80	5.51	55	60	133	133	0.41	0.45
6/17/11		5.48	65		134		0.49	
6/17/11		5.49	60		133		0.45	
7/14/11	6.05	5.61	63	64	135	140	0.47	0.46
7/14/11		5.57	65		144		0.45	
8/16/11	6.30	5.92	55	57	135	135	0.41	0.42
8/16/11		5.88	58		135		0.43	
9/16/11	6.50	5.72	55	55	124	125	0.44	0.44
9/16/11		5.71	56		127		0.44	
10/21/11	6.70	5.75	55	57	127	128	0.43	0.44
10/21/11		5.91	58		129		0.45	
1/17/12	6.70	NM[1]	90	88	160	168	0.56	0.52
1/28/12		NM	85		176		0.48	
2/9/12	6.90	5.97	83	82	166	167	0.50	0.49
2/9/12		5.97	81		169		0.48	
3/1/12	7.10	6.21	80	80	188	180	0.43	0.44
3/1/12		6.29	75		167		0.45	
5/8/12		6.25	85		172		0.50	
5/8/12		6.63	79		193		0.41	

[1] NM – Not measured

Table 0-14: TDS to Electrical Conductivity Relationship for RO Plant's 2nd Stage Concentrate

Date	Target Feed pH	pH 2nd Stg Conc	TDS (mg/L)		Conductivity [EC] (µs/cm)		TDS/EC Ratio	
			2nd Stage Conc.	Ave. 2nd Stage Conc.	2nd Stage Conc.	Ave. 2nd Stage Conc.	2nd Stage Conc.	Ave. 2nd Stage Conc.
6/17/11	5.80	6.35	8646	8642	10440	10435	0.83	0.83
6/17/11		6.32	8681		10390		0.84	
6/17/11		6.36	8570		10460		0.82	
6/17/11		6.29	8672		10450		0.83	
7/14/11	6.05	6.56	8591	8660	10880	10873	0.79	0.80
7/14/11		6.67	8699		10900		0.80	
7/14/11		6.63	8690		10840		0.80	
8/16/11	6.30	6.89	8897	8968	11500	11483	0.77	0.78
8/16/11		6.93	9021		11440		0.79	
8/16/11		6.90	8987		11510		0.78	
9/16/11	6.50	6.93	8670	8699	11350	11385	0.76	0.76
9/16/11		6.96	8729		11420		0.76	
10/21/11	6.70	7.11	8669	8575	11600	11640	0.75	0.74
10/21/11		7.13	8536		11720		0.73	
10/21/11		7.20	8520		11600		0.73	
1/17/12	6.70	NM[1]	8692	9114	11626	11971	0.75	0.76
1/28/12		NM	9536		12315		0.77	
2/9/12	6.90	7.38	8982	8952	11930	11840	0.75	0.76
2/9/12		7.39	8923		11750		0.76	
3/1/12	7.10	7.41	9676	9438	12550	12222	0.77	0.77
3/1/12		7.43	9787		12630		0.77	
3/1/12		7.51	9237		11950		0.77	
5/8/12		7.59	9220		12070		0.76	
5/8/12		7.65	9377		12120		0.77	
5/8/12		7.72	9334		12010		0.78	

[1] NM – Not measured

Table 0-15: TDS to Electrical Conductivity Relationship for Canary Feed (Jun'11 – Sep'11)

Date	Target Feed pH	pH Canary Feed	TDS (mg/L)		Conductivity [EC] (µs/cm)		TDS/EC Ratio	
			Canary Feed	Ave. Canary Feed	Canary Feed	Ave. Canary Feed	Canary Feed	Ave. Canary Feed
6/7/11	5.80	6.60	9538	9072	11650	11076	0.82	0.82
6/7/11		6.60	9364		11740		0.80	
6/17/11		6.45	8810		10680		0.82	
6/17/11		6.38	8763		10720		0.82	
6/17/11		6.36	8847		10800		0.82	
6/17/11		6.39	8859		10770		0.82	
6/21/11		6.36	9323		11350		0.82	
6/28/11		6.42			10920			
6/28/11		6.41			11050			
7/14/11	6.05	6.61	8750	8850	11060	11100	0.79	0.80
7/28/11		6.67	8988		11040		0.81	
7/28/11		6.71	8813		11200		0.79	
8/9/11	6.30	7.09	8926	9024	11220	11535	0.80	0.78
8/16/11		6.94	8971		11610		0.77	
8/16/11		6.98	9106		11660		0.78	
8/16/11		6.97	9095		11650		0.78	
8/31/11	6.50	7.19	9417	9049	12420	11818	0.76	0.77
8/31/11		7.21	9413		12420		0.76	
9/12/11		7.34			11200			
9/16/11		6.99	8502		11640		0.73	
9/16/11		6.95	8991		11670		0.77	
9/16/11		6.93	8922		11560		0.77	

Table 0-16: TDS to Electrical Conductivity Relationship for Canary Feed (Oct'11 – May'12)

Date	Target Feed pH	pH Canary Feed	TDS (mg/L)		Conductivity [EC] (µs/cm)		TDS/EC Ratio	
			Canary Feed	Ave. Canary Feed	Canary Feed	Ave. Canary Feed	Canary Feed	Ave. Canary Feed
10/12/11	6.70	7.18	9468	9012	11290	11611	0.84	0.78
10/12/11		7.36	9257		11410		0.81	
10/21/11		7.26	8789		11610		0.76	
10/21/11		7.22	8720		11660		0.75	
11/2/11		7.32	8718		11150		0.78	
12/1/11		7.29	9399		11610		0.81	
12/7/11		7.15	8890		12150		0.73	
12/7/11		7.15	8855		12010		0.74	
12/20/11	6.70	7.27	9074	9251	12260	11593	0.74	0.80
12/28/11		7.27	9114		11410		0.80	
12/28/11		7.24	9085		11380		0.80	
1/31/12		7.31	9730		11320		0.86	
2/9/12	6.90	7.23	9284	9260	12150	11960	0.76	0.77
2/9/12		7.28	9183		11970		0.77	
2/9/12		7.28	9312		11760		0.79	
3/1/12	7.10	7.45	9938	9354	12800	12211	0.78	0.77
3/1/12		7.47	9296		12160		0.76	
3/1/12		7.54	9383		12200		0.77	
4/3/12		7.61	8847		11780		0.75	
4/3/12		7.68	8787		11620		0.76	
4/10/12		7.59			11900			
4/17/12		7.73	9454		12510		0.76	
4/17/12		7.71	9354		12480		0.75	
5/8/12		7.68	9518		12320		0.77	
5/8/12		7.66	9614		12340		0.78	

Table 0-17: TDS to Electrical Conductivity Relationship for Canary Permeate (Jun'11 – Jan'12)

Date	Target Feed pH	pH Canary Permeate	TDS (mg/L)		Conductivity [EC] (µs/cm)		TDS/EC Ratio	
			Canary Permeate	Ave. Canary Permeate	Canary Permeate	Ave. Canary Permeate	Canary Permeate	Ave. Canary Permeate
6/7/11	5.80	6.05	71.5	76.9	164.5	139.1	0.43	0.55
6/17/11		5.82	75.0		132.1		0.57	
6/17/11		5.80	68.5		129.3		0.53	
6/17/11		5.76	93.5		129.7		0.72	
6/21/11		5.71	76.0		147.3		0.52	
6/28/11		5.78			131.5			
7/14/11	6.05	5.89	46.0	46.3	129.1	130.5	0.36	0.36
7/28/11		5.91	50.0		128.3		0.39	
7/28/11		5.89	43.0		134.0		0.32	
8/9/11	6.30	5.97	50.5	54.8	124.0	127.2	0.41	0.43
8/16/11		6.05	62.0		126.7		0.49	
8/16/11		6.05	52.0		130.8		0.40	
8/31/11	6.50	6.12	57.0	48.7	135.1	122.6	0.42	0.40
9/12/11		5.83			115.7			
9/16/11		5.85	40.0		118.8		0.34	
9/16/11		5.92	49.0		120.9		0.41	
10/12/11	6.70	5.76	114.0	69.7	160.5	186.0	0.71	0.37
10/21/11		6.10	52.0		153.5		0.34	
10/21/11		6.12	28.0		155.8		0.18	
11/2/11		5.95	88.5		223.0		0.40	
12/1/11		5.97	70.5		255.1		0.28	
12/7/11		6.14	65.0		168.3		0.39	
12/20/11	6.70	5.79	61.5	119.5	219.0	222.2	0.28	0.54
12/28/11		5.82	70.5		224.1		0.31	
1/31/12		6.05	226.5		223.5		1.01	

Table 0-18: TDS to Electrical Conductivity Relationship for
Canary Permeate (Feb'12 – May'12)

Date	Target Feed pH	pH Canary Permeate	TDS (mg/L)		Conductivity [EC] (µs/cm)		TDS/EC Ratio	
			Canary Permeate	Ave. Canary Permeate	Canary Permeate	Ave. Canary Permeate	Canary Permeate	Ave. Canary Permeate
2/9/12	6.90	6.12	179.0	183.0	448.0	447.0	0.40	0.41
2/9/12		6.35	187.0		446.0		0.42	
3/1/12	7.10	6.63	166.0	151.8	353.0	325.1	0.47	0.47
3/1/12		6.40	104.5		300.0		0.35	
4/3/12		6.52	110.0		288.0		0.38	
4/10/12		6.59			303.0			
4/17/12		6.62	113.0		337.0		0.34	
5/8/12		6.72	209.1		334.0		0.63	
5/8/12		6.70	208.5		361.0		0.58	

Table 0-19: TDS to Electrical Conductivity Relationship for Canary Concentrate (Jun'11 – Sep'11)

Date	Target Feed pH	pH Canary Conc.	TDS (mg/L)		Conductivity [EC] (µs/cm)		TDS/EC Ratio	
			Canary Conc.	Ave. Canary Conc.	Canary Conc.	Ave. Canary Conc.	Canary Conc.	Ave. Canary Conc.
6/7/11		6.65	10454		13180		0.79	
6/7/11		6.65	10430					
6/17/11		6.43	10006		11930		0.84	
6/17/11		6.44	9958		11930		0.83	
6/17/11	5.80	6.43	9905	10220	11940	12323	0.83	0.83
6/17/11		6.43	10066		11920		0.84	
6/21/11		6.38	10430		12670		0.82	
6/21/11		6.43	10511		12720		0.83	
6/28/11		6.47			12290			
7/14/11		6.72	9932		12330		0.81	
7/14/11		6.75	10073		12340		0.82	
7/14/11	6.05	6.79	9946	10036	12340	12412	0.81	0.81
7/28/11		6.71	10204		12490		0.82	
7/28/11		6.82	10024		12560		0.80	
8/9/11		7.16	9916		12470		0.80	
8/9/11		7.15	9940		12530		0.79	
8/16/11	6.30	7.00	10235	10130	12900	12762	0.79	0.79
8/16/11		7.02	10303		12960		0.79	
8/16/11		6.96	10257		12950		0.79	
8/31/11		7.16	10575		13800		0.77	
8/31/11		7.16			12340			
9/16/11	6.50	7.04	9664	10104	13010	13020	0.74	0.78
9/16/11		7.03	10074		12930		0.78	
9/16/11		7.03	10104					

Table 0-20: TDS to Electrical Conductivity Relationship for Canary Concentrate (Oct'11 – May'12)

Date	Target Feed pH	pH Canary Conc.	TDS (mg/L)		Conductivity [EC] (µs/cm)		TDS/EC Ratio	
			Canary Conc.	Ave. Canary Conc.	Canary Conc.	Ave. Canary Conc.	Canary Conc.	Ave. Canary Conc.
10/12/11	6.70	7.23	10541	10070	12320	12814	0.86	0.79
10/12/11		7.23	10212		13160		0.78	
10/21/11		7.25	9707		13280		0.73	
10/21/11		7.23	9671		13040		0.74	
11/2/11		7.51	9675		12420		0.78	
12/1/11		7.38	10297		12260		0.84	
12/7/11		7.28	10433		12760		0.82	
12/7/11		7.28	10024		13270		0.76	
12/20/11	6.70	7.14	9970	10259	13420	12856	0.74	0.80
12/20/11		7.16	9912		13400		0.74	
12/28/11		7.21	10232		12440		0.82	
1/31/12		7.24	10595		12480		0.85	
1/31/12		7.27	10587		12540		0.84	
2/9/12	6.90	7.29	10181	10251	13000	13055	0.78	0.79
2/9/12		7.28	10321		13110		0.79	
3/1/12	7.10	7.42	11412	10774	14470	13761	0.79	0.78
3/1/12		7.49	11152		14520		0.77	
3/1/12		7.49	10379		13970		0.74	
4/3/12		7.65	10099		13260		0.76	
4/10/12		7.63			13330		0.00	
4/10/12		7.65			13220		0.00	
4/17/12		7.74	10677		13740		0.78	
5/8/12		7.64	10774		13690		0.79	
5/8/12		7.73	10848		13690		0.79	
5/8/12		7.73	10850		13720		0.79	

Table 0-21: Model Inputs and Actual versus Predicted by Model (Models 1-4) for K_{TDS1} on RO Plant

No.	H^+	Temp (°C)	EC (µs/cm)	Viscosity, ν, (ft^2/s)	Ionic Strength	Actual K_{TDS1}	Predicted K_{TDS1} by Model				% Diff From Actual			
							1	2	3	4	1	2	3	4
1	6.29E-07	28.7	4685	8.92E-06	9.38E-02	0.02242	0.02287	0.02293	0.02295	0.02241	-2.0	-2.3	-2.4	0.0
2	7.01E-07	28.6	4700	8.94E-06	9.38E-02	0.02277	0.02331	0.02316	0.02318	0.02279	-2.4	-1.7	-1.8	-0.1
3	9.36E-07	29.5	4700	8.78E-06	9.05E-02	0.02454	0.02446	0.02444	0.02442	0.02491	0.3	0.4	0.5	-1.5
4	9.94E-07	29.6	4695	8.76E-06	9.31E-02	0.02382	0.02471	0.02464	0.02462	0.02489	-3.7	-3.4	-3.3	-4.5
5	5.72E-07	28.4	4890	8.98E-06	9.28E-02	0.02469	0.02392	0.02378	0.02380	0.02368	3.1	3.7	3.6	4.1
6	6.05E-07	28.4	4880	8.98E-06	9.24E-02	0.02430	0.02402	0.02381	0.02383	0.02380	1.2	2.0	1.9	2.0
7	5.24E-07	28.7	4865	8.92E-06	9.37E-02	0.02610	0.02352	0.02374	0.02374	0.02339	9.9	9.0	9.0	10.4
8	2.52E-07	28.7	5030	8.93E-06	8.83E-02	0.02248	0.02327	0.02394	0.02394	0.02411	-3.5	-6.5	-6.5	-7.3
9	2.49E-07	28.6	5130	8.94E-06	9.17E-02	0.02420	0.02391	0.02451	0.02450	0.02444	1.2	-1.3	-1.2	-1.0
10	2.52E-07	28.7	4895	8.93E-06	8.68E-02	0.02153	0.02239	0.02311	0.02312	0.02323	-4.0	-7.3	-7.4	-7.9
11	2.37E-07	28.6	4905	8.93E-06	8.44E-02	0.02451	0.02239	0.02311	0.02312	0.02352	8.7	5.7	5.7	4.0
12	2.13E-07	28.0	5055	9.05E-06	9.11E-02	0.02297	0.02325	0.02352	0.02354	0.02331	-1.2	-2.4	-2.5	-1.5
13	1.48E-07	25.8	5165	9.50E-06	8.71E-02	0.02117	0.02364	0.02245	0.02240	0.02283	-11.7	-6.0	-5.8	-7.8
14	1.59E-07	25.6	5075	9.56E-06	8.88E-02	0.02158	0.02311	0.02175	0.02168	0.02175	-7.1	-0.8	-0.4	-0.8
15	1.48E-07	26.3	5110	9.39E-06	8.95E-02	0.02353	0.02329	0.02246	0.02249	0.02243	1.0	4.5	4.4	4.7
16	1.31E-07	26.5	5460	9.35E-06	8.47E-02	0.02598	0.02548	0.02467	0.02469	0.02590	1.9	5.0	5.0	0.3
17	1.26E-07	26.5	5355	9.35E-06	8.62E-02	0.02387	0.02477	0.02401	0.02404	0.02483	-3.8	-0.6	-0.7	-4.0
18	1.25E-07	26.7	5315	9.29E-06	8.29E-02	0.02555	0.02450	0.02394	0.02399	0.02511	4.1	6.3	6.1	1.7
19	6.07E-08	27.4	5615	9.17E-06	9.97E-02	0.02426	0.02614	0.02606	0.02607	0.02554	-7.8	-7.4	-7.5	-5.3
20	6.48E-08	27.8	5485	9.09E-06	9.72E-02	0.02327	0.02532	0.02559	0.02559	0.02516	-8.8	-10.0	-10.0	-8.1
21	4.75E-08	27.7	5565	9.11E-06	9.19E-02	0.02627	0.02575	0.02596	0.02596	0.02633	2.0	1.2	1.2	-0.2
22	4.46E-08	27.5	5480	9.15E-06	9.28E-02	0.02810	0.02519	0.02526	0.02527	0.02533	10.4	10.1	10.1	9.9
23	4.01E-08	27.7	5505	9.11E-06	9.10E-02	0.02728	0.02533	0.02557	0.02558	0.02593	7.1	6.2	6.2	4.9

Table 0-22: Model Inputs and Actual versus Predicted by Model (Models 5-8) for K_{TDS2} on RO Plant

No.	H^+	Temp (°C)	EC (µs/cm)	Viscosity, ν, (ft^2/s)	Ionic Strength	Actual K_{TDS2}	Predicted K_{TDS2} by Model				% Diff From Actual			
							5	6	7	8	5	6	7	8
1	5.69E-07	28.9	8340	8.88E-06	1.81E-01	0.01261	0.01364	0.01365	0.01364	0.01366	-8.1	-8.2	-8.2	-8.3
2	5.93E-07	29.2	8320	8.83E-06	1.82E-01	0.01463	0.01368	0.01368	0.01368	0.01367	6.5	6.5	6.5	6.5
3	6.06E-07	29.5	8365	8.77E-06	1.81E-01	0.01360	0.01386	0.01386	0.01386	0.01390	-1.9	-1.9	-1.9	-2.2
4	6.36E-07	29.7	8360	8.73E-06	1.83E-01	0.01351	0.01396	0.01396	0.01396	0.01399	-3.4	-3.4	-3.4	-3.5
5	3.56E-07	28.5	8705	8.96E-06	1.80E-01	0.01442	0.01384	0.01384	0.01384	0.01385	4.0	4.0	4.0	4.0
6	3.06E-07	28.7	8700	8.93E-06	1.84E-01	0.01477	0.01362	0.01361	0.01362	0.01353	7.8	7.8	7.8	8.4
7	3.26E-07	29.1	8665	8.85E-06	1.85E-01	0.01452	0.01360	0.01359	0.01359	0.01350	6.3	6.4	6.4	7.0
8	1.35E-07	29.0	9035	8.87E-06	1.80E-01	0.01278	0.01390	0.01388	0.01388	0.01387	-8.7	-8.6	-8.6	-8.5
9	1.46E-07	28.8	9145	8.91E-06	1.85E-01	0.01339	0.01426	0.01425	0.01425	0.01420	-6.6	-6.4	-6.5	-6.1
10	1.56E-07	28.9	8955	8.88E-06	1.76E-01	0.01337	0.01376	0.01374	0.01374	0.01377	-2.9	-2.7	-2.7	-2.9
11	1.55E-07	28.6	8995	8.95E-06	1.72E-01	0.01379	0.01386	0.01385	0.01385	0.01396	-0.5	-0.4	-0.4	-1.2
12	9.62E-08	26.2	9220	9.41E-06	1.77E-01	0.01351	0.01428	0.01431	0.01431	0.01437	-5.7	-6.0	-5.9	-6.4
13	9.86E-08	25.9	9205	9.48E-06	1.81E-01	0.01454	0.01425	0.01429	0.01428	0.01428	2.0	1.8	1.8	1.8
14	9.31E-08	26.5	9160	9.35E-06	1.83E-01	0.01415	0.01410	0.01412	0.01412	0.01408	0.4	0.2	0.2	0.5
15	6.86E-08	26.7	9645	9.30E-06	1.66E-01	0.01760	0.01541	0.01543	0.01542	0.01576	12.5	12.3	12.4	10.4
16	6.70E-08	26.8	9485	9.28E-06	1.67E-01	0.01720	0.01494	0.01495	0.01495	0.01523	13.2	13.1	13.1	11.5
17	4.63E-08	27.7	10000	9.12E-06	1.98E-01	0.01542	0.01635	0.01635	0.01635	0.01627	-6.0	-6.0	-6.0	-5.5
18	4.36E-08	27.8	9670	9.10E-06	1.94E-01	0.01487	0.01538	0.01538	0.01538	0.01528	-3.4	-3.4	-3.4	-2.7
19	2.73E-08	27.9	9795	9.08E-06	1.85E-01	0.01701	0.01568	0.01567	0.01567	0.01573	7.8	7.9	7.9	7.5
20	2.35E-08	27.8	9745	9.09E-06	1.84E-01	0.01569	0.01552	0.01551	0.01551	0.01557	1.1	1.1	1.1	0.7
21	2.73E-08	27.9	9700	9.07E-06	1.82E-01	0.01636	0.01540	0.01539	0.01540	0.01547	5.8	5.9	5.9	5.4

Table 0-23: Model Inputs and Actual versus Predicted by Model (Models 1 and 4) for K_{TDS1} on RO Pilot

No.	H^+	Temp (ºC)	EC (µs/cm)	Viscosity, ν, (ft^2/s)	Ionic Strength	Actual K_{TDS1}	Predicted K_{TDS1} by Model		% Diff From Actual	
							1	4	1	4
1	8.54E-07	24.7	4690	9.76E-06	9.97E-02	0.02142	0.02399	0.01985	-12.0	7.3
2	1.16E-06	29.8	4590	8.71E-06	1.03E-01	0.02149	0.02481	0.02370	-15.5	-10.3
3	1.13E-06	27.2	4565	9.21E-06	1.03E-01	0.02171	0.02452	0.02143	-13.0	1.3
4	1.15E-06	28.6	4780	8.94E-06	1.03E-01	0.02308	0.02603	0.02437	-12.8	-5.6
5	2.95E-07	29.0	4625	8.87E-06	9.99E-02	0.02245	0.02085	0.01979	7.1	11.9
6	2.95E-07	28.9	4625	8.88E-06	1.00E-01	0.02106	0.02084	0.01971	1.0	6.4
7	3.36E-07	28.9	4715	8.89E-06	9.94E-02	0.02231	0.02163	0.02069	3.0	7.2
8	2.95E-07	29.0	4770	8.87E-06	1.01E-01	0.02123	0.02179	0.02077	-2.7	2.1
9	2.27E-07	29.0	4605	8.87E-06	1.00E-01	0.02022	0.02039	0.01930	-0.8	4.5
10	6.45E-08	28.6	4590	8.94E-06	9.62E-02	0.02104	0.01950	0.01866	7.3	11.3
11	5.90E-08	28.7	4600	8.92E-06	9.70E-02	0.02070	0.01953	0.01869	5.6	9.7
12	8.75E-08	28.9	4670	8.88E-06	9.88E-02	0.02140	0.02013	0.01930	5.9	9.8
13	6.51E-08	29.1	4730	8.85E-06	9.56E-02	0.02161	0.02041	0.02020	5.5	6.5
14	5.78E-08	29.1	4725	8.84E-06	9.57E-02	0.02126	0.02034	0.02014	4.3	5.3
15	6.65E-08	28.9	4525	8.89E-06	9.99E-02	0.02109	0.01908	0.01785	9.5	15.4

Table 0-24: Model Inputs and Actual versus Predicted by Model (Models 5 and 8) for K_{TDS2} on RO Pilot

No.	H^+	Temp (ºC)	EC (µs/cm)	Viscosity, ν, (ft^2/s)	Ionic Strength	Actual K_{TDS2}	Predicted K_{TDS2} by Model		% Diff From Actual	
							5	8	5	8
1	6.16E-07	24.2	7870	9.884E-06	1.82E-01	0.01169	0.01246	0.01245	-6.6	-6.5
2	6.25E-07	24.2	7895	9.873E-06	1.83E-01	0.01171	0.01257	0.01255	-7.3	-7.2
3	8.13E-07	30.0	7870	8.676E-06	1.89E-01	0.01242	0.01326	0.01314	-6.8	-5.8
4	8.79E-07	27.4	7675	9.163E-06	1.84E-01	0.01318	0.01296	0.01295	1.7	1.7
5	7.20E-07	28.8	7985	8.901E-06	1.85E-01	0.01247	0.01322	0.01316	-6.0	-5.6
6	2.26E-07	29.1	7590	8.854E-06	1.77E-01	0.01053	0.01007	0.00973	4.4	7.7
7	2.37E-07	29.2	7870	8.826E-06	1.84E-01	0.01002	0.01093	0.01055	-9.1	-5.3
8	2.22E-07	29.3	8010	8.816E-06	1.84E-01	0.01059	0.01127	0.01093	-6.5	-3.2
9	2.13E-07	29.3	8065	8.807E-06	1.84E-01	0.00986	0.01140	0.01106	-15.6	-12.2
10	1.53E-07	29.3	7695	8.816E-06	1.84E-01	0.00885	0.01008	0.00961	-13.9	-8.6
11	4.37E-08	29.0	7635	8.873E-06	1.77E-01	0.01025	0.00946	0.00902	7.7	12.0
12	6.21E-08	29.2	7685	8.826E-06	1.81E-01	0.01137	0.00968	0.00919	14.8	19.1
13	5.27E-08	29.2	7685	8.835E-06	1.81E-01	0.01073	0.00964	0.00916	10.2	14.7
14	4.76E-08	29.4	7845	8.798E-06	1.78E-01	0.01107	0.01009	0.00968	8.9	12.6
15	4.98E-08	29.1	7430	8.854E-06	1.87E-01	0.00997	0.00889	0.00824	10.9	17.4
16	4.74E-08	29.1	7515	8.844E-06	1.86E-01	0.01007	0.00913	0.00851	9.4	15.5

Table 0-25: Model Inputs and Actual versus Predicted by Model (Models 9 and 10) for K_{Na1} on RO Plant

No.	EC (µs/cm)	Na (mg/L)	Viscosity, ν, (ft^2/s)	Actual K_{Na1}	Predicted K_{Na1} by Model		% Diff From Actual	
					9	10	9	10
1	4685	350.7	8.92E-06	0.05395	0.05158	0.05796	4.4	-7.4
2	4700	357.8	8.94E-06	0.05315	0.05089	0.05624	4.2	-5.8
3	4700	351.6	8.78E-06	0.04924	0.05160	0.06081	-4.8	-23.5
4	4695	371.6	8.76E-06	0.05683	0.04926	0.05623	13.3	1.1
5	4890	400.6	8.98E-06	0.04835	0.04763	0.04960	1.5	-2.6
6	4880	409.9	8.98E-06	0.04659	0.04648	0.04712	0.2	-1.2
7	4865	418.2	8.92E-06	0.04592	0.04540	0.04604	1.1	-0.3
8	5030	427.5	8.93E-06	0.04769	0.04577	0.04759	4.0	0.2
9	5130	426.6	8.94E-06	0.04975	0.04674	0.05003	6.1	-0.6
10	4895	443.1	8.93E-06	0.03830	0.04280	0.04058	-11.8	-6.0
11	4905	444.2	8.93E-06	0.04332	0.04276	0.04045	1.3	6.6
12	5055	424.0	9.05E-06	0.04254	0.04638	0.04668	-9.0	-9.7
13	5165	419.5	9.50E-06	0.04198	0.04785	0.04171	-14.0	0.7
14	5075	424.1	9.56E-06	0.04148	0.04654	0.03730	-12.2	10.1
15	5110	416.5	9.39E-06	0.04194	0.04772	0.04335	-13.8	-3.4
16	5460	384.4	9.35E-06	0.05579	0.05444	0.06019	2.4	-7.9
17	5355	386.5	9.35E-06	0.05630	0.05329	0.05715	5.4	-1.5
18	5315	417.8	9.29E-06	0.05141	0.04935	0.04973	4.0	3.3
19	5615	493.6	9.17E-06	0.04759	0.04326	0.04106	9.1	13.7
20	5485	451.6	9.09E-06	0.04527	0.04695	0.04967	-3.7	-9.7
21	5565	467.3	9.11E-06	0.04624	0.04584	0.04744	0.9	-2.6
22	5480	464.6	9.15E-06	0.04668	0.04541	0.04514	2.7	3.3
23	5505	469.1	9.11E-06	0.04649	0.04511	0.04557	3.0	2.0

Table 0-26: Model Inputs and Actual versus Predicted by Model (Models 11 and 12) for K_{Na2} on RO Plant

No.	EC (µs/cm)	Na (mg/L)	Viscosity, ν, (ft^2/s)	Actual K_{Na2}	Predicted K_{Na2} by Model		% Diff From Actual	
					11	12	11	12
1	8340	726.4	8.88E-06	0.04751	0.04759	0.048472	-0.2	-2.0
2	8320	723.2	8.83E-06	0.05383	0.04765	0.049124	11.5	8.7
3	8365	731.0	8.77E-06	0.04550	0.04749	0.049437	-4.4	-8.7
4	8360	712.4	8.73E-06	0.04949	0.04836	0.050949	2.3	-2.9
5	8705	785.8	8.96E-06	0.05293	0.04652	0.045979	12.1	13.1
6	8700	818.1	8.93E-06	0.04469	0.04494	0.044207	-0.6	1.1
7	8665	815.8	8.85E-06	0.04794	0.04488	0.044910	6.4	6.3
8	9035	852.8	8.87E-06	0.04277	0.04492	0.044411	-5.0	-3.8
9	9145	834.7	8.91E-06	0.04366	0.04633	0.045767	-6.1	-4.8
10	8955	862.4	8.88E-06	0.04138	0.04406	0.043280	-6.5	-4.6
11	8995	831.5	8.95E-06	0.04339	0.04574	0.044780	-5.4	-3.2
12	9220	825.7	9.41E-06	0.04110	0.04713	0.041773	-14.7	-1.6
13	9205	829.0	9.48E-06	0.04095	0.04690	0.040794	-14.5	0.4
14	9160	803.0	9.35E-06	0.04255	0.04793	0.043455	-12.7	-2.1
15	9645	764.7	9.30E-06	0.05370	0.05216	0.048951	2.9	8.8
16	9485	766.6	9.28E-06	0.05315	0.05128	0.048158	3.5	9.4
17	10000	976.1	9.12E-06	0.04891	0.04372	0.039490	10.6	19.3
18	9670	819.8	9.10E-06	0.04903	0.04963	0.047692	-1.2	2.7
19	9795	900.5	9.08E-06	0.04727	0.04636	0.043493	1.9	8.0
20	9745	908.3	9.09E-06	0.04723	0.04573	0.042637	3.2	9.7
21	9700	897.5	9.07E-06	0.04839	0.04603	0.043259	4.9	10.6

Table 0-27: Model Inputs and Actual versus Predicted by Model 9 for K_{Na1} on RO Pilot

No.	EC (µs/cm)	Na (mg/L)	Viscosity, ν, (ft^2/s)	Actual K_{Na1}	Predicted K_{Na2} by Model 9	% Diff From Actual
1	4690	422.03	9.76E-06	0.04248	0.04344	-2.3
2	4590	424.79	8.71E-06	0.04527	0.04226	6.7
3	4565	417.93	9.21E-06	0.04346	0.04283	1.5
4	4780	417.70	8.94E-06	0.04326	0.04472	-3.4
5	4625	429.65	8.87E-06	0.03922	0.04200	-7.1
6	4625	431.35	8.88E-06	0.03839	0.04181	-8.9
7	4715	420.10	8.89E-06	0.04118	0.04388	-6.5
8	4770	432.14	8.87E-06	0.03850	0.04297	-11.6
9	4605	410.14	8.87E-06	0.03858	0.04407	-14.2
10	4590	434.90	8.94E-06	0.03746	0.04110	-9.7
11	4600	437.13	8.92E-06	0.03594	0.04093	-13.9
12	4670	437.91	8.88E-06	0.03718	0.04145	-11.5
13	4730	430.74	8.85E-06	0.03825	0.04279	-11.9
14	4725	437.07	8.84E-06	0.03768	0.04202	-11.5
15	4535	458.08	8.89E-06	0.03566	0.03796	-6.4

Table 0-28: Model Inputs and Actual versus Predicted by Model 11 for K_{Na2} on RO Pilot

No.	EC (µs/cm)	Na (mg/L)	Viscosity, ν, (ft^2/s)	Actual K_{Na2}	Predicted K_{Na2} by Model 11	% Diff From Actual
1	7870	793.5	9.88E-06	0.04482	0.04205	6.2
2	7895	799.1	9.87E-06	0.04545	0.04190	7.8
3	7870	804.4	8.68E-06	0.04591	0.04152	9.6
4	7675	774.6	9.16E-06	0.04726	0.04200	11.1
5	7985	771.4	8.90E-06	0.04792	0.04368	8.9
6	7590	772.1	8.85E-06	0.04061	0.04170	-2.7
7	7870	826.0	8.83E-06	0.04199	0.04048	3.6
8	8010	808.2	8.82E-06	0.04375	0.04203	3.9
9	8065	795.2	8.81E-06	0.04227	0.04292	-1.6
10	7695	788.7	8.82E-06	0.03989	0.04142	-3.8
11	7635	846.1	8.87E-06	0.03733	0.03836	-2.7
12	7685	829.3	8.83E-06	0.03964	0.03941	0.6
13	7685	835.9	8.84E-06	0.03916	0.03910	0.2
14	7845	861.9	8.80E-06	0.03788	0.03863	-2.0
15	7430	865.7	8.85E-06	0.03808	0.03641	4.4
16	7515	883.7	8.84E-06	0.03651	0.03596	1.5

REFERENCES

Abdulrazaq, J. A. (2011, June). Transport phenomena analysis for evaluating the optimum operating conditions of reverse osmosis processes. *Research Journal of Chemical Sciences, 1*(3), 26-33.

Agashichev, S. P., & Lootah, K. (2003). Influence of temperature and permeate recovery on energy consumption of a reverse osmosis system. *Desalination, 154*, 253-266.

Ahmad, A., Ismail, S., & Bhatia, S. (2005). Membrane treatment for palm oil mill effluent: effect of transmembrane pressure and crossflow velocity. *Desalination, 179*(1-3), 245-255.

Aimar, P., Baklouti, S., & Sanchez, V. (1986). Membrane-solute interactions: influence on pure solvent transfer during ultrafiltration. *Journal of Membrane Science, 29*(2), 207-224.

Al Smadi, B., Al-Zboon, K., & Al-Azab, T. (2010). Water management and reuse opportunities in a thermal power plant in Jordan. *African Journal of Biotechnology, 9*(29), 4606-4614.

Al-Rammah, A. (2000). The application of acid free antiscalant to mitigate scaling in reverse osmosis membranes. *Desalination, 132*, 83-87.

Al-Shammiri, M., Salman, A., Al-Shammari, S., & Ahmad, M. (2005). Simple program for the estimation of scaling potential in RO systems. *Desalination, 184*, 139-147.

Amjad, Z. (1993). Reverse Osmosis: Membrane Technology. In *Water Chemistry and Industrial Applications.* New York: Van Nostrand Reinhold.

ASCE and AWWA. (1990). *Water Treatment Plant Design* (2nd ed.). McGraw-Hill.

ASTM. (2002). *ASTM D4189-95 Standard test method for silt density index (SDI) of water.* American Society for Testing and Materials.

ASTM. (2010). *ASTM D3739 - 06 Standard Practice for Calculation of the Langelier Saturation Index for Reverse Osmosis.* American Society of Testing and Material.

Atlas, R. M. (1984). *Microbiology - Fundamentals and Applications.* New York, U.S.A: Macmillan Publishing Company.

AWWA. (1999). Manual of water supply practices -M46: Reverse osmosis and nanofiltration. *1st*. Denver: American Water Works Association.

AWWA. (1999). *Water Quality and Treatment: A Handbook of Community Water Supplies* (5th ed.). (R. Letterman, Ed.) New York: McGraw-Hill, Inc.

AWWA. (2005). *Microfiltration and Ultrafiltration Membranes for Drinking Water: Manual of Water Supply Supply Practices M53.* Denver: AWWA.

Baker, J., & Dudley, L. (1998). Biofouling in membrane systems - A review. *Desalination, 118*(1-3), 81-90.

Bartels, C., Franks, R., Rybar, S., Schierach, M., & Wilf, M. (2005). The effect of feed ionic strength on salt passage through reverse osmosis membranes. *Desalination, 184*(1-3), 185-195.

Berdanier, B., & Ziadat, A. (2006). Evaluation of a total dissolved solids model in compariosn to actual field data measurements in the Cheyenne River, South Dakota, U.S.A. *Environmental Monitoring and Assessment, 117*(1-3), 335-344.

Bergamasco, R., Konradt-Moraes, L., Vieira, M., Fagundes-Klen, M., & Vieira, A. (2011). Performance of a coagulation-ultrafiltration hybrid process for water supply treatment. *Chemical Engineering Journal, 166*(2), 483-489.

Bergman, R. (2005). Membrane Processes. In AWWA, & ASCE, *Water Treatment Plant Design* (4th ed., pp. 13.1 - 13.48). McGraw-Hill.

Bergman, R., & Elarde, J. (2005). Post-treatment of reverse osmosis and nanofiltration systems for municipal water supply. *AWWA - Membrane Technology Conference.* AWWA.

Berman, T. (2010). Biofouling: TEP - a major challenge for water filtration. *Filtration + Separation*, 20-22.

Berman, T., & Holenberg, M. (2005, March). *Amiad Filtration Systems.* Retrieved September 27, 2012, from Amiad USA: http://www.amiadusa.com/pdf/articles/TEP%20and%20Biofilm%20Fouling%20on%20Membranes.pdf

Bonne, P., Hofman, J., & van der Hoek, J. (2000). Scaling control of RO membranes and direct treatment of surface water. *Desalination, 132*(1-3), 109-119.

Bonne, P., Hofman, J., & van der Hoek, J. (2000). Scaling control of RO membranes and direct treatment of surface water. *Desalination, 132*, 109-119.

Boyd, C. C., & Duranceau, S. J. (2011). Post-sedimentation ultrafiltration membrane performance for a Florida surface water supply. *AMTA/SEDA Joint Conference & Exposition.* Miami: AMTA/SEDA.

Boyd, C. C., Duranceau, S., Harn, J., & Harn, J. (2010). Beta testing of a new ultrafiltration membrane for treatment of Manatee County's surface water supply. *Florida Section AWWA.* AWWA.

Brezonik, P. L., & Arnold, W. A. (2011). *Water Chemistry - An Introduction to the Chemistry of Natural and Engineered Aquatic Systems.* New York: Oxford University Press.

Butt, F., Rahman, F., & Baduruthamal, U. (1995). Identification of scale deposits through membrane autopsy. *Desalination, 101*(3), 219-230.

Cabibbo, S., Guy, D., Ammerlaan, A., Ko, A., & Singh, R. (1979). *Reverse Osmosis Technical Manual.* Springfield, Virginia, USA: NTIS Publication.

Camp, T. (1965). *Water and its Impurities.* New York: Reinhold Publishing Company.

Carroll, J. J. (1998). *AQUAlibrium.* Retrieved Sep 6, 2012, from Software for Phase Equlibria in Natural Gas-Water Systems: A Discussion of the Effect of pH on the Solubility of Hydrogen Sulfide: http://www.telusplanet.net/public/jcarroll/ION.HTM

Characklis, W. G., & Marshall, K. (1990). *Biofilms.* New York: John Wiley & Sons.

Chellam, S., Jacangelo, J. G., Bonacquisti, T. P., & Schauer, B. A. (1997). Effect of pretreatment on surface water nanofiltration. *American Water Works Association, 89*(10), 77-89.

Cheryan, M. (1998). *Ultrafiltration and Microfiltration Handbook.* Lancaster, Pennsylvania: Technomic Publishing Company,Inv.

Chong, T., Wong, F., & Fane, A. (2007, January 15). Enhanced concentration polarization by unstirred fouling layers in reverse osmosis: Detection by sodium chloride tracer response technique. *Journal of Membrane Science, 287*, 198-210.

Chong, T., Wong, F., & Fane, A. (2008). The effect of imposed flux on biofouling in reverse osmosis: Role of concentration polarization and biofilm enhanced osmostic pressure phenomena. *Journal of Membrane Science, 325*(2), 840-850.

Chua, K. H., & Malek, A. (2003). Pretreatment pf seawater: Results of pilot trials in Singapore. *Desalination*, 225-243.

City of Sarasota. (2008). *Sarasota City Plan - Utilities Support Document.* Sarasota, FL.

Comstock, D. (1991). Reduction of colloidal fouling in membrane systems. *Industrial Water Treatment*, 39-42.

Cooney, M. J., Roschi, E., Marison, I. W., Comminellis, C., & Stockar, U. v. (1996). Physiologic studies with the sulfate-reducing bacterium Desulfovibrio desulfuricans: Evaluation for use in a biofuel cell. *Enzyme Microbiology Technology, 18*(5), 358-365.

Cooper, C. D., & Alley, F. (2012). *Air Pollution Control - A Design Approach* (4th ed.). Waveland Press, Inc.

Cooper, C. D., Dietz, J. D., & Reinhart, D. R. (2000). *Foundations of Environmental Engineering.* Illinois: Waveland Press, Inc.

Cyna, B., Chagneau, G., Bablon, G., & Tanghe, N. (2002). Two years of nanofiltration at the Mery-sur-Oise plant, France. *Desalination, 147*, 69-75.

Darton, E. (1997, November). Scale inhibition techniques used in membrane systems. *Desalination, 113*(2-3), 227-229.

Day, B., & Nightingale, H. (1984). Relationship between groundwater silica, total dissolved solids, and specific electrical conductivity. *Ground Water, 22*(1), 80-85.

Dell'Orco, M., Chadik, P., Bitton, G., & Neumann, R. (1998, Oct). Sulfate-oxidixing bacteria: their role during air-stripping. *AWWA, 90*(10), 107-115.

Dow Water Solutions. (2010). *Filmtec Reverse Osmosis Membranes Technical Manual.* Retrieved September 5, 2012, from http://www.scribd.com/doc/24498057/FILMTEC-RO-Membranes-Technical-Manual

Downs, A., & Adams, C. (1973). *The Chemistry of Chlorine, Bromine, Iodine and Astantine.* Pergamon: Oxford.

Duranceau, J. S., Anderson, R., & Teegarden, R. (1999). Comparison of mineral acid pretreatments for sulfide removal. *American Water Works Association, 91*(5), 85-97.

Duranceau, S. (1990). *Modeling of mass tranfser and synthetic organic compound removal in a membrane softening process.* Orlando, Florida: University of Central Florida.

Duranceau, S. J. (2009). Desalination post-treatment considerations. *Florida Water Resources Journal*, 4-19.

Duranceau, S. J., & Taylor, J. S. (1991). Modeling membrane mass transfer using dimensional analysis. *Membrane Tecnologies in the Water Industry* (pp. 215-222). Orlando, Florida: AWWA.

Duranceau, S. J., & Taylor, J. S. (2011). *Water Quality & Treatment: A Handbook on Drinking Water* (6th ed.). New York, NY, USA: McGraw-Hill.

Duranceau, S., Pfeiffer-Wilder, R., Douglas, S., Pena-Holt, N., & Watson.I.C. (2010). *Post Treatment Stabilization of Desalted Permeate.* Denver: Water Research Foundation.

Duranceau, S., Taylor, J., & Mulford, L. (1992). SOC removal in a membrane softening process. *Journal AWWA, 84*(1), 68-78.

Duranceau, S., Trupiano, V., Lowenstine, M., Whidden, S., & Hopp, J. (2010b, July). Innovative hydrogen sulfide treatment methods: Moving beyond packed tower aeration. *Florida Water Resources Journal*, 5-14.

Eaton, A., Clesceri, L., Rice, E., & Greenberg, A. (2005). *Standard Methods for the Examination of Water and Wastewater* (21 ed.). Washington: American Public Health Association, American Water Works Association, Water Environment Federation.

Eriksson, P., Kyburz, M., & Pergande, W. (2005). NF membarne characteristics and evaluation for sea water processing applications. *Desalination, 184*, 281-294.

Escobar, I., & Randall, A. A. (1999). Influence of NF on distribution system biostability. *AWWA, 91*(6), 76-90.

Escobar, I., Hong, S., & Randall, A. (2000). Removal of sssimilable and biodegradable dissolved organic carbon by reverse osmosis and nanofiltration membranes. *Journal of Membrane Science, 175*, 1-17.

Faborode, J. O. (2010). *Predictive modelling of sulfide removal in tray aerators.* Masters of Science Thesis, University of Central Florida, Civil, Environmental and Construction Engineering, Orlando.

FDEP. (2011, September 21). *Drinking Water Regulations.* Retrieved October 15, 2012, from Florida Department of Environmental Protection: http://www.dep.state.fl.us/water/drinkingwater/inorg_con.htm

Feng, C., Tollin, G., & Enemark, J. H. (2007, May). Sulfite oxidizing enzymes. *Biochim Biophys Acta, 1774*(5), 527-539.

Flemming, H., Schaule, G., McDonogh, R., & Ridgway, H. (1994). *Effects and extent of biofilm accumulation in membrane systems.* USA: CRC Press.

Fuqua, T. M., Bowen, P., & Creighton, R. (1991). Membrane treatment and the use of the Floridan Aquifer in South Florida. *Membrane Tecnologies in the Water Industry* (pp. 649-663). Orlando, Florida: AWWA.

Garcia, L. B., Blanco, G. G., & Meraz, M. (2008). Removal of sulfur inorganic compounds by a biofilm of sulfate reducing and sulfate oxidizing bacteria in a down-flow fluidized bed reactor. *Journal of Chemical Technology and Biotechnology*(83), 260-268.

Gare, S. (2002). RO systems - The importance of pre-treatment. *Flitration and Separation, 39*(1), 22-27.

Garrels, R., & Naeser, C. (1958). Equilibrium distribution of dissolved sulfur species in water at 25 degree celsius and 1 atm total pressure. *Geochim Cosmochimica Acta, 15*, 113-130.

Ghafour, E. E. (2003). Enhancing RO system performance utilizing antiscalants. *Desalination, 153*(1-3), 149-153.

Gottschalk, G. (1986). *Bacterial Metabolism* (2nd ed.). New York,U.S.A.: Springer-Verlag New Tork Inc.

Greenlee, L., Lawler, D., Freeman, B., & Marrot, B. (2009). Reverse osmosis desalination: Water resources,technology, and today's challenges. *Water Research, 43*, 2348-2371.

Haas, C. (2011). Chemical Disinfection. In AWWA, & J. Edzwald (Ed.), *Water Quality & Treatment: A Handbook of Drinking Water* (6th ed., pp. 17.1 -17.56). Denver, Colorado, USA: McGraw-Hill Companies, Inc.

Hajibabania, S., Verliefde, A., McDonald, J., Khan, S., & LeClech, P. (2011, March 4). Fate of trace organic compounds during treatment by nanofiltartion. *Journal of Membrane Science*.

Hem, J. (1985). *Study and interpretation of the chemical characteristics of natural water.* Washington D.C.: US Govt. Printing Office.

Higa, A., Tanioka, A., & Kra, A. (1998, March 18). A novel measurement method of Donnan potential at an interface between a charged membrane and mixed salt solution. *Journal of Membrane Science, 140*(2), 213-220.

Hilal, N., Al-Zhobi, H., Darwish, N., Mohammad, A., & Arabi, M. (2004). A Comprehensive Review of Nanofiltration Membranes: Treatment, Pretreatment, Modelling, and Atomic Force Microscopy. *Desalination, 170*, 281-308.

Hoek, E. M., Allred, J., Knoell, T., & Jeong, B.-H. (2008). Modelling the effects of fouling on full-scale reverse osmosis process. *Journal of Membrane Science, 314*, 33-49.

Hydranautics. (2008, Dec). *Chemical pretreatment for RO and NF*. Retrieved Sep 2010, from Technical Application Bulletin No.111, Revision C: http://www.membranes.com/docs/tab/TAB111.pdf

Jensen, J. (2003). *A Problem-Solving Approach to Aquatic Chemistry.* New Jersey: John Wiley & Sons, Inc.

Johnson, R. A. (2005). *Miller & Freund's Probablity and Statistics for Engineers* (7th ed.). New Jersey: Pearson Prentice Hall.

Kegel, F. S., Rietman, B., & Verliefde, A. (2010). Reverse Osmosis followed by activated carbon filtration for efficient removal of organic micropollutants from river bank filtrate. *Water Science & Technology, 61*(10), 2603-2610.

Keifer, C., Brinson, F., & Suratt, B. (2003). Optimizing the performace of low fouling membranes for the worls's largest nanofiltration plant. *AWWA Membrane Technology Conference.* AWWA.

Kerollis, R., & Mowrey, E. (1993, December 14). *Patent No. 5,269,444.* United States.

Kim, A., Chen, H., & Yuan, R. (2006). EPS biofouling in membrane filtration:An analytic modeling study. *Journal of Colloid and Interface Science, 303*, 243-249.

Kinser, K., Kopko, S., Fenske, A., & Schers, G.-J. (2007). Chemical optimization for a new brackish water RO treatment plant. *AWWA Membrane Technology Conference.* AWWA.

Kinser, K., Kopko, S., Fenske, A., & Schers, G.-J. (2008). Chemical optimization for a new brackish grounwater reverse osmosis treatment plant. *Florida Water Resources Journal*, 34-42.

Knoell, T., Martin, E., Ishida, K., & Phipps, D. (2005). The effects of chlorine exposure on the performance and properties of polyamide reverse osmosis membranes. *AWWA - Membrane Technology Conference*. AWWA.

Knoke, D., Bohrnstedt, G. W., & Mee, A. (2002). *Statistics For Social Data Analysis* (4th ed.). Cengage Learning.

Komlenic, R. (2010). Rethinking the causes of membrane fouling. *Filtration & Separation, 47*(5), 26-28.

Kucera, J. (2010). *Reverse Osmosis - Industrial Applications and Processes.* Salem: John Wiley & Sons and Scrivener Publishing LLC.

Kuzmenko, D., Arkhangelsky, E., Belfer, S., Freger, V., & Gitis, V. (2005, July). Chemical cleaning of UF membranes fouled by BSA. *Desalination, 179*(1-3), 323-333.

Liu, C., Caothien, S., Hayes, J. C., & Otoyo, T. O. (2001). Membrane chemical cleaning: From art to science. *AWWA 2000 Water Quality Technology Conference.* Denver,CO: AWWA.

Liu, T., Chen, Z.-L., Yu, W.-Z., Shen, J.-m., & Gregory, J. (2011). Effect of two-stage coagulant addition on coagulation-ultrafiltration process for treatment of humin-rich water. *IWA Water Reserach, 445*(2011), 4260-4268.

Logan, D., Nehus, H., & Smith.A.L. (1985). Acid free scale control for RO systems. *The International Water Conference Annual Meeting*, (pp. 456-466).

Lovins, W., Duranceau, S., King, T., & Medeiros, S. (2004). Trumping hydrogen sulfide. *Water Environment & Technology, 16*(3), 36-41.

Lyn, T. (1991). Hydrogen sulfide chlorination and turbidity control. Orlando: University of Central Florida.

Lyn, T. L., & Taylor, J. (1992). Assessing sulfur turbidity formation following chlorination of hydrogen sulfide in ground water. *American Water Works Association, 84*(9), 103-113.

Madigan, M. T., & Martinko, J. M. (2006). *Brock: Biology of Microorganism.* Prentice hall.

Maher, W., & Woo, L. (1998). Procedures for the storage and digestion of natural waters for the determination of filterable reactive phosphorus, total filterable phosphorus and total phosphorus. *Analytica Chimica Acta, 375*, 5-47.

Mance, G., O'Donnell, J., & Harriott, P. (1988). *Proposed Environmental Quality Standards for List II Substances in Water: Sulfide.* Medmenham: ESSL.

Mansouri, J., Harrisson, S., & Chen, V. (2010). Strategies for controlling biofouling in membrane filtration systems: challenges and opportunities. *Journal of Materials Chemistry, 20*, 4567-4586.

Maung, H. O., & Lianfa, S. (2009). Effect of pH and ionic strength on boron removal by RO membranes. *Desalination, 246*, 605-612.

Meireles, M., Aimar, P., & Sanchez, V. (1991). Albumin denaturation during ultrafiltration: effects of operating conditions and consequences on membarne fouling. *Biotechnol, 38*(5), 528-534.

Migdisov, A., Williams-Jones, A., Lakshtanov, Z., & Alekhin, Y. (2002, May 15). Estimates of the second dissociation constant of H2S from the surface sulfidation of crystalline sulfur. *Geochimica et Cosmochimica Acta, 66*(10), 1713-1725.

Mo, H., Tay, K. G., & Ng, H. Y. (2008). Fouling of reverse osmosis membrane by protein (BSA): Effects of pH, calcium, magnesium, ionic strength and temperature. *Journal of membrane science, 315*, 28-35.

MWH. (2005). *Water Treatment: Principles and Design* (2nd ed.). New Jersey: John Wiley & Sons, Inc.

MWH. (2012). *MWH's Water Treatment: principles and design* (3rd ed.). New Jersey: John Wiley & Sons, Inc.

Nanda, D., Tung, K.-L., Li, Y.-L., Lin, N.-J., & Chuang, C.-J. (2010). Effect of pH on membrane morphology, fouling potential, and filtration performance of nanofiltration membrane for water softening. *Desalination, 349*(1-2), 411-420.

Nemeth, J., & Seacord, T. (2000). Cost effective RO and NF systems: Importance of O&M considerations in design, procurement and manufacturing. *International Water Conference Annual Meeting.*

Ning, R., & Netwig, J. (2002). Complete elimination of acid injection in reverse osmosis plants. *143*, 29-34.

Ong, S., Zhou, W., Song, L., & Ng, W. (2002). Evaluation of feed concentration effects on salt/ion transport through RO/NF membranes with Nernst-Planck-Donnan Model. *Environmental Engineering Science, 19*(6), 429-439.

Ozaki, H., Li, H., & Saktaywin, W. (2001). Performance of ultra low pressure reverse osmosis membrane for separating heavy metals. *1st IWA ASPAC Regional Conference*, *2*, pp. 587-592. Japan.

Ozaki, H., Sharma, K., & Saktaywin, W. (2002). Performance of an ultra-low-pressure reverse osmosis (ULPROM) for separating heavy metal: effects of interference parameters. *144*(1-3), 287-294.

Parameswara, D., & Prasad, K. (2012). Role of asymmetry effect on the specific conductivity of water - A case study. *Chinese Journal of Geochemistry, 31*, 276-281.

Park, N., Kwon, B., Kim, I., & Cho, J. (2005, August). Biofouling potential of various NF membranes with respect to bacteria and their soluble microbial products (SMP): Characterizations, flux decline, and transport parameters. *Journal of Membrane Science*, *258*(1-2), 43-54.

Patel, S., & Milligan, J. (2008). Magnesium hydroxide deposit control for reverse osmosis system. (pp. 83741-837414). New Orleans: National Assoc. of Corrosion Engineers International.

Petersen, R. (1993). Composite reverse osmosis and nanofiltartion membranes. *Journal of Membrane Science, 83*, 81-150.

Powell, S., & von Lossberg, L. (1948). Removal of Hydrogen Sulfide from Well Water. *AWWA, 40*(12), 1277-1283.

Prihasto, N., Liu, Q., & Kim, S.-H. (2009). Pre-treatment strategies for seawater desalination of reverse osmosis system. *Deslination, 249*, 308-316.

Quevedo, N., Sanz, J., Ocen, C., Lobo, A., & Tejero, I. (2011, January). Reverse osmosis pretreatment alternatives: Demonstartion plant in the seawater desalination plant in Carboneras, Spain. *Desalination, 265*(1-3), 229-236.

Rajinder, S. (2006). *Hybrid Membrane Systems for Water Purification : Technology, Systems Design and Operation.* Elsevier.

Ray, C., & Jain, R. (2011). Drinking Water Treatment Technology - Comparative Analysis. In C. Ray, & R. Jain, *Drinking Water Treatment, Strategies for Sustainability* (pp. 9-35). Springer Science.

Reynolds, T. D., & Richards, P. A. (1995). *Unit Operations and Processes in Environmental Engineering* (2nd ed.). Boston: PWS Publishing Company.

Richarson, D., Blom, L., & Taylor, E. (2009). The effect of pH on membrane performance in treatment of paper inductry effluent. *63rd Appita Annual Conference andExhibition*, (pp. 249-255). Melbourne, Australia.

Saad, M. A. (2004). Early discovery of RO membrane fouling and real-time monitoring of plant performance for optimizing cost of water. *Desalination, 165*, 183-191.

Sawyer, C. N., McCarty, P. L., & Parkin, G. F. (2003). *Chemistry for Environmental Engineering abd Science* (5th ed.). New York: McGrawHill.

Schafer, A., Pihlajamaki, A., Fane, A., Waite, T., & Nystrom, M. (2004). Natural organic matter removal by nanofiltration:effects of solution chemistry on retention of low molar mass acids versus bulk organic matter. *Journal of Membrane Science, 242*, 73-85.

Schock, M. (1984). Temperature and ionic strength corrections to the langelier saturation index - revisited. *AWWA, 76*(8), 72-76.

Seacord, T., Cushing, R., White, P., Grimes, G., & Dieffenthaller, A. (2001). Process design implications of no-acid RO/NF treatment of grounwater containing hydrogen sulfide. *AWWA Membrane Conference.* AWWA.

Singer, P. C., & Reckhow, D. (2011). Chemical Oxidation. In J. Edzwald (Ed.), *Water Quality & Treatment : A Handbook on Drinking Water* (6th ed., p. 7.42). Denver, Colorado, USA: AWWA.

Singh, R. (2006). *Hybrid Membrane Systems for Water Purification - Technology, Systems Design and Operation.* Colorado Springs: Elsevier.

Smith, P., Vigneswaran, S., Ngo, H., Ben-Aim, R., & Nguyen, H. (2006). A new approach to backwash initiation in membrane systems. *Journal of Membrane Science*(278), 381-389.

Snoeyink, V., & Jenkins, D. (1980). Water Chemistry. New York: John Wiley and Sons, Inc.

Song, Y., Xu, J., Xu, Y., Gao, X., & Gao, C. (2011, March 11). Performance of UF-NF integrated membrane process for seawater softening. *Desalination*.

Stokke, J., Seacord, T., Maillakakis, M., & Hawes, R. (2010). Acid elimination study for the North Lee County RO water treatment plant. *Florida Section AWWA Conference Proceeding.* Orlando: AWWA.

Stokke, J., Seacord, T., Maillakakis, M., & Hawes, R. (2011). Acid elimination study for the North Lee County RO water. *FSAWWA.* Orlando: AWWA.

Stumm, W., & Morgan, J. (1996). *Aquatic Chemistry: Chemical Equlibria and Rates in Natural Waters.* New York: John Wiley & Sons,Inc.

Subramani, A., & Hoek, E. (2008). Direct observation of initial microbial deposition onto reverse osmosis and naofiltration membranes. *Journal of Membrane Science, 319*, 111-125.

Sungur, E. I., & Cotuk, A. (2005). Characterization of sulfate reduicng bacteria isolated from cooling towers. *Environmental Monitoring and Assessment*(104), 211-219.

Sutzkover-Gutman, I., & Hasson, D. (2010). Feed water pretreatment for desalination plants. *Desalination, 264*(3), 289-296.

Taylor, J. S., & Jacobs, P. E. (1996). Reverse Osmosis and Nanofiltration. In M. J., P. E. Odendall, & M. R. Wiesner, *Water Treatment Membrane Processes* (pp. 4.1-4.20). New York: McGrawHill.

Taylor, J., Dietz, J., Randall, A., & Hong, S. (2005). Impact of RO-desalted water on distribution water quality. *Water Science & Technology, 51*(6-7), 285-291.

Tharamapalan, J., Duranceau, S. J., & Perez, P. (2011). Demonstration of sulfuric acid elimination in a brackish water reverse osmosis membrane process. *American Membrane Technology Association and Southeast Desalting Association Joint Conference.* Miami Beach: AMTA.

Thompson, D., Olson, C., & Wagner, W. (1993). Colloidol sulfur turbidity control and offgas treatment. *AWWA Annual Conference.* San Antonio: AWWA.

Tian, J., Chen, Z., Yang, Y., Liang, H., Nan, J., & Li, G. (2010). Consecutive chemical cleaning of fouled PVC membrane using NaOH and ethanol during ultrafiltration of river water. *Water Research, 44*(1), 59-68.

Tro, N. J. (2008). *Chemistry : Amolecular Approach.* New Jersey: Pearson Prentice Hall.

Trupiano, V. (2010). *Evaluation of oxidized media filtration processes for the treatment of hydrogen sulfide in groundwater*. Orlando, Florida, United States: University of Central Florida.

U.S. EPA. (1979). *Handbook for Analytical Quality Control in Water and Wastewater Laboratories.* Cincinnati, Ohio: Environmental Monitoring and Support Laboratory,U.S. EPA.

USEPA. (1992). *Rules and Regulation (40 Code of Federal Regulations).* Washington: U.S. Government Printing House.

USEPA. (2005). *Membrane Filtration Guidance Manual EPA 815-R-06-009.* Cincinnati,OH: EPA.

USEPA. (2012, May 21). *Secondary Drinking Water Regulations: Guidance for Nuisance Chemicals*. Retrieved Aug 31, 2012, from United States Environmental Protection Agency: http://water.epa.gov/drink/contaminants/secondarystandards.cfm

Van der Bruggen, B., & Vandecasteele, C. (2003). Removal of pollutants from surface water and groundwater by nanofiltration: Overview of possible applications in the drinking water industry. *Environmental Pollution, 122*, 435-445.

Verdugo, P., & Santschi, P. (2010). Polymer dynamics of DOC networks and gel formation in sea water. *Deep Sea Research II*, 1486-1493.

Villacorte, L., Kennedy, M., Amy, G., & Schippers, J. (2009). The fate of transparent exopolymer particles (TEP) in integrated membrane systems: Removal through pre-treatment processes and depostion on reverse osmosis membranes. *Water Research, 43*, 5039-5052.

Vrouwenvelder, J. (2009). *Biofouling of Spiral Wound Membrane Systems.* Delft, The Netherlands: Ipskamp Drukkers,Enschede, The Netherlands.

Vrouwenvelder, J., Beyer, F., Dahmanai, K., Hasan, N., Galjaard, G., Kruithof, J., & Van Loosdrecht, M. (2010). Phosphate limitation to control biofouling. *Water Reserach, 44*(11), 3454-3466.

Walton, N. (1989). Electrical conductivity and total dissolved solids - What is their precise relationship. *Deslination, 72*(3), 275-292.

Wang, X., Zhang, C., & Zhao, J. (2000). Separation mechanism of nanofiltration membranes and its applications in food and pharmaceutical industries. *Membrane Science and Technology, 20*(1), 29-30.

Wells, S. (1954). Hydrogen sulfide problems of small water systems. *AWWA, 46*(2), 160-170.

White, G. (1972). *Handbook of Chlorination.* New York: Van Nostrand Reinhold Company.

White, G. (1999). *Handbook of Chlorination* (4th Edition ed.). New York: John Wiley & Sons, Inc.

Xu, J., Ruan, G., Gao, X., Pan, X., Su, B., & Gao, C. (2008). Pilot study of inside-out and outside in hollow fiber UF modules as direct pretreatment at low temperature for reverse osmosis. *Science Direct, 219*(1-3), 179-189.

Yongsiri, C., Vollertsen, J., & Jacobsen, T. H. (2004, January). Effect of temperature on air-water transfer of hydrogen sulfide. *Journal of Environmental Engineering,* 104-109.

Zhao, Y., & Taylor, J. (2005, September). Incorporation of osmotic pressure in an integrated incremental model for the predicting of RO and NF concentration. *Desalination, 174*(2), 145-159.

Zhao, Y., & Taylor, J. S. (2005b). Assessment of ASTM D 4516 for evaluation of reverse osmosis membrane performance. *Desalination, 180*, 231-244.

Zondervan, E., Zwijnenburg, A., & Roffel, B. (2007). Statistical analysis of data from accelerated ageing tests of PES UF membranes. *Desalination, 300*(1-2), 111-116.